Rainfall-Runoff Modelling of Meso-Scale Catchments in the Upper Ewaso Ng'iro Basin, Kenya

Diplomarbeit
der Philosophisch-naturwissenschaftlichen Fakultät
der Universität Bern

vorgelegt von
Benedikt Notter
2003

Leiter der Arbeit:

Dr. Hanspeter Liniger
Centre for Development and Environment (CDE)
Geographisches Institut

Prof. Rolf Weingartner
Gruppe für Hydrologie
Geographisches Institut

ABSTRACT

The Ewaso Ng'iro Basin in Kenya is a classical example of a highland-lowland interaction: Mt. Kenya, which receives high precipitation, contributes a major share to the discharge of the rivers in the basin, but growing demand for irrigation water on its foothills produces water shortage in the lowlands. Water scarcity leads to conflicts that can only be solved by community self-help mechanisms like the recently founded River Water Users Associations, but their work is hindered by a lack of knowledge on the present and future availability of water resources.

This study tries to make a contribution to better water management in the area by:

- evaluating a new version of the land-use sensitive NRM^3 Streamflow Model (Thomas 1993, McMillan 2003) in three meso-scale perennial catchments on the Mt. Kenya slopes, as a potential tool for water management. The performance of the NRM^3 Streamflow Model is tested in predicting discharges, specifically low flows, under various geographic and data availability conditions;
- creating better insight into the hydrology of the study catchments;
- analysing scenarios of land use and climate change; the NRM^3 Streamflow Model is run with modified GIS (for land use scenarios) and meteorological time-series inputs (for climate change scenarios) according to possible trends.

As a prerequisite to hydrological modelling, groundwater influences in the Naro Moru, Burguret and Nanyuki catchments are assessed by profile measurements of discharge, electric conductivity and temperature. The results indicate that the lower forest belt and the footzone are groundwater discharge areas and the savannah zone is an area characterized by transmission losses. Hydrological modelling of the catchments is considered possible without major modifications of the NRM^3 Streamflow Model structure. The great insecurities on the anthropogenic influences (namely water abstractions) are a serious drawback to the validity of the results. River water abstractions are assessed based on a campaign during the field work period and data from previous monitoring by NRM^3, resulting in a naturalised flow series that model outputs can be compared to.

In a second step, the NRM^3 Streamflow Model is calibrated and validated in the Naro Moru, Burguret and Nanyuki catchments using the time period 1987 – 1991 for calibration and the period 1992 – 1996 for validation. The experiments show a reasonably good performance on the decadal time-step and an acceptable performance on the daily time-step. The model can be used without extensive calibration. GIS input data produce good results up to a spatial resolution of 500 m. It is crucial, however, to use good quality rainfall data from a well-distributed measuring network, which is only given in the Naro Moru catchment. Improvements on the model could mainly be made by modifying the simulation of groundwater discharge (introduction of a second groundwater store or variable groundwater parameters), by introducing an altitude-dependent method of precipitation interpolation and by making the programme more user-friendly.

In the last part of the study, the NRM^3 Streamflow Model is run in the four nested Naro Moru subcatchments with modified GIS land use maps representing five scenarios of changed land use, and with meteorological time-series modified according to the climate projections of the IPCC SRES illustrative marker scenarios A2 and B2. It is shown that degradation of the land cover would mainly result in higher peak flows; low flows would be slightly, if at all, reduced. More dramatic is the output of the climate change scenario A2: With precipitation drastically reduced in June to August, low flows are significantly reduced, increasing the water scarcity; on the other hand, in the dry season and rainy season months floods are projected to increase dramatically. Scenario B2 causes similar but less severe impacts.

TABLE OF CONTENTS

LIST OF FIGURES

LIST OF ABBREVIATIONS

AGCM	Atmospheric Circulation Model
ASAL	Arid and Semi-arid Lands
a.s.l.	above sea level
CETRAD	Centre for Training and Integrated Research for ASAL Development (the former LRP)
CDE	Center for Development and Environment
E_2	Nash and Sutcliffe Efficiency Score
EC	Electric Conductivity
ENNDA	Ewaso Ng'iro North Development Authority
ET	Evapotranspiration
GCM	General Circulation Model
HRU	Hydrological Response Unit
IDW	Inverse Distance Weighting interpolation technique
ITCZ	Inner tropical convergence zone
KMD	Kenya Meteorological Department
LRP	Laikipia Research Programme (today: CETRAD)
MoWD	Ministry of Water Development
NMQ30	The lowest 30-day mean of discharge in a hydrological year
NRM^3	Natural Ressources Monitoring, Modelling and Management
OGCM	Ocean Circulation Model
P	Precipitation
Q	Discharge
R1COEFF	Slow groundwater discharge coefficient of the NRM^3 Streamflow Model
R2COEFF	Fast groundwater discharge coefficient of the NRM^3 Streamflow Model
r^2	Coefficient of determination
RCM	Regional circulation model (of the atmosphere)
Res.	Resolution
RGS	River gauging station
ROCOEFF	Runon coefficient of the NRM^3 Streamflow Model
RWUA	River Water Users Association
S – O	Simulated – Observed Discharge
SCOEFF	Deep seepage coefficient of the NRM^3 Streamflow Model
SSZTH	Threshold of saturated zone moisture between fast and slow groundwater discharge in the NRM^3 Streamflow Model
T	Temperature
WMO	World Meteorological Organization

1. INTRODUCTION

1. 1. BACKGROUND

Water is one of the most basic resources of life. Especially in developing countries, where a majority of the population directly relies on the productivity of the land, it is a fundamental prerequisite to development. On the other hand, water is said to be the first resource to become scarce worldwide in the 21st century, and conflicts around the allocation of water are expected to become more severe in the future.
These facts are well known, and their importance has lead to enormous efforts in research, management, and politics. However, big challenges remain. They include (Gichuki&Ngigi 2001: 1):

- improving data and knowledge basis for decision
- water allocation, considering the social, economic and ecological context
- water saving technologies
- policy reforms
- improvements in water governance

This study aims at improving the knowledge basis for decision in an area where water is naturally scarce, and is becoming more and more so due to socio-economic developments in the recent past.

Mt. Kenya as an over 5000 metres high mountain in the East African savannah zone is destined to be a water tower for the region. The streams originating on its slopes are, due to orographic precipitation, a reliable source of surface fresh water for the surroundings, especially during the dry seasons. Ewaso Ng'iro River, the main river draining the Laikipia plains, receives the greatest contribution to its runoff from Mt. Kenya (by Naro Moru, Burguret and Nanyuki Rivers) and the Aberdare Range (Ewaso Narok, Seghera and Soguroi Rivers) (see map, Fig. 2.1).

Fig. 1.1: Mt. Kenya seen from the Laikipia plains (picture by J. Aeschbacher)

In the past two decades the Ewaso Ng'iro and its tributaries have increasingly often fallen dry over long stretches during the dry seasons. The reason for this is not a change of climatic conditions – there is no decreasing trend in precipitation in this time span. The water scarcity in the lowlands is primarily caused by increasing water demand for irrigated agriculture in the footzone of the mountain ranges. A second possible reason are land use changes in the river catchments.
As a consequence of the water shortage, conflicts arise

between pastoralists and agriculturalists on one hand, but also among agriculturalists using the water of the same river. The uncontrolled intensification of agriculture through continued immigration worsens the situation. Water laws are not enforced.
To face these problems, in the last years a self-help movement has been taking place with the formation of River Water Users Associations (RWUAs) in some of the catchments on the slopes and in the footzone of Mt. Kenya (where most of the irrigation is concentrated). Their objectives are to enhance co-operation between water users, government agencies, national park staff, and scientists; create awareness of the water scarcity; monitor water resources; and to try to ensure a fair distribution of the water resources.
However, the achievement of these goals is hindered by a lack of knowledge on:

- **who** uses how much water: the number of small-scale farmers abstracting water for irrigation is constantly increasing. Because water laws are not enforced and most abstractions are illegal, neither the abstraction points nor the used water amounts are registered anywhere.
- **how much** water is there to be used: the unknown amounts of abstracted water and the lack of knowledge about the reaction of the catchments to a given rainfall make it impossible for decision-makers to know how much of the resource can be counted with.
- how will the situation evolve in the **future**: given the current trends in land use changes and the projections about global climate change, how much water can be expected in the future?

1. 2. AIMS OF THIS STUDY

The objective of this study is to make a contribution to better water management in the Upper Ewaso Ng'iro Basin by improving the knowledge base on the hydrology of the meso-scale perennial catchments on the slopes and foothills of Mt. Kenya, and by testing a potential tool for water management in the area. This is achieved by:

- Evaluating the performance of a **land-use sensitive hydrological model**, the NRM3 Streamflow Model, at predicting discharges in the Naro Moru, Burguret and Nanyuki catchments. The sensitivity to model parameters, the applicability of the model at different spatial scales and the need for input data are assessed, as well as the model's user-friendliness and applicability as a potential tool for water management in the context of NRM^3 and the RWUAs.
- Creating better insight into the hydrology of the study catchments – on one hand by assessing the magnitude of **groundwater influences** and by identifying areas of groundwater recharge and discharge (which is a prerequisite to modelling), and on the other hand by the modelling results as a measure for how well the hydrological processes are understood.
- Evaluating **scenarios** of changed land use and climate and their impact on water availability according to possible trends in the near future.

1. 3. INSTITUTIONAL AND CONCEPTUAL FRAMEWORK

1. 3. 1. Institutional framework

This study has been realized within the framework of NRM^3. Natural Resources Monitoring, Modelling and Management (NRM^3) in Nanyuki is a project that evolved as part of the LRP

(Laikipia Research Programme, initiated by the University of Berne), with the aim of promoting sustainable use of natural resources in the Upper Ewaso Ng'iro Basin by:

- establishing a Natural Resources Information System (NRIS) containing baseline information on climate, water, soil, vegetation and land use
- analysing natural variability or trends as well as the human impact on resources
- collecting long-term data series that can be used for model development and validation
- developing a data and knowledge base for decision makers to plan and implement sustainable management of resources

According to these goals, NRM^3 has been assisting in the formation of RWUAs in the river catchments of the Upper Ewaso Ng'iro Basin and is supporting their decision-making process with its database.

This study has also been carried out in close collaboration with Jos Aeschbacher, who in his MSc thesis (Aeschbacher 2003) analyses the development of abstractions as well as the low flows of Naro Moru River. The field work in summer 2002 was carried out together. The naturalized discharge data series (observed discharge plus abstracted amounts) resulting from Aeschbacher's investigations was used to calibrate and validate the NRM^3 Streamflow Model. The outputs of the NRM^3 Streamflow Model for Naro Moru, in turn, could be used to infill data gaps for the estimation of total water use in the catchment.

1. 3. 2. Conceptual framework

A hydrological model, the NRM^3 Streamflow Model, is applied to simulate discharge from the study catchments.
Hydrological models are numerical models that calculate the discharge from a catchment from given input data: informations on catchment characteristics, such as topography, land use, soils etc., and time-series information on the meteorological variables, such as precipitation and evapotranspiration.
Hydrological models are mainly used to overcome the limitation of measuring hydrological processes in space and time: in space, by their application to ungauged catchments, and in time, by making predictions of discharge into the future. The other benefit of hydrological models is that they assemble knowledge on processes in a neat package and will show if the theory is in conflict with reliable measured data, thus giving a feedback on how well processes are understood (Beven 2001: 1).

Given the aims of applying a hydrological model in the Upper Ewaso Ng'iro Basin and of assessing the impact of land use changes, the chosen model must

- be able to be run with the input data that are available in the region
- be land-use sensitive, i. e. land use types in a catchment are included in the calculation of discharge

These requirements are met by the NRM^3 Streamflow Model. Its use is a continuation of the efforts of previous NRM^3 studies.
The NRM^3 Streamflow Model was originally developed by Mike Thomas (1993) for use in rural, ungauged catchments in Kenya. It is a conceptual, semi-distributed, three-layer water balance model which runs on a daily time-step. It needs precipitation and pan evaporation as time-series input data; further required information is soil type (and soil depth, water capacity and infiltration properties), and land use respectively associated crop coefficients. The original model version used the Hydrological Response Units (HRUs) as basic units to

calculate water balances, irregularly shaped patches of land with an (assumed) homogenous hydrologic response.
Mike Thomas and Lindsay McMillan (2003) introduced as main development the use of a grid in which for each cell the water balance is calculated. The model can now be run at any desired spatial resolution of the grid. McMillan tested and calibrated the new version of the NRM^3 Streamflow Model on small-scale (ephemeral) catchments in the Ewaso Ng'iro Basin, namely the Mukogodo catchment.

This study makes the scale-shift to meso-scale/perennial catchments, which is the type of catchments the RWUAs are mainly active in.

In a first step, (described in Section 5) hydrological influences on the water balance of the study catchments that cannot be modelled with the NRM^3 Streamflow Model are identified: the magnitude of groundwater influences and areas of groundwater re- and discharge are assessed based on profile measurements of discharge, electric conductivity, and temperature along the rivers (carried out during field work in July and August 2002).
River water abstractions are accounted for by estimating total abstractions in a catchment and adding these to the observed flow series, resulting in a naturalized flow series that the model outputs can be compared to. This is done based on the abstractions campaigns carried out during field work, earlier monitoring data from the NRM^3 database, and the work of J. Aeschbacher (2003).

For the actual evaluation (Section 6) of the NRM^3 Streamflow Model, hydrometeorological data from the NRM^3 database for the years 1987 – 1996 are used to calibrate and validate the model. This is done under varying geographic conditions (catchment size, land use, ecological zones) and varying data quality (spatial and temporal resolution of the input data). The four nested catchments of Naro Moru (A3 – A6) and the Burguret (A8) and Nanyuki (A9) catchments are modelled. Data requirements are assessed as well as the performance of the model and its applicability.

In the last part of the study (Section 7), the model is run with modified inputs: To evaluate the impact of land use changes, GIS information on land cover is altered to produce five scenarios of changed land use, such as conversion of forest and savannah into cropland or grazing land, or contrarily, the re-conversion from cultivated land to forest and savannah.
To evaluate the impacts of climate change, outputs from an atmospheric General Circulation Model (GCM) for the years 2040 – 2069 are used to calculate monthly change fields of precipitation and evaporation according to the guidelines of the Task Group on Scenarios for Climate Impact Assessment (IPCC-TCGIA, 1999). These changes are applied to the baseline meteorological data series to be used as forcing for two climate scenario runs based on the A2 and B2 IPCC SRES illustrative marker scenarios.
For the base case that the outputs of all land use and climate change scenario runs are compared to, meteorological data from the years 1987 to 2001 and the land use map of 1988 are used in order to reflect current conditions.

2. DESCRIPTION OF THE STUDY AREA

2. 1. PHYSICAL ENVIRONMENT

2. 1. 1. Highland-lowland interactions: Mt. Kenya as the water tower of Laikipia

The Ewaso Ng'iro North Basin covering 210'226 km^2 is the largest of the five major Kenyan drainage basins. The Upper Basin (reaching down to Archer's Post) covers an area of 15'200 km^2. It is located to the North and West of Mt. Kenya between longitudes 36°30' and 37°45' East and latitudes 0°15' South and 1°00' North.
Topographically, the Upper Ewaso Ng'iro Basin is characterized by the tertiary volcano ranges of Mt. Kenya (5'199 m a.s.l.) and the Aberdares or Nyandarua Range (3'999 m a.s.l.), between which the vast, gently undulating Laikipia Plains extend at an elevation of 1700 – 1900 m a.s.l. To the north of the Plains, the Loldaiga Hills on the so-called basement complex reach altitudes of 2500 m a.s.l. before dropping to the lowlands around Archers Post (862 m a.s.l.).

The Ewaso Ng'iro Basin can be subdivided into three main subbasins: The Ewaso Narok subbasin which drains the Aberdares and the western part of the Laikipia Plateau; the Ewaso Ng'iro-Mt. Kenya subbasin on the slopes of Mt. Kenya and the eastern Plateau; and the Ewaso Ng'iro Lowland subbasin. The common point of the three is the Confluence of Ewaso Ng'iro and Ewaso Narok at Junction (see Fig. 2.1).

This study focuses on three catchments in the Ewaso Ng'iro-Mt. Kenya subbasin: The Naro Moru, Burguret and Nanyuki catchments. These rivers are the three main tributaries to Ewaso Ng'iro originating on the western slopes of Mt. Kenya. With their elongated shape from the peak of the mountain down to the Laikipia plains the catchments cross all ecological zones, including the moorland and forest belt which is the zone where most of the crucial dry season runoff is generated (see Fig. 2.2).

The Upper Ewaso Ng'iro Basin is a classical example of highland-lowland interactions. Topography and atmospheric circulation produce steep climatic and ecological gradients, resulting in humid and subhumid conditions in the Mt. Kenya and Aberdare ranges, semi-arid conditions in the Laikipia Plains and arid conditions in the lowlands around Archers Post. Annual rainfall ranges from around 300mm in the lowlands to around 700mm in the plateau and reaches its maximum values in the highlands with 1500 – 2000mm (Leibundgut et al. 1986, p. 29). 99% of the Upper Ewaso Ng'iro Basin experience a rainfall – evaporation deficit (Gichuki 2001: 1). Given this dependence of the whole basin on dry season flows generated on the mountain slopes, Mt. Kenya can be described as being the water tower for Eastern Laikipia.

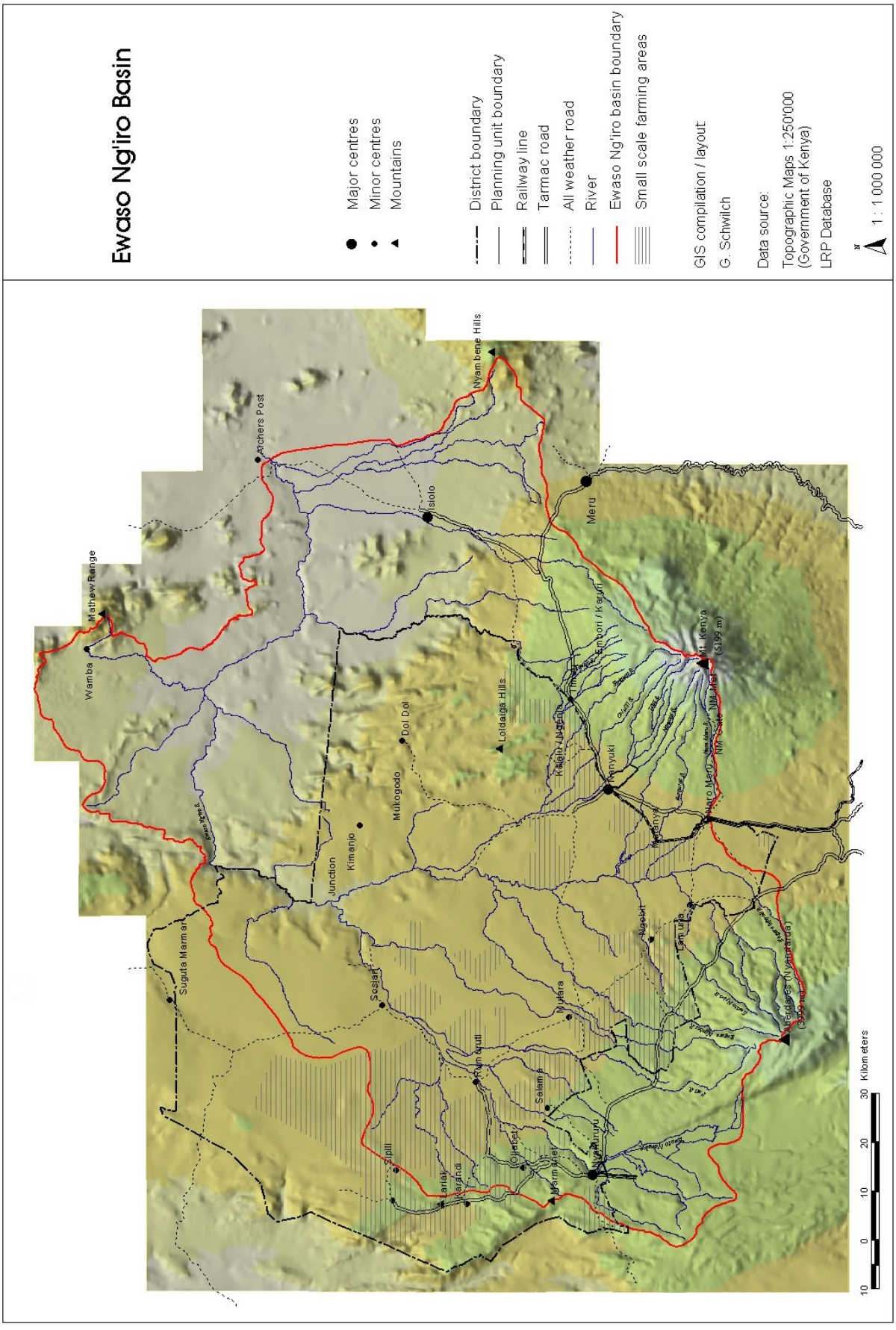

Fig. 2.1: The Upper Ewaso Ng'iro Basin (Source: LRP Database/Gudrun Schwilch)

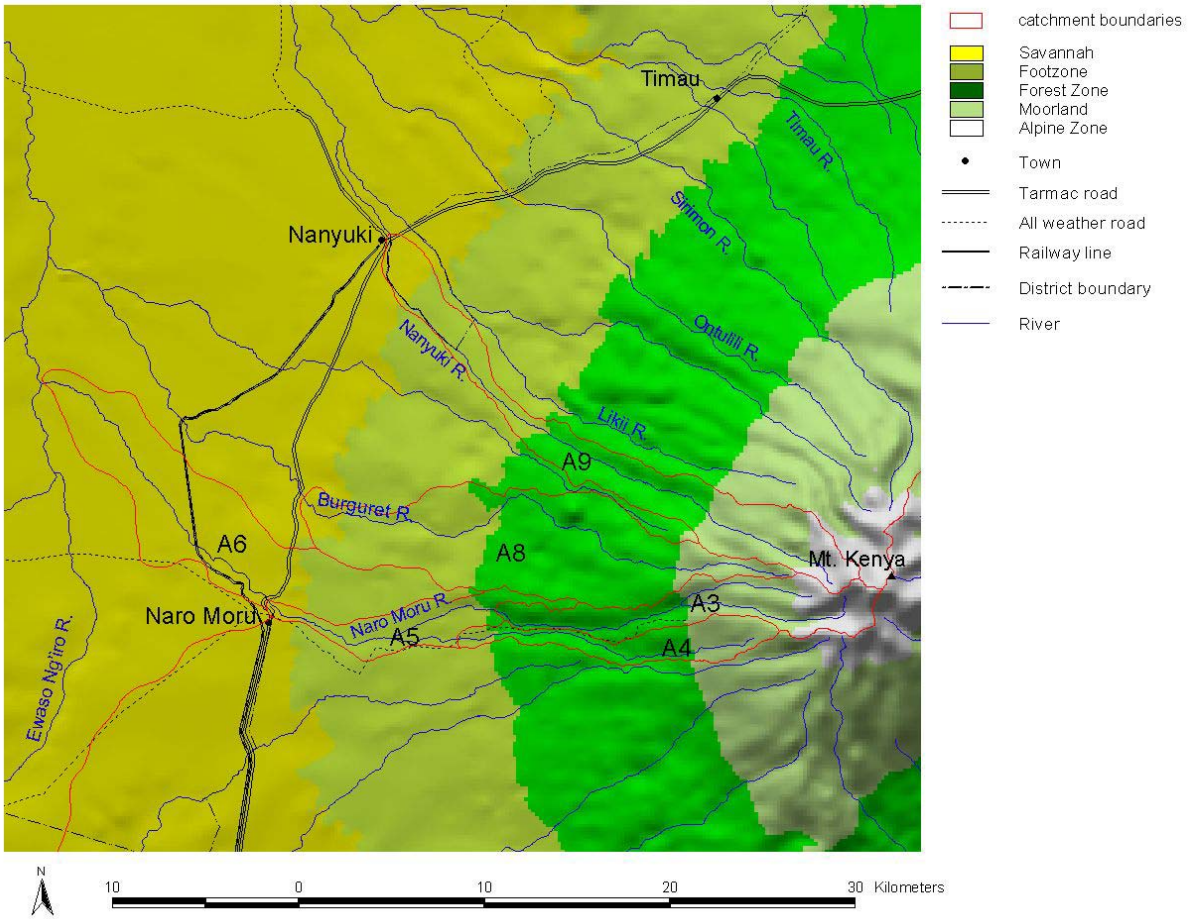

Fig. 2.2: The study catchments A3 – A6 (Naro Moru), A8 (Burguret) and A9 (Nanyuki) and the ecological zones.

2. 1. 2. Climate

The climate of the study region is a result of the interactions of the atmospheric circulation with topography. Its yearly fluctuations are mainly dominated by the position of the ITCZ (Inner Tropical Convergence Zone).

The ITCZ, according to the traditional cell model of atmospheric circulation, generally is the zone on the meteorological equator that receives the highest amount of radiation, which causes high-reaching convection (up to 16 km). When the rising air cools at higher altitudes due to pressure reduction, its relative humidity rises, and clouds and rains form. Near the surface the rising air is constantly replaced by air streaming in from the North and the South, forming the trade winds, whose lateral direction is additionally modified by the Coriolis force towards the West. In the upper Stratosphere, the outflow from the ITCZ diverges again towards the North and the South. The resulting convection cells on both sides of the meteorological equator are called Hadley cells. The air in the upper stratosphere on both sides of the ITCZ runs in the opposite direction to the trade winds, and by its tendency to sink prevents the trade winds from rising, causing an inversion. This way, while the region on which the ITCZ is centered will receive much precipitation, the areas further to the North and the South will remain relatively dry.

Additionally, East Africa and the Western part of the Indian Ocean are under the influence of extensive subsidence of the zonal Walker circulation on the equator, that is also one of the driving forces of the ENSO phenomenon (Berger 1989: 22).

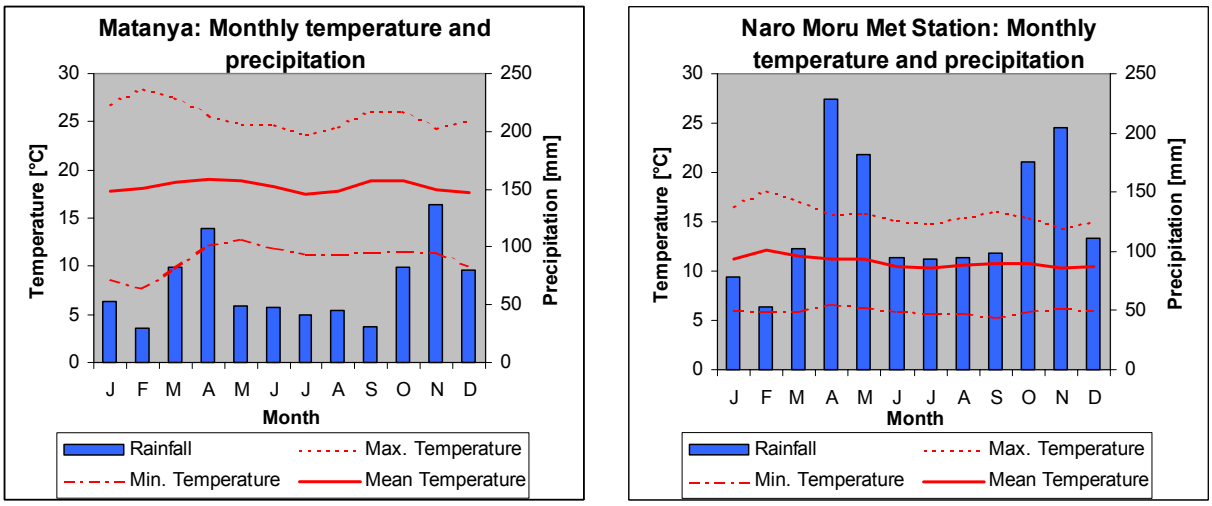

Fig. 2.3: Climate diagrams (monthly temperature and precipitation) of Matanya (1840 m a.s.l., savannah zone) and Naro Moru Met Station (3050 m a.s.l., upper forest zone).

Because of the inclination of the Earth's axis and its movement around the sun, the ITCZ moves each year from the Southern to the Northern hemisphere and back. The position of the ITCZ generally follows the declination of the sun but is largely modified by surface characteristics. Where fast-warming surfaces occur, such as the Tibetan High Plateau, the ITCZ will move further away from the Equator.

This situation results in four distinguishable seasons in the study area (Gichuki et al. 1998b):

- During the **Dry Season** from January to February the ITCZ is positioned south of the equator, over the southern Rift Valley and Madagascar. The northerly trade winds originating in Saudi Arabia and then crossing the arid areas of Somalia and Northern Kenya are dry, and therefore almost no rainfall can be observed in the study area.
- During the **Long Rains** from March to June the ITCZ is crossing the equator. The resulting high-reaching convection causes extended rains to set in.
- During the **Continental Rains** season from July to September the ITCZ is located over Southern Arabia. The trade winds from the South-East originate over the Indian Ocean and are therefore not as dry as the northerly trade winds in January and February. The Western part of the Upper Ewaso Ng'iro Basin receives more precipitation than the Eastern part in this season, which could be caused by a second convergence zone on the 700 mB level over Lake Victoria (Sturm 2002: 21).
- The **Short Rains** season from October to December is again characterized by the ITCZ causing convection and precipitation over the study area.

Topography is the second great influence on climate. Mt. Kenya and the Aberdares as obstacles cause the trade winds to rise, cool down and release part of their moisture. This causes the rains on the mountain slopes that sustain the dry season flows in the rivers. The sinking air from the upper troposphere, however, prevents the air from rising all the way to the peak regions. This is why the cloud layer around the mountain can often be observed reaching up to a certain height only, leaving the view of the peak clear. It also causes the maximum of the precipitation (around 1600 mm/year) to occur at an altitude of around 3000 to 3500 m a.s.l. Further above, precipitation decreases to reach around 800 mm/year in the peak region (Berger 1989: 22).
The exposition of a site also influences rainfall patterns. The Eastern and Southern slopes of Mt. Kenya are much wetter than the Western and Northern slopes, because the South-Eastern

trade winds originating over the Indian Ocean carry more moisture than the North-Eastern trade winds originating over the Arabian desert. This situation is also clearly reflected in the vegetation pattern: While rainforest covers the Eastern and Southern slopes of the mountain, dry montane forest grows in the lower forest zone to the West, and to the North of Mt. Kenya the forest belt even narrows towards a small gap.

Generally the climate in the study area can be characterized as semi-arid in the savannah zone (between 600 and 750 mm/year) and semi-humid to humid in the forest and moorland zones (up to 1600 mm/year). The rainfall pattern is bimodal, according to the two distinct rainy seasons. Potential evaporation is high, reaching 1700 – 2000 mm on the Laikipia plateau and decreasing with altitude. Only on the upper mountain slopes precipitation exceeds potential evapotranspiration, which causes the natural disposition of the area for water scarcity (see Fig. 2.4).
The onset of the rainy seasons is unreliable, and their duration varies. Sometimes dry periods occur within rainy seasons. This is a big restraint for crop production. Interannual rainfall variability is high as well; for some rain gauging stations in the Laikipia Plateau the coefficient of variation of annual rainfall amounts to up to 35%. A fluctuation of yearly rainfall totals can be observed that could be explained with the QBO (Quasi-biannual oscillation), but clearly the influence of El Niño also plays a major role. It caused for example the years 1997/98 to be wet and the years 1999 and especially 2000 to be very dry. Longer periods with precipitation above or below average can also be distinguished. For example, the 1960's were quite wet, while the first half of the 70's and the 80's respectively was dry (Berger 1989: 15).

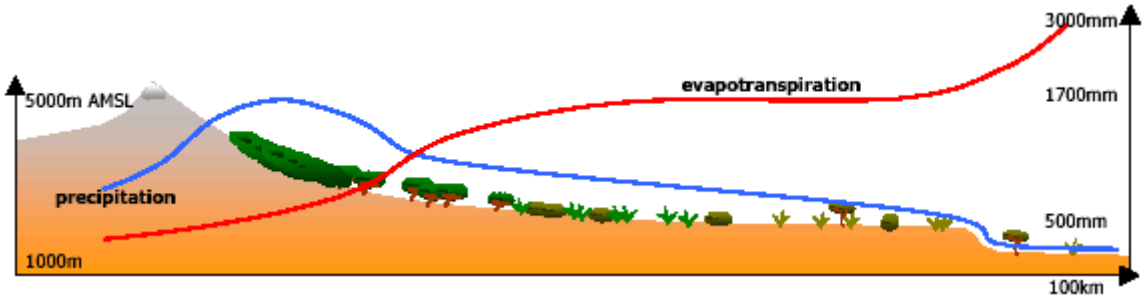

Fig. 2.4: Precipitation and evapotranspiration between the peak of Mt. Kenya and the lowlands (Source: Liniger et al. 1998b).

Temperatures lie between 16° and 22° C in the savannah zone and decrease with altitude towards the glaciated peak of Mt. Kenya. Daily temperature fluctuations by far exceed yearly fluctuations, which is typical for the tropics (see also Fig. 2.3).
Typical is also the high proportion of convective rainfall generation (adversed to advective rains caused by larger-scale circulation), which results in storms often confined to small, limitied perimeters (Berger 1989: 24). Such storms are difficult to capture by rainfall monitoring if the measuring network is not very dense. This can be an obstacle to hydrological modelling, as is shown in Section 6.

2. 1. 3. Ecological zones: vegetation and land use

The climatic conditions cause a clear altitudinal zonation of vegetation and land use that is modified by orientation. On the Western slopes of Mt. Kenya, where the study catchments are located, the following major zones can be distinguished from the peak downwards to the Laikipia plains:

Fig 2.5: The alpine zone on Mt. Kenya (picture by J. Aeschbacher)

2. 1. 3. 1. Alpine Zone (> 4000 m a.s.l.)

The two highest peaks of Mt. Kenya, Batian and Nelion, rise up to 5199 m a.s.l. The major part of the alpine zone is made up of bare rock, steep slopes, snow and ice. Vegetation is only apparent in its lower parts: tussock grasses on the valley bottoms and Giant Groundsels *(Senecio Keniodendron)* on the better drained valley sides.

2. 1. 3. 2. Moorland (3200 – 4000 m a.s.l.)

In the upper part of the moorland tussock grasses grow on valley bottoms and Giant Groundsels on the valley sides. The lower part is dominated by heather vegetation, mostly Erica and Philippia (Decurtins, 1992: 25).

2. 1. 3. 3. Forest Zone (2300 – 3200 m a.s.l.)

The upper part of the forest zone down to about 2600 m a.s.l. is characterized by dense, humid bamboo forest mixed with huge Podocarpus and cedar trees. Below 2600 m evergreen dry montane forest with Podocarpus, Olea and Locotea species grows. In the forest zone also

Fig. 2.6: The forest zone in the Naro Moru catchment (picture by B. Notter).

human influences are visible: small illegal clearings where vegetables are grown, and in the lower parts forestry use and plantations with exotic species such as Eucalyptus or pines. First traces of man-induced soil erosion can be noticed here.

Fig. 2.7: The footzone of Mt. Kenya in the Naro Moru catchment (picture by J. Aeschbacher)

2. 1. 3. 4. Footzone (2000 – 2300 m a.s.l.)

The vegetation in the footzone is greatly influenced by man: much of the forest is cleared or replaced with plantations of eucalyptus and pine, and large areas are used for small-scale partly rainfed agriculture, mainly potatoes and maize. Settlement, roads and infrastructure also exist. Under the shamba system (shamba meaning field), some forest areas get cleared and replanted with tree seedlings. Between the seedlings the land can be cultivated until the replanted trees are too competitive for the crops.

2. 1. 3. 5. Savannah (1700 – 2000 m a.s.l.)

Open grasslands alternate with bushlands; acacia species and the funny-looking Euphorbia trees (succulents) are the most conspicuous species. The river courses are lined by dense riverine vegetation including red cedar, podocarpus and fewer acacias. Wetlands with papyrus swamps exist at the confluence of Burguret with Ewaso Ng'iro. The natural vegetation is subject to much human-induced change through the increasing number of small-scale farmers settling down along the rivers (growing mostly vegetables, maize, or sugar cane). Acacias are often slashed by farmers to produce coal, in order to get some additional income. In some parts the valuable vegetation protection has been completely removed from the river banks.

Fig. 2. 8: The savannah zone near Matanya with the characteristic Euphorbia trees (picture by B. Notter).

2. 1. 4. Geology

Mt. Kenya is a volcano that formed at the end of the Tertiary, about 3 million years ago. Its original height is estimated to have been over 6500 m. It has been subject to much erosion, including at least two periods of glaciation, which has given the peak, the remnants of the central volcano plug, its present sharp shape. The volcano is of Vesuvian type and made up of lavas, pyroclastic rocks, and ashes (Decurtins 1992: 12).
The central volcano plug consists of intrusive rock masses, porphyric phonolites and nepheline syenites. A zone of trachytes, fissile phonolites, tuffs and agglomerates then follows. The moorland zone is in the upper part underlain with Kenytes and Kenyte agglomerates. They are well permeable and should allow groundwater formation, as well as the porphyric phonolites and agglomerates that underlie the forest and footzone. In the savannah zone, pyroclastic rocks and intermediate igneous rocks form the plateaus while fluvial accumulations of weathered pyroclastic and igneous rocks form the valley bottoms (Decurtins 1992: 24ff, see also Fig. 2. 9).

2. 1. 5. Soils

Soil formation depends on geology, climate, vegetation, topography, and the time the soil had to form. The distribution of soil types in the study area generally follows the ecological zonation.

In the alpine zone only lithosols and dystric regosols are found. They are, after the U. S. Department of Agriculture's Soil Conservation Service hydrological soil group classification system (USDA SCS, 1985), poorly drained, and reach only thicknesses of 10 cm.
In the moorland zone rankers occur next to lithosols and regosols. Soil thickness is 25 cm on average, and the drainage is poor.
The upper forest zone, the bamboo belt, is characterised by moderately well to well drained humic andosols that reach thicknesses of around 80 cm on the slopes, and poorly drained humic gleysols on the valley bottoms. In the lower forest zone the andosols are replaced by around 150 cm deep well drained humic acrisols.
In the footzone moderately ferric luvisols are dominant on the slopes and undulating plateaus, and dystric gleysols in the valley bottoms. They are around 150 cm deep on average. Their drainage properties extend from imperfectly to moderately well drained.
In the savannah zone imperfectly to poorly drained luvic Phaeozems and Vertisols with a thickness of 150 to 180 cm make up the soils on the plateau. They tend to crust formation. On the valley sides excessively drained lithosols and ferric luvisols are found (Decurtins 1992: 30) and on the valley bottoms poorly drained gleyic soils and fluvisols (Speck 1983, Liniger et al. 1998a).

2. 1. 6. Hydrology: drainage network, natural water availability

2. 1. 6. 1. Surface water

The **drainage pattern** of Mt. Kenya is clearly radial, which is typical for a volcano with a relatively young drainage network. In their uppermost reaches the rivers are fed by glaciers, snow and icefields, and lack well-defined riverbeds where they flow through swamps dammed by glacial moraines. Down to around 4000 m a.s.l. the valleys are glacially U-shaped. Below 4000 m fluvial V-shaped, deeply incised valleys with many cascades dominate. In the moorland, many diffuse groundwater outflows feed the streams. In the forest zone a dense network of deeply incised tributaries exists. In the footzone there are fewer well marked river courses. In the savannah zone, the rivers are meandering and incised about ten to twenty metres into the plateau, and most tributaries are ephemeral.
In accordance with the climate of the area, the **discharge regime** of the rivers is bimodal with peaks in April/May and November. The areas with the highest contributions to discharge lie in the moorland and upper forest zone, where precipitation is highest and evaporation is low. Water yield is in the dry season only sustained by the uppermost regions of the catchment with 10 – 50 mm. In the rainy seasons the upper forest and lower moorland zones yield around 300 mm or even more, while the contributions to surface flow lie around 60 – 150 mm in the lower forest zone and around 160 – 250 mm in the alpine zone (figures for the years 1983/84, taken from Decurtins 1992: 83ff).
From the point of view of **surface water availability** two main zones can be distinguished: the zone from the peak of Mt. Kenya down to the tarmac road (lower end of the footzone) which is well supplied with water, and the zone below the tarmac road characterized by low river density and less surface water.

2. 1. 6. 2. Groundwater

The springs around Mt. Kenya are clear evidence of an aquifer system. Actually two systems can be distinguished according to their geology: The sediments of the alluvial systems on one hand, and the fractured and weathered volcanic rocks on the other hand (NRM^3 2002b: 8).
The chemical properties of the groundwater have been investigated by Schotterer and Mueller (1985). With the use of isotopes they showed that most of the spring water in the area is more

than 30 years old. Only some springs in the forest and footzone area of Naro Moru and Burguret have younger water (residence times of a few years); Decurtins (1991) and Gathenya (1992), whose investigations deal with water balances of the Naro Moru river, agree that the upper forest and moorland zone with high precipitation and low evaporation are the recharge areas of this local groundwater system, and that most of it is discharged in the lower forest zone and footzone. The foothills and savannah zone have limited infiltration capacity; only very limited local flow systems exist. In variable depths old hyperthermal (around 30°C warm) groundwater can be found, that is also being tapped by boreholes on larger farms. Schotterer and Mueller (1985) point to the possibility that this water, which shows ^{14}C ages of 4000 – 10'000 years, might have accumulated under a different climatic regime and is not renewed under current conditions. This fact, the costs of exploitation and its too high content of mineral salts prevent this old groundwater reservoir from being a solution to water scarcity problems.

The subject of groundwater recharge and discharge areas is more extensively discussed in Section 5.

Flury stated in 1987 with view to the general water availability in the area: "The water resources (surface and subsurface water) are sufficient to cover the domestic needs of the people and their livestock. Minor garden irrigation may in some cases be possible. With some few exceptions, production must depend on rainfall only. Water conservation and harvesting methods should receive very high priority. Considering the water resources in the area, irrigated crop production is not realistic" (Flury 1987: 2).

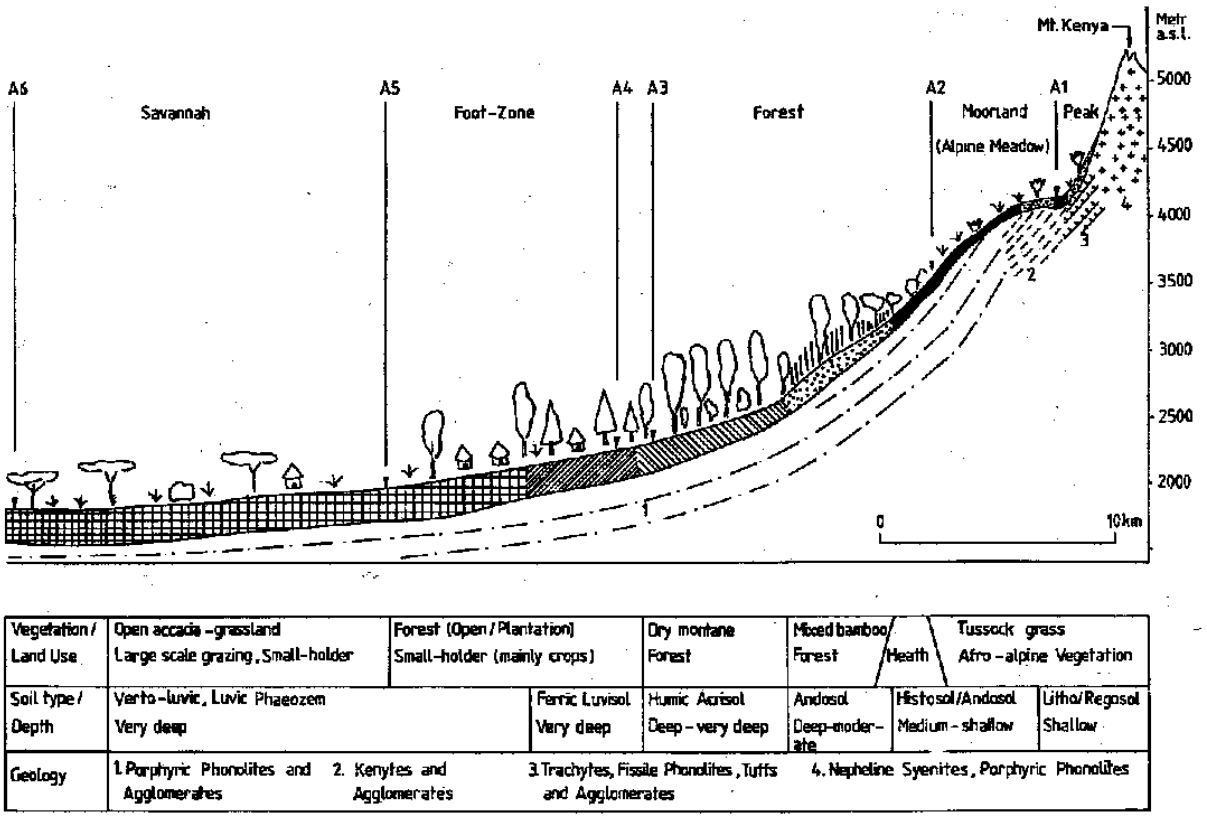

Fig. 2.9: Profile of Mt. Kenya West: Land Cover, Soils, Geology, and Ecological Zones (Source: Liniger 1992: 367).

2. 2. SOCIO-ECONOMIC SETTINGS

2. 2. 1. Population growth and immigration

The Upper Ewaso Ng'iro Basin today is divided into the administrative districts of Meru, Nyeri (Eastern Province), Laikipia, Samburu and Isiolo (Central Province) and Nyambene (Rift Valley Province). The study catchments belong to Nyeri district in their upper part, down to the Nyeri – Nanyuki tarmac road, and their lower part belongs to Laikipia.
The socio-economic situation in the area is characterised by rapid land use transition due to subdivision of former large-scale ranches and subsequent immigration of peasant households from the high-potential areas of Kenya (Wiesmann 1998: 17). This results in very high and continuous population growth and pressure on natural resources.

In pre-colonial times, the savannah of the Laikipia plains between Mt. Kenya and the Aberdares was used as grazing land by semi-nomadic Masai pastoralists. The agriculturalist tribes of the Kikuyu, Embu and Meru inhabited the moister Southern and Eastern slopes of Mt. Kenya. Lord Delamere, who came to the Laikipia plains in 1898, noticed that the Laikipia plains were unoccupied, since the Purko Clan of the Masai had annihilated the Laikipia clan. In 1902 the Purko Clan occupied the Plains but at the same time the British government already carried out a survey in order to prepare Laikipia for white settlement. In 1910 the Masai were moved out on the grounds of a dubious contract "to protect the forest from their burning activities" and white settlers were allocated land in the area (Decurtins 1992: 2). It was a basic misunderstanding by the British at the beginning of the colonial era that unoccupied land belonged to no one (and could thus be taken for settlement), ignoring the fact that in reality the indigenous tribes had very meticulously subdivided all land among themselves (Kenyatta 1965).

In the colonial era huge ranches were established in the so-called "White Highlands". While the Masai pastoralist economy had used very little water – basically the perennial streams and rivers were essential for livestock watering and human consumption only – the white ranchers began to dig the first furrows for irrigation. Their agriculture was still very extensive, however, due to the huge sizes of the properties, and did not put much pressure on water resources.

After Kenya's Independence in 1964, many of the ranches, starting at the moister slopes of Mt. Kenya, were either taken over by the government or sold to private land-buying companies. Subsequently they were subdivided into small plots of 0.5 to 5 ha and sold to small-scale farmers that were driven out from their high-potential homelands in the fertile highlands in the South and Southeast by population pressure. This triggered heavy and continuous immigration. The population of Laikipia district rose from approximately 30'000 in the early 1960's to 250'000 in 1989, which equals an annual growth rate of 7 – 8 % (Wiesmann 1998: 93).

Today the footzones and an expanding area in the savannah zone around Mt. Kenya and the Aberdares are characterized by small-scale agriculture. Ethnically mostly Kikuyu (almost 90%) and Meru (around 7%, Wiesmann 1998) live in these areas. The central part of Laikipia with very low water availability still largely belongs to white large-scale ranchers. Masai continue to live in Mukugodo division and further down in the lowlands.

2. 2. 2. Water scarcity and associated conflicts

Water scarcity is a main issue in the development of the Upper Ewaso Ng'iro Basin. The river flows at Archer's Post show a clear decreasing trend since 1970. The Ewaso Ngiro has since dried up for a stretch of up to 60km upstream of Buffalo Springs in 1984, 1986, 1991, 1994, 1997 and 2000 (Gichuki et al. 1998: 21). But also some of its tributaries, like Naro Moru, have started to fall dry – in July 2002 the riverbed downstream from the Kenya Railways Bridge was dry except for some pools.
The water scarcity is clearly primarily caused by increasing water demand. Rapid population growth combined with the transformation of the land use into small-scale farming and the development of urban centres (like Naro Moru and Nanyuki in the study catchments) is putting heavy pressure on water resources. Many irrigation schemes, dams and boreholes already existing on the formerly white farms suffered degradation after the transformation to small-scale farms, widening the gap between supply and demand even more.
Many of the migrant farmers are not organized socially or politically. Without organization and without financial resources it is impossible to maintain or build functioning water supply schemes. So the water demand is primarily centered on the perennial rivers, which represent the most easily accessible and reliable source of water (Wiesmann 1998: 93ff).

Water scarcity results in conflicts. Gichuki et al. (1998b: 23) identify three main types of conflicts associated with water scarcity in the region:

- Upstream vs. downstream conflicts: the principle of "first come, first serve" is applied. The first to suffer are the Masai pastoralists in Samburu who rely on the Ewaso Ng'iro as water source in the dry seasons. When the rivers fall dry they are forced to move upstream with their herds, resulting in conflict potential with the agriculturalists when they reach the farming land. Conflicts take place also among the small-scale farmers along the tributaries, when there is no water anymore for downstream users.
- Conflicts among members of water supply projects: water shortage that tail-enders are suffering from has in the past resulted in political struggles in communities, vandalizing of water supply installations, and even a high-school riot in Matanya. Latent conflicts due to inherent inequalities remain dormant until they are reawakened by crisis (Gichuki & Ngigi 2001).
- Water use vs. conservation of nature: The reduced river flows also have a negative ecological impact. Swamps and valuable wetland habitats are drained. The savannah animals lose their watering places. Ecosystems are damaged. A degradation of Samburu National Park as a generator of income could also have heavy economic consequences. Animals, like elephants, moving upstream in search of water destroy cultivated fields.

2. 2. 3. River water abstractions: development, types, distribution, water use

Since the late seventies the number of abstraction works for irrigation has been growing continuously and increasingly fast. The numbers given in Fig. 2.10 and 2.11 are valid for Naro Moru River, but are representative for the development along all perennial rivers. Most water is used for irrigation. Other principal water uses are livestock watering and domestic demand.

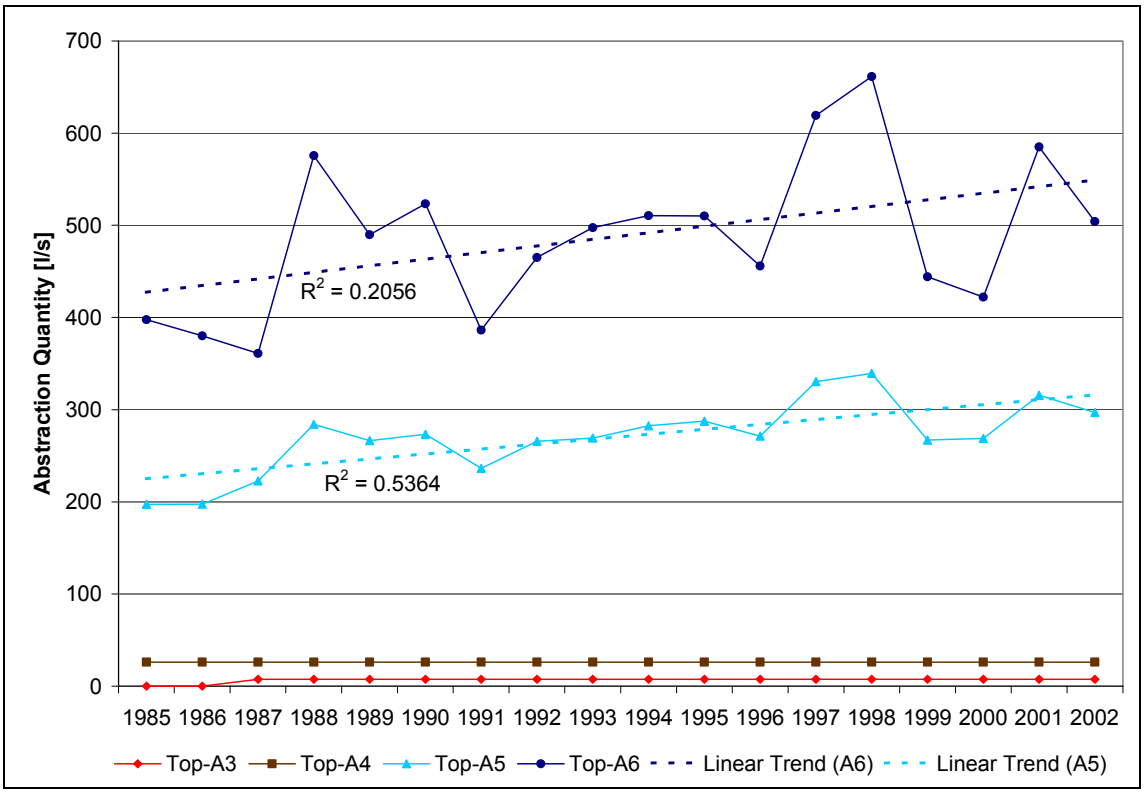

Fig. 2.10: Development of the quantity of abstracted river water in the four Naro Moru subcatchments A3 to A6 between 1985 and 2002 (Source: Aeschbacher 2003).

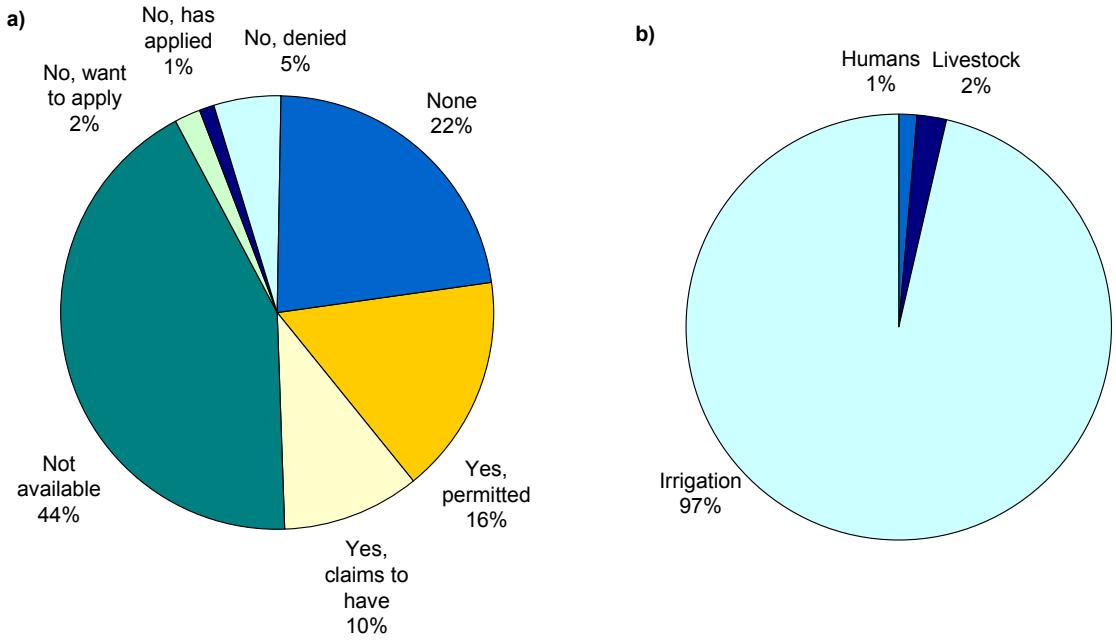

Fig. 2.11: a) Legal status of the abstraction points on Naro Moru in 2002. The largest proportion of water users does not have a permit. b) Principal water uses on Naro Moru in 2002: Almost all abstracted water is used for irrigation, domestic use and livestock watering only make up for 3% of the water use.

From interviews with farmers but also from evidence of abandoned fields in the lower catchment there is reason to believe that the peak of abstractions on Naro Moru occurred in

the year 2000. Falling market prices for agricultural produce, and maybe simply too little water in the river have caused some installations to have been abandoned in the meantime.

There are different types of abstraction works that can be associated with different zones along the rivers and also up to a certain extent with different social backgrounds.

- **Gravity pipelines** are dominant in the upper parts of the catchments. They require a certain slope in order to work, which is why they can only be installed in the steeper regions. Most of the intakes are situated in the lower forest zone. A weir dams the river, and the water is let through a filter chamber into the pipeline, from where it flows by gravity to reservoirs and fields. Due to the containment in a pipe and storage mostly in big covered tanks this technique is quite water-saving. On the other hand very large amounts of water can be abstracted by such a pipe (around 50 l/s), and not in all cases there is enough storage space, or water is distributed from the tanks to the members by unlined furrows. It is clear that the work effort and the financial requirements to install such a system are heavy. Only well-organized communities, sometimes with financial support from NGOs, can afford to build these systems. In the upper regions of the catchments generally community organization is better because the people have been living there for a longer time, and the better water availability leads to time and financial surpluses that can be invested. Gravity pipes are responsible for the greatest amount of abstracted water, although they make up a much smaller percentage of the number of abstraction points.

Fig. 2.12: The weir at the intake of Gitwe Water Project on Naro Moru North. The gravity pipe, with a sluice gate to control the flow, is visible on the left side (Picture by J Aeschbacher).

- **Furrows** are the oldest type of abstraction works. Some of them have been installed by the former white owners of the area and have continued to be used. Furrows usually belong to projects with several hundreds of members. Furrows can take a lot of water, depending on the water level in the river. The amount of abstracted water through a furrow can fluctuate between 0 and 200 l/s. In many cases the sluice gates are broken or inexistent, so there is no regulation. All furrows on Naro Moru are unlined (no lined furrow is known to the author from other rivers either), so there are great losses to seepage

Fig. 2.13: Aguthi Furrow in the Naro Moru A5 catchment (picture by B. Notter).

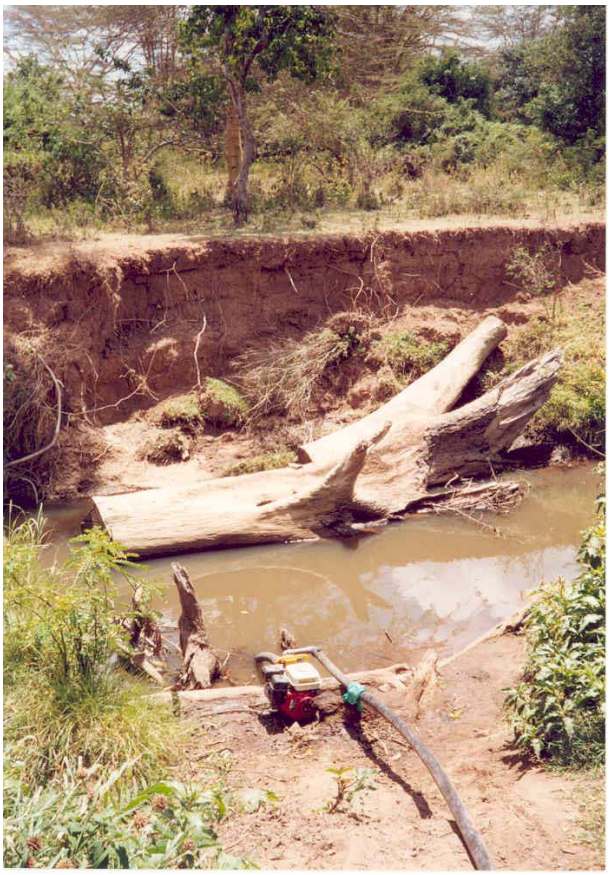

Fig. 2.14: A portable pump installed for irrigation in the savannah zone on Naro Moru river (picture by B. Notter).

and evaporation. The fine distribution to the project members often happens by the individual users digging their own side-canals or pumping from the furrow. Furrows exist in the upper as well as in the lower reaches of the catchments. Although they are few in number, they follow the gravity pipes closely in terms of the water amount abstracted.

- **Portable pumps:** This simplest way of abstracting water is mostly and increasingly used in the lower catchments, mostly by the least socially organized people with the poorest financial background. The pump can simply be placed by the river and connected with plastic pipes; then the fields are irrigated directly. In most cases there are no water storage facilities. Water losses are high with the so-called flood irrigation. In the lower Naro Moru catchment (savannah zone) a pump can be found almost every 100 metres along the river nowadays. But also in the footzone pumps exist. Some members of water project also started using

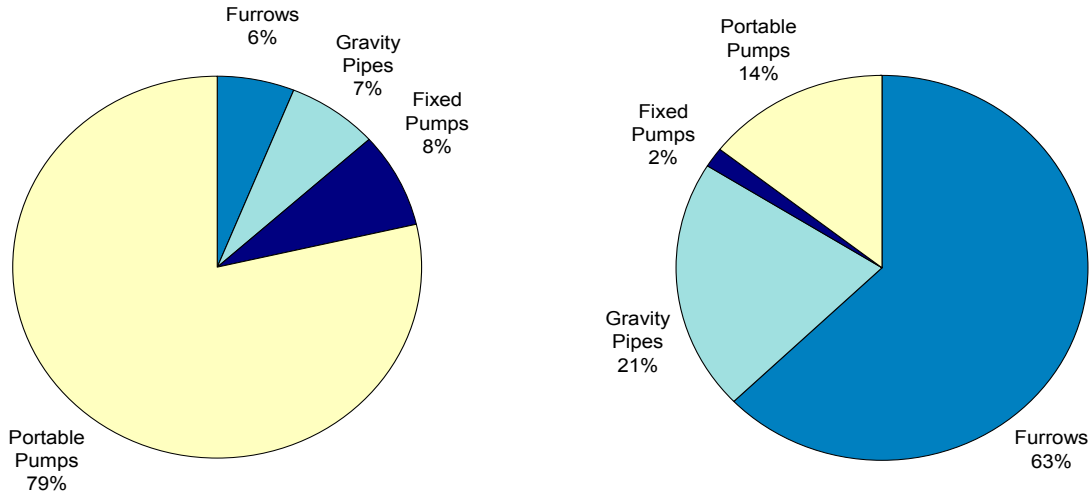

Fig. 2.15: Frequency and water use of different types of abstraction works: Although portable pumps make up 79% of all reported abstraction points on Naro Moru in 2002, they are responsible of only 14% of the total abstracted water amount. Furrows make up only 6% of the abstraction points but take up 63% of all abstracted water.

pumps when they didn't consider the supply through the project reliable anymore. Most pump abstractions are illegal and registered nowhere. Portable pump abstractions make up by far the largest number of abstraction works; but due to their small capacity, they take a much smaller proportion of the amount of water abstracted.

- **Other systems**, like fixed pumps, hydrams, or turbines, are rather rare. Fixed pumps are used for example by large-scale commercial irrigators like Vitacress, who pumps water out of Naro Moru with a large fixed pump to a dam in dry valley of the other side of the hill. Hydrams and turbines are mostly older installations that do not take much water per time period but operate continuously through the force of water and gravity.

2. 2. 4. Water management activities

2. 2. 4. 1. Governmental management

The solution of conflicts around water is not made easier by the existing legislation and administration of the water resources. There is a number of reasons for this:

- **Unclear and complicated legislation:** There is a number of boards, ministries and authorities that have a say in the allocation of water on different administrative levels. The Water Act, Cap. 372 of the Laws of Kenya, declares water as a common resource owned by the government. Highest priority is given to the use of domestic water. The MoWD (Ministry of Water Development), the practical authority to construct works and impose water rates, supports equity between water uses. The MARD (Ministry of Agriculture Development) on the other hand promotes irrigation for sufficient food production. Then there is the WAB (Water Apportionment Board) with the catchment boards at the basin level, the Water Resources Authority who is supposed to investigate and give advice, and a number of offices and authorities at the regional level. This causes insecurity about the legislation and so people do not take it serious anymore. The law with the highest respect among the people is the Chief's Act, a law that gives certain powers to the local chiefs, which are known by the people and generally have a positive impact (Gichuki & Ngigi 2001: 11).
- **Obstacles to complying with the law:** A water permit is needed to legally abstract water from a river. But from the moment one applies for a permit it can take years until it is issued. The catchment board, which issues the permits, meets once in two years for two days, and some farmers have been waiting for ten years or more for their permits. For the average small-scale farmer this procedure takes much too long and is too expensive.
- **Random allocation:** The amount of water permitted to abstract is most of the times determined by a single gauging at the site, regardless to the season or the discharge at the moment. It is not clear what "high flow" or "low flow" is. There is minimum consultation between up- and downstream district officers. This results in over-allocation of water in the upper reaches (Gichuki 2001: 8).
- **Lack of enforcement:** As abstractions along the rivers are rarely monitored by the Water Office (the district office of the MoWD), illegals are seldom detected. Penalties for over-abstracting are very low and do not prevent the farmers from taking more water than they are permitted
- **Administrative Boundaries:** The administrative boundaries do not follow the catchment or basin boundaries but often divide drainage units. Naro Moru, Burguret and Nanyuki Catchments for example belong in their upper part to Nyeri and in their lower part to Laikipia district. There is a strong need for an inter-district agreement on water resources.

2. 2. 4. 2. River Water Users Associations (RWUAs)

To face the water shortage, in the past years a self-help movement has been taking place with the formation of River Water Users Associations (RWUAs) in some of the catchments of the Ewaso Ng'iro tributaries. They are relatively new in the management of water resources in the region. The need to increase community participation has been addressed in various forums concerning water scarcity, and has triggered the formation of the Ngare Nything RWUA in 1997, the Ngushishi and Upper Naro Moru RWUAs in 1998, the Likii and Burguret RWUAs in 1999 and the Nanyuki RWUA in 2000. The Ontulili and Sirimon RWUAs are in their formative stages.

Their objectives are:

- to promote legal water use activities that recognize the needs of all communities relying on the river water
- to enhance co-operation between water users, government agencies, national park staff, and scientists; create awareness of the water scarcity;
- to monitor water resources
- to try to ensure a fair distribution of the water resources.

The scope of the associations can wide depending on what level of water management the members want to achieve (NRM^3 2002: 6).

NRM^3 has assisted the RWUAs in their formation and is supporting them with a data and knowledge base for decision-making. From time to time workshops are organized that bring together the stakeholders in water-management in the Upper Ewaso Ng'iro Basin.

The lack of knowledge or data and the difficulties in communication are not the only obstacles to the solution of water scarcity. It is also the attitude of people towards water that complicates things. Some problematic attitudes and resulting feedbacks are:

- Water is still seen as a free resource. People do not want to pay for water or the costs to install and maintain supply works. This way water use fails to generate the funds necessary for its management.
- The former white settlers were allocated generous shares of water, because demand downstream was low. There was no need to maintain furrows in a good state. The present small-scale farmers have adopted this attitude in a way, saying that the pastoralists downstream use the water less efficiently anyway.
- Among the large-scale horticulturers also the attitude is prevailing that they are using the water most efficiently. And, with the water supply in the rivers becoming less and less reliable, they are also less ready to invest in supply schemes.

2. 2. 5. Land use changes

A series of land use change trends can be observed in the Upper Ewaso Ng'iro Basin that are closely linked to the socio-economic developments:

- **Conversion of savannah to cropland:** The subdivision of the large-scale ranches to small-scale farms has brought an enormous intensification of agriculture. In the footzone[1] of Mt. Kenya and the Aberdares cropland has almost doubled between 1984

[1] Note that with "footzone" not the ecological zone described in Section 2. 1. 3. is meant here, but a larger zone downwards extending in the ecological savannah zone and occupying more or less the upper half of Laikipia. See Niederer (2000) for details.

and 1995 at the expense mainly of grassland and grassland with trees (Niederer 2000: 91).

Fig. 2.16: Slashing acacias for the production of coal in order to generate some cash income is a common practice with the irrigation farmers along the savannah stretches of the rivers (Picture by B. Notter).

- **Conversion of forest to cropland:** Natural forest has in the same time lost one tenth of its area. This happened on one hand in the lower river reaches, where much of the alley vegetation had to give way to the farms along the rivers, resulting in riverbank erosion. On the other hand illegal clearings in the mountain forest zone were increasing up to 1998, when a change of policy allowed Mt. Kenya National Park to protect its area by force.

- **Conversion of wetlands to cropland:** Thenya et al. (2001) warn that with no intervention wetlands will have disappeared from the area in few years. This has mainly ecological impacts because the swamps are refuges to animals in the dry season, but also hydrological consequences (loss of the sponging effect of wetlands at floods), and the resulting cropland will rapidly decrease in fertility because of the oxidising soils.

- **Expansion of urban areas:** Urban areas have increased by 300% between 1984 and 1995 (Niederer 2000: 91).

- **Conversion of natural forest to plantation forest:** Under the rotating shamba system continously areas of forest are cleared, while others are replanted. As a consequence natural forest is increasingly replaced by plantation forest with exotic species such as eucalyptus or pine.

3. THEORY

3. 1. THE HYDROLOGICAL CYCLE AND PROCESSES IN RIVER CATCHMENTS

The constant turning over of water in the biosphere by the sun as the driving force is called the hydrological cycle. The elements of this cycle and the processes in river catchments shall be described in this section before getting into their representation in hydrological models in the next sections.

The sun makes water **evaporate**. Evaporated water rises with the air and as the air cools down due to pressure reduction, the relative humidity of the air rises. This eventually results in cloud formation and **precipitation**. When rain or snow falls on a catchment, it may be first **intercepted** by a vegetation cover. The remaining water falls on the ground. According to the structure of the ground a part of the incoming water flows off on the surface to either directly reach a water body – forming direct **runoff** or to **infiltrate** in another place, which is called **runon**. The infiltrated water in the soil is then subject to further processes: It may be sucked in by plants and **transpirated** from their stomata. It may be evaporated directly from the ground. It may **seep** deeper into the soil, contributing to a **groundwater store**. It may also **flow laterally**, maybe following preferred subsurface flowpaths, like **macropores**. Eventually, groundwater will form the **baseflow** contribution to a stream, unless **deep seepage** removes it for indefinite time from the hydrological cycle – for months, years, centuries, millions of years or forever. Of course there are also other **stores** for water – for example ice, snow, or lakes.

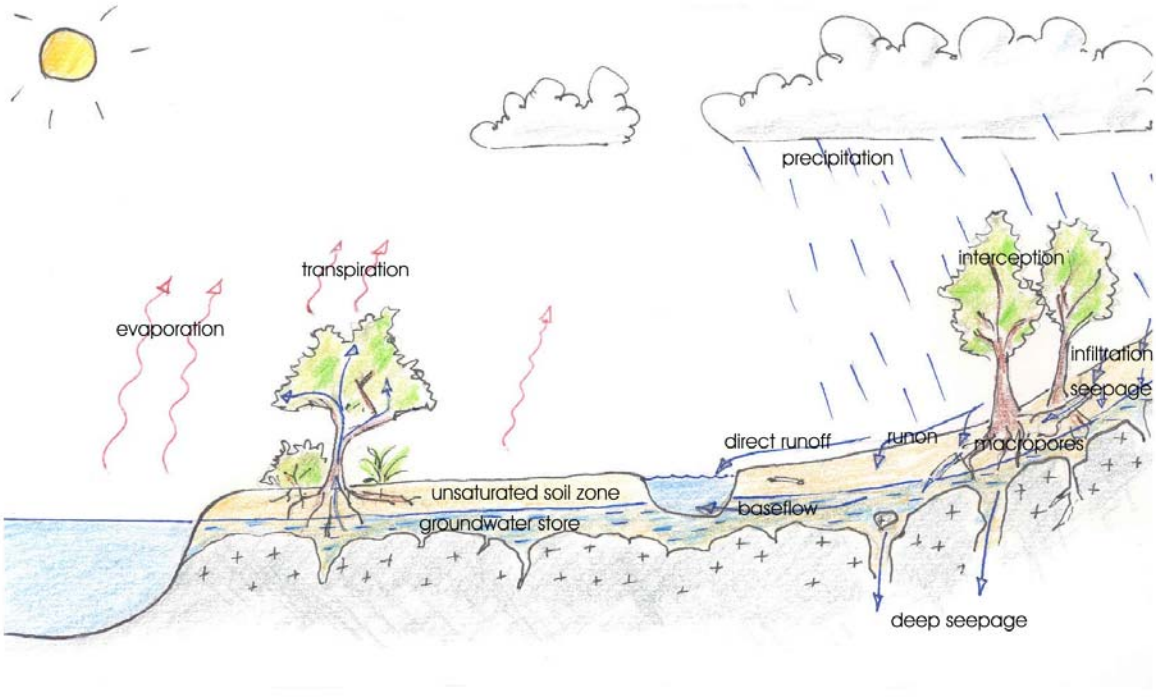

Fig. 3.1: The hydrological cycle and processes in river catchments.

It can be said that when looking at a river catchment as a system, the amount of incoming water must equal the amount of outgoing water plus or minus the difference in the water amount that is trapped in stores. This is mathematically formulated with the water balance equation:

$$Q + ET = P \pm \Delta S \qquad (3.1)$$

With Q = runoff
ET = evapotranspiration
P = precipitation
ΔS = changes in the stores

The water balance equation is the mathematical foundation for hydrological modelling.

3. 2. HYDROLOGICAL MODELLING IN PAST AND PRESENT

Hydrological models are numerical representations of the processes in river catchments. Today they mostly take the shape of computer programmes that calculate values of discharge and/or other elements of the hydrological cycle from a catchment, given time-series inputs of meteorological variables and information on the catchment characteristics.
Hydrological models are mainly used for two reasons (Beven 2001: 1):

a) the more practical reason is to overcome the limitation of not being able to measure all hydrological information of interest. Models allow to extrapolate existing knowledge in space, by applying them to ungauged catchments, and in time, by making projections into the future.
b) The more scientific reason is that a model assembles the knowledge on hydrological processes in a neat package. When model outputs are compared to reliably measured variables, conflicts between theory and reality will show.

The earliest approach to hydrological modelling was made in 1851 by Thomas James Mulvaney, an Irish Engineer who wanted to estimate maximum flood flow for constructing bridges. The "Rational Formula" he came up with had the form

$$Q_p = CAR \qquad (3.2)$$

Where Q_p = peak runoff
R = rain
A = area of catchment
C = "runoff coefficient"

This simple formula already contains the principal ideas of hydrological modelling: An output flow variable (here the peak flow) is calculated from input information on meteorology (rain) and catchment characteristics (catchment area and a "runoff coefficient" summarizing the response of the catchment) (Beven 2001: 25).
Ross in 1921 made the first attempt in distributed modelling: A catchment is divided into different units that are expected to show homogenous hydrologic responses by their surface characteristics and travel time of the water to the catchment outlet.
A next big step was the introduction of the Unit Hydrograph by Sherman (1932) who tried to quantify the amount of discharge that one unit of precipitation produces in a catchment. The

principle of superposition could then be applied (if one unit of rain produces y discharge, then x units will produce xy discharge). Many models have since been built on this principle, since it also allowed to account for the time lag of water arriving from more distant corners of a catchment (channel routing). But it also raised the question of hydrograph separation: How do you determine the amount of discharge produced by one unit of rain if measured discharge at a site not only consists of the direct runoff from the present storm but also from the baseflow caused by earlier storms?
The first digital computer models arrived on the scene in the early 1960's with the Stanford Watershed Model by Crawford and Linsley. In the first years computing power was the limiting factor, but on the other hand almost every hydrologist with access to a computer began to develop his own model. In this time the first ESMA type models ("Explicit soil moisture accounting" models – lumped models including the calculation of soil moisture over time) were developed, an approach that also later in combination with semi-distributed models has proved quite successful (the NRM^3 Streamflow Model can also be counted to this category).
In 1969 Freeze and Harlan introduced the first distributed process description based models. They gave the possibility of defining parameter values for many elements and processes, but also led to the restraint of difficult calibration and validation. Their attraction lies not only in the simulation of processes that affect only part of a catchment and the feedback of processes within a catchment, but also in the possibility of building as much understanding of processes as possible into a model.
Today computer power allows more and more complex modelling. The linking of hydrological models with Geographical Information Systems (GIS) has allowed to include big amounts of information on catchment characteristics in ever-increasing resolution with little effort into models. The development of supporting software is sometimes faster than the development of the hydrological models themselves. But more complexity always means more parameters, more calibration, and increased uncertainty in predictions, particularly outside the calibration range of a model. Simple models still have a lot to offer. In essence, hydrological modelling is still mainly limited by the available measured data (Beven 2001: 45).

3. 3. DEVELOPMENT AND TYPES OF HYDROLOGICAL MODELS

Models are always a simplified representation of reality – there is no model that can do everything and that can be used universally (Spreafico 2.1)!

Generally the hydrological models available today can be categorized in two dimensions: The first dimension is whether a deterministic or stochastic approach is chosen. A deterministic model produces a single outcome for one set of input data and parameter values, whereas a stochastic model produces an outcome accounting for randomness and uncertainty of the predictions.
The second dimension is the extent to which a model goes into details: We distinguish between so-called "lumped" and "distributed" models. In a lumped model the catchment is represented as a black box that is assigned certain characteristics according to which the uniform response of the catchment to an incoming rainfall is determined. A distributed model calculates the water balance for each gridpoint in a catchment according to its actual physical properties.
Of course the transitions between the types of models are gradual: Some deterministic models add stochastic error to outcome, and some stochastic models make predictions in a

deterministic way. The transition between lumped and distributed models is gradual – Hydrological Response Unit (HRU) models (like the first version of the NRM^3 Streamflow Model) for example work like lumped models but allocate the "black boxes" on the level of (assumingly) homogenous parts of a catchment, and most (if not all) grid-based models must use average values and parameters at a scale greater than the scale of the actual processes ("semi-distributed" models).

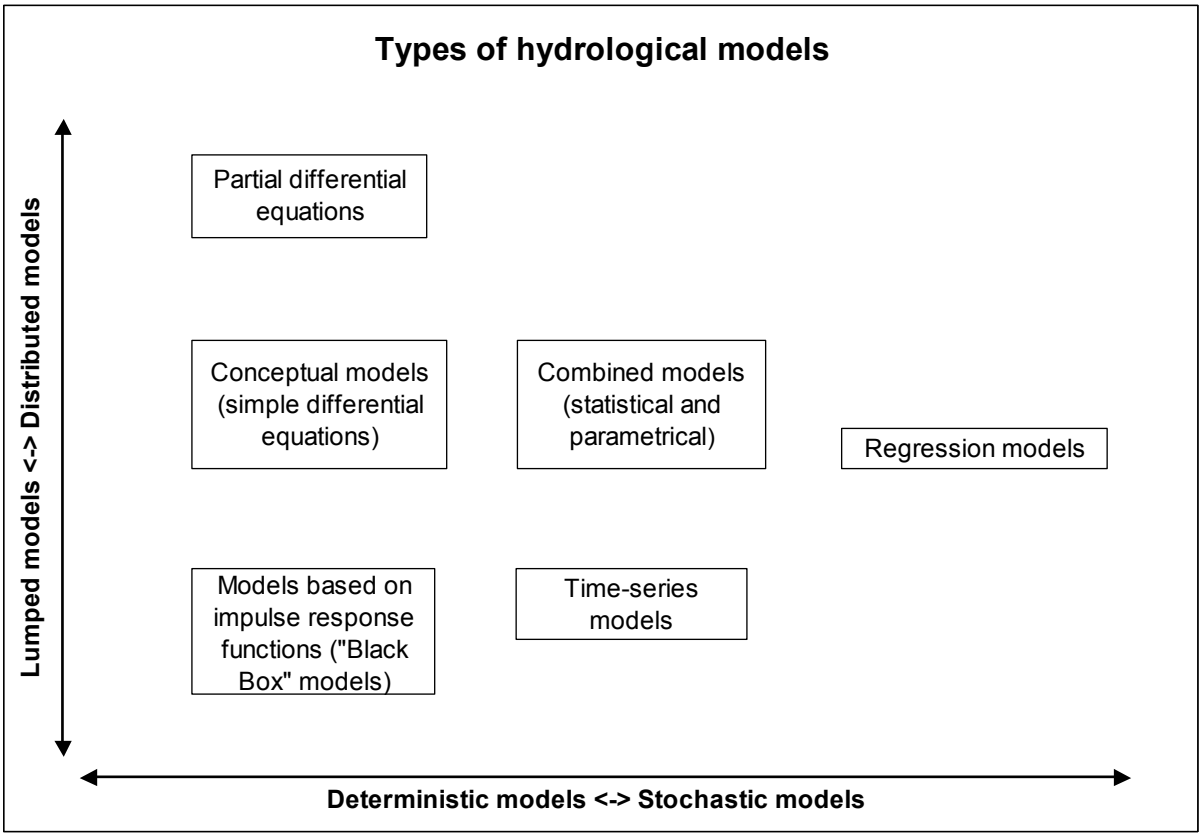

Fig. 3.2: Types of hydrological models categorized according to the mathematical approach (deterministic/statistic) and the level of detail (lumped vs. distributed models) (Source: Spreafico 2000: 1.4)

Beven (2001: 3ff) distinguishes five steps in the development of hydrological models, the first three of which are not part of this study but are important to be reflected in order to comment on the validity and reliability of the results:

1) Development of a perceptual model: the hydrologist developing the model decides, with his perception of processes in a catchment, which processes are to be modelled in which way. The resulting decisions are necessarily personal to a certain degree.
2) Development of a conceptual model: the mathematical formulation of the processes.
3) Development of a procedural model: getting the program code to run on a computer
4) Model parameter calibration
5) Validation and evaluation of the predictions

There are different practical and scientific criteria that influence the development or the choice of an appropriate model structure. Spreafico (2000: 2.1) categorizes them as follows:

- Model structure as a function of the goal of the study: Which variables are the ones of primary interest (peak flows, low flows, average runoff)? What kind of answer is looked for, and how accurate does it have to be?

- Model structure as a function of resolution: On which spatial and temporal scale do the processes take place that we are interested in?
- Model structure as a function of catchment characteristics: What is the size of the catchments, and which processes do take place or are dominant? (for example, snow melt is not of primary importance in a tropical catchment but surely is in boreal climate)
- Model structure as a function of available data: For which meteorological variables do we have existing, long-enough time series? In what resolution do we have information on catchment characteristics like topography, land use, etc.?
- Model structure as a function of process knowledge: What do we know about the processes involved?
- Model structure as a function of available means: How much money do we need or have? How much time? Can we meet software requirements?

The choice of the NRM^3 Streamflow Model to be used as a potential tool for water management and impacts assessment in the Upper Ewaso Ng'iro Basin is on one hand very much based on the above criteria. It has been developed in order to be run with the available rainfall and pan evaporation data and with the available GIS information in the NRM^3 database. Its development has been carried out with the available funds. It is intended for the modelling of small to middle-sized catchments. For others of the above criteria there are question marks – is the model appropriate for meso-scale perennial catchments? Is its performance good enough to be used in water management or impact assessment? Can it be run flexibly enough with the software available? – It is also a goal of this study to determine if these criteria are met by the NRM^3 Streamflow Model.

3. 4. THE NRM^3 STREAMFLOW MODEL

The NRM^3 Streamflow Model is a conceptual, semi-distributed, three-layer water balance model which runs on a daily time-step. The spatial resolution can be chosen by the user. It needs precipitation and pan evaporation as time-series input data; further required information is soil type and soil depth, water capacity and infiltration properties, and land use respectively associated crop coefficients. The separation of incoming precipitation into surface runoff and infiltration is based on the U. S. Soil Conservation Service Curve Number method (USDA SCS, 1985). In principle, the model is also suitable for ungauged catchments. The original model version developed by Thomas (1993) used the Hydrological Response Unit (HRU) as basic unit to calculate water balances. Mike Thomas and Lindsay McMillan introduced as main development the use of a grid in which for each cell the water balance is calculated (McMillan 2003).

3. 4. 1. History and theory of the US SCS Curve Number Method

The US SCS curve number method was developed in the late 1940's and early 1950's as a low-cost method for estimating floods of a selected return period from a given rainfall, for the design of small-scale civil engineering structures (brigdes, drainage systems, soil conservation terraces etc.). Its simplicity is at the same time the source of its historical success and its limitation.

The basic idea of the Curve Number Method is that as P (precipitation) tends to infinity, P-Q (retention, Q being discharge) asymptotically reaches a constant value S. So S is the potential

retention, i. e. the maximum amount of water that can be absorbed by the catchment in a storm (McMillan 2003).
Proportionality is assumed between retention and runoff: The relation of potential to actual retention equals the relation of discharge to rain.

$$(P - Q)/S = Q/P \quad (3.3)$$

In reality, an initial amount of rainfall will be lost to interception, surface ponding and infiltration before runoff is generated. Introducing these losses as I to equation (3.3) results in:

$$(P - I - Q)/S = Q/(P - I) \quad (3.4)$$

which can be rearranged in terms of Q, yielding the SCS runoff equation:

$$Q = (P - I)^2/(P - I + S) \quad (3.5)$$

In order to simplify the equation, a linear relation between I and S was assumed based on empirical studies in small catchments:

$$I = 0.2S \quad (3.6)$$

And the SCS runoff equation becomes

$$Q = (P - 0.2S)^2/(P + 0.8S) \quad (3.7)$$

(when $P > 0.2S$; otherwise $Q = 0$)

For convenience, S was converted into a dimensionless parameter CN, the curve number:

$$S = 25'400/CN - 254 \quad (3.8)$$

(when P and Q are expressed in mm)

This results in a set of curves relating rainfall to runoff for different Curve Numbers (see Fig. 3.3). In theory the Curve Numbers range from 0 to 100, but in practice values have been narrowed by experience to the range 40 – 98 (McMillan 2003).

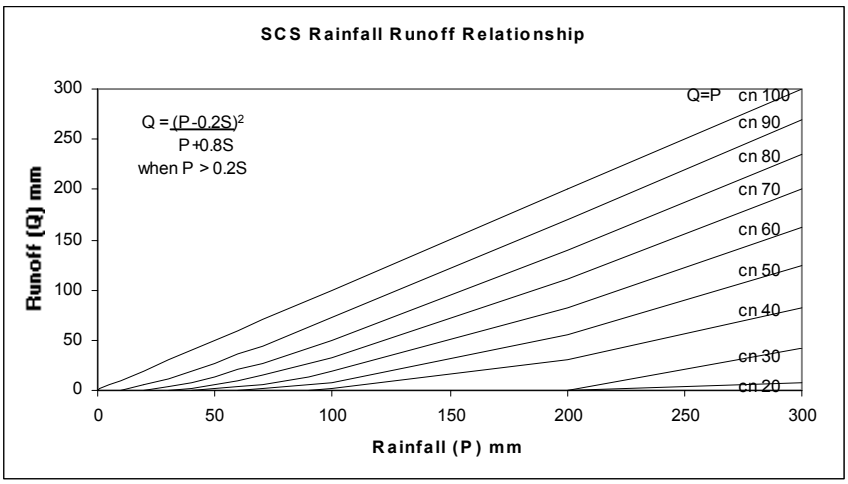

Fig. 3.3: SCS Rainfall Runoff Curves (Source: McMillan 2003)

It has been subject to much discussion how exactly the Curve Number method was developed and which processes of runoff generation it describes.
McMillan (2003) notes that no complete account of the method's origins is available to date. According to Beven (2001: 30) it can be traced back to the analysis of rainfall and runoff by Mockus (1949) in many small US-midwestern catchments from which the hydrologic soil group, land use class and surface condition were known. The data from each catchment were plotted as P in the abscissa and Q in the ordinate, and the curve number corresponding to the line separating half of the plotted data from the other half was taken as the median curve number for the catchment.
The curve numbers can be regarded as representing various processes and catchment characteristics:

- **Land use and soils:** In combination with the SCS hydrologic soil group classification (assigning all soil types to four groups according to their drainage characteristics) the Curve Number method has extensively been used to estimate surface runoff from ungauged catchments given the land use or treatment class, as for example described in the SCS National Engineering Handbook (USDA SCS, 1985).

- **Antecedent Catchment Conditions:** The scatter in rainfall-runoff plots suggests that in reality a catchment would have more than one curve number. This can be related to the antecedent moisture status of a catchment. Various methods of adjusting the Curve Numbers to dry, wet and average antecedent conditions have been proposed (USDA SCS 1985). Doing this can be an advantage but it means again to use empirical parameters without physical justification (Beven 2001: 205). The example of the Upper Ewaso Ng'iro Basin shows one of the problems: In the proposed methods of relating CN's to antecedent conditions it is assumed that wetter conditions will produce higher curve numbers (less storage space in the catchment). Modelling experience in the Upper Ewaso Ng'iro Basin, however, has shown that after long dry periods direct runoff is often underestimated because of the soil's tendency to form a crust which results in higher surface runoff.

- **Infiltration processes:** It is widely said that the CN method represents Hortonian overland flow as runoff-generating mechanism, a saturation-excess on hillslopes. On the other hand this would mean that it could not be used in forested areas where subsurface stormflow tends to be the dominating mechanism (Beven 2001: 12). It is agreed by most authors, however, that the method is only an approximation of the infiltration process.

Generally it can be said that the Curve Number method is a purely empirical method lacking physical justification. It "incorporates some empirical knowledge of fast runoff generation, by whatever process, at the small catchment scale" (Beven 2001). Its choice by many hydrologists (see Table 3.1 for other hydrological models making use of the method) is based on its simplicity and the fact that it repeatedly fits the selected data well.

Some issues have to be taken into consideration when using the Curve Number Method within a model for continuous daily streamflow prediction in meso-scale catchments in East Africa, since this is a significant change from the method's original intended use. There are three main concerns (McMillan 2003):

- The transfer of a design flood event based methodology to a model for continuous streamflow prediction: This has been done before successfully with other models (see

also Table 3.1). The appropriate modifications include the introduction of evapotranspiration loss and soil water balance modules, which are also present in the NRM^3 Streamflow Model.

- The transfer of curve numbers based on flood series in the Midwestern US to Kenya: Despite the method being designed for ungauged catchments, it would be imprudent to transfer the curve numbers to other regions of the world without testing it there against measured discharges. The studies of Thomas (1993) and McMillan (2003) with the NRM^3 Streamflow Model have shown that the method – with curve numbers specially assigned to Kenyan land use classes can be applied in Kenya.

- The scale issue: Originally the curve number method was intended for small catchments. Some modellers have more or less successfully tested it in large basins, however, for example with SWRRB in rural basins in the USA or in a 263 km^2 arid basin in India (Sharma and Singh 1992, cited in McMillan 2003). The original version of the NRM^3 Streamflow Model was tested on the decadal time-step in Naro Moru catchment yielding r^2 values of 0.7 – 0.83 (Thomas 1993). Its present version has been calibrated and validated on the daily time-step in the small catchment of Mukogodo.

Models which use the SCS Curve Number Methodology	
AGNPS	Agricultural Nonpoint Source Model (Young et al. 1995)
CREAMS	Chemicals, Runoff and Erosion from Agricultural Management Systems (Knisel 1980)
EPIC	Erosion, Productivity Impact Calculator (Williams 1983)
GWLF	General Watershed Loading Functions (Haith and Shoemaker 1987)
PERFECT	Productivity, Erosion, Runoff Functions to Evaluate Conservation Techniques (1989)
SPUR	Simulation of Production and Utilisation of Rangelands (Wight and Skiles 1987)
SWAT	Soil Water Assessment Tool (Arnold et al. 1998)
SWRRB	Simulator for Water Resources in Rural Basins (Williams et al. 1985)
TAMS	Tibbetts-Abetts-McCarthy-Stratton (Kenya National Water Plan, 1980)
WEPP	Water Erosion Prediction Project (1991)

Table 3.1: Models that use the SCS curve number methodology (Source: McMillan 2003; authors cited in McMillan 2003)).

3. 4. 2. Model structure

The NRM^3 Streamflow model conceptualises the hydrology of a catchment as a population of soil stores represented vertically by three layers and horizontally by HRUs (original model version by Thomas 1993) or a grid (present model version by McMillan 2003). For each unit, daily water balances are maintained with mathematical equations describing the fluxes between the stores. Being fully distributed at the surface, semi-distributed in the unsaturated zone and lumped in the saturated zone, it can be described as a semi-distributed model. Required input data are daily precipitation and pan evaporation time series and seven GIS layers: catchment boundaries, topography, drainage network, soils, land use, rain gauges, and evaporation pans.
A list of parameters is given in Table 3.2. In total the model has 19 parameters. This seems like a large number, but in fact most of the parameters can be derived from measurements or

earlier calibration in the region. Only the four parameters influencing groundwater discharge should be subject to optimisation when applying the model to a new catchment.

STREAM1 Model Parameter Listing	
Stream Flow Simulation Parameters	
PTHRESH	Rainfall Threshold for Rainfall Files
ROCOEFF	Runon Coefficient (% Runoff going to adjacent d/s HRU)
R1COEFF	Groundwater Discharge Coefficient (Long term)
R2COEFF	Groundwater Discharge Coefficient (Short term)
SCOEFF	Deep Seepage Coefficient
SSZTH	Groundwater Discharge Threshold
NSD	Number of Soil Depths to be simulated
SLDEP(J)	Soil Layer Depths (mm) to be simulated
SDEPTH(I)	Total Soil Depth (mm) for each soil type
SCNGR(I)	Soil Curve Number Drainage Class (1-5)
SWC(I)	Soil Water Capacity (mm)
SCSCN(I,J)	Soil Curve Number for each US SCS Soil Group (refer to Section 4.1.5)
CSDEP(I)	Critical Soil Depth
KC(I)	Crop Coefficient
ROOTD(I)	Soil Root Depth
LEAFI = LINT	Daily Leaf Interception (mm) for each land cover category
ABSTR	Catchment Abstractions m3/day
CSLOPE	Average Catchment Slope (%)
HYDLEN	Hydraulic Length of Stream along main channel (m)

Table 3.2: NRM³ Streamflow Model parameters (McMillan 2003)

The simulation of a hydrological day can be described as follows (McMillan 2003 – see also Appendix C. 1. for a summary of the simulation process):

The model operates on the basis of the **water balance**. For any grid cell

$$P - ET \pm \Delta S = Q \qquad (3.9)$$

is maintained (see also Section 3.1; P = precipitation, ET = evapotranspiration, Q = discharge, ΔS = changes in stores).

At the start of the day (prior to rainfall) actual **evapotranspiration** (ETK) is computed. For each grid the nearest three precipitation pans are determined and the closest for which data are available is used as the potential evaporation (ETP). This is then modified according to interception (ILOSS), the crop coefficient (KC) of the land use on the cell, the soil moisture (SMF) in the critical soil depth and a pan coefficient (KPAN) that allows for the use of different types of pans:

$$ETK = (ETP - ILOSS) * KPAN * KC * SMF \qquad (3.10)$$

The soil moisture factor replaces the 5-day precipitation index used in the original SCS method to account for the influence of catchment wetness on runoff generation. It is calculated as follows: The water available to plants (TOTWAT) is first calculated as a fraction (ALPHA) of the maximum possible (MAXWAT):

$$ALPHA = TOTWAT/MAXWAT \quad (3.11)$$

If 80% (= threshold THRESH) or more of TOTWAT are available, then SMF will be = 1. If less water is available, then SMF is:

$$SMF = ALPHA/THRESH \quad (3.12)$$

Precipitation is computed using the inverse distance interpolation technique to determine the rainfall over each grid cell: The two nearest rain gauges are determined and their rain amounts weighted inversely – i. e. the closer a gauge to a grid, the higher its weight.
Snow accumulation and melting is not simulated.

Interception is represented as a simple store. Intercepted water is assumed to evaporate, and potential evaporation is subsequently reduced by ILOSS (see above).

Direct runoff from a grid is determined using the SCS curve number method (described in the previous section). The base curve number (CNK2) for each cell is determined at the beginning of the simulation based on soil type and land-use category. In the day-to-day simulation loop, a final curve number (CNK) is computed modifying the base curve number according to soil moisture (TOTWAT). The lowest (CNK1) and the highest possible curve number (CNK2) are calculated according to Ponce and Hawkins (1996):

$$CNK1 = CNK2/(2.281 – (0.01821 – CNK2)) \quad (3.13)$$
$$CNK3 = CNK2(0.427 + (0.00573 – CNK2)) \quad (3.14)$$

A linear relation between CNK1 and CNK3 is then assumed based on the actual soil moisture (TOTWAT) and maximum soil moisture (MAXWAT):

$$CNK = (CNK3 – CNK1)*(TOTWAT/MAXWAT) + CNK1 \quad (3.15)$$

So the final curve number is lowest when the actual soil moisture corresponds to the maximum possible. Most water thus infiltrates into the soil when it is most dried out.

All direct runoff is assumed to leave the catchment within the day unless the **runon** routine is activated. This simple routine is intended to represent Hortonian overland flow which has been described by Thomas (1993) as a dominant process in the region. It lets surface runoff run on to downslope cells that still have infiltration capacity and be reinfiltrated there. This is why the flow paths have to be identified based on topography at the beginning of a model run: An order of the computation of cells is identified so that when it comes to calculating the runoff from the cells all upslope cells have already been computed.

The model writes GIS outputs for days on which one of the rain gauges records more precipitation than the threshold specified in the control file. These show from which cells how much direct runoff is generated.

The water not running off directly **infiltrates** into the soil.

The **unsaturated soil zone** is represented as a number of layers that can be set by the user; in this study, five layers are used. Infiltration enters the uppermost layer first and fills it to its field capacity before starting to fill the next lower level. If all layers become saturated, the excess flow percolates to the shallow saturated zone. Moisture is abstracted from the soil to meet the evaporative demand from the wettest layer first until it becomes as dry as the second wettest layer, then from both layers simultaneously and so on. The water balance for the unsaturated zone is maintained for each cell:

$$USZ_t = USZ_{t-1} + INF - ETK - PERC \quad (3.16)$$

Where USZ_t = moisture in unsaturated zone at the end of the simulation day
USZ_{t-1} = moisture in unsaturated zone at the end of the previous day
INF = infiltration
ETK = actual evaporation
PERC = percolation

No lateral flow is modelled in the unsaturated soil zone. Also preferential flow paths such as root holes or animal burrows are considered implicit in the method.

The **saturated soil zone** is represented in a lumped manner as a large single reservoir with water entering from all unsaturated soil columns. The daily groundwater discharge to the streamflow is determined by a two component linear model controlled by a threshold value. If the moisture in the saturated zone (SSZ) is less or equal to the threshold value SSZTH, then the slow groundwater discharge coefficient RCOEFF1 is used, otherwise the fast groundwater groundwater coefficient RCOEFF2 determines baseflow contribution (GWQ):

$$\text{IF } SZZ \leq SSZTHRESH \text{ THEN } GWQ = SSZ * RCOEFF1 \quad (3.17)$$
$$\text{IF } SZZ > SSZTHRESH \text{ THEN } GWQ = SSZ * RCOEFF2 \quad (3.18)$$

This is intended to reflect the contrast between higher groundwater contributions after rainy periods and lower contributions during dry periods.
A water balance is also maintained here:

$$SSZ = SSZ + SUMPCK - GWQ - GWAQR \quad (3.19)$$

Where SSZ = moisture in the saturated zone
SUMPCK = aggregated percolation from the unsaturated zone of all cells
GWQ = groundwater discharge
GWAQR = deep seepage

GWAQR is determined from the moisture in the saturated zone and a coefficient SCOEFF set by the user:

$$GWAQR = SSZ * SCOEFF \quad (3.20)$$

The **daily streamflow** as the main output variable is simply calculated as the aggregated direct runoff (SUMQ) and the aggregated groundwater runoff(GWQ) plus the total catchment abstractions for water use (ABSTR):

$$Q = SUMQ + GWQ - ABSTR \quad (3.21)$$

Note that in this study the abstractions were not set as a daily average in the control file as is intended in the model. As the abstracted amounts are significant and vary greatly between months and seasons, no abstractions were modelled but model outputs compared to a naturalised flow series. This issue will be described in more detail in Section 5.2.
Channel routing is absent from the model, which is no problem as long as streamflow reaches the catchment outlet within one day. This works for smaller catchments but is a drawback from modelling larger catchments as will be shown in Section 6.2.4.
The structure of the NRM^3 Streamflow Model is summarised in Fig. 3.4.

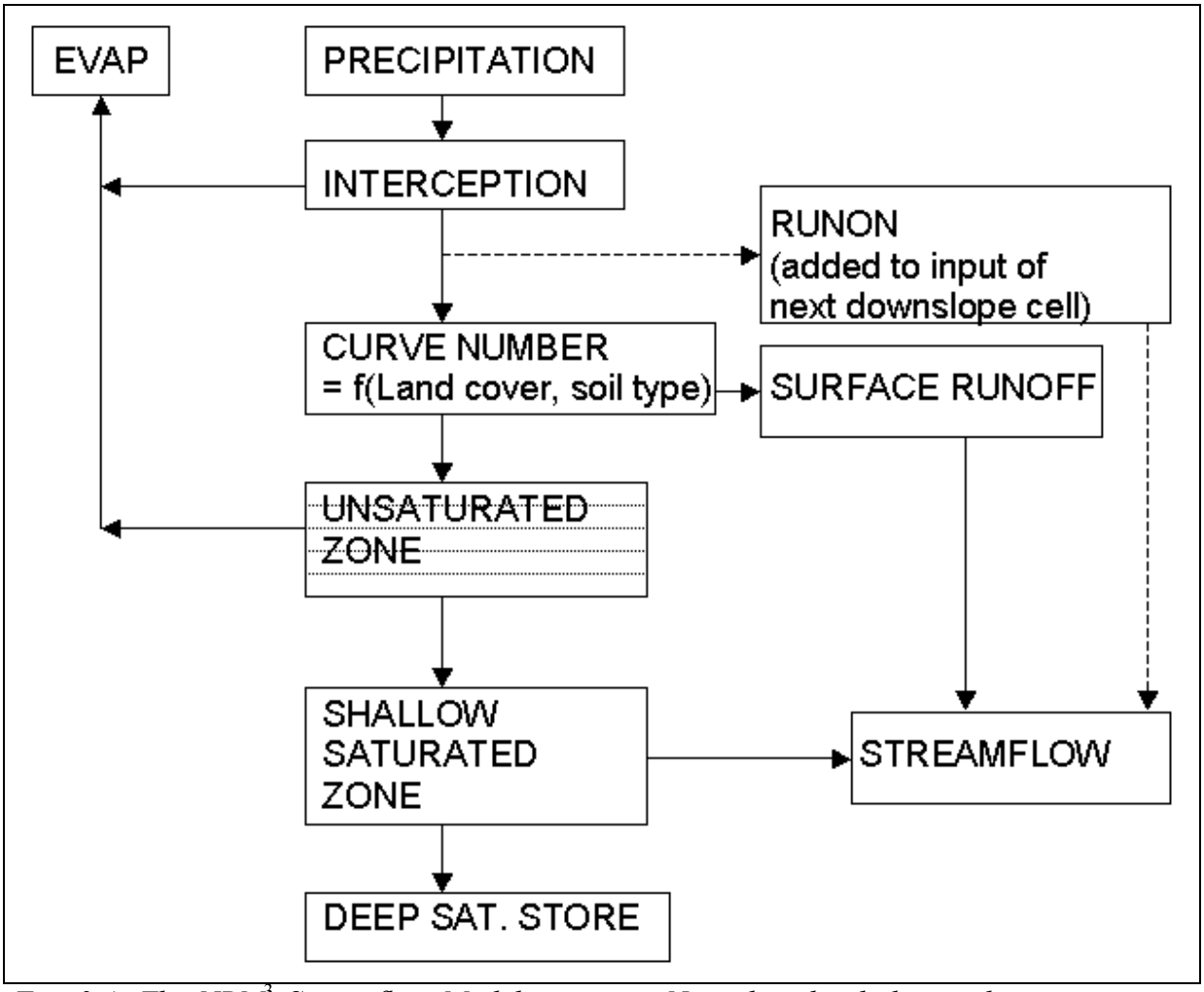

Fig. 3.4: The NRM^3 Streamflow Model structure. Note that the daily simulation routine is calculated for each cell separately down to the level of the unsaturated zone. The shallow saturated zone and the deep saturated store are represented in a lumped manner, i. e. averaged over the whole catchment.

3. 4. 2. Differences between Thomas (1993) and McMillan (2003) versions

Apart from the transition from using hydrological response units (HRUs) to using grid cells as the basic unit for calculating water balances some additional developments were made by McMillan (2003) that make her version differ from Thomas's (1993) original version. They are listed in Table 3.3.

Thomas 1993 version features	McMillan 2003 version features
• HRUs as basic unit for calculating water balances • Precipitation interpolation: Altitude instead of distance is inversely weighted • Snowmelt included • Weather generator within model	• Grid cells as basic unit for calculating water balances • Precipitation interpolation: Inverse Distance Weighting (IDW); inclusion of gauges outside catchments • Multiple evaporation stations • Dynamic curve number component (version stm4d) • Impact of crusting soils • Impact of cracking soils

Table 3.3: Differences between Thomas 1993 and McMillan 2003 versions of the NRM3 Streamflow Model

The most important developments by McMillan (2003) are:

- **The Dymanic Curve Number Component:** It was observed in the study catchment of Mukogodo that in the deterioration of the grass cover during long dry periods had a hydrological influence. To account for this a routine was developed to change curve numbers according to the long-term moisture status of the catchment. The identification of wet and dry periods is done outside the model according to the classification procedure described in Table 3.4 resulting in a series of wet, dry or average seasons (fixed months). These are listed in a season file. In a simulation run, curve numbers are then increased if the seasonal status is dry and decreased when it is wet. The Dymanic Curve Number Component is only included in McMillan's version stm4d (for this study also version stm2ci was used, the only difference between the two versions being the Dymanic Curve Number Component).

- **Impact of cracking soils:** cracking soils occur in the drier zones of the study region. They have a twofold effect: On one hand water can flow directly through the cracks bypassing the usual infiltration, resulting in lower surface runoff. On the other hand when the soil swells at wetting, the cracks are closed with impermeable swollen clays, increasing direct runoff. It was observed, however, that the second effect rarely takes place. In the model, crack flow is calculated as a proportion of incoming rainfall that flows directly to the deepest unsaturated soil zone layer. With more soil water available, actual evaporation is assumed to increase. Both factors have to be entered in the control file and have to be obtained from literature or by trial and error (McMillan 2003).

- **Impact of crusting soils:** Certain soils in the study region develop a hard, impermeable crust dependent on their vegetative cover, resulting in Hortonian overland flow and higher direct runoff. As a consequence in the model, if land cover that allows crust formation occurs in combination with a soil type prone to crusting, it is assumed that a crust will have developed and the soil group is changed to D, the one with the lowest infiltration capacities (McMillan 2003).

Classification:	Reclassification:
1. Wet1 if 125% < P < 140% of mean seasonal rainfall (P = seasonal rainfall in the year of interest) 2. Wet2 if P > 140% of 3. Dry1 if 50% < P < 75% 4. Dry2 if P < 50% 5. Ave if 75% < P < 125% except special case of dry season when only very wet scenarios classified (wet2 when P >150%)	1. dry if dry2 or two drys in previous 2 seasons 2. wet if wet2 or if wet in two consecutive seasons 3. Ave if dry1(2) follows wet1(2) and vice versa Priority order 3,2,1

Table 3.4: Classification procedure for the determination of wet, dry, or average season conditions for the use of the Dynamic Curve Number Component of model version stm4c.

3. 4. 4. Computational requirements, in- and outputs

The model code is written in the programming language Fortran77 and takes the form of subroutines for each activity, a list of which is given in Appendix C.1. It can be run on DOS, or on Linux when cell arrays beyond the compiling capacity of DOS are generated by high resolution of the GIS input layers.

To run the model, all required input files have to be placed in one folder. The main parameters for each run and the names of the in- and output files are entered into the control (text) file. The necessary information on soil and land use types as well as the time series inputs are also stored in simple text files. GIS inputs have to be in the Idrisi16 format that has already been outmoded by the newer Idrisi32 version – conversion to Idrisi16 can easily be done within Idrisi32, however. Manuals on how to produce the input files and to run the model on Windows and Linux are presented in Appendix C. 2 – 4.

A model run will produce a text file with the extension .out as the main output file containing time series information on catchment rain/evaporation, streamflow, baseflow, and soil moisture (changes). Output files of the same format containing the same information, but for selected single cells, are produced if output file names and row/column number of the selected cells have been specified in the control file.
Further the model produces GIS outputs in Idrisi16 format: Maps with the base curve numbers and the flowpaths are printed in every run. Additionally for every day one or more of the rain gauges record precipitation higher than the rainfall threshold set in the control file, maps are printed containing rainfall, areas where runoff is generated, plant available water, and final curve numbers.

3. 5. MODEL CALIBRATION AND VALIDATION ISSUES

A hydrological model in order to be used has to be calibrated and validated. Calibration is the determination of model structure and parameter values with which the model best simulates real conditions. In order to determine this, the model is run with measured input variables and outputs compared to the corresponding measured time series of the chosen output variable (mostly discharge). Validation is the test of running the model with the structure and parameter values chosen in calibration in a different time period and again comparing its outputs to measured time series of the output variable.

Model input files/formats	Model output files/formats
Text input files: • Control file (extension .con) • Rainfall file (extension .prn) • Evaporation file (extension .prn) • Seasonal moisture status file (extension .prn) • Land cover information file (extension .gen) • Soil information file (extension .gen) **GIS input files (Idrisi16, two files each with the extensions .doc and .img):** • Catchment boundaries • Topography/elevation • Drainage network • Soils • Land cover • Rain gauges • Evaporation pans **The program:** streamlm.exe The **empty but essential** file temp.req	**Text output files:** • Catchment daily water balance (extension .out) • Cell water balance (extension .out) **GIS output files (Idrisi16, two files each with the extensions .doc and .img):** • Base curve numbers • Flowpaths • Rainfall on a given day • Final curve numbers on a given day • Runoff generated on a given day • Plant available water on a given day • Soil moisture on a given day

Table 3.5: NRM³ Streamflow Model in- and outputs.

The problem with this procedure is: there are mostly too many combinations of model structure and parameter sets that give a reasonable fit, so that in terms of discharge prediction alone it is difficult to validate any individual model (Beven 2001: 5). Where it is possible, a multiple-response verification should be done, i. e. the comparison of various output variables to measured time-series. A good example of this is the multiple-response verification of the model PREVAH carried out by Zappa (2002), where the evaluation of the model not only included the validation of discharge but also of soil moisture and snow cover simulation. Unfortunately the existing time-series in the study area only allow the comparison to discharge.

Two main reasons for calibration and validation problems can be identified (Beven 2001: 20):

- The scale of the measurement techniques is not the same as the scale of the needed parameter values. Measured and calibrated parameters may be called the same but in reality they are incommensurate, meaning different quantities on different scales.
- Trying to find a "best fit" of the parameter values is based on the assumption that both model structure and observations are error-free – which is never the case. A "best set" of parameter values may be very sensitive to small changes in observations, periods of observations, and changes in model structure.

This implies that the concept of a "best" parameter set may be ill-founded. There will often be parameter sets of different models nearly as good as the one calibrated and validated. Beven (2001: 20) calls this the concept of equifinality. In fact, this can also be an advantage, since it allows the prediction of uncertainty as part of the decision-making process.

There is also the issue of the performance measures, which indicate which set of parameters performs better. The performance measures used in this study will be described more in detail in Section 6.1.3.

The measures most used are the coefficient of determination (r^2) and the Nash-Sutcliffe efficiency score (E_2). Problems arising with their use are (Beven 2001: 225):

- The highest residuals tend to occur around flow peaks; a higher weight is given to the simulation of flow peaks than low flows.
- These measures do not recognize that there may be a time lag between simulated and observed values – if there is one, the measure will be as low as for a poor performance without time lag.
- Residuals may be autocorrelated – with variance changing consistently over time.

Generally it has to be said that the use of statistical measures in the calibration of hydrological models does not conform well to requirements of statistic theory, such as no bias, purely random error, and no autocorrelation. But still the use of statistical measures greatly supports the decision for final parameter values (or ranges), although it cannot replace the visual inspection of the simulated and observed hydrographs by eye.

4. DATA

The development and use of hydrological models requires a lot of data. Information on the modelled catchments has to be fed to the model in order to run it. The NRM^3 Streamflow Model is designed to be run with comparatively easily accessible catchment information – but still topographical maps had to be read into a GIS database, and studies had to be carried out in order to develop a soil map or to classify satellite images to land use maps.
To calibrate and validate a model additionally requires measured long-term time series of the in- and output variables of the model. To obtain these, a monitoring network has to be maintained, including rain gauges, met stations, river gauging stations, or soil test plots. NRM^3, in accordance with its goals, is keeping such a hydrometeorological measuring network (Gichuki et al. 1998), one out of only three comparable ones in size and time range on the whole continent of Africa (oral communication by Th. Kohler).
The data gathered by monitoring, together with data gathered by official departments covering the time before NRM^3 existed (for example from KMD, the Kenya Meteorological Department), are kept in the NRM^3 database, which consists of relational databases in Microsoft Access format as well as a GIS database in ArcView format. (Note that for this study most GIS information was processed starting from the CDE database, which contains the same information but is kept in Arc/Info format. This is why the Manual describing the conversion of GIS data to Idrisi16 starts off with Arc/Info).

So the largest part of the data necessary for this study has been existing thanks to the monitoring efforts of NRM^3. Some information, however, still had to be gathered. This was done in the field work period for this study, conducted in July, August and September 2002. The targets of the field work were to obtain profile measurements of key parameters along the study rivers in order to identify areas of groundwater recharge and discharge, as a prerequisite for modelling; to carry out an abstractions campaign on Naro Moru river, resulting in a new method of generating naturalized flow series that model outputs can be compared to (see Aeschbacher 2003); and to gather the latest meteorological data from farms and KMD stations and to enter it into the NRM^3 database in order to be used in this and other studies.

Data quality is an important issue, especially when dealing with a model that has to be calibrated based on reliable data and that will also show conflicts between different kinds of measured data. This is why the last chapter of this section is dedicated to error ranges, data processing and quality control within the NRM^3 database.

4. 1. THE HYDROMETEOROLOGICAL MONITORING NETWORK OF NRM^3

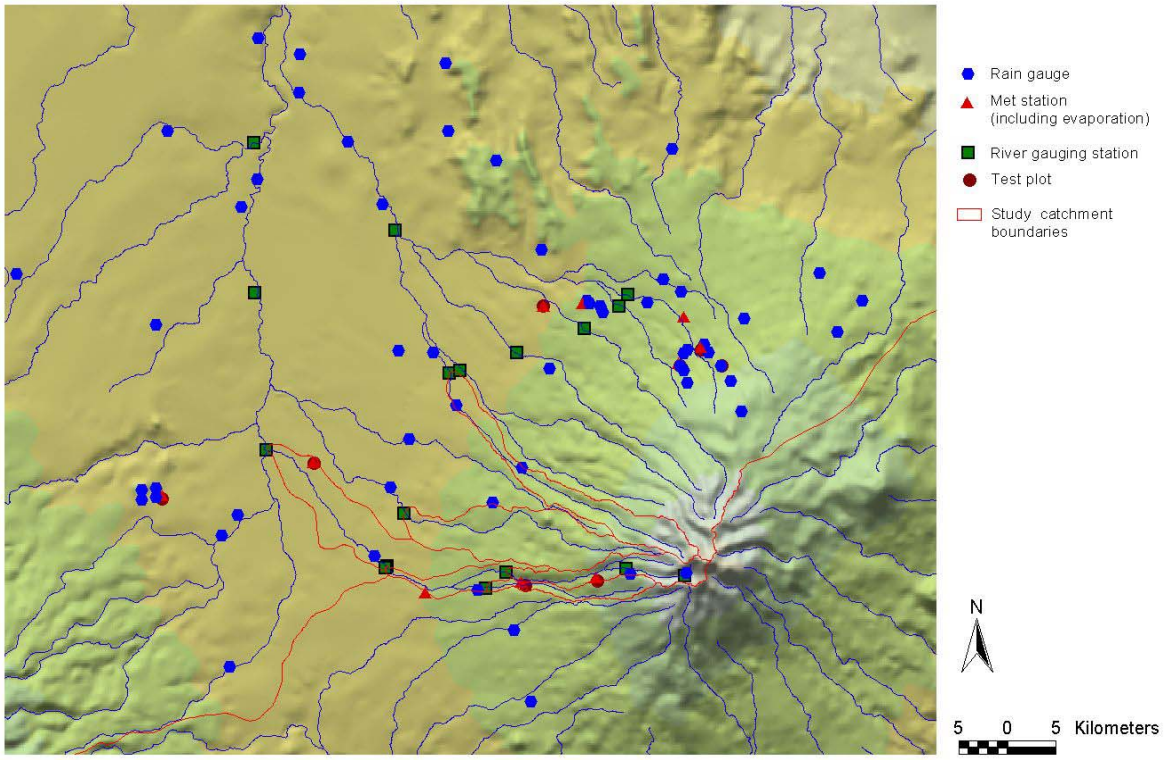

Fig 4.1: The NRM^3 monitoring network

4. 1. 1. Rain gauges

The rainfall monitoring network of NRM^3 comprises 116 gauges distributed over the whole Upper Ewaso Ng'iro Basin. Ten of these gauges belong to met stations installed by NRM^3. The rest are maintained privately on farms (mainly on the large-scale ranches belonging to white settlers in the Laikipia Plains and the Loldaiga Hills) or by KMD (Kenya Meteorological Department). The first measured daily rainfall event in the database was recorded on the 1. 1. 1934.
Most of the gauges used are operated manually, i. e. the amount of rain fallen has to be recorded every day. This is normally done at 9 o'clock in the morning, but there are some gauges where it is done earlier (between 7 and 9 o'clock). Most gauges are glass cylinders of make Casella, but there are also plastic cylinders of unknown make in use at some locations. The Moorland and Teleki gauges in the high regions on Mt. Kenya are equipped with automatic rain gauges of the type Belfort, which work with batteries and record precipitation amounts on a chart. Hellmann type automatic gauges have also been used in the past, but presently none of these is in use anymore.

In general, the density of the rainfall monitoring network is rather high compared to WMO standards, which recommend an area of 600 – 900 km^2 to be represented by one gauging station in flat terrain (Sturm 2002: 35). The area of the Upper Ewaso Ng'iro Basin and its surroundings (175km x 150km = 26'500 km^2) divided by the number of gauges (116) results in an average area of 228.45 km^2 represented by one gauge. It has to be taken into account, however, that the distribution of these gauges is not even – the density of the measuring network is highest in the footzone of Mt. Kenya, and some of the gauges are very close to

each other whilst long distances separate others. Not all gauges are classified as reliable, either (Sturm 2001). Limiting for this study is the fact that on the mountain slopes there are not many gauges. Along the Naro Moru profile there is a series of gauges almost up to the peak of the mountain, but apart from that gauges are rather scarce on the mountain. For mountainous areas, on the other hand, WMO recommends one gauge per 150 – 200 km^2. Additionally, it has to be taken into account that WMO recommendations are very generalized and that in tropical regions heavy storms can occur very locally, leaving places only a few kilometres away completely dry. It is very difficult to capture such storms with a measuring network. For hydrological modelling in the area this represents a serious limitation, as the main areas that generate runoff are located on the mountain. Problems associated with this are discussed in Section 6.4.1. An overview of the rainfall data used in this study is given in Appendix A.1.

Fig. 4.2: An NRM^3 Met Station with an evaporation pan (left foreground) and a rain gauge behind it (picture by Hanspeter Liniger).

Fig. 4.3: River gauging station A6 before the confluence of Naro Moru with Ewaso Ng'iro (picture by B. Notter).

4. 1. 2. Evaporation pans

All ten NRM^3 stations are also equipped with evaporation pans. They represent a very simple but effective way of measuring potential evaporation. The pan is a large container of water with a surface area of 1m^2, covered by a mesh to keep animals out. One liter of water taken or added from the pan equals the difference of one millimetre in the water depth. A vertical metal needle is fixed in the pan. When recording evaporation, which has to be done manually every day, 0.5-litre cups of water are added to the pan or taken out until the water level is exactly on the height of the tip of the metal needle. If only evaporation took place on one day, the amount of water evaporated in mm is twice the number of cups added to the pan. If there has been rain, the amount of rain has to be subtracted.

A list of the evaporation pans used in this study and an overview of available data is given in Appendix A.2.

4. 1. 3. River gauging stations

The NRM[3] database contains data from 43 river gauging stations (RGS). Many of them have been started as part of the MoWD (Ministry of Water Development) surface water monitoring network in the 1950's. The MoWD gauges were simple staff gauges where water levels had to be read twice every day excluding Sundays and public holidays. The data collected this way give very valuable information on the long-term behaviour of the rivers, although information on flood flows is inaccurate due to the measuring method (Decurtins 1992: 33). In the study region the staff gauges have been replaced by the LRP (Laikipia Research Project, the project that NRM[3] developed out of) by automatic water-level recorders of type OTT. Their working principle can be seen in Fig. 4.4. Charts have to be changed monthly, which is done by either NRM[3] or MoWD staff.

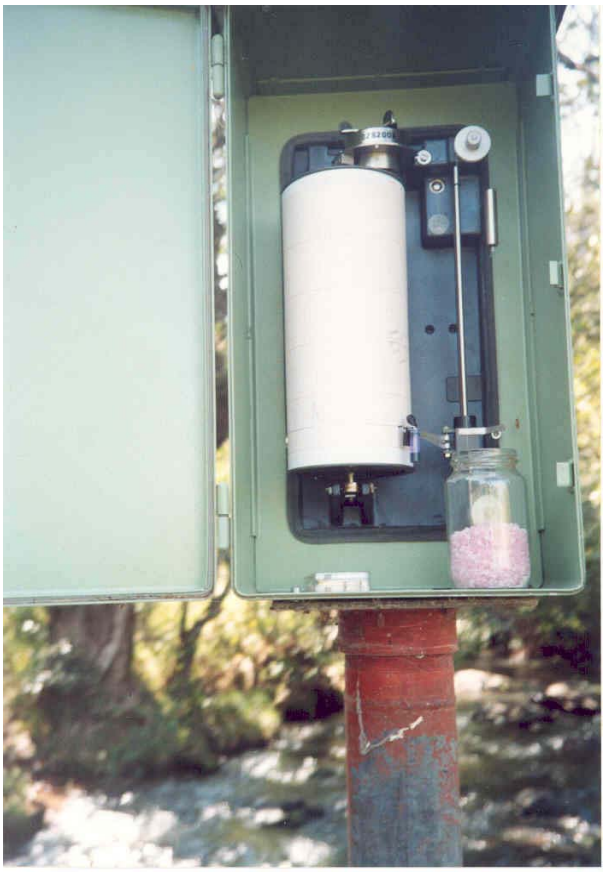

Fig. 4.4: The interior of a water level recorder. A needle actuated by a floating device in the tube of the gauging station records the water level on a chart that has to be changed monthly (picture by B. Notter).

In the study catchments, there are nine river gauging stations. Seven of them have been placed at the lower boundary of each ecological zone on Naro Moru River; three of these are not operating anymore: Mwichuiri because its mostly dry river valley has been converted into a water reservoir of Vitacress with a dam; and A1 (Naro Moru Alpine) and A2 (Naro Moru Moorland) because of the high maintenance costs due to their remoteness.
The other two river gauging stations are located at the lower boundary of the footzones in Burguret and Nanyuki catchments, both near the Nyeri-Nanyuki tarmac road. An overview of the gauging stations in the study catchments is given in Appendix A.3.1.

4. 1. 4. Land use

Two land use maps classified from satellite images are available of the Upper Ewaso Ng'iro Basin, one of 1988 (Roth 1997) and one of 1995 (Niederer 2000). The classification was done according to a scheme developed by Liniger and Thomas (Liniger et al. 1998) resulting in 20 land use classes according to their hydrological properties (see Appendix A.5).
In this classification scheme, a letter is used to describe each land use. Composites are possible. The symbols comprise one to three components:

- the first component indicates the percentage of the ground covered by a canopy layer
- the second component indicates the primary land use on the herbaceaous layer (>50% of the ground cover)
- the third component indicates the secondary land use on the herbaceaous layer (20 – 50% of the ground cover)

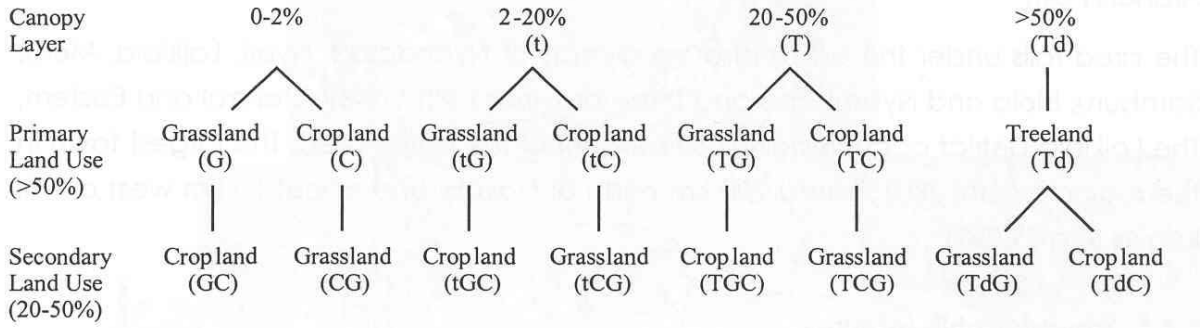

Fig. 4.5: Classification system of land use by Liniger and Thomas 1991 (Source: Liniger et al. 1998)

4. 1. 5. Soils

The soil map used in the study is a combined and slightly modified GIS layer based on the soil maps by Speck (1983) and Klingl (1996). Speck developed a map of the Mt. Kenya soils based on satellite and aerial photo interpretation, field observations and laboratory analyses of 34 profiles. Klingl's synthetic soil map of Laikipia West was produced by GIS modelling of geology, landforms, slope, drainage and vegetation.
The soil types and their associated parameter values for hydrological modelling can be viewed in Appendix A. They are classed into the four hydrological groups A to D based on the SCS soil classes. These groups have the following characteristics (Thomas 1993: 80):

- **Group A:** Soils with high infiltration rates and low runoff potential. They consist mainly of deep, well to excessively drained sands or gravels.
- **Group B:** Soils with moderate infiltration rates, moderately deep to deep, and with a moderately fine to moderately coarse texture.
- **Group C:** Soils with slow infiltration rates. Often with a layer that impedes downward movement of water, or soils with moderately fine to fine texture.
- **Group D:** Soils with very slow infiltration rates and high runoff potential. Often clay soils with high swelling potential, a high water table, or shallow soils over nearly impervious material.

4. 1. 6. River water abstractions monitoring

NRM^3 has monitored river water abstractions for more than a decade. The data are stored in the "ABST-COM 2000" database within the NRM^3 database. They come from various sources:

- John Gathenya (1992) continuously monitored all abstractions points on Naro Moru that were existing at that time between November 1st, 1990, and June 30, 1991. He used the data to calculate daily water balances for the footzone and savannah reaches of the river.

- Between 1993 and 1997, monthly measurements of the abstraction amounts of most known abstractions points along all three study rivers were made. Most abstractions can be assigned a monthly average water amount value for these years, although the average is not always based on measurements in all four years.

- Snapshot campaigns capturing all abstractions along a river were held by John Gikonyo (2003) in all three study catchments in 1996/97. Similar campaigns have been held in 2001 and 2002 by NRM^3 in the Nanyuki and Burguret catchments (NRM^3, 2001 and 2002a); the 2002 campaign in Naro Moru catchment was held by Jos Aeschbacher, two NRM^3 staff members and the author of this study during the field work period (see also Section 4.2.). These campaigns yielded information on ownership, water use, legal status, water quality; the recorded amounts of abstracted water taken (measured or estimated) are of course momentary. The problem of their temporal extrapolation is dealt with by Gikonyo (2003) and Aeschbacher (2003) and will also be discussed in Section 5.2.

4. 2. FIELD WORK

Field work for the study was carried out between July 17 and September 23, 2002, together with Jos Aeschbacher (see also Aeschbacher 2003). The main targets of the field work were:

- To obtain information on discharge, temperature, electroconductivity, and turbidity along a profile of each study river (Naro Moru, Burguret, Nanyuki) in order to assess the magnitude of groundwater influence and to identify regions of groundwater recharge and discharge. Measurements of these parameters were carried out in regular intervals along each river. Jumps in the values of these parameters, when plotted along the profile of a river, should indicate groundwater recharge or discharge areas. The profile measurements had to be carried out in one or two days each, in order to minimize jumps due to the nightly breaks or to rainfall in the catchment.

- To carry out an abstractions campaign on Naro Moru River as done before by NRM^3 in two- to four-yearly intervals (campaigns on Burguret and Nanyuki rivers had already been conducted by NRM^3 in 2001 and 2002) targeting information on ownership, method of abstraction, water use and used amounts on each abstraction point along the river. The obtained information was used for the analysis of abstractions and low flows by Aeschbacher (2003); of interest for this study was ultimately the production of a naturalized flow series that NRM^3 Streamflow Model outputs could be compared to.

- To gather post-1997 rainfall and evaporation data from farms and KMD stations where these records are manually kept, to quality-control them and enter them into the NRM^3 database, in order to be used in model calibration/validation and in impacts assessment.

All field work was carried out in a team of four, namely Jos Aeschbacher (MSc student from Berne), James Mwangi (NRM^3, normally responsible for maintenance of the NRM^3 met stations), Ben Mwangi (NRM^3, driver) and the author of the study.

4. 2. 1. River Profiles

The measurements of the four parameters discharge, electric conductivity, temperature and turbidity were carried out for Naro Moru on July 26 and 27, 2003, yielding data from 14 points along the river; for Burguret, on August 20 and 21, 2002, yielding data from 14 points along the river; and for Nanyuki on August 22 and September 23, 2002, yielding data for 15 points along the river. Additionally, the four parameters were also measured at four springs

and a borehole, in order to obtain a base for comparison. This was done on Juli 27 and 30, 2002.
The measurements were carried out in periods of low flow and without rainfall, so it can be assumed that the flow in the rivers at that time was made up mostly of baseflow and no direct runoff. The profile points along each river were chosen in intervals of 2 to 5 kilometres, determined by accessibility of the river due to topography, roads, and private property. Tributaries were gauged at least one time before their confluence with the main river. The uppermost measurements were made in the lower forest zone, and the last at the confluence of the Rivers with Ewaso Ng'iro (except Nanyuki river, where the lowest measurement was made at its confluence with Timau river).

Instruments and methods used were:

Current meter gauging of discharge
The Baby Ott current meter was used to measure discharge. A propeller is fixed near the lower end of a 1m metal stick with a handle at its upper end. Electric signals are sent through wires to a counter that records each turn of the propeller.

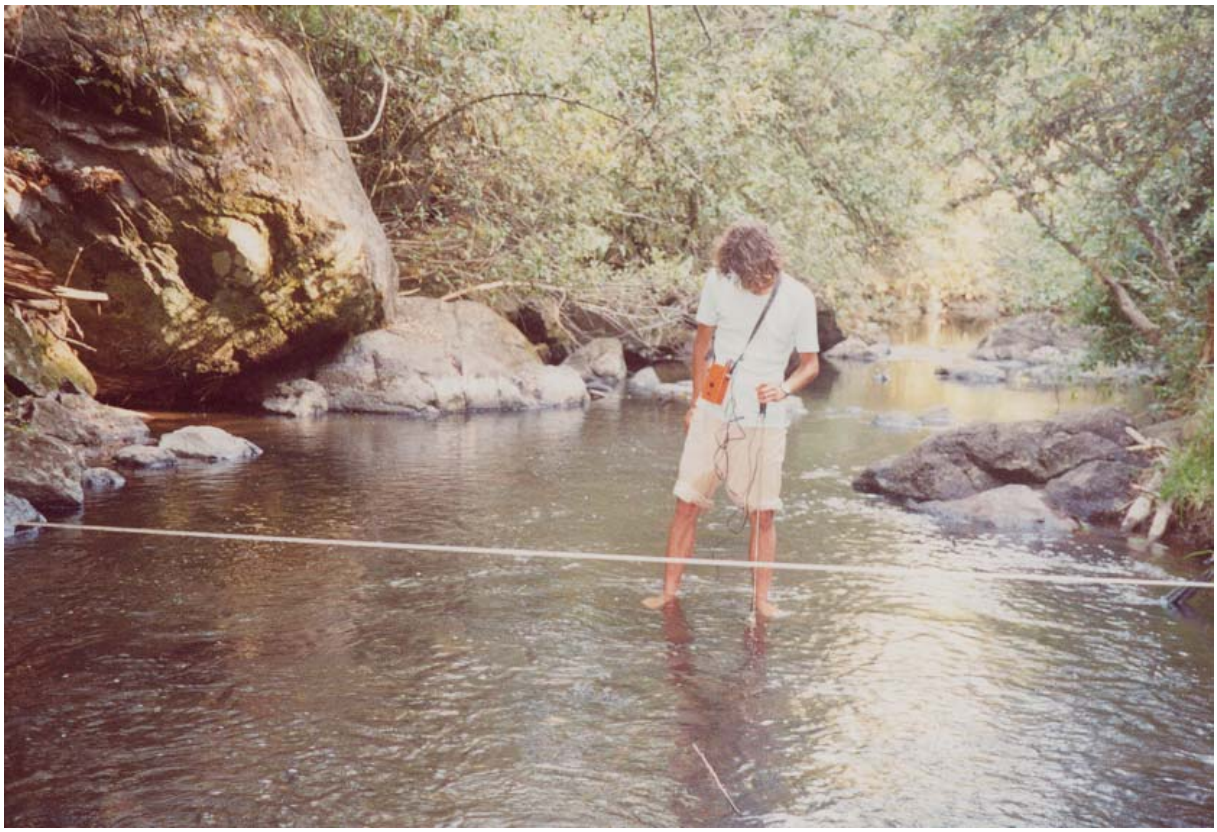

Fig 4.6: Current meter gauging on Burguret River (picture by J. Aeschbacher)

To measure discharge, a line has to be fixed crossing the river just a little above the water, designing a cross section of the river. The cross section has to be chosen very carefully: There should be no big stones, no turbulent water or countercurrents and enough flow for the propeller to turn across the whole width of the channel. Sometimes the search for a suitable cross-section can be very time-consuming, and sometimes big rocks had to be removed to create a cross-section where a current meter gauging was possible.
Point measurements of flow velocity and water depth are then made in regular intervals (10 to 30 cm, according to water depth and river width) along the cross-section from one shore to the other. The measured values (distance from starting point, number of propeller turns in 30

or 60 seconds and water depth in cm) are noted on a gauging sheet. The sheets used in this study are the "Current Meter Gauging (Mid-Section Method)" sheets by the Hydrology Section of the Republic of Kenya (see Appendix B.2). The values are later entered into a Microsoft Access form within the database which automatically calculates discharge in m^3/s.

Measurements of electric conductivity and temperature
The electric conductivity and temperature measurements were done with an EC meter equipped with batteries. Its metal sensor simply has to be held into the water, yielding instant results on the display of the machine.

Turbidity measurements
Water samples were taken in PET bottles at each site but unfortunately could only be processed weeks later, at the end of the field work period, because there was no turbidity meter available at NRM^3. It could finally be done at Rural Focus (the company of Mike Thomas who developed the first version of the NRM^3 Streamflow Model), but the results were unusable due to error ranges of up to almost 100% - reasons can only be speculated on, ranging from the bottles over the turbidity meter to the long waiting time.

4. 2. 2. Abstractions campaign on Naro Moru River

The abstractions campaign on Naro Moru River was held between July 29 and August 16, 2002. For practical reasons, the furrows were visited first, then the gravity pipes and finally the pumps.
At each abstraction point, an interview was made with the owner. In addition, GPS position, temperature and electric conductivity were measured and a water sample taken. A questionnaire was filled in with the following information:

- Geo-reference and ownership
- Principal water uses
- Legal status of abstraction
- Type of abstraction
- Methods of irrigation and diversion
- Area of irrigation
- Quantity of abstracted water
- Water quality

For measuring or estimating the quantity of abstracted water for each abstraction point, different methods had to be used:

- **Furrows:** Besides measuring furrow discharge with the current meter (method described above), the sites of all intakes were surveyed. This way a temporal extrapolation of furrow flow was made possible: the Manning-Strickler Formula, which needs the hydrologic gradient, the hydrologic radius of the cross-section and the Strickler coefficient (for the bottom friction) as input parameters, can be used to calculate discharge given the water level in the river.

- **Gravity pipes:** The capacity of each gravity pipe was measured by twice gauging the river below the intake, once with sluice gate at intake opened and once closed. The difference of the two gaugings gives us the quantity of abstracted water.

- **Pumps:** For different reasons (pumps are usually portable and therefore often not around, the water level in the dry spell is too low to double gauge, for some irrigated plots no owner or even informant could be found, current meter gauging is very time consuming) it was not possible to carry out a precise measuring of the abstracted water by pumps. However, the experience of the previous campaigns showed that an estimation based on demand (size of the irrigated plot) or on pumping hours and capacity gives acceptable results.

The sites of most intakes of the furrows and the gravity pipes were already been known from the previous campaigns and could therefore be approached by car. For the pumps there was no other possibility than walking along the river looking for signs of pumping or flood irrigation. In the lower reaches, this was sometimes difficult as acacia thickets, fences, and the river itself had to be crossed repeatedly. Since most of the pumps are portable, often only the end of a pipeline at the river bank or the typical signs of flood irrigation gave a hint of an abstraction point.

4. 2. 3. Rainfall and Evaporation Data Collection

Rainfall data were needed for a region roughly delimited by the peak of Mt. Kenya, Embori Farm (on the North slope of the mountain), Junction (the confluence of Nanyuki with Ewaso Ng'iro River) and Lamuria. Since rainfall data from all stations had previously only been entered and checked up to 1998, the recent data had to be collected. The collection of these data from the gauges, which are kept mostly either at farms of white settlers or at government stations (Kenya Meteorological Department, Forest Stations), was carried out between the August 26 and 29, 2002, by car. The records are almost everywhere kept on paper. They had to be copied manually onto record sheets (see Appendix B.3) and, back in Nanyuki, entered into the NRM^3 database.
When gathering the data, great care was given to the question whether the person responsible for the daily measurements wrote down the amount of fallen rain on the day of the measurement or on the day of the rainfall – since rain is always measured in the morning (at 9.00 a. m. at most stations). Afterwards, when entering the data into the database, this proved very useful since there had apparently already been a great deal of confusion over this question. Many rainfall amounts from after 1997 that had been entered previously were entered on the wrong day. Luckily, with the help of the archived original datasheets and the station documentation by Bernhard Sturm, the datasets could be corrected. This points to the importance of quality control, discussed in the next section.

4. 3. DATA PROCESSING, QUALITY CONTROL AND ERROR RANGES

Data of reliable quality are of prime importance to any scientific application. Measured data can never be absolutely accurate, there is always a measurement error. To reflect the methods of measuring and processing data and to estimate error ranges of the measured variables is necessary to comment on the validity of research results.
This principle is also followed by NRM^3. Guidelines for quality control of the gathered data exist. Unfortunately it seems that the scarce financial resources have prevented the maintenance of high standards in some cases, primarily in the establishment of reliable rating equations for river discharge.

4. 3. 1. Discharge

The automatic river gauges continuously record the water level at a site. In order to transform gauge height values to discharge values so-called rating equations are used. A rating equation describes the relation of discharge and gauge height at one site and is established plotting measured discharge values (with the current meter method, or the salt dilution method) against their corresponding gauge heights. The equation of the form

$$Q = a(H + b)^x \qquad (4.1)$$

With Q = discharge
H = gauge height
a, b, x = site-specific coefficients

best fitting the plotted data is used as the rating equation for the site. In some cases, if a river bed has an irregular cross-section, the rating equation has to be segmented, meaning that different equations have to be used for different ranges of gauge heights. There is special software available for the computation of rating equations, for example HYDATA from ….

It is obvious that a higher number of gaugings and a greater range of flows covered by the gaugings increase the reliability of a rating equation. In addition, when floods modify the mostly natural river channels at the gauging sites, the relationship between gauge height and discharge is changed as well. Nevertheless, the same rating equations have been used for years for some of the gauging stations in the NRM^3 database, and these equations are sometimes based on a very low number of gaugings, or on gaugings done a long time ago. The last comprehensive quality control of discharge data in the NRM^3 database was done by Lindsay McMillan in December 1996 (McMillan 1996, see Appendix A.3.3), and since then rating equations have been continued to be used largely unchanged. (For comparison: In the test catchment of the Group for Hydrology of the Institute of Geography in Bern, new rating equations are established every two years for sites where artifical concrete cross-sections have been constructed).
There is evidence that the present gauging equations are inaccurate: Conflicts were noted between the amounts of water recorded at AF (Nanyuki-Timau confluence) and AJ (Confluence of Ewaso Ng'iro and Nanyuki) when comparing water balances in the study regions (Notter 2002: 6). At A9 (Burguret river in footzone) a difference of almost 100% was noted when comparing the measured flow at this station during the profile measurements to the flow calculated from the gauge height at the same time and the rating equation.

The error range of a current meter gauging lies around 5 – 10%, depending on the number of flow velocity measurements taken in the cross-section and the channel properties (width, flow velocity, turbulence, rocks). The errors of the rating equations of the river gauging stations in the study area range between 3.9% (Naro Moru A2) and 15.7% (Naro Moru A6). The exact values are given in Appendix A.3.3. Gaps in the flow data used in this study are shown in Appendix A.3.2.

4. 3. 2. Precipitation and evaporation

Quality control of precipitation and evaporation data takes place at different stages:
During the data collection campaign, every value is copied manually onto the record sheet, because these values are also manually noted by the gauge operators. This is a very time-

consuming process that can form another source of errors, but on the other hand doubtful values can already be identified during the manual copying process. In addition the values are double-checked by the second person taking part in the data collection campaign.
When the values are entered into the database, the software automatically performs various checks, such as inch-to-millimetre conversion and gap identification.
The entered data is cross-checked by another person who ideally was not involved in the data collection process.
Further quality control within the database includes the flagging of unusually high values. Gaps can be identified with a database query, but this query only recognizes gaps when the date of the missing values is also missing. The exact identification of missing rain and evaporation values for this study was done in Excel. An overview over available data is given in Appendix A.1.2 and A.2.2. Detailed descriptions of most rain gauges including the method of measurement, station history, etc. by Sturm (2001) can be found in the NRM^3 database.

The error in measuring the amount of precipitation is more difficult to assess. It is largely determined by wind velocity: The gauge forms an obstacle to wind, and to flow around it, the wind has to speed up, which reduces the probability of a drop falling into the cylinder. In mountainous areas the error is higher because of stronger winds. No figures were found on the study area; in Switzerland the measuring error is around 5% in the flatlands and up to 30% in alpine areas for rain – for snowfall the measuring error can be up to 50%.

5. GROUNDWATER AND ABSTRACTIONS: ASSESSMENT OF EXTERNAL INFLUENCES

The NRM^3 Streamflow Model calculates daily discharge on the basis of time series of precipitation/evaporation and information on topography, land cover, soils, and drainage network. There are two important influences on the water balance in the study catchments, however, that the model deals with only in a very generalized way:

- Influences of groundwater are only included as long as the water does not leave the modelled cycle – if it stays underground in deeper stores for longer times, it can only be included in the model as a constant loss factor (parameter SCOEFF). Groundwater inflow from deep aquifers into the rivers cannot be simulated by the NRM^3 Streamflow Model.
- River water abstractions can be entered as a constant value in m^3/day, and there is no possibility to include variable abstraction amounts in the model. In reality much more water is abstracted through furrows during the rainy season (when river water levels are high) than in the dry season; for pumps it's the opposite – farmers will only pump when the weather is dry. Large differences exist between the day-to-day abstractions abstraction amounts.

Both influences were considered too important in the study catchments to just use constants or constant factors without further assessment of the magnitude and variability of their impact. In consequence,

- River profiles measurements of discharge, electric conductivity and temperature were carried out during the field work period (as described in Section 4.2.1.) in order to assess the magnitude of groundwater influences and identify areas of groundwater recharge and discharge.
- In model calibration and validation, river water abstractions were not accounted for by subtracting them as a constant value from the simulated discharge (as can be done within the model), but by comparing the modelled natural flow values to naturalized observed discharge (meaning measured discharge plus total daily abstraction amounts within a catchment). The methods of naturalization used are described in Section 5. 2.

5. 1. GROUNDWATER RECHARGE AND DISCHARGE AREAS

5. 1. 1. Measured parameters and their characteristics

The river profile measurements during the field work period yielded sets of three parameters for various points along every river in more or less regular intervals (see Fig. 5.1). The measured values for all points are listed in Appendix B.4.

Discharge is the most direct parameter for identifying groundwater influences. A higher value at one point than at the last point upstream indicates groundwater discharge (as far as there are no tributaries), a lower value indicates transmission losses due to groundwater recharge, bank storage or evaporation.

There are two main problems, however: one is that when measuring total discharge in the river, one cannot tell the difference between groundwater reaching the river from the saturated soil zone (that is included in the simulation of the NRM[3] Streamflow Model) and groundwater from deeper aquifers. The other problem concerns potential errors: As mentioned in Section 4.2.1, the error in one current meter gauging is around 0 – 10%. In addition to this, there is the influence of river water abstractions, that amount to a great percentage of the natural flow in a dry period. This influence has to be accounted for and the flows naturalised. The errors in the estimation of the abstracted water amount at each point at the exact time of the profile measurements, when added up for naturalization, can result in a very large error. At some points where discharges are higher than upstream but EC values do not increase substantially in the same stretches, the probability is large that an intake or a pump might have been turned off in the meantime.

Temperatures: Groundwater with longer residence times is generally expected to have higher temperatures than river water. River water temperatures rise from 8°C in the forest zone to around 22°C in the lower reaches. Springs have generally higher temperatures, between 20 and 25°C, but as it turned out to be, the difference to the river waters is not so big that the origin of the water can easily be distinguished by temperature. Also temperatures of river water of course show the influence of air temperature – in the morning the lower river water temperatures were measured than in the afternoon.

Electric conductivity (EC) of water rises with its mineral content. Naturally groundwater with long underground residence times will have dissolved more minerals from the rock than river water or soil water. Electric conductivity proved to be the best parameter to identify inflow of groundwater with longer underground residence times: River water in the upper

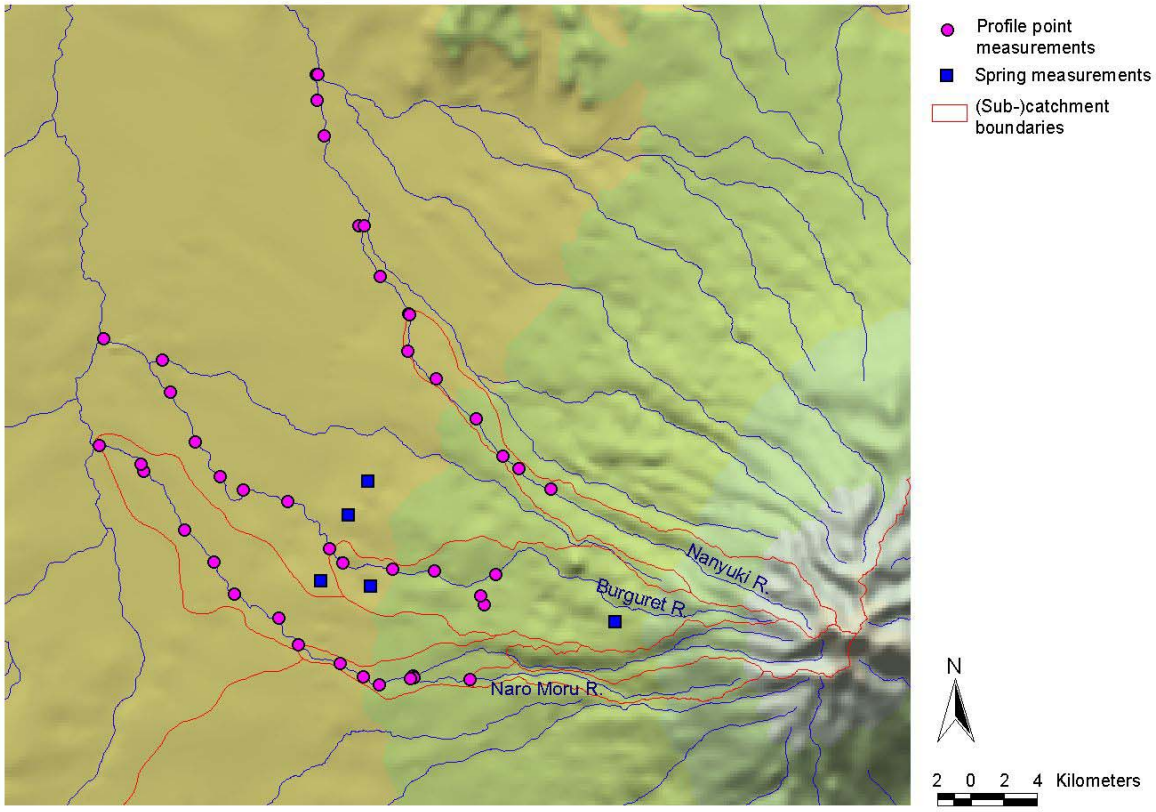

Fig. 5.1: Profile points along Naro Moru, Burguret and Nanyuki rivers (purple circles) and springs measured for comparison (blue squares).

reaches of the study rivers generally has values between 30 and 40 µS/cm. They gradually rise to about 100 µS/cm in lower Burguret and Nanyuki and almost 200 µS/cm in lower Naro Moru, with the higher values in Naro Moru being at least in part explained by the extremely low flow, which results in a higher concentration of dissolved minerals. Spring water on the other hand shows values between 300 and 760 µS/cm, and small quantities of spring water substantially increase the EC of river water. If large percentages of river flow are made up of groundwater from deep aquifers, this shows in a large increase of river water EC. The small spring on lower Naro Moru with an EC of "only" 236 µS/cm is probably part of a local groundwater system, probably within the sediments of the river bed.

5. 1. 2. Results

The results of the river profiles are summarized in Figures 5.2 to 5.7. Generally the picture of the footzone being an area of groundwater discharge, presented by Decurtins (1991) and Gathenya (1992), can be supported: The measurements beginning in the lower forest zone all show decreasing amounts of observed flows, due to the large amounts of abstracted water. When naturalized, the discharge profiles of Naro Moru and Burguret show an increase in the beginning where contributions of tributaries come in, followed by a further small increase down to the lower boundary of the footzone (tarmac road, RGS A5/A8). The savannah zone following downstream is characterized by small losses due to either evaporation, bank storage or seepage into the alluvial sediments.

5. 1. 2. 1. Springs

The measured springs show very high electric conductivity (over 300 µS/cm) and rather high temperatures. The values are shown in Table 5.1 and can be regarded as representative for groundwater with longer residence times (Leibundgut et al. 1986). None of these springs had much water at the time of the measurements. Probably very little, if any at all, of this water ever reaches the main rivers directly.

The borehole on Satima Farm, a farm situated on Naro Moru river below RGS A5, penetrates a profile of 146 m depth. The water rest level lies at 54 m and the measured water was pumped from a depth of 74 m. The yield of the borehole based on a rating done after its construction is 1.5 m^3/s (oral communication of the owner of Satima Farm on July 27, 2002). The water of the borehole can be assumed to originate in the regional aquifer system around Mt. Kenya (refer to Section 2.1.6.).

Name	Spring/Borehole	Drains to:	Discharge (estimates) [l/s]	EC [µS/cm]	T [°C]
Satima Farm	Borehole	Naro Moru	1500 (yield)	301	25.5
Mureru Springs	Spring	Burguret	8.5	400	20.6
Karichota (Waguziru) Spring	Spring	Burguret	2.5	303	21.1
Burguret Springs	Spring	Burguret	very little	*562*	22
Ragati Spring	Spring	Burguret	0.5	760	20.5

Table 5.1: Discharge, electric conductivity and temperature of some springs in the study catchments

5. 1. 2. 2. Naro Moru

While the observed **flows** decrease almost over the whole length of the profile, the naturalized flows of Naro Moru show a large increase in runoff at the lower boundary of the forest zone (at the confluence of Naro Moru North with Naro Moru South), and then a small increase down to A5. Below A5 the observed discharge is further reduced and reaches zero at the crossing of the railway bridge. From there on water is only found in still pools in the riverbed, except for a small spring (discharge about 1 – 2 l/s) in the riverbed near Matanya that seems to emerge from the alluvial sediments. Naturalised discharge stays more or less the same below A5.

Electric conductivity increases all over the profile. The increase is most pronounced in the upper footzone and in the lower part of the savannah zone, where no flow was observed anymore. EC was measured in still pools also used for livestock watering, which is a partial explanation for the increase.

Temperatures naturally show an increase due to decreasing altitude and increasing air temperatures, and a downward jump due to the nightly break at A5. Only one unexpected jump can be seen at the small spring near Matanya, but as temperatures due to the dry rivers also had to be measured in pools, this does not allow the conclusion that the water comes from a deep aquifer, especially since its EC is lower than the one of the springs measured for comparison.

On Naro Moru river the impact of river abstractions is most dramatic. The large insecurities in naturalization due to river water abstractions become evident in the three graphs of naturalized flow in Fig. 5.2. Naro Moru is the river where most data are available on abstractions in 2002; at most abstraction points the amounts have been measured or estimated with various methods (demand based estimate, gauging, estimate based on physical properties of the abstraction works). The three graphs shown in Fig. 5.2 were calculated using

a) the lowest estimate for each abstraction point
b) the final ("most probable") amount taken for the campaign report by NRM[3]
c) the highest estimate for each abstraction point.

This results in a quite wide range of discharge amounts; the relative changes between the profile points are similar for all three naturalizations, however.

The fact that no flow was measured below the railway bridge signifies that below that point losses could not be detected anymore, so the lower part of the curves has to be treated with care.

It seems, in agreement with the findings of Decurtins (1991) and Gathenya (1992), that on Naro Moru the lower forest and footzone can be described as areas of groundwater discharge while the savannah zone is an area of no great changes. Water lost to bank storage and seepage in the savannah zone seems to stay well-confined within the alluvial sediments of the riverbed and remains visible in pools or reappears, like at the small spring near Matanya.

The groundwater contributions in the footzone do not seem to consist of significant amounts of groundwater with long residence times. Old groundwater probably plays a minor influence, but if amounts significant for the hydrological modelling of the catchment were involved, it would show in more dramatically rising EC values. A modelling experiment showed that the NRM[3] Streamflow Model results for the day of the measurements lie well within the range of naturalised river flows and also follow the pattern of increase towards A5 and a slight decrease towards A6 (see also Fig. 5.2).

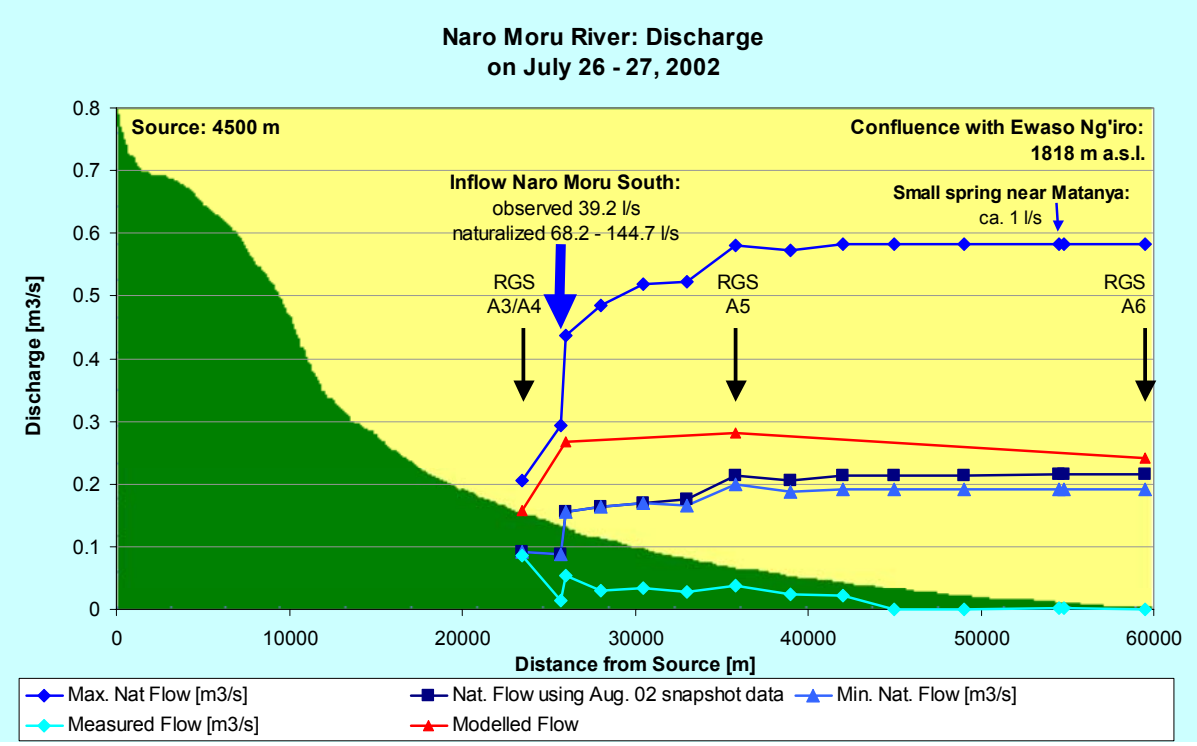

Fig. 5.2: Profile of discharge along Naro Moru river on July 26 and 27, 2002. The light blue line is observed discharge, the three dark blue lines show naturalizations using the minimal, the "most probable" and the maximal estimate for each abstraction point. The red line shows the discharge simulated by the NRM^3 Streamflow Model for the subcatchments on the two particular days.

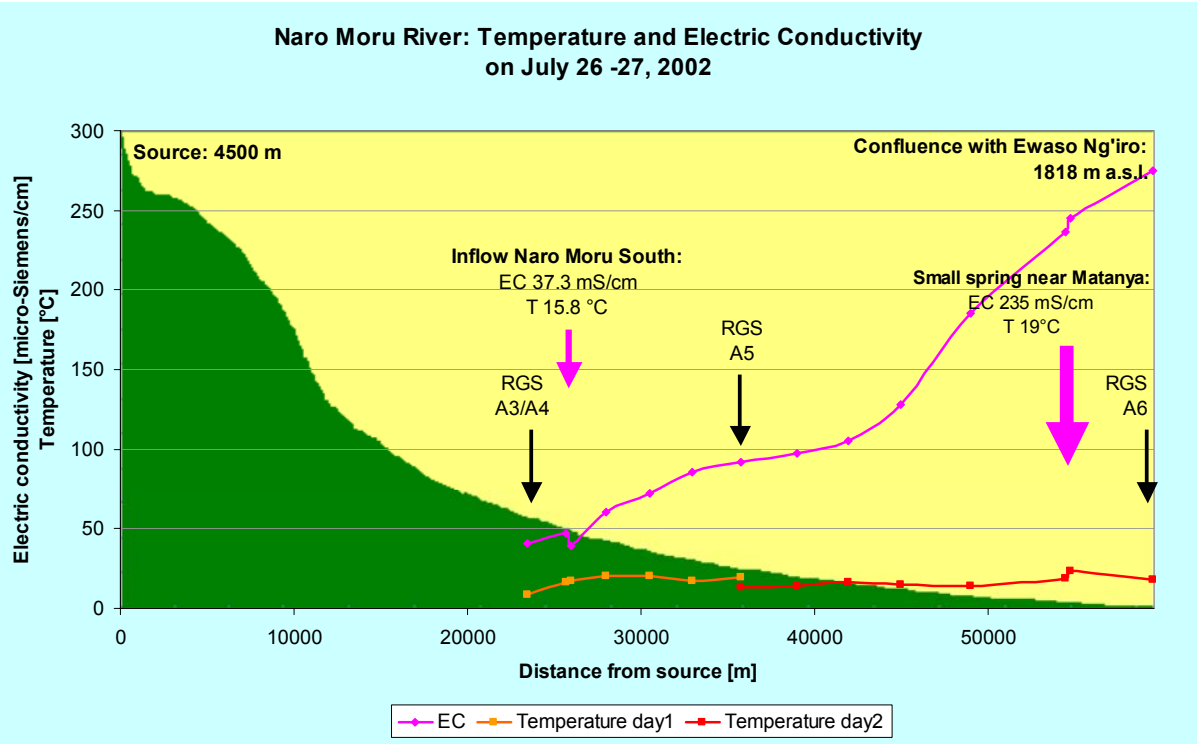

Fig. 5.3: Profile of electric conductivity and temperature (orange: first day, red: second day) along Naro Moru river

5. 1. 2. 3. Burguret

The situation on Burguret (Fig. 5.4 and 5.5) is similar to that on Naro Moru. A large increase in naturalized discharge due to the confluence of Burguret South and North is followed by a very small increase down to RGS A8. Further downstream losses are more pronounced than on Naro Moru, especially in the last kilometres before the confluence with Ewaso Ng'iro, where Burguret river crosses the Marura swamp. This swamp is almost totally drained today and converted to cropland, but apparently has either kept its function of a sponge for riverflows, or the abstractions in that river stretch are largely underestimated, which seems likely given the large irrigated area. In the Burguret catchment only the abstraction estimates used for the 2002 campaign report (NRM[3] 2002a) was available for the naturalization of the flows.

EC values are generally lower than on Naro Moru. They show an upward jump at the inflow of the tributary Waguziru, which is mainly fed by springs and has an electric conductivity of 366 µS/cm. This shows the magnitude of the impact of a small amount of spring water (3.8 l/s) on the overall EC of river water. The generally lower values in the lower reaches of Burguret than on Naro Moru are explained mainy by the fact that the measured flow was higher. Burguret did not fall dry and so there was no possibility for minerals, or pollutants caused mainly by the watering of animals, to concentrate in pools.

Temperatures show a steady increase in the downstream direction only interrupted by the nightly measuring break.

In the Burguret catchment groundwater discharge influences seem to be effective in the lower forest and footzone. There is some groundwater with long residence times, as evidenced by the springs and the tributary Waguziru that is mainly fed by springs. But also here old groundwater does not seem to occur in large enough amounts to produce significant limitations for hydrological modelling.

5. 1. 2. 4. Nanyuki

On Nanyuki river (Fig. 5.6 and 5.7) the interpretation of the results is made difficult due to incomplete information on abstractions. The discharge graphs (both observed and naturalised) show a decrease followed by an increase in flow in the uppermost part of the measured profile, which is with the highest probability due to the intake of a gravity pipe just upstream of the second gauging point. It was probably turned on at the time of the gaugings at the second and third point and turned off again in the time between the gauging of the second and the third point (oral communication by Ben Mwangi on August 22, 2002). However, there is no information in the abstraction database on this intake. The data availability situation on abstractions is worst on Nanyuki of all three study rivers, so the results of this profile have to be treated with extreme caution.

Apart from that, the measurements seem to indicate a more or less steady decline in flow until the confluence with Likii, that for unknown reasons apparently is abstracted so little that it still sustained a flow of over 200 l/s just before the confluence. After the inflow of Likii a further increase in flow was observed. The reasons for this are not clear; groundwater is not probable because it would show in an EC increase as well; probably it can be attributed to measurement errors or water that is abstracted upstream and then led back to the river, or again the closing of a water intake.

Temperature and EC show a constant but small increase in the downstream direction. EC makes a sudden upward jump at the downstream side of Nanyuki town, which is probably due to pollution by the city. EC values are lowered again by the inflow of Likii to stay around 80 µS/cm until the confluence with Timau.

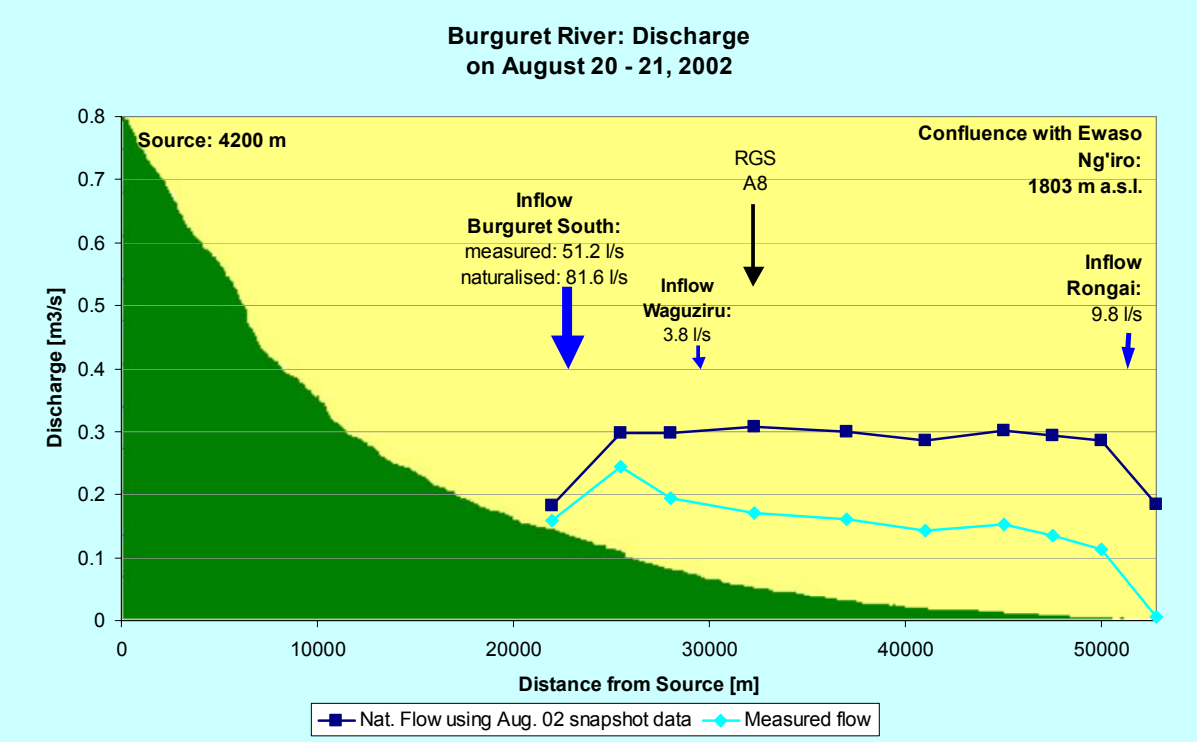

Fig. 5.4: Profile of measured and naturalised discharge along Burguret river on August 20th and 21st, 2002.

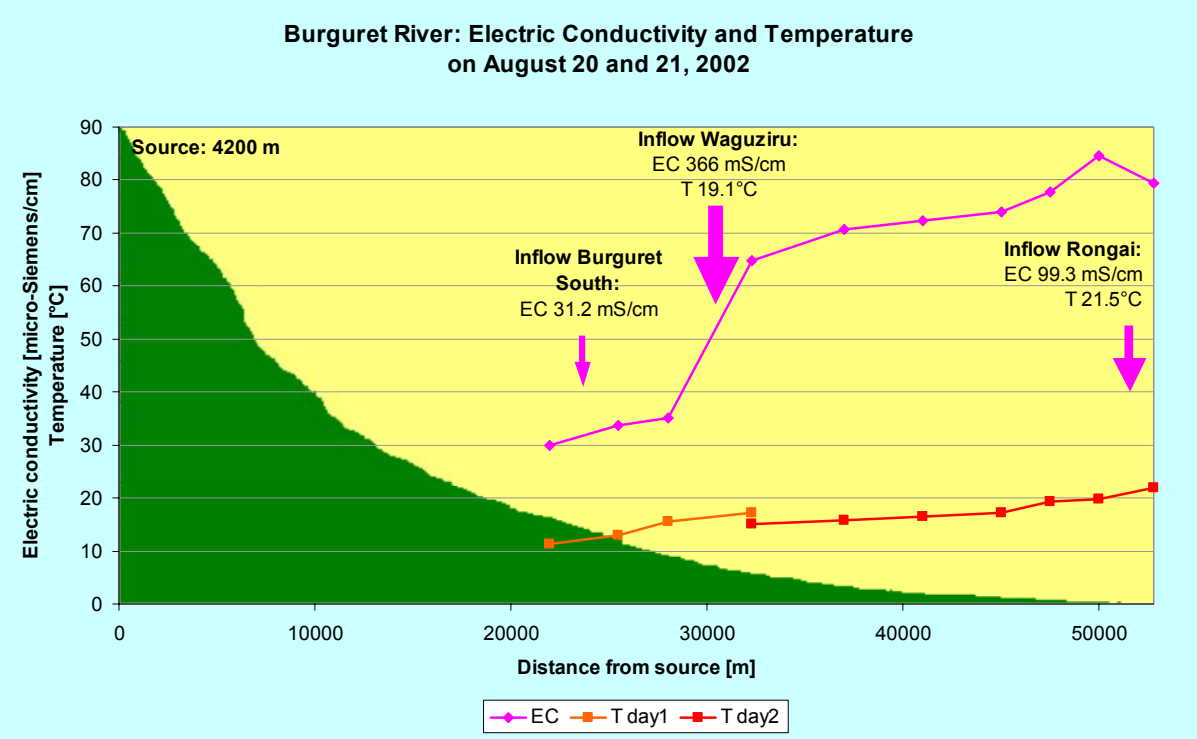

Fig. 5.5: Profile of electric conductivity and temperature along Burguret river on August 20th and 21st, 2002. The influence of tributaries with a higher/lower electric conductivity than the main river is well visible: Waguziru with only 3.8 l/s but an EC of 366µS/cm causes a large upward jump in electric conductivity. Rongai with 9.8 l/s and 99.3µS/cm causes a decrease.

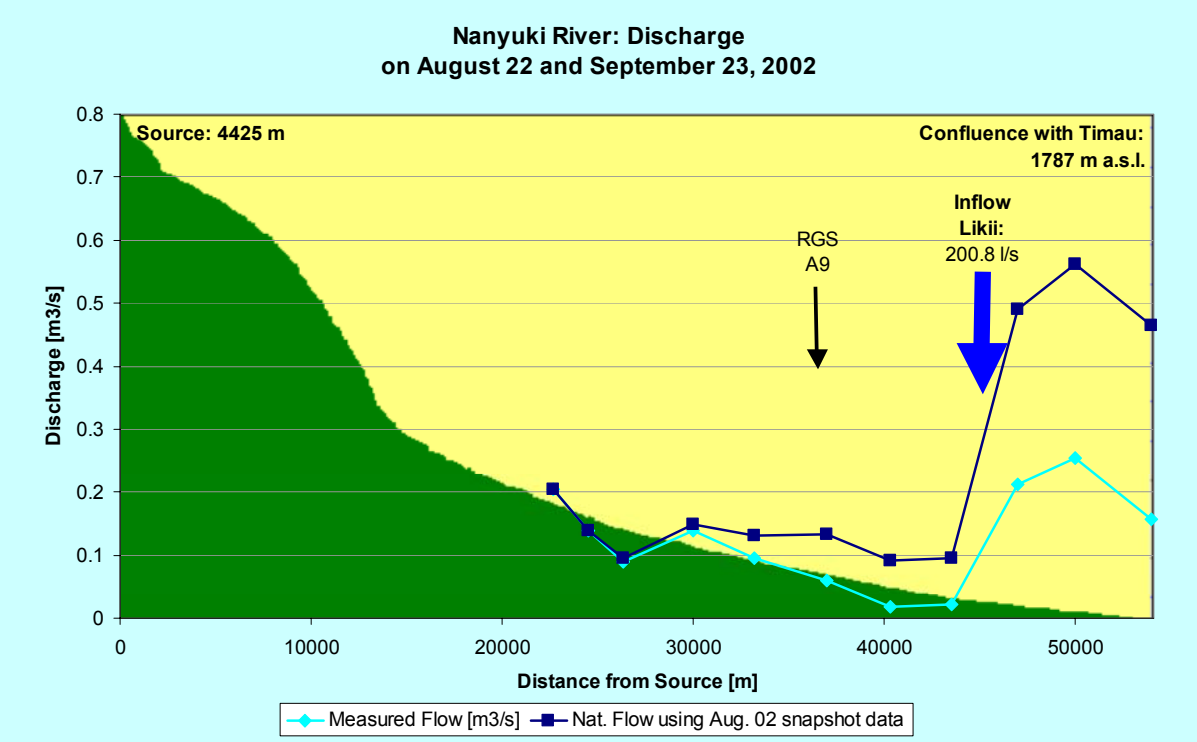

Fig. 5.6: Profile of measured and naturalised discharge along Nanyuki river on August 22nd and September 23rd, 2002.

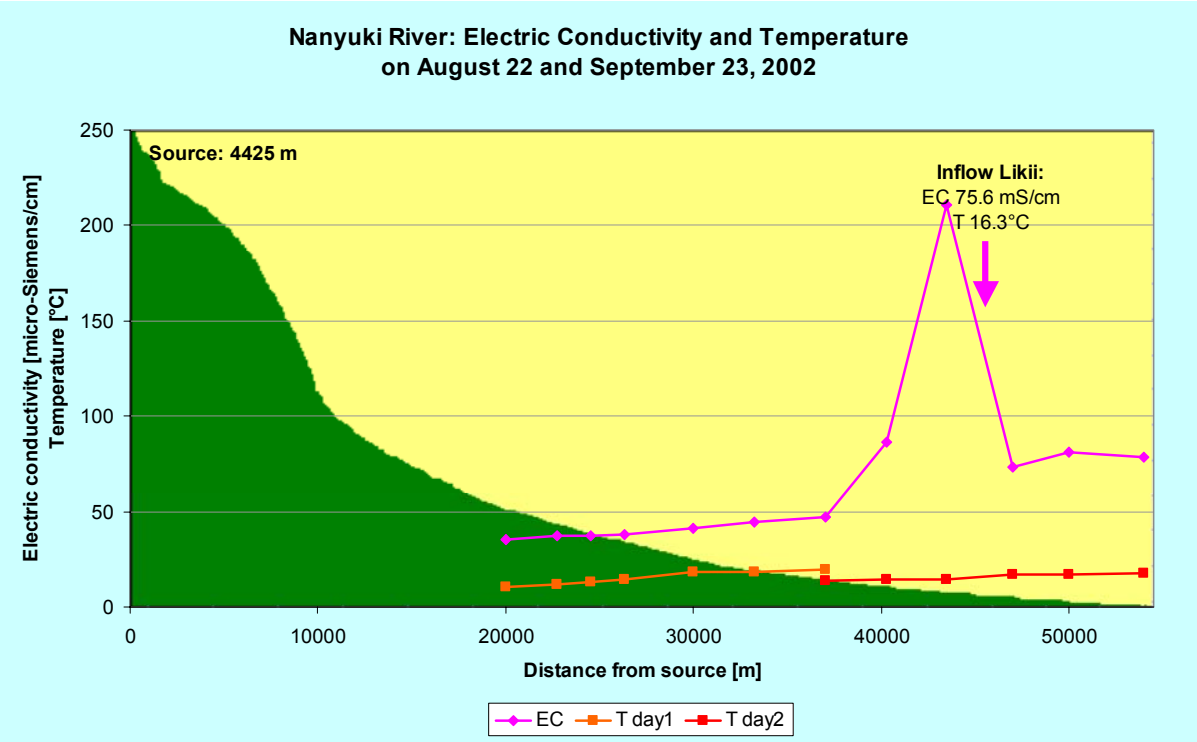

Fig. 5.7: Profile of electric conductivity and temperature along Nanyuki river on August 22nd and September 23rd, 2002. The peak before the inflow of Likii river is probably caused by pollution from Nanyuki town.

Considering the relatively constant EC and temperature values in combination with the unreliable flow data, the statement can be made that at least down to RGS A9 groundwater influences seem to play a minor role. Downstream towards the confluence with Timau river the uncertainties about the anthropogenic influences (pollution, water supply systems) in this quite urbanized catchment do not allow statements on groundwater influences. The poor results of the Nanyuki profile show the necessity of better data on abstractions and generally a better water management that does not let a valuable resource like water go unaccounted for.

5. 2. NATURALIZATION OF OBSERVED STREAMFLOW RECORDS

The available data on river water abstractions is described in Section 4.1.6. Using this data, naturalised flow series had to be produced by adding the total daily abstraction amounts in a catchment to the observed flow data, in order to be compared to NRM^3 Streamflow Model outputs for calibration and validation.
Basically two methods were used for naturalization:

a) Using as much as possible of the measured data from the NRM^3 database, available mainly from the years 1990/91 (continuous abstractions monitoring on Naro Moru, Gathenya 1992), and 1992 – 97 (monthly monitoring of abstractions on all rivers by NRM^3, NRM^3 database). This method is described in Section 5.2.1.
b) Using the Abstractions Calculation Tool by Aeschbacher (2003), an Access Query that aims at temporally extrapolating abstraction amounts from the data collected in the snapshot campaigns, based on the methods used by Gikonyo (2003) and the surveys of the furrows carried out in the field work periods. Its workings are described in Section 5.2.2.

Since the Abstractions Calculation Tool didn't become available almost until the end of the work on this study, calibration and validation was done mainly based on naturalized flow series produced with the first method. This was also more appropriate with the choice of the years 1987 – 1996 as calibration/validation period, because the parameters used in the Abstractions Calculation Tool are based on the campaigns in 1996/97 and 2001/02.

5. 2. 1. Naturalisation using measured data from the NRM^3 database

Total river abstractions were estimated using the data from the table "Abstractions_Data" in the ABST-COM 2000 database. They include the monitoring data by Gathenya (1992) and NRM^3, covering:

- All abstraction points on Naro Moru between November 1st, 1990, and June 30, 1991, on a daily basis.
- The furrows on Naro Moru on a daily basis: Aguthi from November 1990 until July 1997, and Thome and Matanya from November 1990 until December 1992, and from January 1994 until July 1997, in parts with large gaps.
- Spot measurements done once or twice monthly on most of the known abstraction points in the years 1993 – 1997, also including many gaps.

Total abstraction amounts were calculated as follows:

- For the period 1993 – 1997 monthly averages were calculated from all abstraction points with the help of an Access Query (Monthly average query, see Appendix A.3.4), based on the assumption that the average of the spot measurements could be taken as

representative for 24 hours a day for the whole month. With the portable pumps this is unrealistic so the rate was halved.

- For the period 1987 – 1992 it was assumed based on an analysis by Lindsay McMillan (not published) that the main driving force for the development of abstraction amounts, including furrows, was rising demand. So a 10% decrease per year was projected backwards from the 1993 – 1997 averages.
- For Naro Moru the measured daily data were taken where available.

5. 2. 2. Naturalisation using the Abstractions Calculation Tool

The Abstractions Calculation Tool is a Microsoft Access Query developed by Aeschbacher (2003) in order to temporally extrapolate abstracted water amounts with the data that can be gathered in a snapshot abstractions campaign. This includes data of the following kinds:

- Measurements: Current meter gaugings (furrows, double gauging with intake turned on and off at gravity pipelines) or volumetric measurements.
- Surveys of the profiles of furrows and the river in order to apply the Strickler-Manning Formula to estimate furrow flow from the river water level (carried out during field work).
- Technical information on the water supply works: Altitude differences, pipe diameters, pumping capacities, etc.
- Information on water demand (how many persons, livestock, irrigated area), storage (tanks), and operation of the technical devices (operating hours per day or week) gathered in the interviews with the water users.

This information is used as parameters for calculating daily estimates of water use above a desired point in Naro Moru catchment. With some adaptations and the necessary data available the Abstractions Calculation Tool could also be used in other catchments.

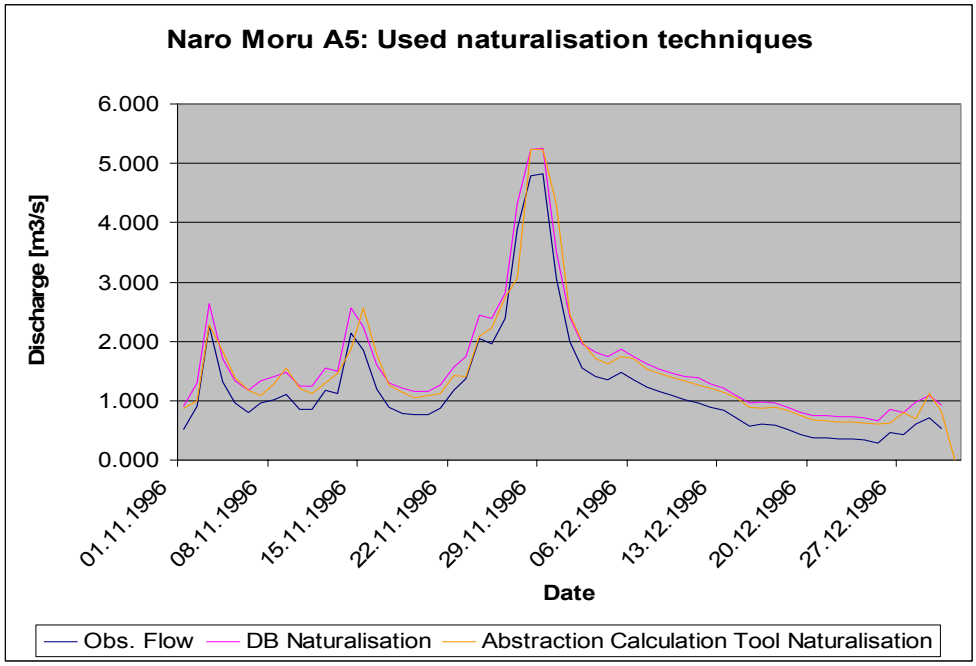

Fig. 5.8: Observed flow at Naro Moru A6 (blue line), naturalized flow using measured data from the NRM[3] database (pink line) and naturalized flow using the Abstractions Calculation Tool (orange line) in November and December 1996.

For the final runs the naturalised values using measured data from the NRM^3 database were used. They resulted in better performance measures than the Abstractions Calculation Tool values. The following reasons are possible:

- The better results with the data series using the NRM^3 measured values are coincidental
- The Abstractions Calculation Tool parameters or structure are not optimised yet
- Not enough information on the developments in the earlier years is included
- The method of extrapolating abstractions from snapshot measurements cannot approximate the real abstractions amounts as closely as regular measurements, even if there are many gaps in the latter.

Fig. 5.8 shows a comparison of observed daily discharge and discharge naturalised with the two described methods. It can be seen that the naturalised series calculated from the NRM^3 database is generally higher and follows the pattern of observed discharge more closely. Fig. 5.9 shows a comparison of the abstracted river water amounts modelled with the Abstractions Calculation Tool to the values measured in the campaigns and by regular monitoring for the Naro Moru A6 catchment. As can be seen, the measured amounts in the years 1990/91 and 1996 show a larger increase of abstractions than is modelled by the Abstractions Calculation Tool, which estimates a quite steady increase over the whole period. This is possibly due to the fact that the modelled amounts are derived only from information gathered in 2002, but there is no proof that the measured amounts from the years 1990/91 and 1996 are more accurate.

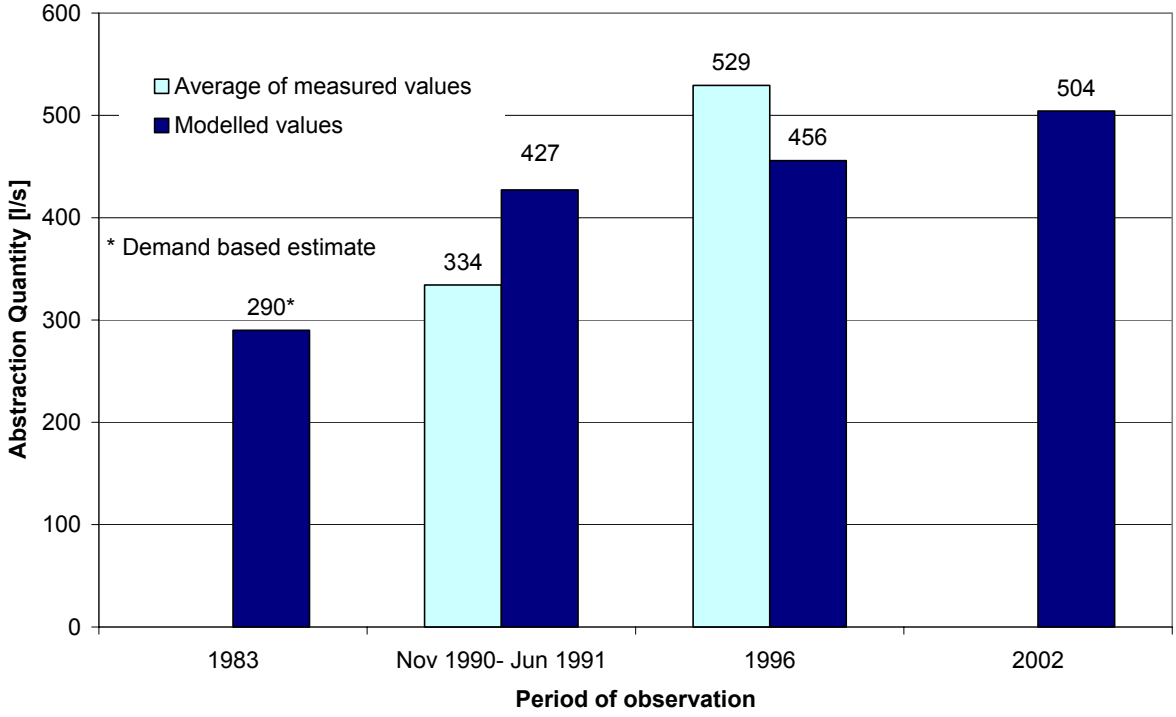

Fig. 5.9: Comparison of total amounts of abstracted river water in the Naro Moru A6 catchment modelled with the Abstractions Calculation Tool (based on information gathered in 2002) to the amounts measured in the NRM^3 monitoring campaigns in the respective years (Source: Aeschbacher 2003).

6. EVALUATION OF THE NRM^3 STREAMFLOW MODEL IN THE STUDY CATCHMENTS

The NRM^3 Streamflow Model is a relatively new hydrological model that has not been extensively used yet. Its original HRU based version by Thomas (1993) was calibrated and validated in the Naro Moru catchment using the two-year period September 1989 – August 1991 for calibration and the period September 1983 – August 1985 for validation. Lindsay McMillan (2003), besides developing further new features (see Table 3.3) adapted the model to a grid-based calculation of the water balance (which greatly facilitates the use of GIS inputs) and evaluated it in the small ephemeral savannah catchment of Mukogodo. The intended use of the model as a tool for water management within the context of NRM^3 and the RWUAs (most of which are active in the meso-scale perennial river catchments on the slopes and in the footzone of Mt. Kenya) requires further evaluation. This section aims at giving such an evaluation, namely of:

- The performance of the model in simulating observed discharges in the study catchments (calibration and validation), with a special focus on the critical low flows;
- The sensitivity of the simulation to parameter values and the question whether the model can be used without extensive parameter calibration;
- The sensitivity of the model to the temporal and spatial resolution of input data;
- The applicability of the model within the context of NRM^3 and the RWUAs with respect to computer requirements and user-friendliness;
- Further need for improvements.

6. 1. CALIBRATION AND VALIDATION STRATEGY

Zappa (2002: 22) summarizes the calibration and validation process as follows:

"The available data sets for hydrological simulations in a catchment are divided into two not overlapping periods. If the global time series is longer than five years, at least three years are used as the calibration period. The remaining period is used for the verification of the model quality without further adjustments of the free parameters. The analysis of the hydrological behaviour of the catchment generally includes the entire available time series. The quality of the model simulation can be assessed by using different observed variables."

As in most hydrological model applications, discharge is the observed variable that model outputs are compared to in this study. Other hydrometeorological observations that would allow a multiple-response verification (like soil moisture time series, groundwater level fluctuations, snow patterns etc.) are not available in the form of time-series.

6. 1. 1. Choice of time periods

In a first step appropriate time periods for calibration and validation had to be selected. The main criteria for the selection were:

- Availability and quality of data
- Length of the time periods to capture the natural variability of the hydrological processes

Based on these criteria the five-year period 1987 – 1991 was chosen for calibration and the following five-year period 1992 – 1996 for validation of the NRM^3 Streamflow Model. The reasons for this choice were:

- The availability of evaporation data: Daily evaporation records in the NRM^3 database start on March 12, 1986.
- The reliability of discharge data: Data recorded by automatic water level recorders are available from the early 1980's on. Discharge data in the NRM^3 database have been quality controlled including the revision of the rating equations up to 1997; after 1997, the rating equations have not been changed or updated anymore and thus the reliability of discharge data decreases.
- The availability of abstractions data has been discussed in the previous sections. Monitoring was most intensive in the period 1990 – 1997. Before 1990 the impact of the abstractions was not so great yet (apart from the furrows, that have been existing for a longer time span, the development of most abstraction points took place in the 1990's). Between 1997 and 2001 there is no quantitative information on the development of abstraction amounts; statements of water users even point to the possibility that the number of abstraction points peaked in the year 2000, but no data is available on this.
- The natural interannual variability of the climate and the hydrological processes: In the beginning the two-year period with the highest availability of abstractions data (1990 – 1991) was chosen for calibration. As it turned out, various parameter values would have been chosen differently than if a longer period was used. For example, the groundwater discharge parameters, if fitted to a period of below-average flows (like 1991), will produce a too fast recession of the hydrograph in periods with more rainfall.

The selected time series were examined and improbable or faulty data excluded. A list of the excluded data with the respective reasons for exclusion is given in Table 6.1.

Dataset	**Excluded dates**	**Reason**
Discharge A3	29.04.1988	Very high peak
	19.07.1988	Very high peak
Discharge A4	24.04.1988	Very high peak
Discharge A5	03.05.1994 – 17.05.1995	Weir leakage
Discharge A8	02.08.1991 – 17.12.1991	Constant flow values – probably needle of water level recorder stuck
Rainfall NM Met Station	11.04.1989	Too heavy rainfall with no corresponding observed flow peak or after the flow peak– probably cylinders were not emptied or measured for some days
Rainfall Teleki	06.07.1989	
Rainfall NM Met Station	09.12.1989	
Rainfall Moorland	01.09.1995	
Rainfall Teleki	06.10.1995	

Table 6.1: Data excluded from the calibration and validation of the NRM^3 Streamflow Model

6. 1. 2. Calibration procedure

The calibration of the NRM^3 Streamflow Model is completed manually by repeatedly entering sets of parameter values in the control file and running the model. Parameter values can be estimated from the characteristics of the hydrograph or background knowledge on the catchment, or determined by trial and error. In most cases a first set of values was estimated based on catchment or hydrograph characteristics and then modified by repeated model runs. The outputs of each model run with a given set of parameter values are compared to observed values and evaluated

a) by a graphical comparison between observation and simulation for a subjective estimation of the simulation quality and
b) by means of objective measures of model performance: statistical criteria (Equations 6.1 to 6.5) and the quantitative differences between characteristics of the observed and simulated flow data.

Attention was not primarily directed to reaching the best performance measures – more importance was given to using physically plausible parameter values. Adaptations of the parameter values were only where they can be argumented based on physical facts.

The catchment specific parameters that were subject to calibration in this study are:

a) The groundwater discharge parameters:

R1COEFF	Groundwater Discharge Coefficient (Long term)
R2COEFF	Groundwater Discharge Coefficient (Short term)
SSZTH	Groundwater Discharge Threshold
SCOEFF	Deep Seepage Coefficient

The first three of these parameters shape the form of the hydrograph in the time of flow recession after a peak. They can be fitted by trial and error or estimated from observed hydrographs with a semi-quantitative method which is described in Section 6.3.1.1.

b) The Runon Coefficient ROCOEFF

The runon coefficient makes a constant proportion of surface runoff reinfiltrate on downslope cells. It was introduced supposing that Hortonian overland flow is a dominant process in the region (Thomas 1993). It has to be fitted by trial and error.

The other parameters of the NRM^3 Streamflow Model (like the curve numbers, the soil layer depths etc., see list in Table 3.2) did not have to be calibrated in the course of this study – their values, which should be representative for the Upper Ewaso Ng'iro Basin, could be taken from the work of McMillan (2003). The topographic parameters CSLOPE and HYDLEN only affect the simulation of daily peak flows (daily average discharge is not affected), for which there are no observed prepared and quality-controlled datasets available.

In each of the catchments first the catchment specific parameters were fitted; the resolution of the base grid is 500m. With the resulting best set of parameter values additional runs were then performed to determine the effect of other variations in inputs: resolution, selection of rain gauges, land use map of 1988 or 1995, and the use of the season-dependent dynamic curve numbers.

6. 1. 3. Model performance measures

6. 1. 3. 1. Statistical measures of model performance

The objective statistical coefficients which were used to evaluate simulated (S) with respect to the observed (O) values are:

The coefficient of determination (r^2):

$$R^2 = \left(\frac{\sum_{i=1}^{N} (S_i - \overline{S})(O_i - \overline{O})}{\sqrt{\sum_{i=1}^{N} (S_i - \overline{S})^2 \sum_{i=1}^{N} (O_i - \overline{O})^2}} \right)^2 \qquad (6.1)$$

with N being the number of observations. r^2 tends to 1 the more the simulated values have similar dynamics with respect to the observations.

The Nash and Sutcliffe Efficiency Score E_2:

$$E_2 = 1 - \frac{\sum_{i=1}^{n} | O_i - S_i |^2}{\sum_{i=1}^{n} \left| O_i - \left[\frac{1}{n} \sum_{i=1}^{n} O_i \right] \right|^2} \qquad (6.2)$$

E_2 quantifies the mean improvement of the model compared with the mean of the observations. Any positive value represents an improvement. E_2 is 0 when the estimation of the observed values by the simulation is no better than using the mean of the observed values as an estimate.

Both measures were applied to daily and decadal resolution of the output data and the coefficient of determination also to daily low flows below a threshold value and to the annual NMQ30 (see next section).

In literatures several thresholds of these measures to accept or reject a simulation are proposed: A generally accepted minimum of E_2 is 0.5 (Zappa 2002: 64). For r^2 different thresholds are used, ranging between 0.5 and 0.8.

Additionally the following measures were considered:

The Root Mean Square Error (RMSE):

$$RMSE = \sqrt{\frac{\sum_{i=1}^{N} (S_i - O_i)^2}{N}} \qquad (6.3)$$

The Root Mean Square Error allows to quantify the magnitude of the deviation of the simulated from the observed values.

The mean absolute deviation (MAD):

$$MAD = \frac{\sum_{i=1}^{N} |S_i - O_i|}{N} \qquad (6.4)$$

The mean absolute deviation must be minimised to obtain the best possible quantitative agreement for the simulated variable with respect to the observation.

6. 1. 3. 2. General flow measures

The following measures describing characteristics of the hydrograph were compared from observed and simulated data per year and over the whole calibration/validation period:

- Mean, maximum, and minimum discharge
- Median and quartiles
- Total runoff

6. 1. 3. 3. Seasonal distribution measures

The Pardé Coefficient PC_i is a dimensionless measure to describe the discharge regime of a river. It is calculated for each month as the ratio of the average monthly runoff (MQ_i) and the average yearly runoff (MQ_y) (Weingartner and Aschwanden 1989):

$$PC_i = \frac{MQ_i}{MQ_y} \qquad i = 1 \ldots 12 \qquad (6.5)$$

In addition, the monthly deviation of simulated from naturalized observed values in percent was considered.

6. 1. 3. 4. Low flow measures

Special attention is directed towards the simulation of low flows, as they occur in the critical periods of drought when water demand is highest. The model should be able to simulate water yield in low flow periods and their duration as well as the interannual variability of the lowest flows, if it is to be used for streamflow prediction in the context of the RWUAs. The conventional measures used for the assessment of simulation quality tend to give a higher weight to peak flows because they consider the absolute deviations of the simulated from the observed values, which are of course higher around the flow peaks. This is why some additional specific low flow measures as proposed by Smakhtin (2001) were considered in this study to assess the quality of low flow simulation:

- The duration (and the water yield) of observed and modelled low flow periods, "low flow" being defined as periods when discharge is below a certain low flow threshold. As threshold for the low flow periods the median of discharge from a catchment was chosen, based on the fact that this figure closely corresponds to the average water demand in the year 2002 in most catchments, and the situation gets critical when water demand is higher than what flows in the river.
- The coefficient of determination of the data which lie below the low flow threshold.
- The NMQ30, which is the mean discharge of the 30 consecutive days with the lowest flow in the hydrological year (from May to June) (that is also subject to analysis in the work of Jos Aeschbacher 2003) and its coefficient of determination between simulated

and observed values, as a measure of how well the interannual variability of the lowest flows is captured.

6. 1. 3. 5. Weight given to the used measures

Of course considering all above mentioned measures of model performance in combination does in most cases not give a clear answer to the question which model run is best. Some model runs will always perform better in some respects while others perform better in other respects. So the above described measures of model performance have to be given an order of importance. In this study the following measures were given priority to decide which runs performed best:

- The coefficient of determination and the efficiency score; in contradicting cases the coefficient of determination was given priority because it is the more widely used measure;
- The difference between simulated and observed runoff in mm/year (total water yield);
- The coefficient of determination of the yearly NMQ30.

After setting these priorities, it is still possible that two or more model runs show equivalent overall performance. In this case the parameter set closest to the originally estimated (and physically plausible) one was chosen for evaluation and use in the environmental change scenarios.

6. 1. 4. Production of the input datafiles

The time series data format required by the NRM^3 Streamflow Model is an ASCII text file structure. These files are the easiest produced copying the Access database values into Excel, where they can be edited and then saved in the desired format.
For GIS inputs, the CDE database maps in ArcInfo format were used as basis and converted to the Idrisi16 format required by the model. Layers with two different extensions were used (corner points in UTM coordinates):

a) Long. 278400 – 312900
Lat. 9979000 – 9985000

These layers were used for Naro Moru A3 – A5 catchments and only in a resolution of 500 m. This way the model could be run under the Windows system for these catchments, which were given priority in calibration and validation due to the best data availability.

b) Long. 265000 – 312900
Lat. 9975000 – 5000

These layers comprise all study catchments (A3 – A6, A8, A9) and were used in 50, 100, 500 and 1000 m resolution.
Guidelines for producing the input files are given in Appendix C.4.

6. 1. 5. Analysis of outputs

As the NRM^3 Streamflow Model in its present version only prints the daily catchment water balance in the outfile (a text file with the extension .out), a Microsoft Excel tool, the StreamflowAnalysisMacro (see Appendix C.7.), was developed to quickly analyse the model outputs for the calibration and validation periods. The outfile of a model run can be opened in

Excel and the data copied to the data table ("alldata") in this Macro Spreadsheet. When the Macro is run all above mentioned measures of model performance are calculated and graphs of the output variables in different resolutions are produced. Catchment-specific parameters (catchment size, low flow threshold) and information on the model run have to be entered into the table "alldata" of "StreamflowAnalysisMacro".
An overview of all model runs presented in the following sections is given in Appendix D.1.

6. 2. CALIBRATION AND VALIDATION RESULTS

6. 2. 1. Naro Moru A5 catchment

Priority was given to the Naro Moru A5 catchment in calibration and validation, because there is the highest availability of data on rainfall (stations along the profile up to the peak of Mt. Kenya) and river water abstractions, and the catchment comprises all major land use classes from the alpine zone to the footzone of Mt. Kenya. A summary of catchment characteristics is given in Box 6.1.

Naro Moru A5 catchment

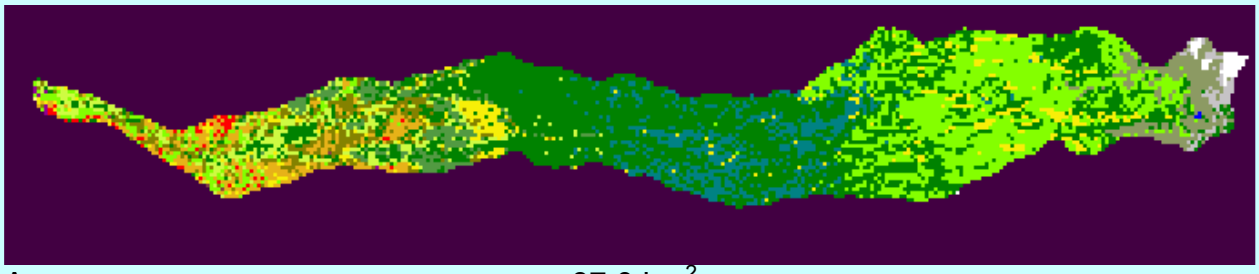

Area:	87.0 km^2
Lowest point:	1961 m a.s.l.
Highest point:	5080 m a.s.l.
Average elevation:	3036 m a.s.l.
Catchment slope:	22.75%
Average base curve number:	64.32

Land use:

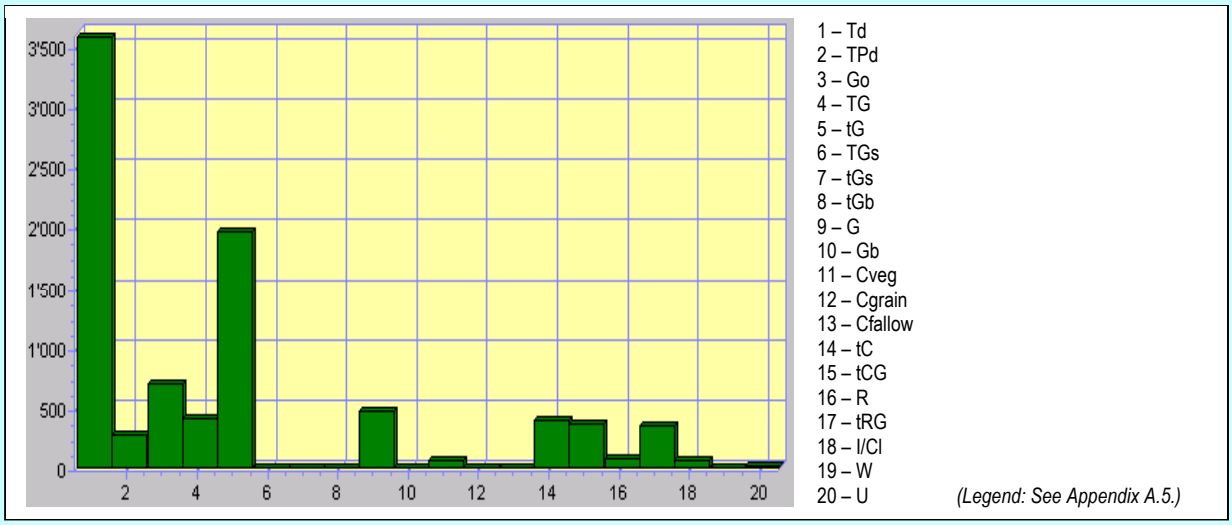

Box 6.1: Naro Moru A5 catchment characteristics. The map layer is in 100 m resolution.

6. 2. 1. 1. Calibration

Run Name	Res.	R1 COEFF	R2 COEFF	SSZTH	S COEFF	RO COEFF	r^2 daily	E_2 daily	r^2 dec.	E_2 dec.	S – O /year [mm]	r^2 NMQ30
a5500gw3	**500**	**0.03**	**0.3**	**20**	**0**	**0**	**0.655**	**0.693**	**0.820**	**0.760**	**-49.157**	**0.618**
a5500ro1	500	0.03	0.3	20	0	0.1	0.655	0.692	0.820	0.760	-49.167	0.618
a5100a01	100	0.03	0.3	20	0	0	0.656	0.690	0.822	0.760	-45.779	0.622

Table 6.2: Calibration runs in the Naro Moru A5 catchment with equivalent overall performance. The parameter set of a5500gw3 was chosen as final parameter set for the A5 catchment. Abbreviations are listed on page 12; run names are explained in Appendix D.1.1.

Table 6.2 shows the best performing calibration runs in the Naro Moru A5 catchment. The r^2 and E_2 scores for daily resolution of the discharge outputs are between 0.6 and 0.7. For decadal data r^2 is above 0.8 and E_2 is above 0.7. This indicates a fair reproduction of runoff-generation dynamics in high and low flow periods. Annual runoff is underestimated by 49.16 mm/year or 11.25%, which is a large percentage but is opposed to the overestimation in the validation period.
The model run a5500gw3 shows the best overall performance, but the runs a5500ro1 (runon coefficient set to 0.1) and a5100a01 (100m grid resolution) performed almost equivalently, if not better in some respects. Nevertheless the parameter set of a5500gw3 was chosen as the final parameter set for A5, because the model should always be kept as simple as possible. Daily simulated and observed naturalized discharge for the calibration period is shown in Fig. 6.1. It can be seen that the greatest deviations occur at observed flow peaks following rains that were probably not recorded by the measuring network, and in periods of high observed baseflow (which could not be reproduced by the model due to the constant groundwater coefficients).

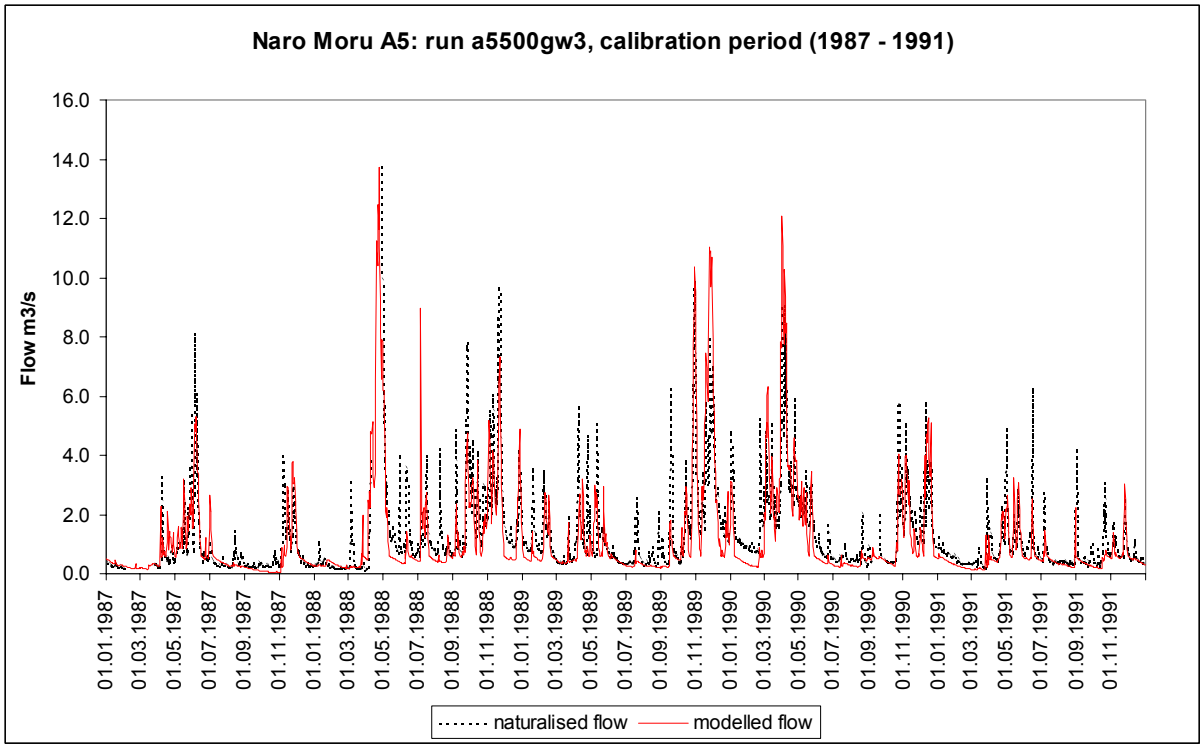

Fig. 6.1: Calibration result at Naro Moru A5 (daily data).

6. 2. 1. 2. Validation

Run Name	Res.	R1 COEFF	R2 COEFF	SSZTH	S COEFF	RO COEFF	r^2 daily	E_2 daily	r^2 dec.	E_2 dec.	S – O /year [mm]	r^2 NMQ30
a5500gw3	**500**	**0.03**	**0.3**	**20**	**0**	**0**	**0.564**	**0.513**	**0.721**	**0.659**	**13.044**	**0.906**
a5500ro1	500	0.03	0.3	20	0	0.1	0.564	0.513	0.721	0.659	13.044	0.906
a5100a01	100	0.03	0.3	20	0	0	0.563	0.499	0.722	0.646	16.132	0.903

Table 6.3: Validation runs in Naro Moru A5 catchment. Abbreviations are listed on p. 12; run names are explained in Appendix D.1.1.

The validation period covers the years 1992 – 1995. Unfortunately the period 03/05/1994 – 18/05/1995 had to be removed from the observed discharge data due to weir leakage. This has to be kept in mind when looking at the statistical measures for the years 1994 and 1995.
The measures of model performance given in Table 6.3 show that the NRM[3] Streamflow Model is able to simulate the daily and decadal hydrographs with the parameter set of the run a5500gw3 with r2 values of 0.56 for daily and 0.72 for decadal resolution and E_2 scores of 0.51 for daily and 0.66 for decadal resolution. The run with the runon coefficient set to 0.1 performed equivalently, while the run in 100 m resolution interestingly shows slightly lower values in almost all performance measures, indicating that the land use map or the calibration of the curve numbers might be inaccurate. Total runoff is now slightly overestimated, in contrast to the calibration period. The daily hydrograph for the validation period is shown in Fig. 6.2.

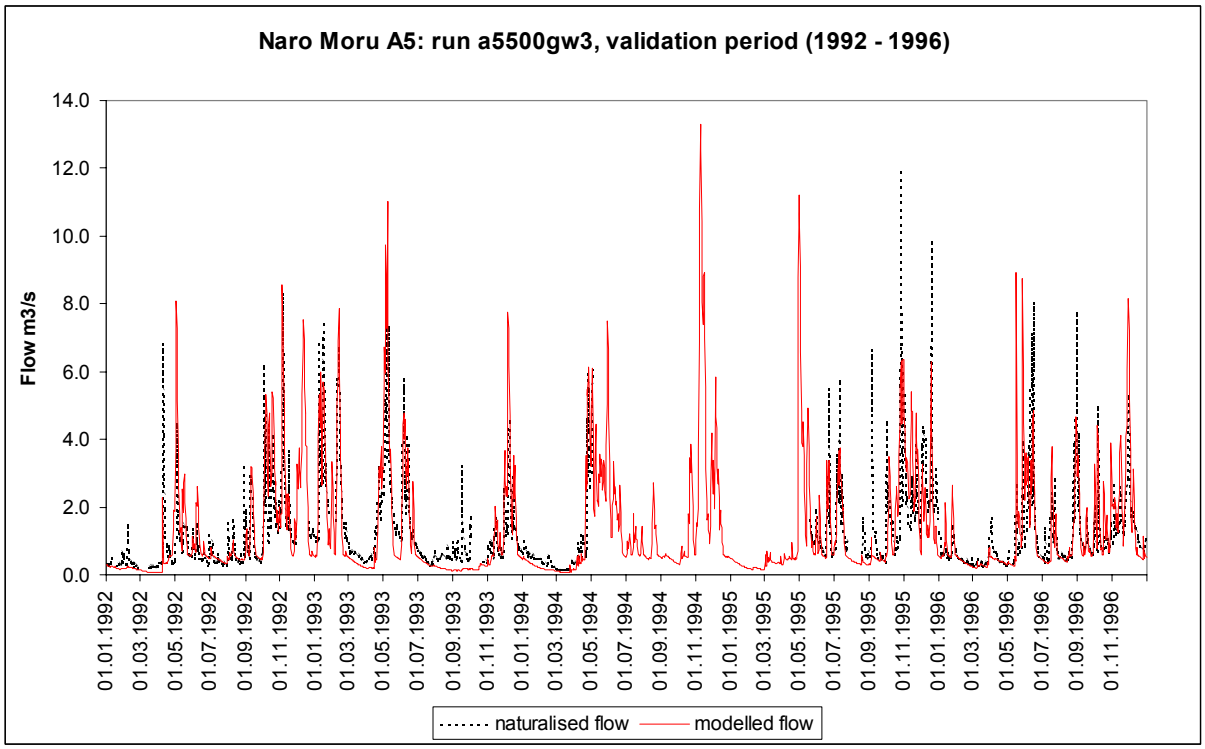

Fig. 6.2: Validation result at Naro Moru A5 (daily data). The period 03/05/1994 until 18/02/1995 had to be removed from the observed discharge data due to weir leakage.

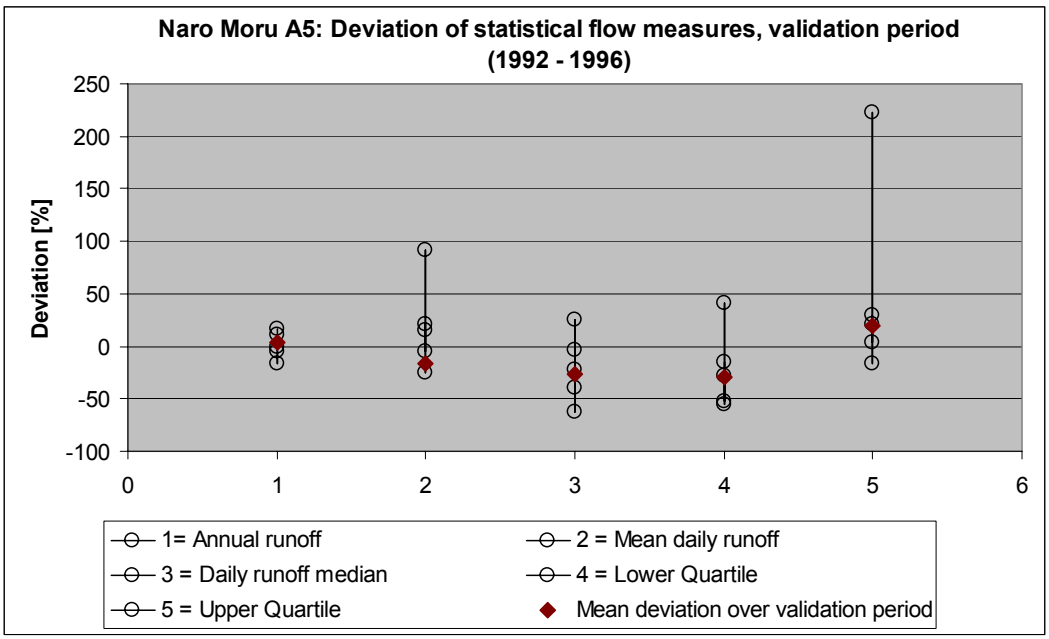

Fig. 6.3: Deviations of simulated statistical flow measures with respect to the naturalized observed values over the whole validation period (diamonds) and for single years (circles) in percent.

Annual flow statistics: The deviation in percent of total annual runoff, median, upper and lower quartile per year and over the whole validation period is shown in Fig. 6.3. It has to be considered that large parts of the 1994/95 hydrograph are missing from the observed records. The figures show that although total annual runoff is overestimated by 4% over the calibration period it is mainly the flood flows that are overestimated. Mean, median and lower quartile are simulated lower than observed.

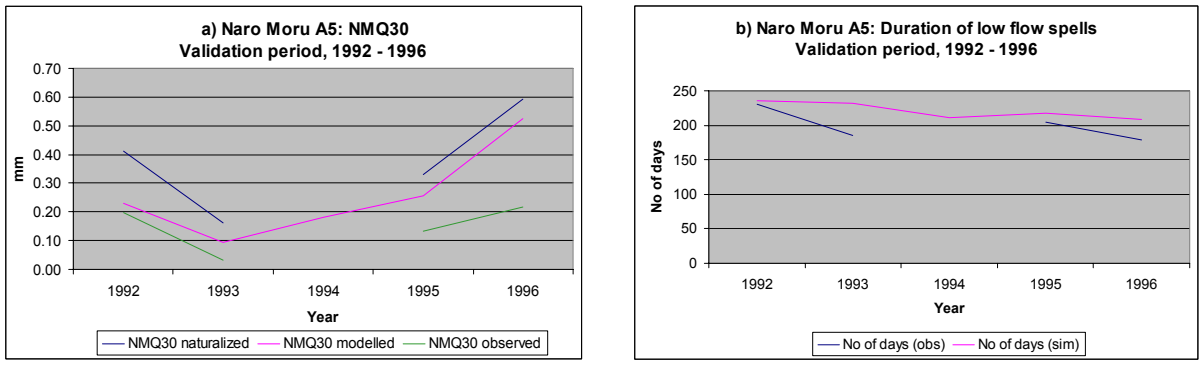

Fig. 6.4: Simulated, observed and naturalized NMQ30 in the validation period (a) and duration of low flows below the low flow threshold. Since NMQ30 was in accordance with the thesis of Jos Aeschbacher (2003) calculated for the hydrological year from May to April, the NMQ30 of 1994 would lie exactly in the missing data period.

Low flows: Low flows tend to be underestimated by the model. Modifying the groundwater discharge coefficients can only help this up to a certain degree without sacrificing the ability of the model to follow the observed pattern of the hydrograph. Especially after periods of heavy rainfall the real catchment sustains a much higher baseflow than the model simulates.

Partly the underestimation of low flows may also be due to an overestimation of abstractions (see also Aeschbacher 2003). The comparison of the modelled, naturalized and unnaturalized observed NMQ30 (Fig. 6.4) shows that it is generally underestimated by the model with respect to naturalized observed discharge, but the modelled values are between 30 and 300 l/s higher than the unnaturalized observed amounts. The modelled NMQ30 lies between the observed and the naturalized values in all years, however, and the interannual pattern is followed fairly well.
The duration of flows below the chosen low flow threshold is predicted too long by the model. Please note again the missing observed hydrograph values in 1994/95.

Seasonal distribution of runoff: As shown in Fig. 6.5 the runoff is underestimated in dry months (Jan – Mar, Jul – Sep) while wet season runoff is overestimated. This is again due to the tendency of the model to overestimate peaks and underestimate baseflow, which under the current model structure (single groundwater reservoir, constant groundwater coefficients) cannot be improved in calibration (see also Section 6.3.1.1).

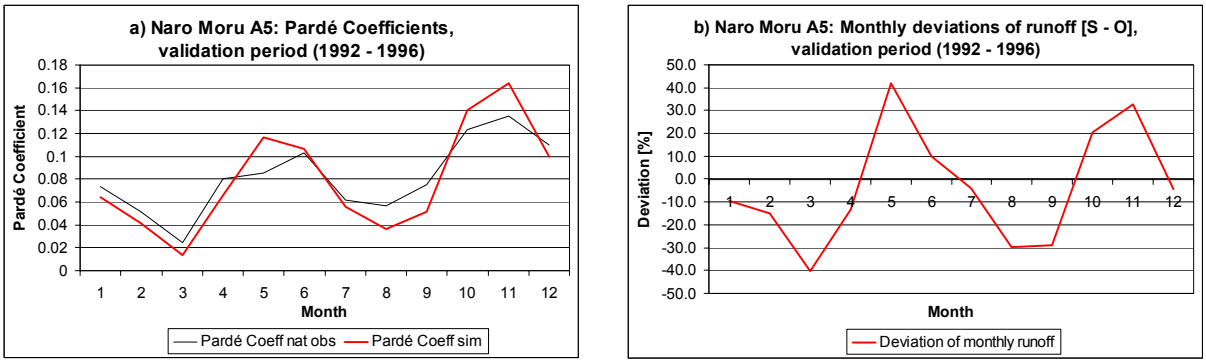

Fig. 6.5: Simulated and naturalized observed Pardé Coefficients (a) and monthly deviations of simulated from observed runoff in percent (b) in the validation period.

6. 2. 2. Naro Moru A3 catchment

A3 is the catchment of Naro Moru North that reaches from the peak down to near the lower boundary of the forest zone. A summary of catchment characteristics is given in Box 6.2.

Naro Moru A3 catchment characteristics

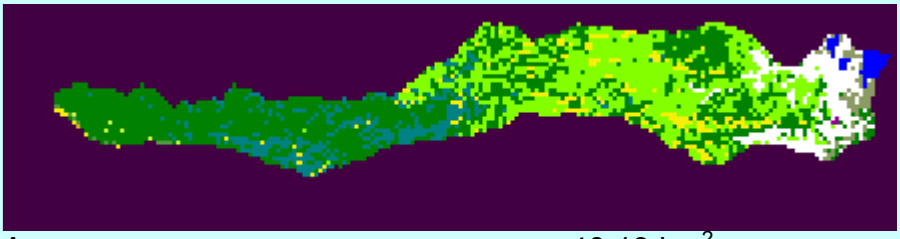

Area:	40.13 km^2
Lowest point:	2298 m a.s.l.
Highest point:	5080 m a.s.l.
Average elevation:	3541 m a.s.l.
Catchment slope:	31.38%
Average base curve number:	65.86

Land Use:

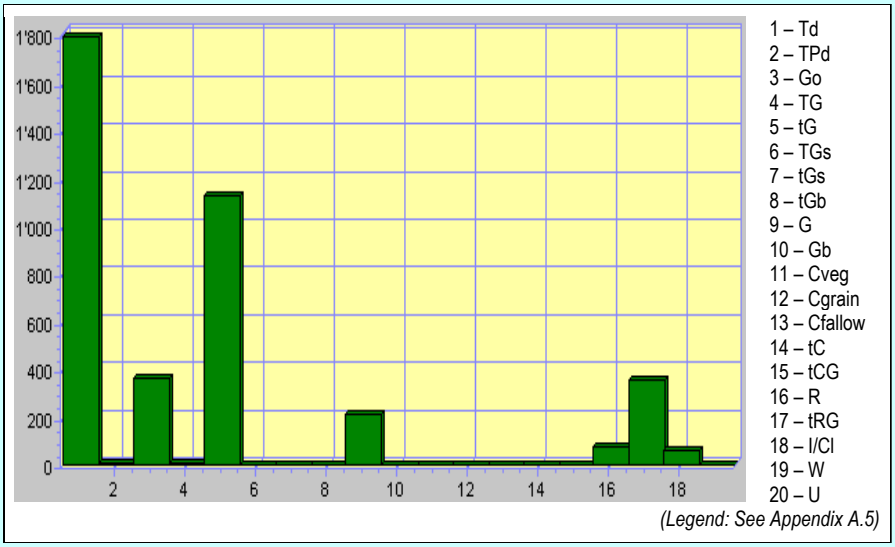

(Legend: See Appendix A.5)

Box 6.2: Naro Moru A3 catchment characteristics. The map layer resolution is 100 m.

6. 2. 2. 1. Calibration

Run Name	Res.	R1 COEFF	R2 COEFF	SSZTH	S COEFF	RO COEFF	r^2 daily	E_2 daily	r^2 dec.	E_2 dec.	S – O /year [mm]	r^2 NMQ30
a3500a03	**500**	**0.03**	**0.4**	**26**	**0**	**0**	**0.306**	**0.514**	**0.533**	**0.917**	**7.804**	**0.960**
a3500a04	500	0.04	0.4	34	0	0	0.298	0.554	0.520	0.926	11.488	0.930
a3500ro1	500	0.03	0.4	26	0	0.1	0.306	0.514	0.533	0.917	7.804	0.960

Table 6.4: Calibration runs in the Naro Moru A3 catchment with equivalent overall performance. The parameter set of a3300a03 was chosen as final parameter set for the A5 catchment. Abbreviations are listed on p. 12; run names are explained in Appendix D.1.1.

The scores of three almost equivalently performing model runs in the Naro Moru A3 catchment (Table 6.4) show a big difference between the Coefficient of determination (r^2) and

the Nash and Sutcliffe Efficiency score (E_2). The latter lies above the threshold 0.5 mentioned in Section 6.1.3. for daily and decadal data, while r^2 is below its respective threshold. The low r^2 is largely due to peak flow outliers (mainly in the year 1988) and the small recorded part of the 1989 hydrograph that does not at all match the modelled flows (see Fig. 6.6). Total runoff is overestimated by 7.8 mm/year or 2.12%. The overall performance measures indicate that the modelling results provide a good estimate of discharge, although the pattern (mainly the peaks) is not followed well in some parts. Again this can be attributed to missing rainfall inputs (the gauge Moorland, located in the middle of the catchment, has many data gaps, see Appendix A.1.2.).

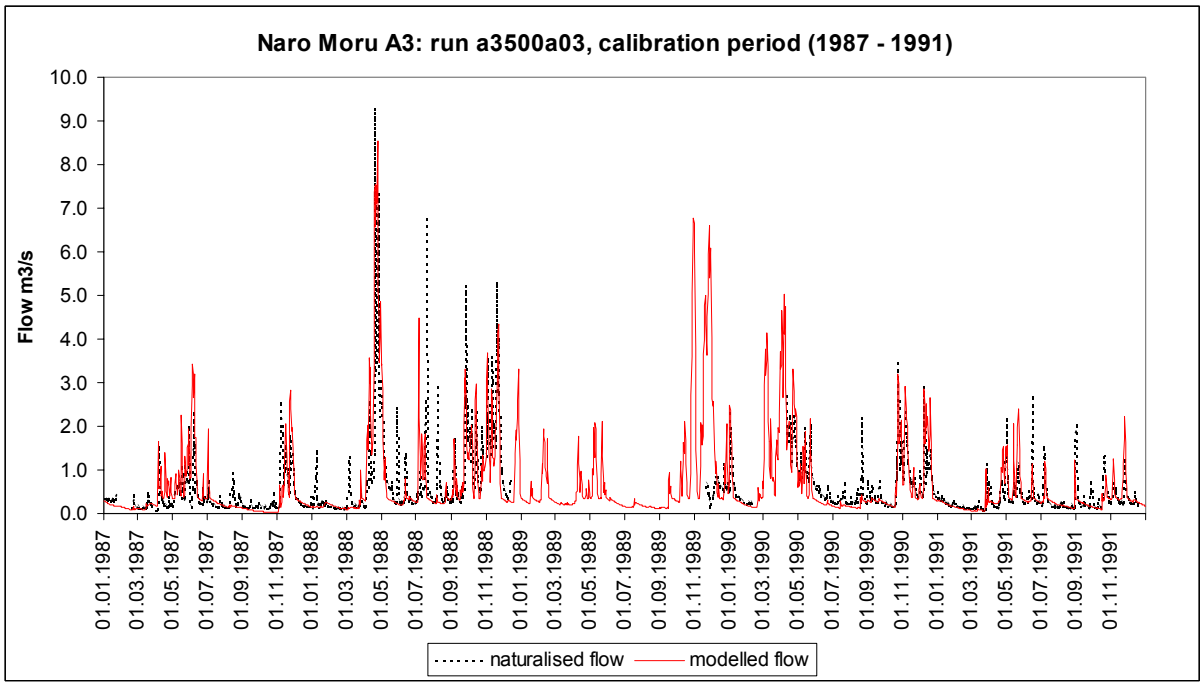

Fig. 6.6: Calibration result at Naro Moru A3 (daily data).

6. 2. 2. 2. Validation

Run Name	Res.	R1 COEFF	R2 COEFF	SSZTH	S COEFF	RO COEFF	r^2 daily	E_2 daily	r^2 dec.	E_2 dec.	S – O /year [mm]	r^2 NMQ30
a3500a03	**500**	**0.03**	**0.4**	**26**	**0**	**0**	**0.578**	**0.280**	**0.841**	**0.892**	**81.867**	**0.914**
a3500a04	500	0.04	0.4	34	0	0	0.559	0.391	0.845	0.909	81.211	0.940
a3500ro1	500	0.03	0.4	26	0	0.1	0.578	0.280	0.841	0.892	81.839	0.914

Table 6.5: Validation runs in the Naro Moru A3 catchment. Abbreviations are listed on p. 12; run names are explained in Appendix D.1.1.

In the validation period r^2 is higher – around 0.58 for daily and 0.85 for decadal values, while E_2 is low (around 0.3) for daily values and high (around 0.9) on the decadal time-step. Annual runoff is now overestimated by 82 mm/year or 16.5%, the same trend towards overestimation in the validation period as at A5. The run a3500a04 shows better overall performance in the validation period than the chosen run a3500a03, which illustrates the concept of equifinality (there is no "best" parameter set).
The results at A3 show how much the performance measures depend on capturing flow peaks (or not): the coefficient of determination will increase if an observed peak is reproduced by the model – but mainly its pattern, not its magnitude. The Nash and Sutcliffe score reacts very strongly to over- respectively underestimation of absolute values (this is why it is so much

higher on the decadal time-step –peaks disappear there). The simulated and naturalized observed daily hydrographs for the validation period are shown in Fig. 6.7.

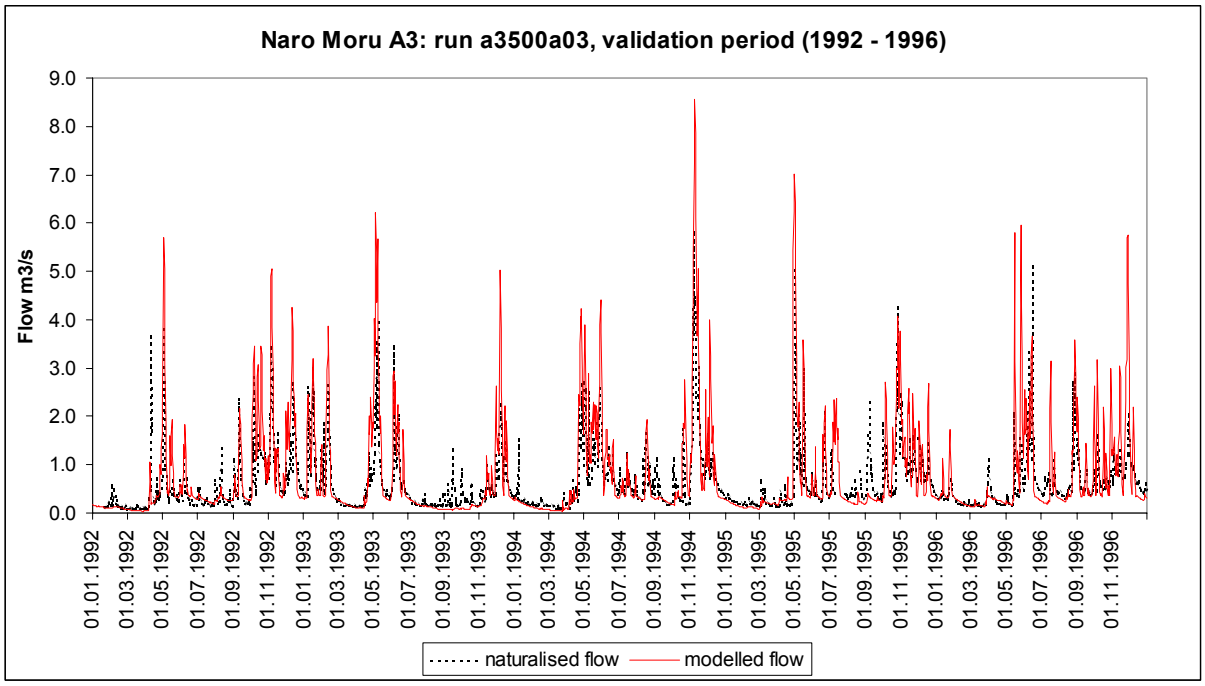

Fig. 6.7: Validation result at Naro Moru A3 (daily data).

Annual flow statistics: The deviations of annual runoff and mean of daily runoff over the whole validation period as well as for the single years are positive in the range of 20%, illustrating the overestimation of runoff over the whole period (see Fig. 6.8). Low flows are again underestimated as indicated by the negative deviations of median and lower quartile, while the deviation of the upper quartile with 9% indicates a not too great overestimation of flood flows compared to total runoff. The range of deviations is smaller than at A5 mainly because there are only small gaps in the recorded hydrograph in the validation period.

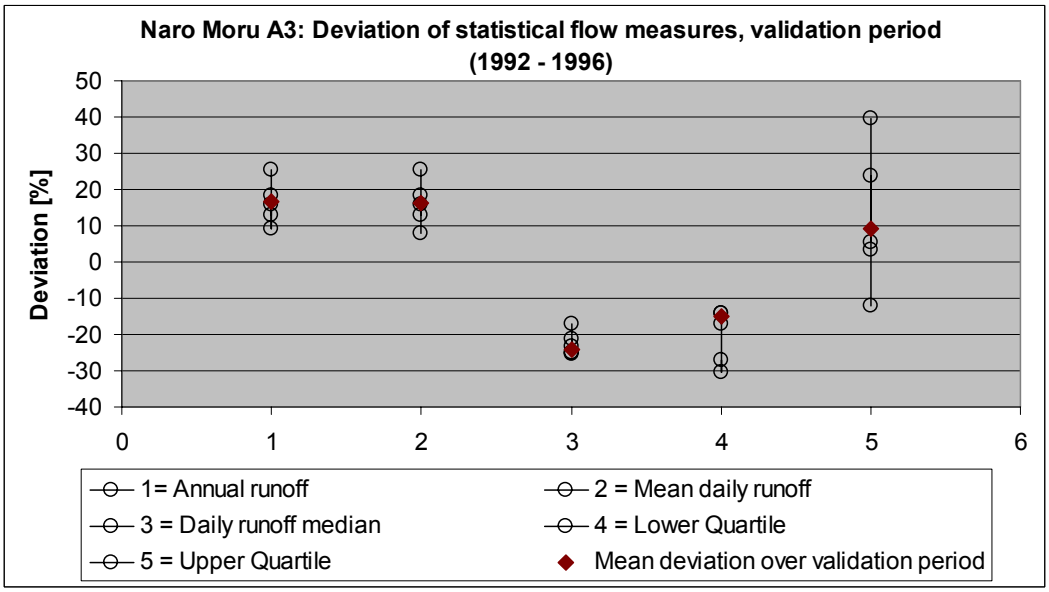

Fig. 6.8: Deviations of simulated statistical flow measures with respect to the naturalized observed values over the whole validation period (diamonds) and for single years (circles) in percent.

Low flows: The NMQ30 is underestimated and the duration of flows below the threshold (0.32 m^3/s for A3) is overestimated. As can be seen in Fig. 6.9, the interannual pattern is again followed fairly well. One reason for the underestimation of low flows could be that too high evaporation values are interpolated for the upper catchment regions (the highest recording evaporation pan being situated at 3050 m a.s.l., which is almost 500 m below the average catchment altitude).

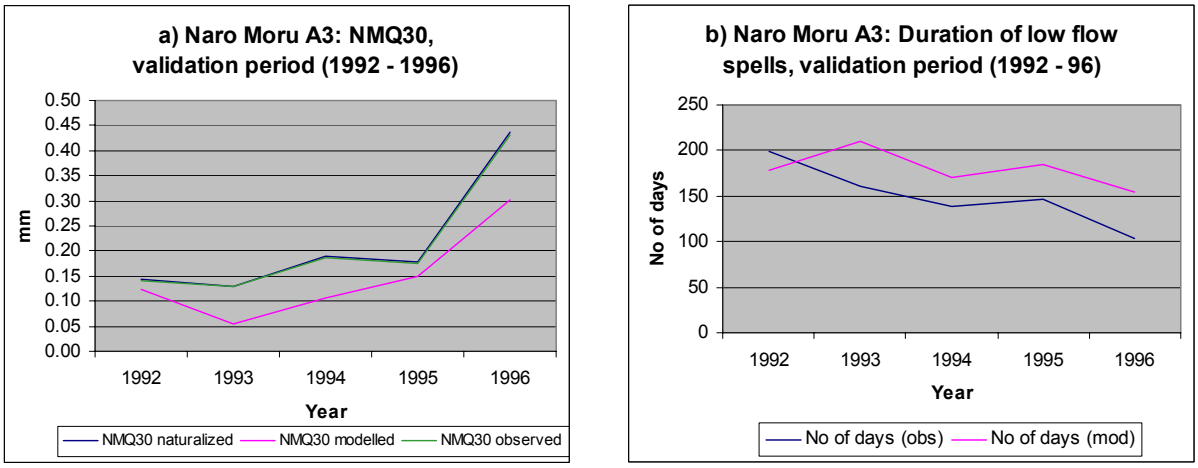

Fig 6.9: Simulated, observed and naturalized NMQ30 in the validation period (a) and duration of low flows below the low flow threshold (b).

Seasonal distribution of runoff: Fig. 6.10 shows an overestimation of runoff in the wetter months (April – June, October – December) of 11% (June) to 67% (May) while in the driest months too little discharge is predicted (-1.6% in January, -55.4% in March). This problem could only be solved by modifying the groundwater discharge simulation within the NRM^3 Streamflow Model structure (refer to Section 6.3.1.1).

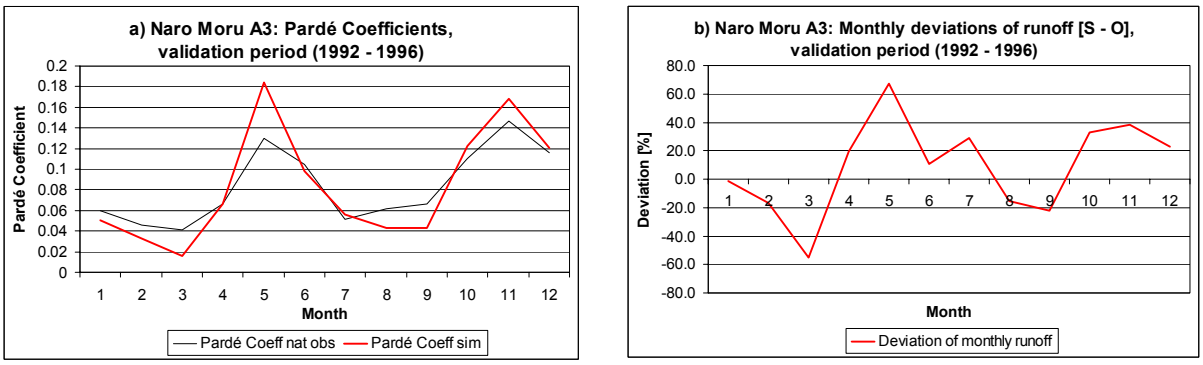

Fig. 6.10: Simulated and naturalized observed Pardé Coefficients (a) and monthly deviations of runoff in percent (b) for the validation period at A3.

6. 2. 3. Naro Moru A4 catchment

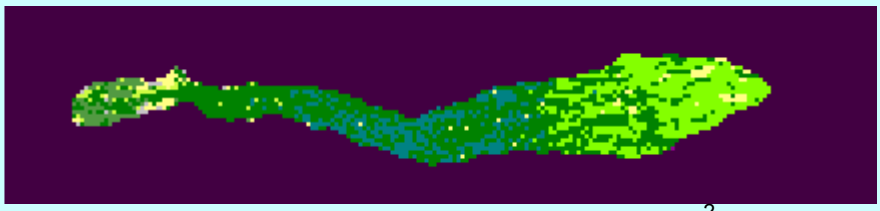

Area:	23.06 km^2
Lowest point:	2199 m a.s.l.
Highest point:	4146 m a.s.l.
Average elevation:	3017 m a.s.l.
Catchment slope:	24.05%
Average base curve number:	62.44

Land Use:

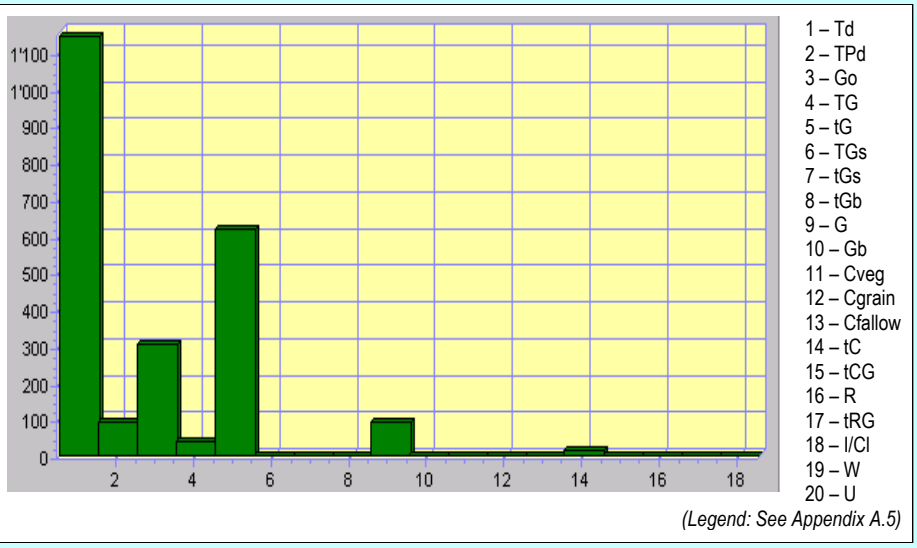

(Legend: See Appendix A.5)

Box 6.3: Naro Moru A4 catchment characteristics. The map layer resolution is 100 m.

Naro Moru A4 is the catchment of Naro Moru South. This tributary of Naro Moru has its source at about 3900 m a.s.l. south of the Naro Moru North valley; the catchment thus crosses only the ecological zones moorland and forest. A summary of catchment characteristics is given in Box 6.3.

6. 2. 3. 1. Calibration

Run Name	Res.	R1 COEFF	R2 COEFF	SSZTH	S COEFF	RO COEFF	r^2 daily	E_2 daily	r^2 dec.	E_2 dec.	S – O /year [mm]	r^2 NMQ30
a45003	500	0.05	0.5	35	0	0	0.583	0.628	0.744	0.982	-178.12	0.468
a45004	**500**	**0.04**	**0.4**	**30**	**0**	**0**	**0.595**	**0.625**	**0.741**	**0.982**	**-178.94**	**0.514**
a4500ro1	500	0.04	0.4	30	0	0.1	0.595	0.625	0.741	0.982	-178.99	0.514

Table 6.6: Calibration runs in the Naro Moru A4 catchment with equivalent overall performance. The settings of run a45004 were chosen as the final parameter settings. Abbreviations are listed on p. 12; run names are explained in Appendix D.1.1.

The Coefficient of Determination and the Nash and Sutcliffe Efficiency score for daily and decadal outputs indicate a fair to good reproduction of runoff dynamics. Annual runoff, however, is underestimated by 179 mm or almost 26%. This is probably caused by too low interpolated rainfall (which is best visible in the hydrograph towards the end of the calibration period, Fig. 6.11): Various authors locate the maximum of precipitation at different altitudes between 3000 and 3500 m a.s.l. (Decurtins 1992: 40); the rain gauges used in this study are situated at 3050 m a.s.l. (Met Station) and 3771 m a.s.l. (Moorland). So there is no rain gauge to capture the probable maximum of precipitation. In the other study catchments this systematic error could be made up for by the fact that the highest rain gauge with daily data available, Teleki, is located at 4262 m a.s.l., and above this altitude precipitation decreases even more according to Decurtins (1992: 40).

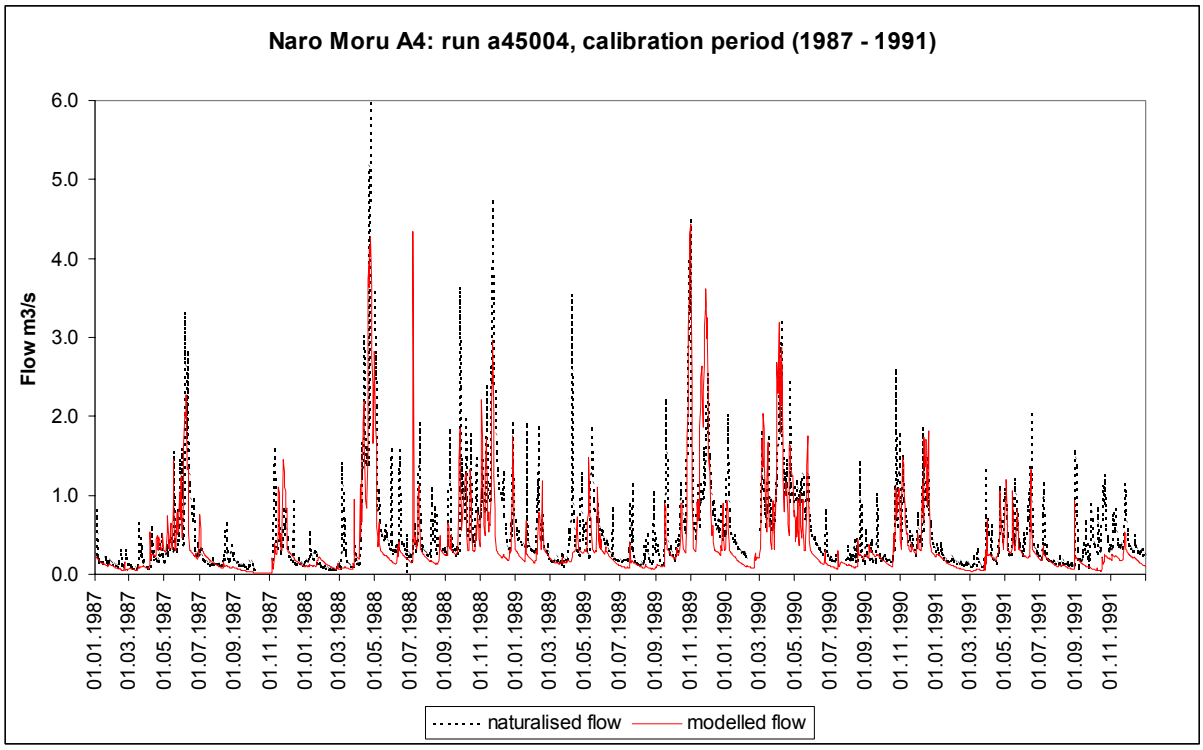

Fig. 6.11: Calibration result at Naro Moru A4 (daily data).

6. 2. 3. 2. Validation

Run Name	Res.	R1 COEFF	R2 COEFF	SSZTH	S COEFF	RO COEFF	r^2 daily	E_2 daily	r^2 dec.	E_2 dec.	S – O /year [mm]	r^2 NMQ30
a45003	500	0.05	0.5	35	0	0	0.517	0.405	0.635	0.978	-92.807	0.047
a45004	**500**	**0.04**	**0.4**	**30**	**0**	**0**	**0.520**	**0.362**	**0.635**	**0.977**	**-91.337**	**0.037**
a4500ro1	500	0.04	0.4	30	0	0.1	0.520	0.362	0.635	0.977	-91.327	0.037

Table 6.7: Validation runs in the Naro Moru A4 catchment. Run a54004 is analysed below. Abbreviations are listed on p. 12; run names are explained in Appendix D.1.1.

In the validation period the daily r^2 and E_2 scores are close to or below their critical values for an acceptable simulation quality, while the decadal E_2 score is quite high. This indicates again that great deviations occur at the flow peaks (see also Fig. 6.12), which disappear when ten-day means are applied. As in the other catchments considered so far, the difference from simulated to observed annual runoff is far more positive in the validation period, but in

absolute terms there is still an underestimation by 91 mm or 13.3 %, which supports the theory that catchment rainfall is interpolated too low.

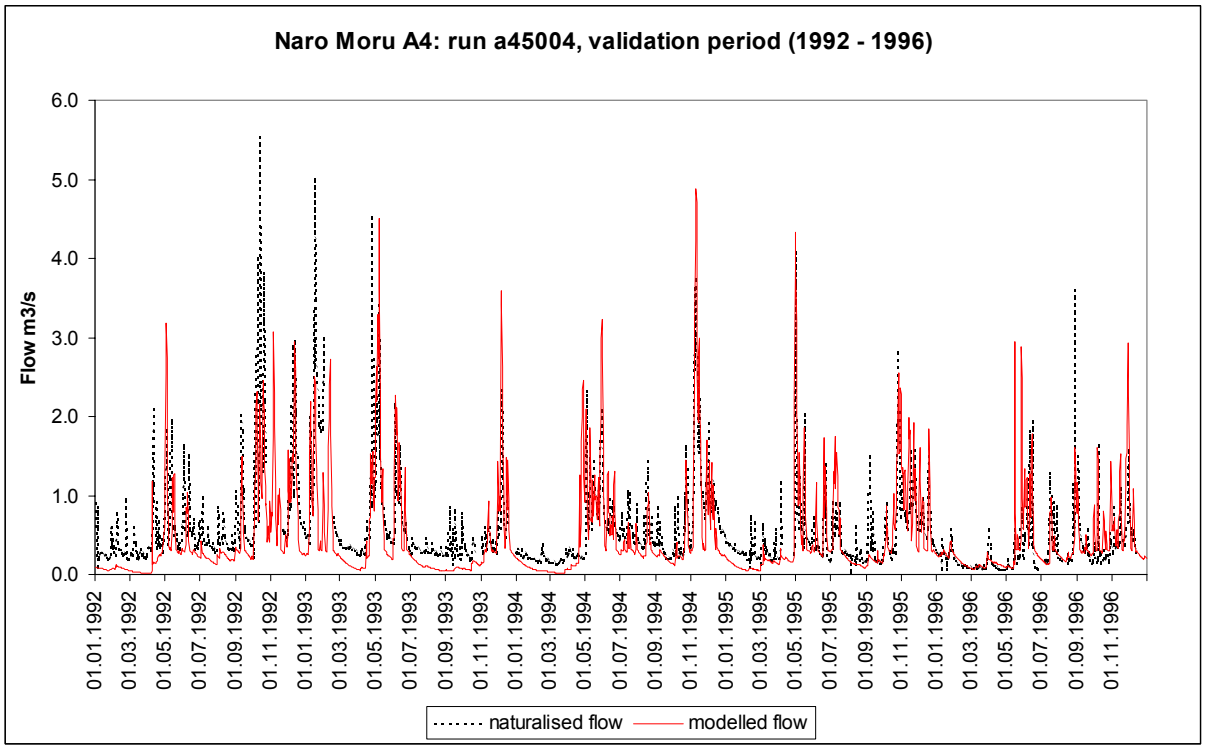

Fig. 6.12: Validation result at Naro Moru A4 (daily data).

Annual flow statistics: In accordance with the underestimation of total runoff there is a negative deviation to all statistical flow measures for the mean of the validation period. The greatest deviation is at the lower quartile, that also shows the highest positive deviation for a single year (1996).

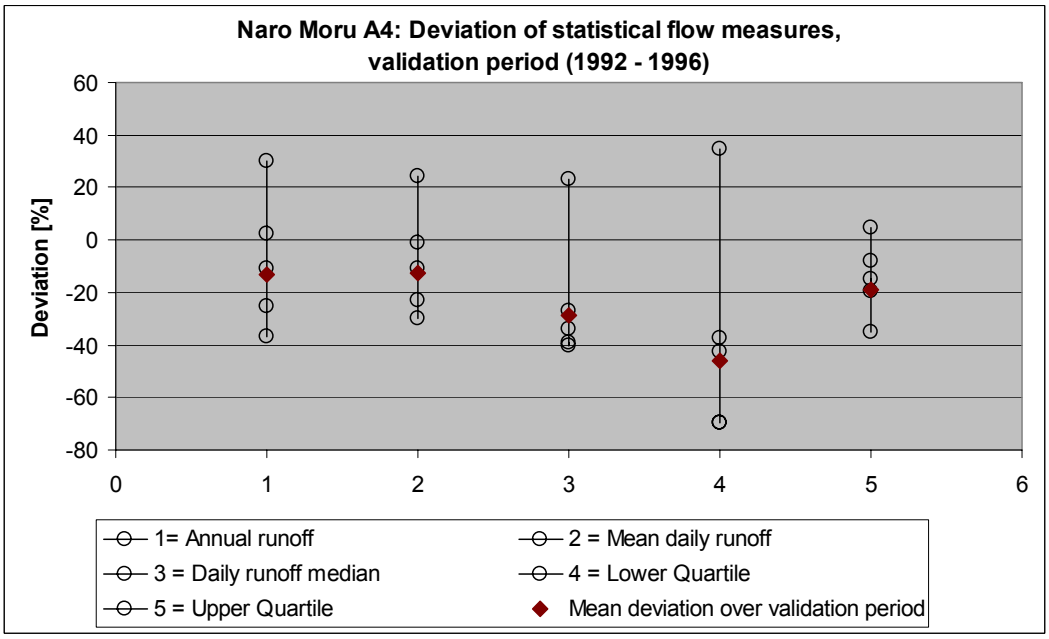

Fig. 6.13: Deviations of simulated statistical flow measures with respect to the naturalized observed values over the whole validation period (diamonds) and for single years (circles) in percent.

Low flows: NMQ30 is greatly underestimated and does not follow the interannual pattern of the observed low flows well (Fig. 6.14 a). The duration of flows below the threshold of 0.32 m^3/s is overestimated (Fig. 6.14 b). An exception is the year 1996. Reasons besides the general tendency of the model to underestimate low flows are the underestimation of catchment rain, an overestimation of evaporation or processes of runoff generation in the moorland and upper forest zone that are not represented adequately by the model.

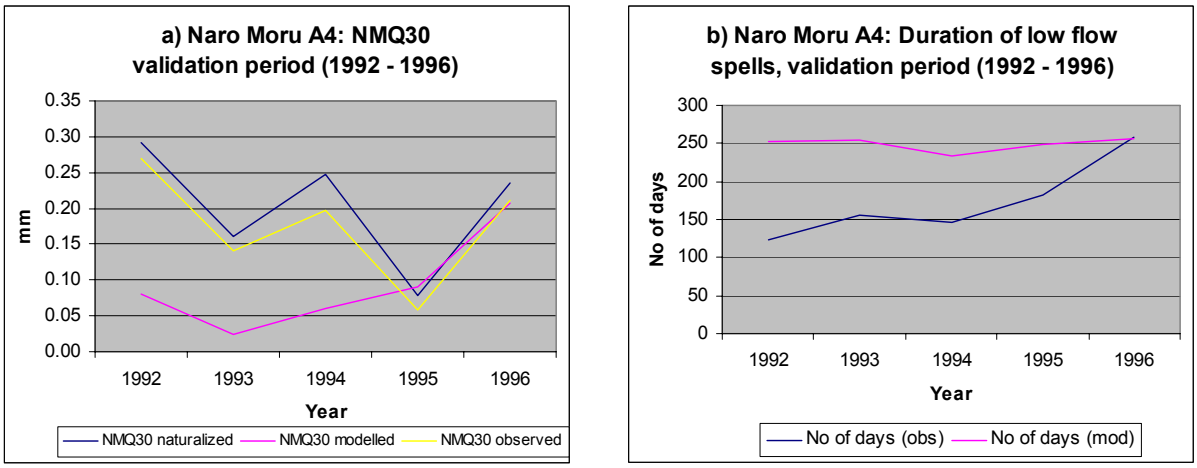

Fig 6.14: Simulated, observed and naturalized NMQ30 in the validation period (a) and duration of low flows below the low flow threshold (b).

Seasonal distribution of runoff: As in the other catchments, too much runoff is simulated in the wet months and too little in the dry months (Fig. 6.15). The negative deviations reach values of 61.4% (March). As mentioned before, the solution to this problem would be a modification of the groundwater discharge simulation (discussed in Section 6.3.1.1).

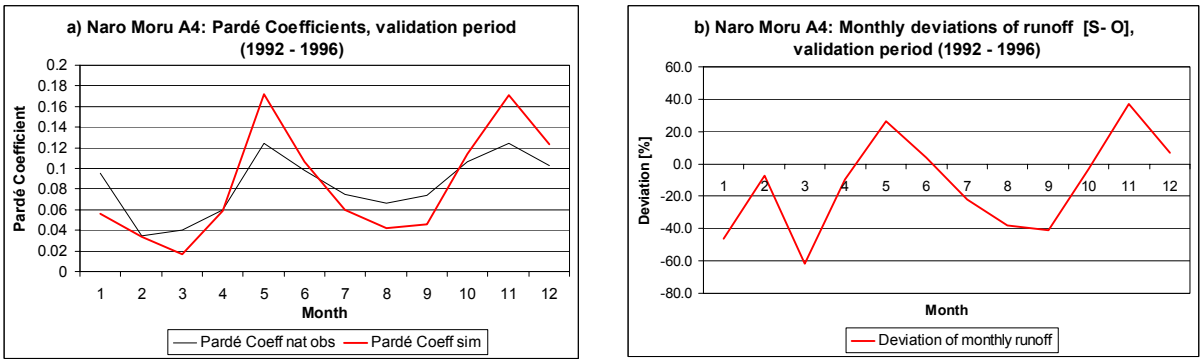

Fig. 6.15: Simulated and naturalized observed Pardé Coefficients (a) and monthly deviations of runoff in percent (b) for the validation period at A4.

6. 2. 4. Naro Moru A6 catchment

Naro Moru A6 includes the whole Naro Moru catchment from the source to its confluence with Ewaso Ng'iro. A large part belongs to the savannah zone, where the river meanders in an incised valley of about 10 m depth through the plateau, followed by riverine forest and small-scale cultivation. A summary of catchment characteristics is given in Box. 6.4.

Naro Moru A6

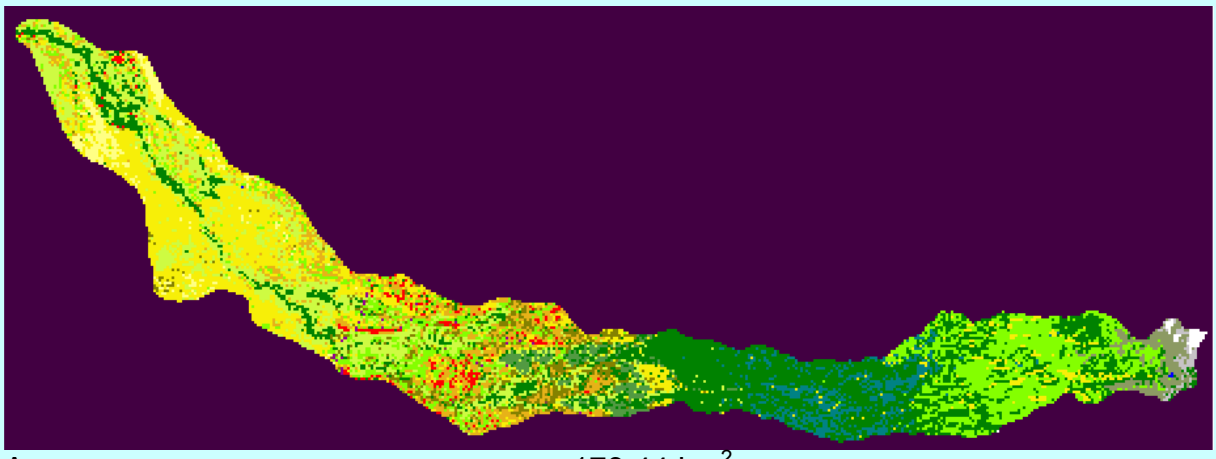

Area:	173.44 km^2
Lowest point:	1797 m a.s.l.
Highest point:	5080 m a.s.l.
Average elevation:	2484 m a.s.l.
Catchment slope:	12.69%
Average base curve number:	70.71

Land Use:

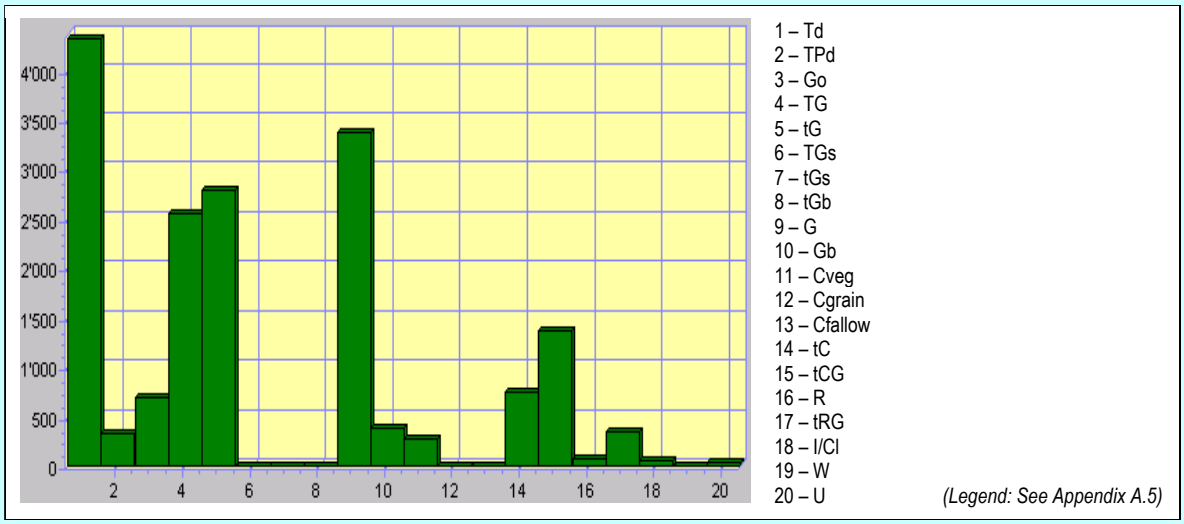

Box 6.4: Naro Moru A6 catchment characteristics. The map layer resolution is 100 m.

6. 2. 4. 1. Calibration

In Naro Moru A6, r^2 values of only 0.47 for daily and 0.65 for decadal streamflow data and Efficiency Scores of 0.48 for daily and decatdal data could be reached in the calibration period. This is partly due to overestimation and the time lag of flow peaks (due to the large catchment area resulting in a travel time of 12 hours of a flood wave through the savannah zone (Gathenya 1992: 134) and the lack of channel routing in the NRM^3 Streamflow Model),

Run Name	Res.	R1 COEFF	R2 COEFF	SSZTH	S COEFF	RO COEFF	r^2 daily	E_2 daily	r^2 dec.	E_2 dec.	S – O /year [mm]	r^2 NMQ30
a65003	500	0.02	0.25	18	0	0	0.439	0.412	0.643	0.438	26.230	0.775
a6500ro5	**500**	**0.02**	**0.25**	**18**	**0**	**0.8**	**0.473**	**0.483**	**0.652**	**0.483**	**17.960**	**0.801**

Table 6.8: Calibration runs in the Naro Moru A6 catchment. The settings of run a6500ro5 (runon coefficient set to 0.8) were chosen as the final parameter settings. Abbreviations are listed on p. 12; run names are explained in Appendix D.1.1.

and to processes of water storage and release (bank storage, seepage) in the savannah zone that the model is not able to simulate. An example is the year 1988 shown in Fig. 6.17. It can be seen that simulated flow peaks appear before the observed ones. In the months of the continental rains (June to September) the observed flows are much higher than the simulated discharge, which could be due to a release of water stored in the channel sediments or the deep savannah soils after flow peaks. Gathenya (1992) also noted such processes in the savannah zone. However, a systematic error in the recording of discharge cannot be ruled out either, since in no other year of the considered period this effect can be observed so pronouncedly.
Total discharge in the calibration period is overestimated by 18 mm/year or 8.82%. This is probably mainly caused by some simulated flow peaks that in reality were "swallowed up". This is also why a high runon coefficient results in a clearly better simulation quality (other than in the rest of the catchments that do not reach into the savannah zone): Inappropriate flow peaks are broken by the runon coefficient. This indicates that the Hortonian Overland Flow, that the runon routine is intended to simulate, occurs mainly in the savannah zone, but other processes might also be responsible for this effect.

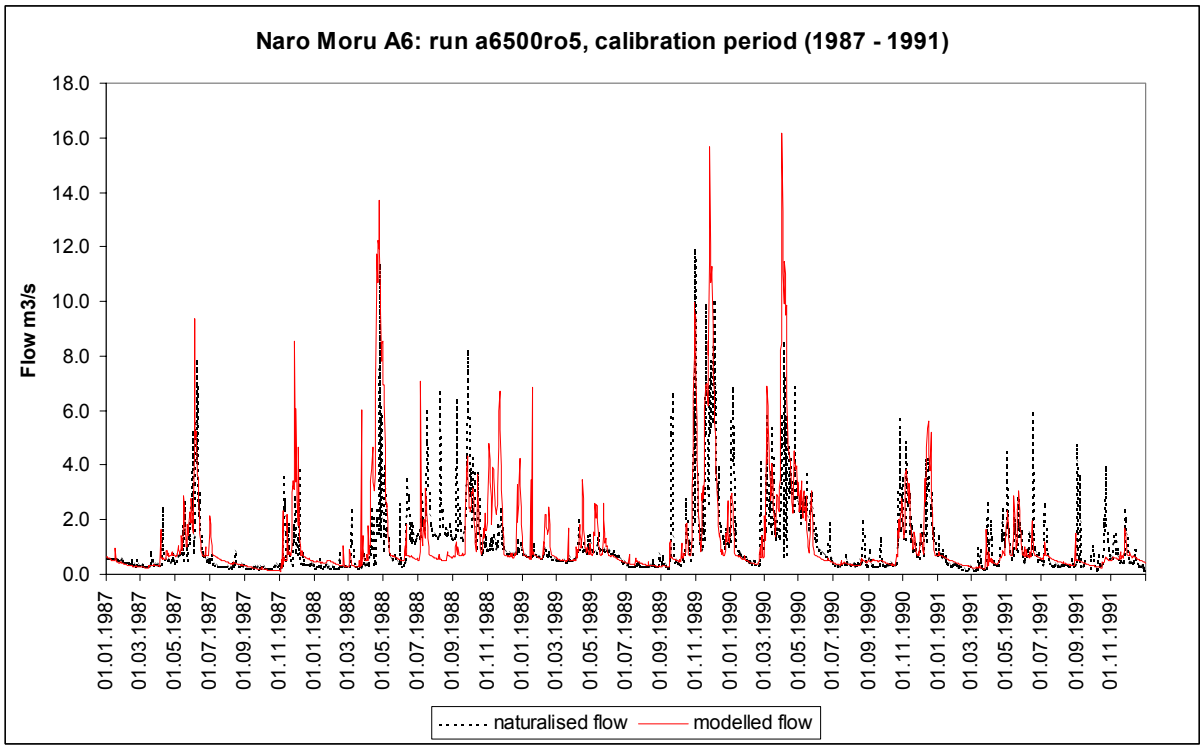

Fig. 6.16: Calibration result at Naro Moru A6 (daily data).

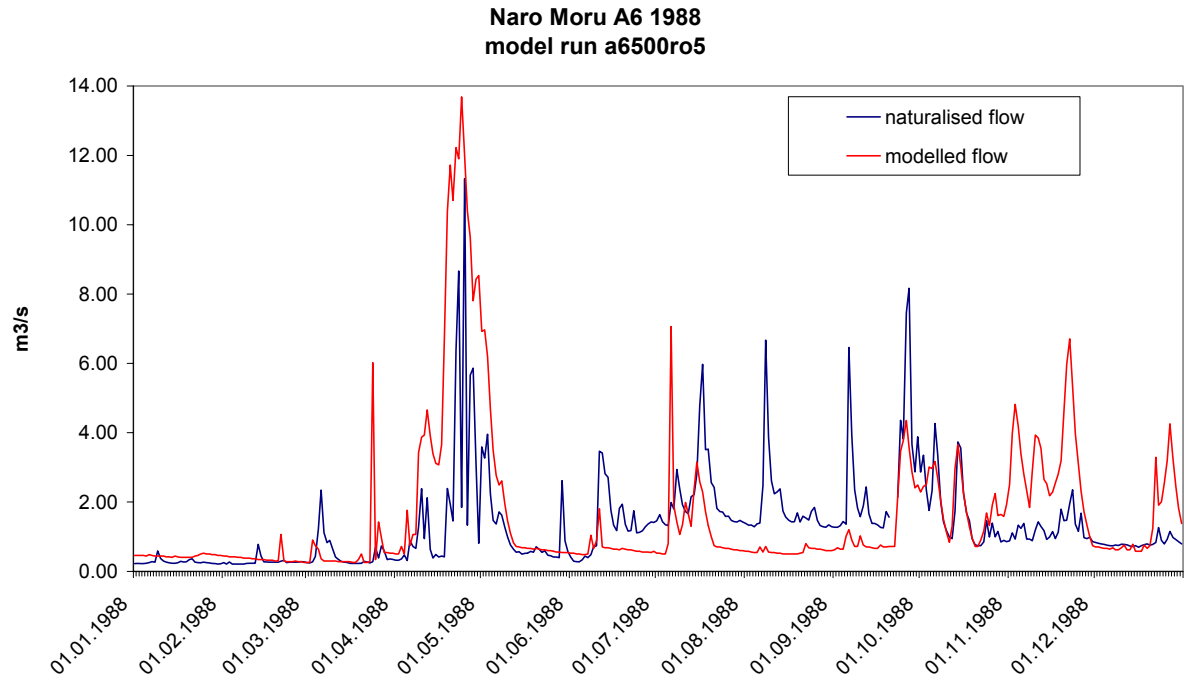

Fig. 6.17: The calibration year 1988 at Naro Moru A5. Note the time lag in flow peaks and the high baseflow from mid-June to September in the naturalized observed hydrograph that is probably caused by release of bank storage water.

6. 2. 4. 2. Validation

Run Name	Res.	R1 COEFF	R2 COEFF	SSZTH	S COEFF	RO COEFF	r^2 daily	E_2 daily	r^2 dec.	E_2 dec.	S – O /year [mm]	r^2 NMQ30
a65003	500	0.02	0.25	18	0	0	0.516	0.478	0.843	0.785	10.713	0.754
a6500ro5	**500**	**0.02**	**0.25**	**18**	**0**	**0.8**	**0.570**	**0.542**	**0.835**	**0.797**	**2.633**	**0.792**

Table 6.9: Validation runs in Naro Moru A6 catchment. Run a6500ro5 is analysed below. Abbreviations are listed on p. 12; run names are explained in Appendix D.1.1.

In the validation period higher performance measures are reached, which can be explained by the lack of a year like 1988, where the model shows very low accordance with the observed hydrograph. Total runoff is overestimated by only 2.6 mm/year or 1.15%, which is a reversal of the effect noted at A3 to A5 where runoff is simulated much higher in the validation period with respect to the observed data than in the calibration period.
Again the time lag from simulated to observed flow peaks can be observed throughout the period.

Annual flow statistics: The deviation of statistical flow measures shown in Fig. 6.19 lie in the range of 0 – 10% over the whole validation period except for the median, that is underestimated by 22.7%. The large scatter in the median is caused by overestimation of baseflows in the dry year 1992 (deviation +30.1%) and underestimation in the years 1994 – 1996, where the recorded hydrograph shows strange up-and-down jumps between 0.1 and 1 m3/s in baseflow periods that must be caused by anthropogenic influences if not by a gauging error. Unlike in the other catchments, low flows are not systematically underestimated as the overall positive deviation of the lower quartile indicates.

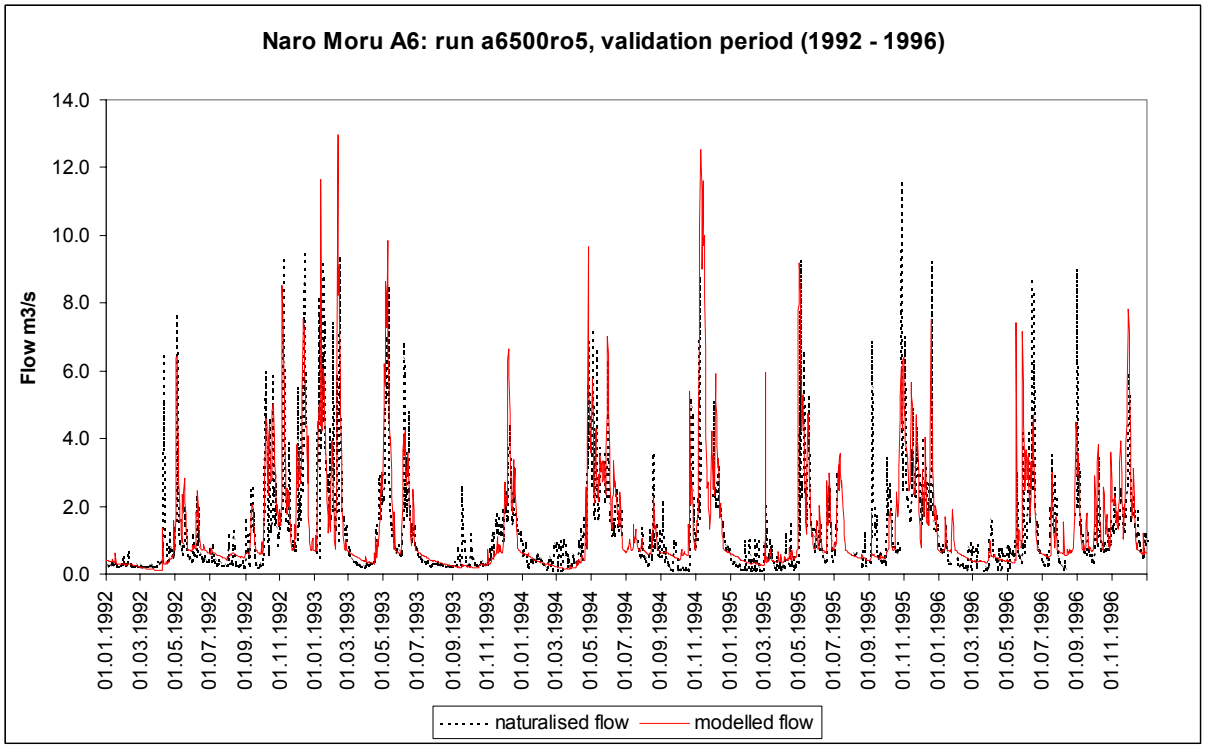

Fig. 6.18: Validation result at Naro Moru A6 (daily data).

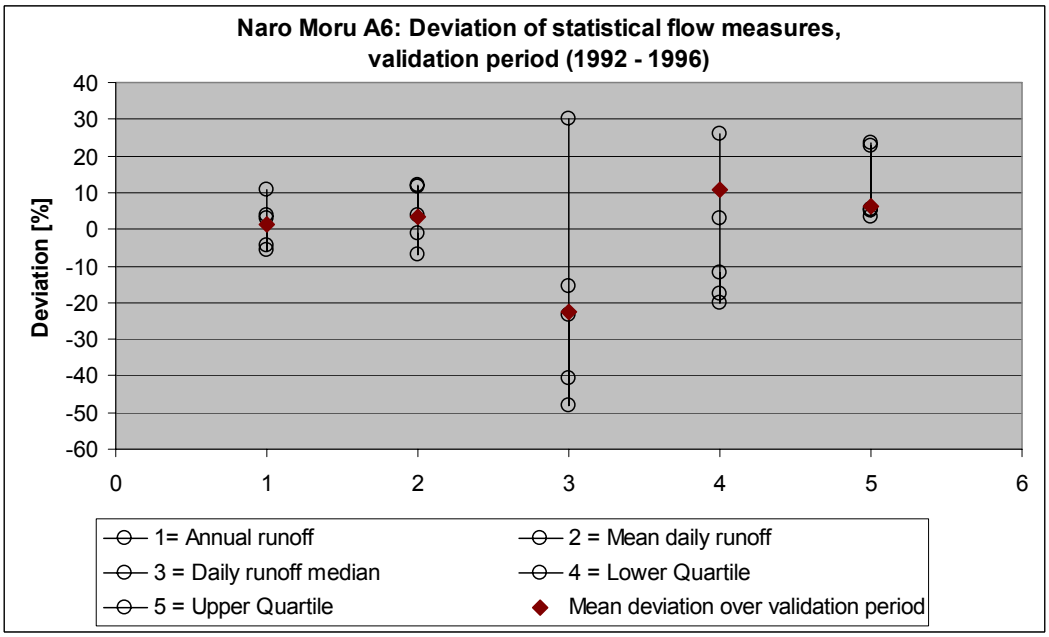

Fig. 6.19: Deviations of simulated statistical flow measures with respect to the naturalized observed values over the whole validation period (diamonds) and for single years (circles) in percent.

Low flows: The graphs of the low flow measures NMQ30 and duration of low flows (Fig. 6.20) show that dry period discharge amounts are captured quite well. The coefficient of determination of the NMQ30 is quite high with 0.792. In contrast to the other catchments, the model here slightly overestimates low flows. It has to be mentioned that at A6 the insecurity

concerning the amount of river water abstractions is greatest, so deviations could as well be due to naturalisation as to modelling errors.

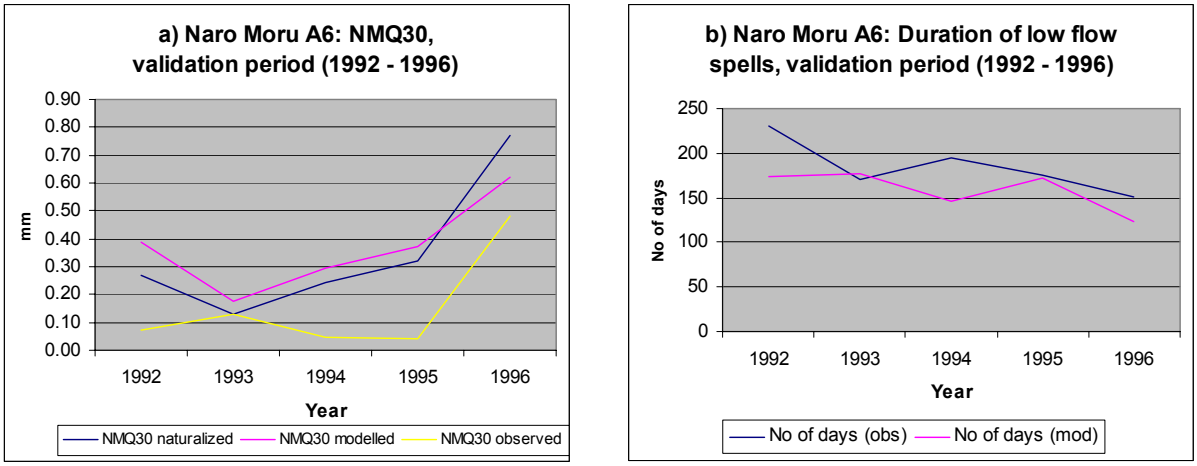

Fig 6.20: Simulated, observed and naturalized NMQ30 in the validation period (a) and duration of low flows below the low flow threshold (0.61 m^3/s) (b).

Seasonal distribution of runoff: The tendency to underestimate discharge in the dry months and to overestimate it in the wet season can only be observed to a limited extent in the A6 catchment (Fig. 6.21). The greatest underestimation occurs again in March (-44.9%), but the greatest positive deviation occurs in the dry month of July (+93.9%). Of course the high percentage is also caused by the low absolute amount. In the rainy seasons the positive deviations lie in the range of –23.3% (April) up to 56.5% (November).

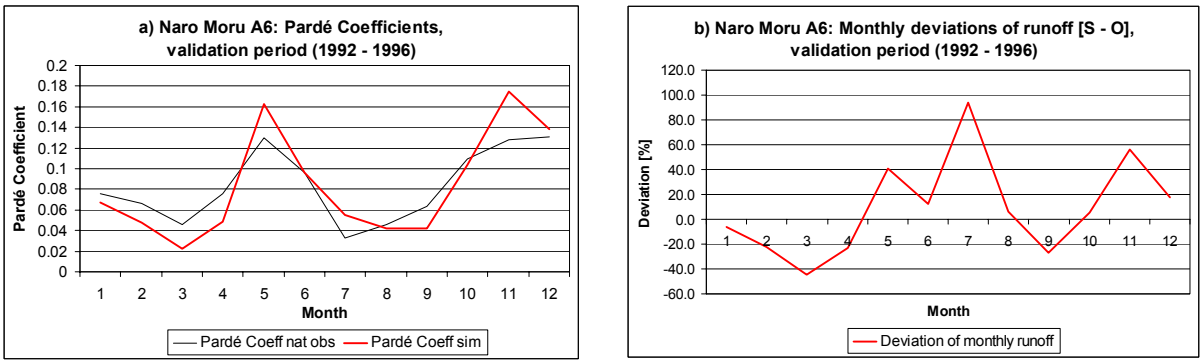

Fig. 6.21: Simulated and naturalized observed Pardé Coefficients (a) and monthly deviations of runoff in percent (b) for the validation period at A6.

6. 2. 5. Burguret A8 catchment

Burguret catchment lies to the north of Naro Moru and has a less elongated shape than the latter, which is due to its not reaching up to the the peak of Mt. Kenya and the many tributaries in the forest zone. Cultivation is not as widespread in the footzone as in Naro Moru catchment, making Burguret the catchment with the lowest average base curve number (see Box 6.5).

Burguret A8

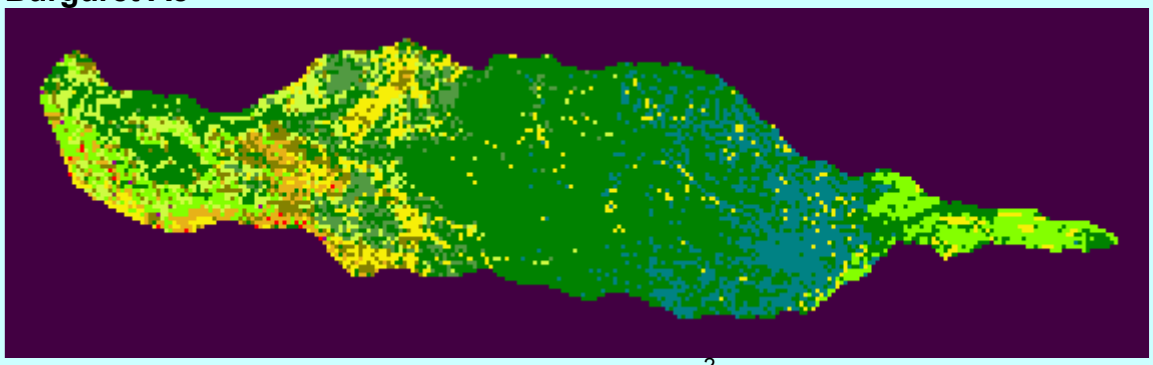

Area:	98.88 km^2
Lowest point:	1939 m a.s.l.
Highest point:	4287 m a.s.l.
Average elevation:	2510 m a.s.l.
Catchment slope:	15.03%
Average base curve number:	55.14

Land Use:

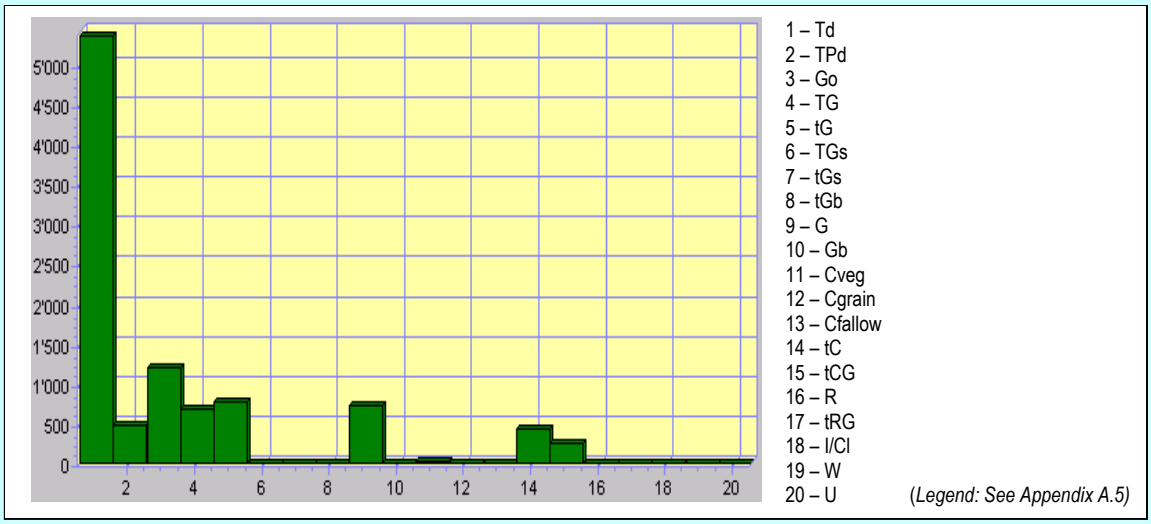

Box 6.5: Burguret A8 catchment characteristics. The map layer resolution is 100 m.

6. 2. 5. 1. Calibration

In the calibration period coefficients of determination of 0.66 for daily and 0.73 for decadal data are reached, while the Efficiency Score stays below its threshold of 0.5 for both temporal resolutions (Table 6.10). The reason is the systematic underestimation of runoff that amounts to –149 mm/year or 38.3% (see also Fig. 6.22). This could be caused by the distribution of rain gauges – the altitudinal belt of maximum precipitation is not represented by any rain gauge in the Burguret catchment, lower values are interpolated from neighbouring gauges – or groundwater influences that are not yet understood.

Run Name	Res.	R1 COEFF	R2 COEFF	SSZTH	S COEFF	RO COEFF	r^2 daily	E_2 daily	r^2 dec.	E_2 dec.	S – O /year [mm]	r^2 NMQ30
a8500a01	**500**	**0.03**	**0.25**	**18**	**0**	**0**	**0.650**	**0.569**	**0.729**	**0.414**	**-148.62**	**0.610**
a8500nmr	500	0.03	0.25	18	0	0	0.618	0.549	0.692	0.420	-133.44	0.592
a8500a8r	500	0.03	0.25	18	0	0	0.646	0.559	0.740	0.447	-137.07	0.652

Table 6.10: Calibration runs at Burguret A8. The runs differ in the rain gauges used: For run a8500a01 (which was chosen as the final run), all gauges were used. For a8500nmr only the gauges along the Naro Moru profile were used, and for a8500a8r only the stations within or near Burguret catchment. Abbreviations are listed on p. 12.

This effect can only be reduced to a certain extent by leaving away data from certain gauges in order to get a more even distribution of gauges in altitude, as tried with the runs a8500nmr (only rain gauges along the Naro Moru profile) and a8500a8r (only gauges within or nearest to A8 catchment). Considering all performance measures and the fact that in the validation period runoff is overestimated again the run using all rain gauges was chosen as the final run.

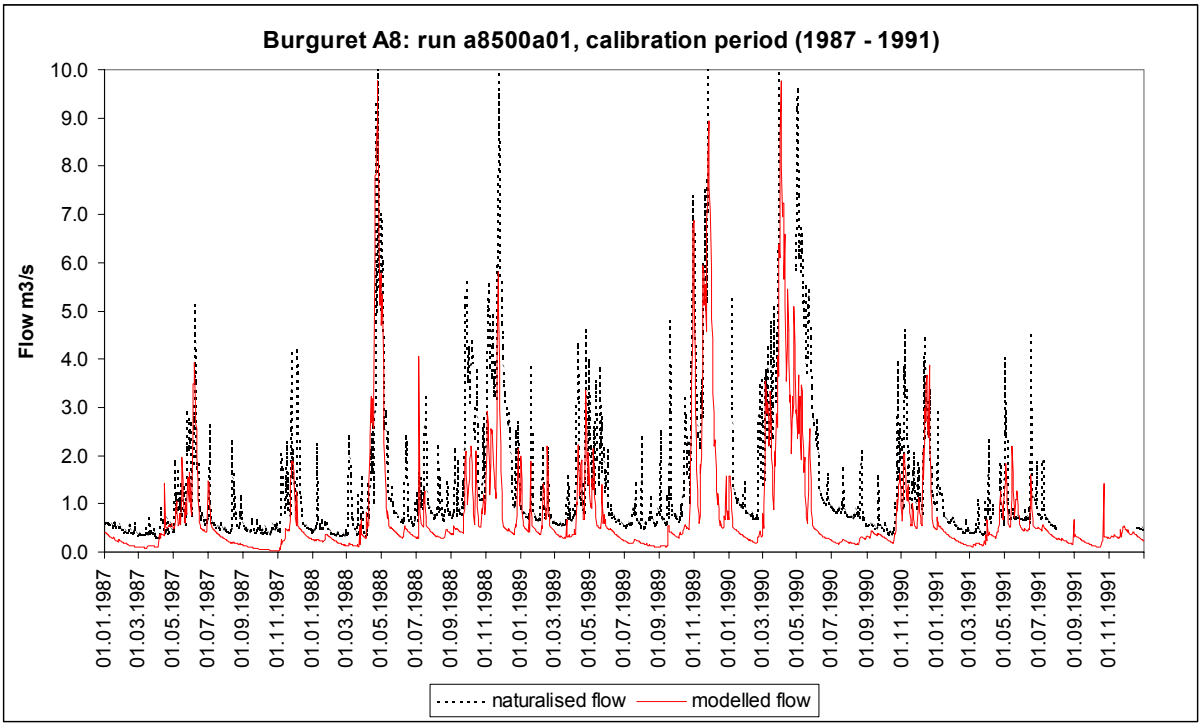

Fig. 6.22: Calibration result at Burguret A8 (daily data).

6. 2. 5. 2. Validation

Run Name	Res.	R1 COEFF	R2 COEFF	SSZTH	S COEFF	RO COEFF	r^2 daily	E_2 daily	r^2 dec.	E_2 dec.	S – O /year [mm]	r^2 NMQ30
a8500a01	**500**	**0.03**	**0.25**	**18**	**0**	**0**	**0.558**	**0.631**	**0.649**	**0.611**	**37.359**	**0.243**
a8500nmr	500	0.02	0.2	16	0	0	0.533	0.510	0.632	0.473	65.225	0.058
a8500a8r	500	0.03	0.25	18	0	0.1	0.567	0.588	0.655	0.555	46.409	0.052

Table 6.11: Validation runs at Burguret A8 using different sets of rain gauges. The run a8500a01(using all available rainfall data) is analysed below. Abbreviations are listed on p. 12; run names are explained in Appendix D.1.1.

As shown in Table 6.11, the coefficient of determination slightly decreases with respect to the calibration period while the Nash and Sutcliffe Efficiency score is higher, indicating an

acceptable simulation quality. Total runoff is now overestimated by 37 mm/year or 12.5% in the run a8500a01. The other runs overestimate runoff even more, demonstrating the same effect as already observed in the A3 – A5 catchments (also discussed in Section 6.2.7). The comparison of simulated and observed hydrographs nevertheless shows a general underestimation of low flows (Fig. 6.22).

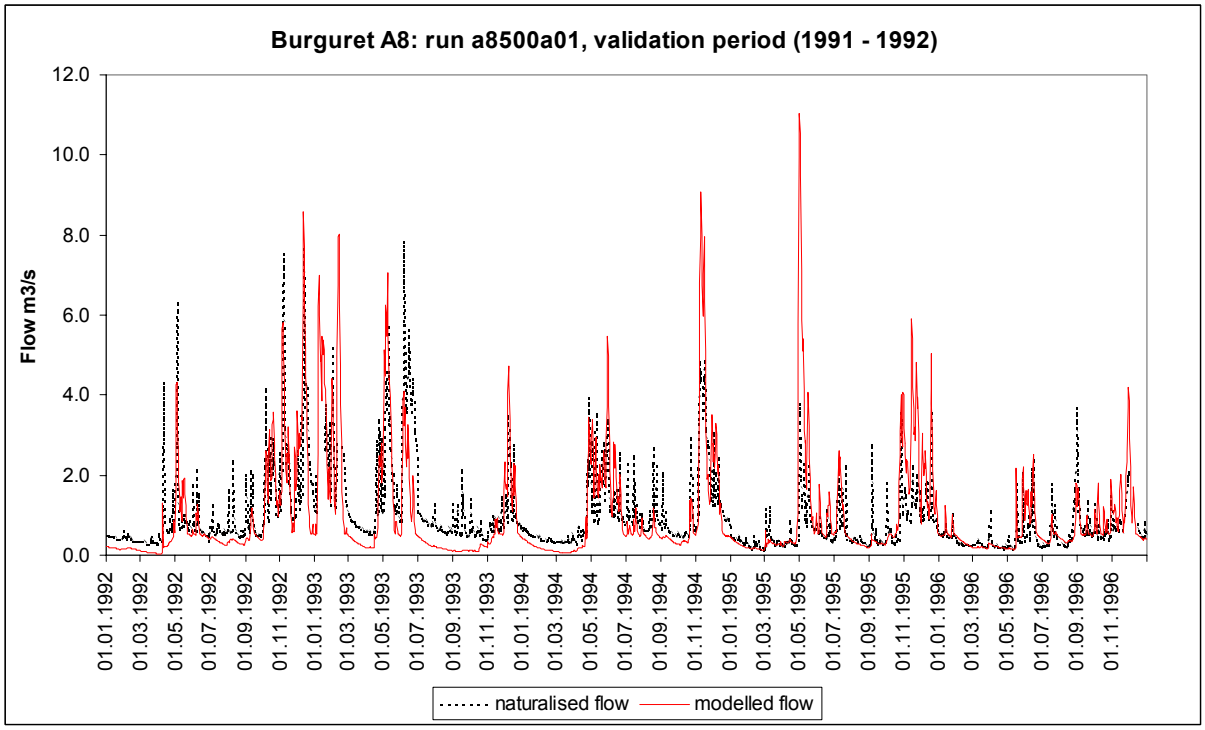

Fig. 6.22: Validation result at Burguret A8 (daily discharge).

Annual flow statistics: Annual runoff, mean and upper quartile show positive deviations while the median and the lower quartile are underestimated by the simulation. The greatest positive deviatons are found in the year 1995, caused mainly by highly overestimated flood peaks in the rainy seasons. The most negative deviations take place in the year 1993, where the recorded hydrograph is consistently higher than the simulated one.

Low flows: Except for the year 1996 low flows are underestimated by the model, as shown in Fig. 6.24 The interannual pattern is followed less well than at Naro Moru, which could again be due to the less accurate rain data. The small difference between observed and naturalised flows in Fig. 6.24 a) (due to relatively few abstraction points above A8) indicates that abstractions represent a smaller insecurity here than in the Naro Moru catchment; on the other hand the rating equation of A8 has to be questioned – in the field work period 2002 an overestimation by almost 100% by the rating compared to a current meter gauging of low flows was noted. Probably the deviation was not this great up to 1996 but it shows that the recorded discharge data have to be eyed with care.

Seasonal distribution of runoff: The seasonal deviations are again most negative in dry months (March: - 49.2%) and most positive in wet months (November: +55.8%) (see Fig. 6.25 b). The overestimation in January is mainly caused by the duration of the Short Rains season 1992 into January and February 1993. The exaggerated shape of the simulated Pardé Coefficients graph (Fig. 6.25 a) as in the other catchments indicates greater groundwater stores than can be simulated with the (current) NRM^3 Streamflow Model structure.

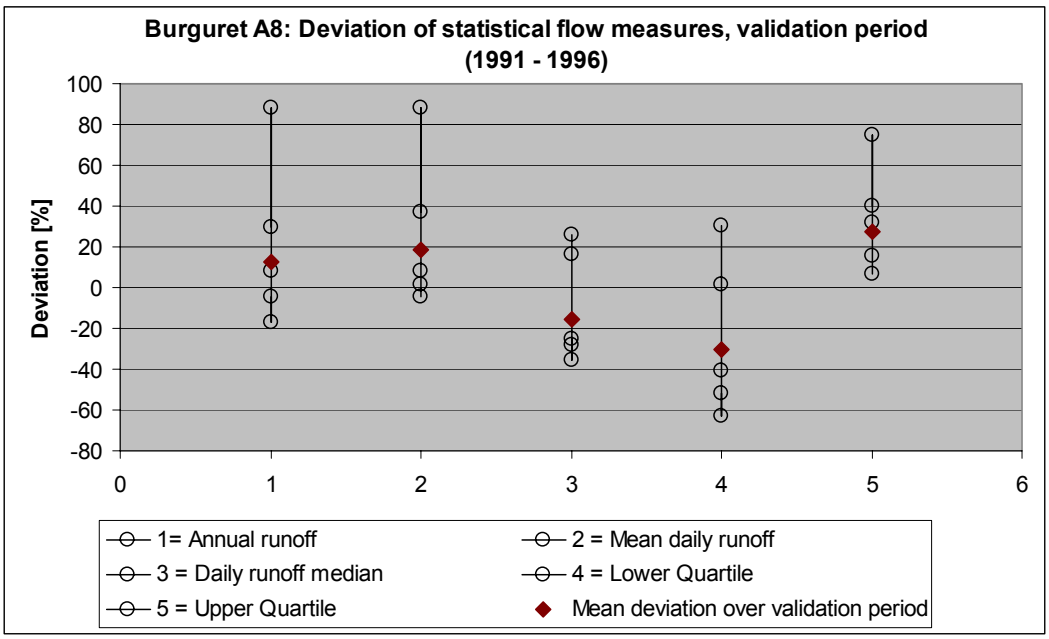

Fig. 6.23: Deviations of simulated statistical flow measures with respect to the naturalized observed values over the whole validation period (diamonds) and for single years (circles) in percent.

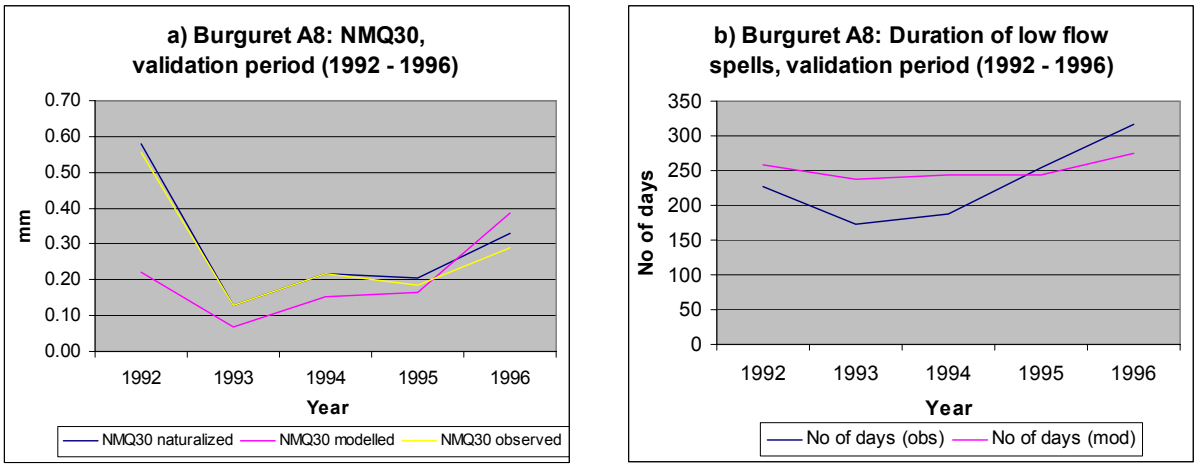

Fig 6.24: Simulated, observed and naturalized NMQ30 in the validation period (a) and duration of low flows below the low flow threshold (0.77 m^3/s) (b).

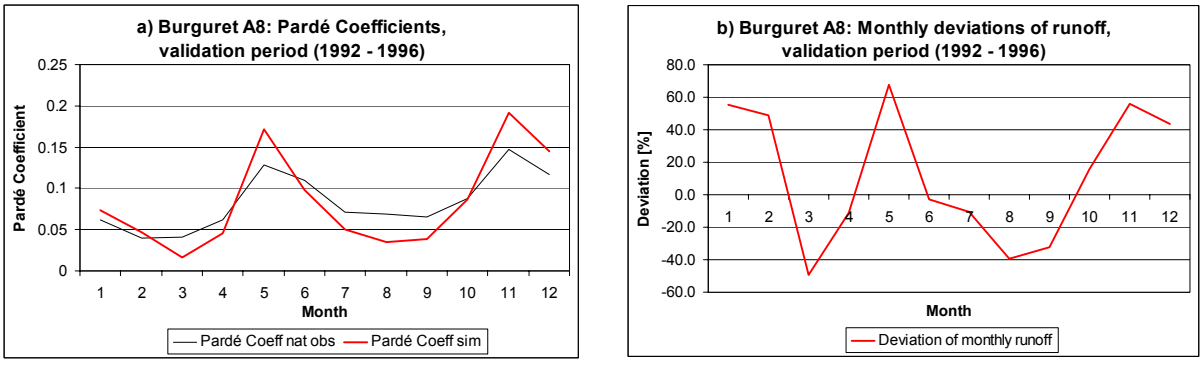

Fig. 6.25: Simulated and naturalized observed Pardé Coefficients (a) and monthly deviations of runoff in percent (b) for the validation period at A8.

6. 2. 6. Nanyuki A9 catchment

Nanyuki A9 catchment has a very elongated shape and reaches from the peak region down to Nanyuki town. A summary of catchment characteristics is given in Box 6.6.

Nanyuki A9

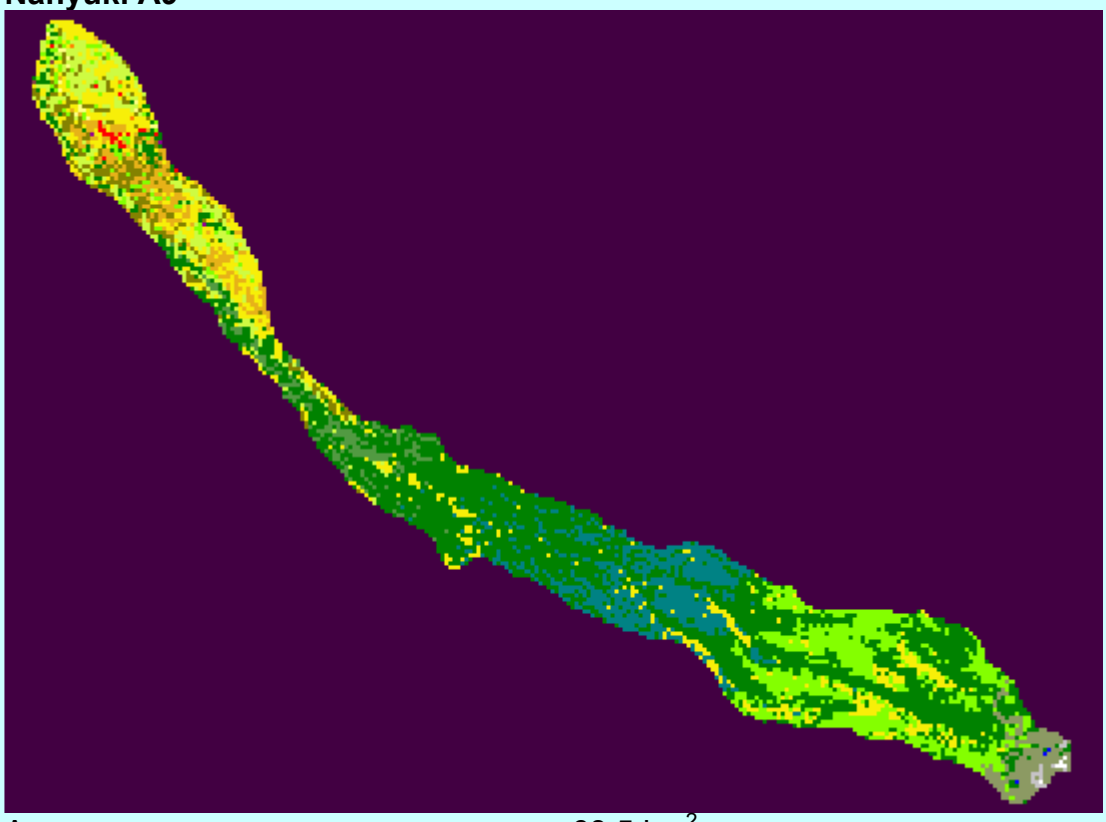

Area:	68.5 km^2
Lowest point:	1968 m a.s.l.
Highest point:	4860 m a.s.l.
Average elevation:	2929 m a.s.l.
Catchment slope:	22.76%
Average base curve number:	61.22

Land Use:

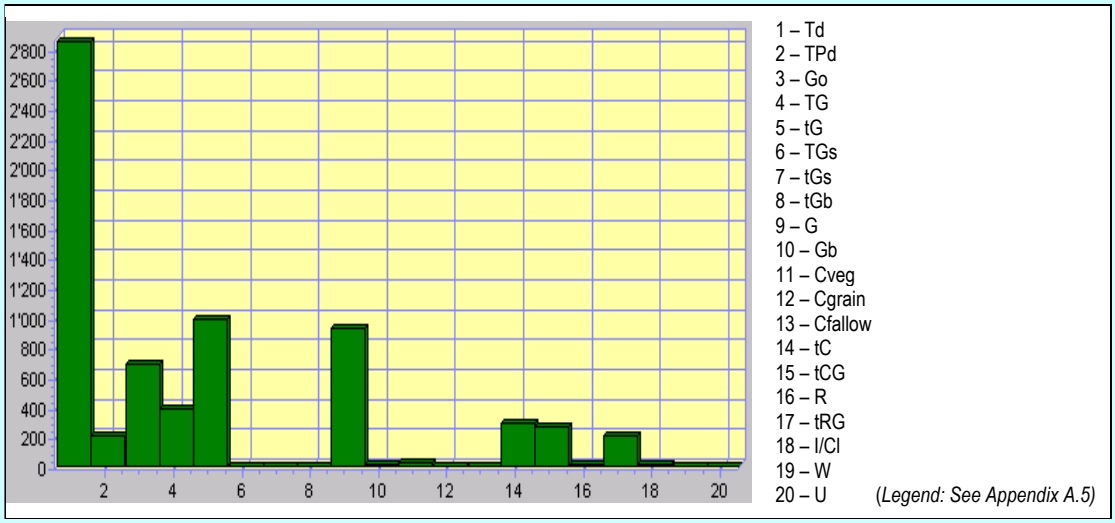

Box 6.6: Nanyuki A9 catchment characteristics. The map layer resolution is 100 m.

6. 2. 6. 1. Calibration

Run Name	Res.	R1 COEFF	R2 COEFF	SSZTH	S COEFF	RO COEFF	r^2 daily	E_2 daily	r^2 dec.	E_2 dec.	S – O /year [mm]	r^2 NMQ30
a9500a01	500	0.03	0.3	20	0	0	0.605	0.166	0.736	0.623	95.719	0.862
a9500a03	**500**	**0.02**	**0.25**	**18**	**0**	**0**	**0.613**	**0.175**	**0.740**	**0.620**	**95.285**	**0.905**
a9500ds4	500	0.03	0.3	20	0.02	0	0.601	0.454	0.738	0.528	11.221	0.853
a95001st	500	0.03	0.3	20	0	0	0.271	0.007	0.383	0.078	5.789	0.611
A9500a9r	500	0.03	0.3	20	0	0	0.602	-0.165	0.739	0.550	128.825	0.915

Table 6.12: Calibration runs in the Nanyuki A9 catchment. For the first three runs all available rainfall data were used. For run a95001st only the rainfall data from Nanyuki Forest Station were used and for run a9500a9r only data from stations in and near A9 catchment. The a9500a03 parameters were chosen as the final parameter settings. Abbreviations are listed on p. 12.

In the Nanyuki A9 catchment coefficients of determination of 0.61 for daily and 0.62 for decadal data and Efficiency Scores of 1.75 for daily and 0.62 for decadal data are reached. The low daily Efficiency Score is mainly due to the missing of flow peaks; some flow peaks are completely out of proportion since there is only one rain gauge within the catchment (Nanyuki forest station). Using only this gauge (run a95001st) or only gauges near the catchment (run a9500a9r) does not result in better overall performance.
Since an overall overestimation of runoff can be observed, the modification of the deep seepage parameter was also explored (run a9500ds4). This results in better accordance of total runoff, but low flows are greatly underestimated this way, which is why deep seepage was set to 0 in the final settings.

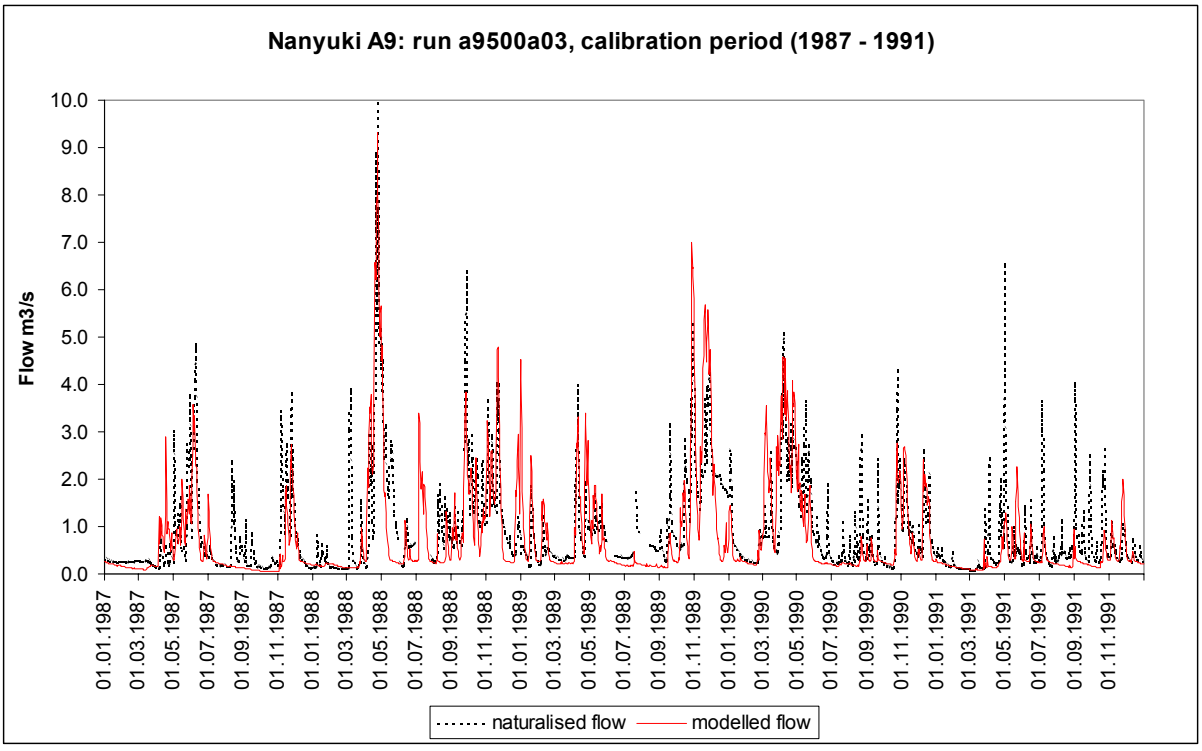

Fig. 6.26: Calibration result at Nanyuki A9 (daily discharge).

6. 2. 6. 2. Validation

Run Name	Res.	R1 COEFF	R2 COEFF	SSZTH	S COEFF	RO COEFF	r^2 daily	E_2 daily	r^2 dec.	E_2 dec.	S – O /year [mm]	r^2 NMQ30
a9500a01	500	0.03	0.3	20	0	0	0.554	-0.350	0.712	0.597	139.145	0.377
a9500a03	**500**	**0.02**	**0.25**	**18**	**0**	**0**	**0.558**	**-0.364**	**0.711**	**0.569**	**138.805**	**0.417**
a9500ds4	500	0.03	0.3	20	0.02	0	0.548	0.208	0.706	0.546	49.889	0.304
a95001st	500	0.03	0.3	20	0	0	0.331	-0.635	0.445	0.119	95.771	0.063
A9500a9r	500	0.03	0.3	20	0	0	0.516	-0.496	0.685	0.532	144.427	0.474

Table 6.13: Validation runs at A9. Run a9500a03 is analysed below. Abbreviations are listed on p. 12; run names are explained in Appendix D.1.1.

The measures of model performance in Table 6.13 indicate low accordance of the simulated with the observed hydrograph on the daily scale, and fair accordance on the decadal time-step. Again it can be observed that total simulated runoff is higher with respect to observed runoff in the validation period than in the calibration period – the overestimation is 139 mm/year or 60.8%. The comparison of the simulated and the naturalised observed hydrograph (Fig. 6.27) shows that generally low flows are underestimated and flow peaks both under- and overestimated by the model.

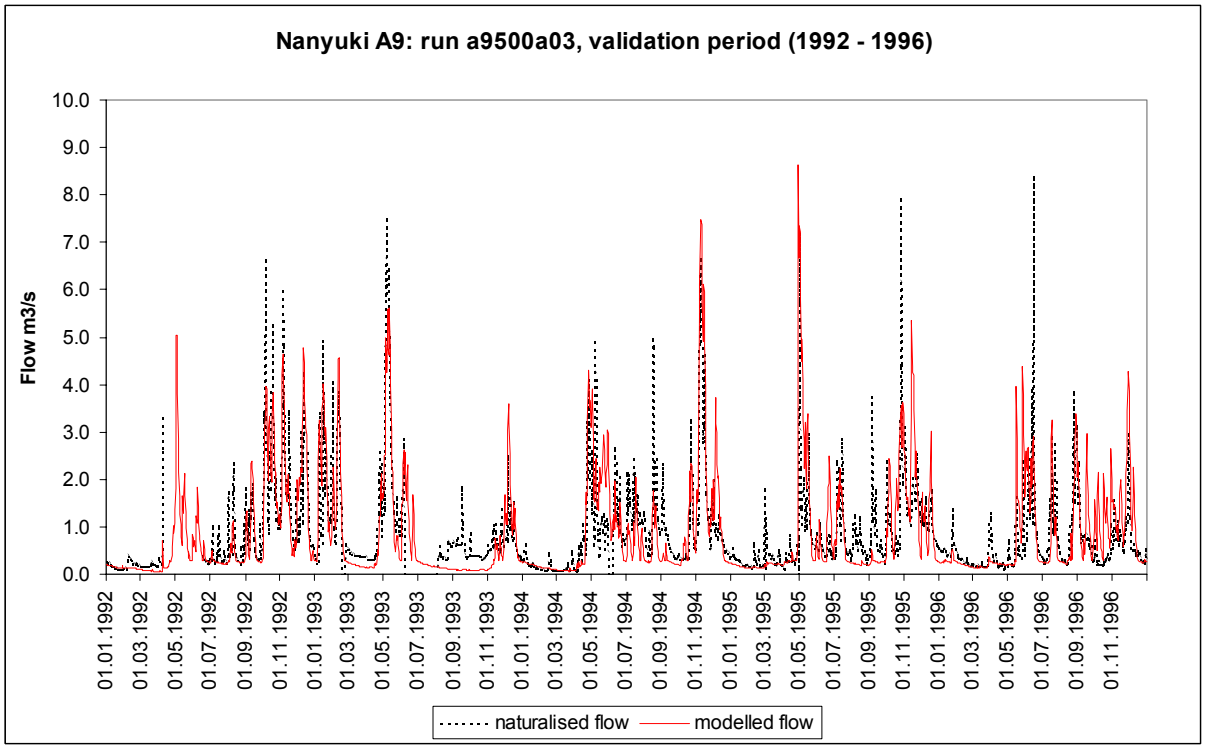

Fig. 6.27: Validation result at Nanyuki A9 (daily discharge).

Annual flow statistics: Except for the median of daily runoff all statistical measures of the modelled hydrograph show a positive deviation for the mean of the validation period, which is in accordance with the overall overestimation of runoff (Fig. 6.28). The explanation for the low median is that many of the smaller flow peaks are not simulated because the rainfall monitoring network failed to capture the rains that caused them. The largest positive deviations (+99% in annual runoff and mean, +163% in the upper quartile) are found in the year 1996, when the reverse effect occurs: several flow peaks in the observed hydrograph are caused by storms that were apparently not as strong over the A9 catchment area as they were measured at their respective gauges.

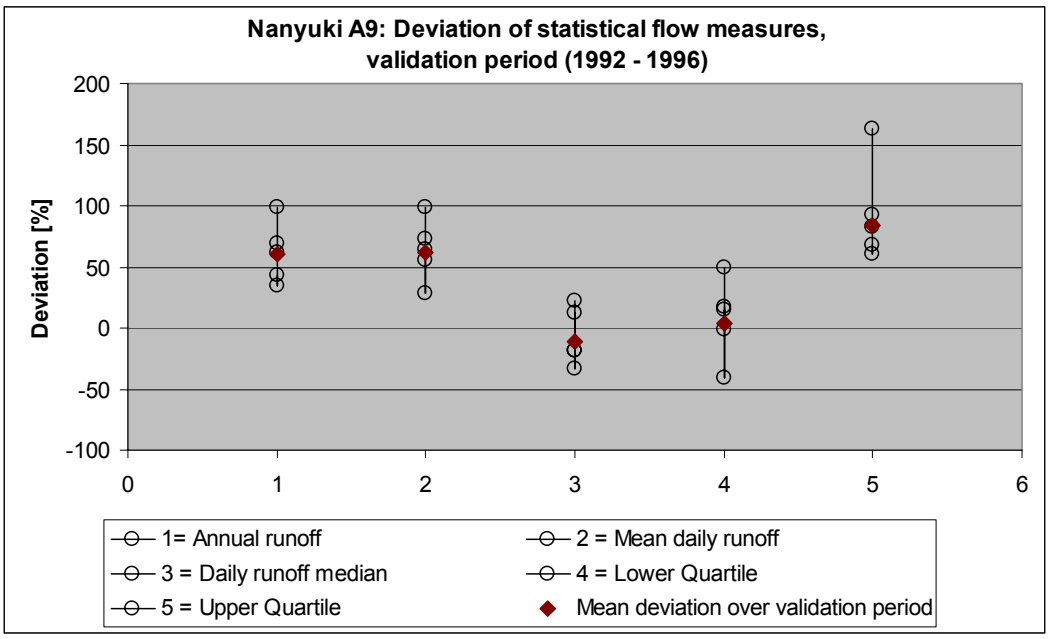

Fig. 6.28: Deviations of simulated statistical flow measures with respect to the naturalized observed values over the whole validation period (diamonds) and for single years (circles) in percent.

Low flows: As can be seen in Fig. 6.29 a), the absolute values of the lowest monthly flows (NMQ30) are again underestimated but the year-to-year pattern is followed fairly well. The duration of flows below the threshold of 0.45 m^3/s is overestimated except for the year 1992, when almost all flow peaks are captured by the model.

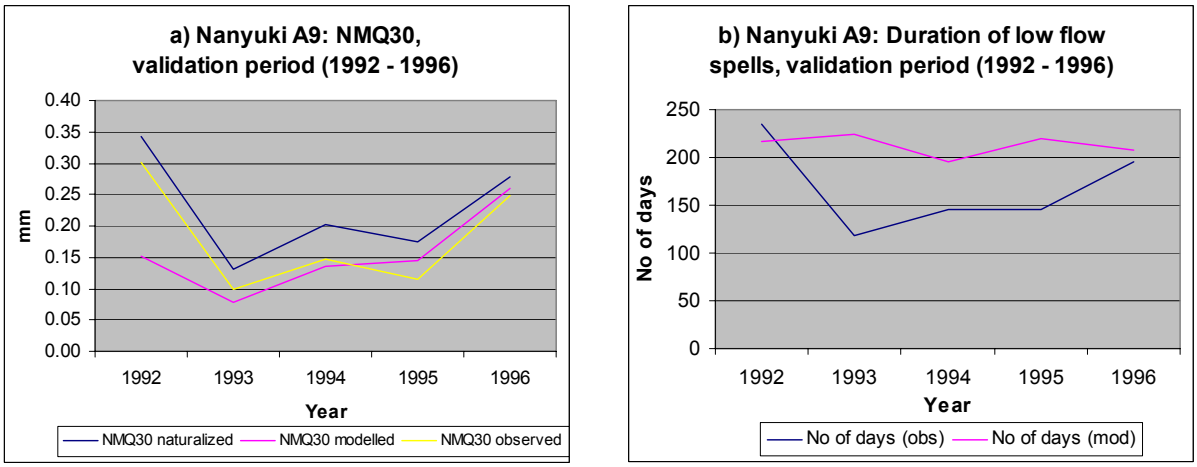

Fig 6.29: Simulated, observed and naturalized NMQ30 in the validation period (a) and duration of low flows below the low flow threshold (0.45 m^3/s) (b).

Seasonal distribution of runoff: The comparison of observed and modelled Pardé Coefficients (Fig. 6.30 a) shows that the model allocates too much of the total runoff in the wet seasons, mainly in the long rains around May. Monthly deviations from the absolute values (Fig. 6.30 b) are positive except for March and August; the highest deviation occurs in May with +168.4%.

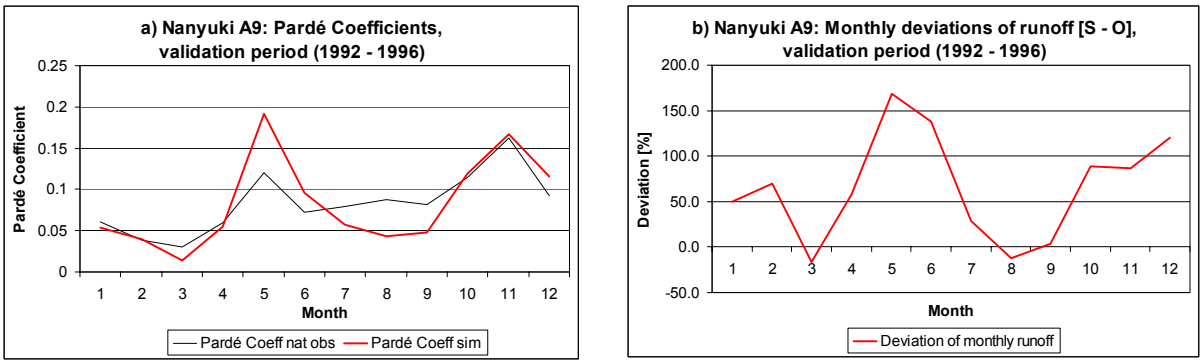

Fig. 6.30: Simulated and naturalized observed Pardé Coefficients (a) and monthly deviations of runoff in percent (b) for the validation period at A9.

6. 2. 7. Overall results

Modelling performance: As can be seen in Fig. 6.31, the coefficients of determination for daily data are lie between 0.5 and 0.6 for daily data in the validation period and between 0.6 and 0.9 for decadal data; the Nash and Sutcliffe Efficiency Score shows a greater scatter – daily values range from -0.36 to 0.63 and decadal values from 0.57 to 0.98. This indicates an acceptable reproduction of runoff dynamics on the daily scale and a reasonably good reproduction on the decadal scale, considering the common thresholds for E_2 of 0.5 and for r^2 between 0.5 and 0.8. The low E_2 scores occur where the absolute discharge amounts of flow peaks were not reproduced well, such as in the Naro Moru A3, A4 and A9 catchments at daily resolution. This mainly due to missing rain inputs, where local storms were not captured by the NRM[3] monitoring network.

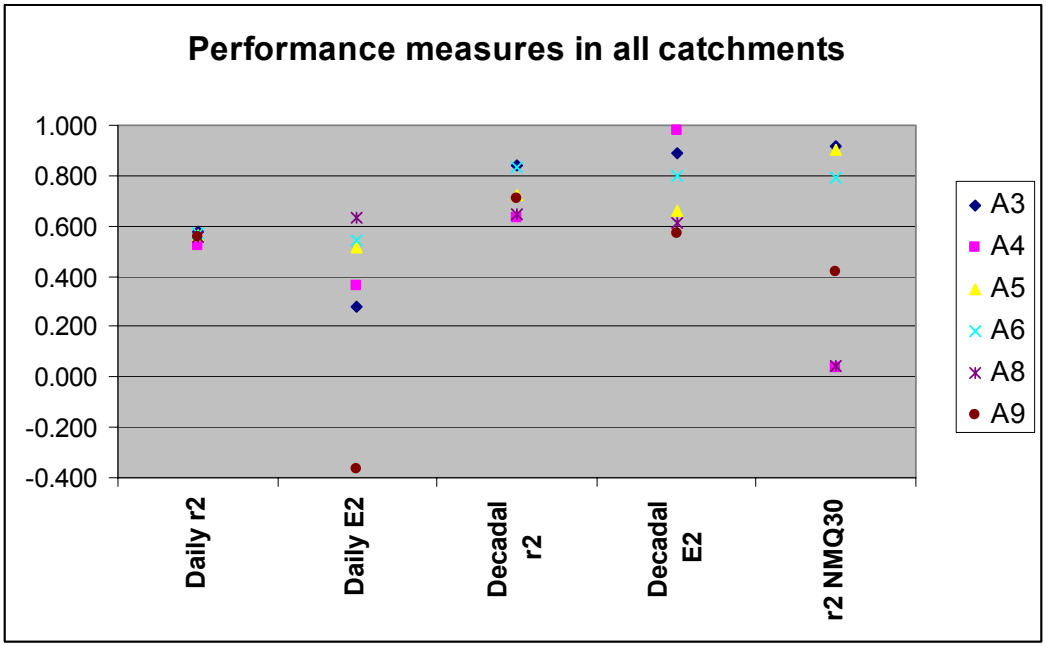

Fig. 6.31: Model performance measures in all study catchments (validation period).

Low flows: Low flows tend to be underestimated by the model. Modifying the groundwater discharge coefficients can only help up to a certain degree without sacrificing the ability of the model to follow the observed pattern of the hydrograph. Especially after periods of heavy

rainfall the catchments sustain much higher baseflow than modelled. Here a modification of the model structure (introduction of variable groundwater parameters or a second groundwater reservoir, see also Section 6.3.1.1.) could help.
Another reason for the underestimation of low flows might be an overestimation of evapotranspiration in the upper catchment parts (refer to Section 6.4.2.1.) Partly the underestimation of low flows could also be due to an overestimation of abstractions and to inaccurate rating curves. The latter reason certainly explains only the smaller part of the underestimation of low flows, however.
As can also be seen in Fig. 6.31, the high coefficient of determination for the NMQ30 in the A3, A5 and A6 catchments indicates that in spite of the general underestimation, the interannual pattern of low flows is followed well. In the other catchments, high deviations in low flows coincide with great under- or overestimation of total discharge, which suggests that the bad performance is caused by inaccurate rain and evaporation inputs.

Simulated - Naturalised Observed total runoff [%]						
Catchment	**A3**	**A4**	**A5**	**A6**	**A8**	**A9**
Calibration period	1.122	-25.96	-11.523	8.824	-38.337	39.26
Validation period	16.500	13.300	4.000	1.150	12.500	60.800

Table 6.14: Deviations from simulated to naturalised observed total runoff in percent for the calibration and validation period.

Total runoff: In all catchments except A6 it can be observed that the model predicts much more runoff in the validation period with respect to the naturalised observed values than in the calibration period (Table 6.14). The deviations are greatest where rainfall inputs are suspected to be most inaccurate: at A4 because of the missing altitudinal precipitation maximum (see Section 6.2.3) and at A8 and A9 because of the greater distances to most rain gauges.
Fig. 6.32 shows the deviations of the major water balance elements (rain, evaporation, flow) from the validation to the calibration period. While catchment rainfall increases by 0 - 10%, catchment evaporation decreases by around 5 – 10%. Subsequently the mean of modelled runoff is raised by 15 – 20%, but naturalised observed runoff stays more or less the same for most catchments (except for a slight increase at A6 and a heavy decrease at A8), resulting in an overall overestimation of modelled discharge.

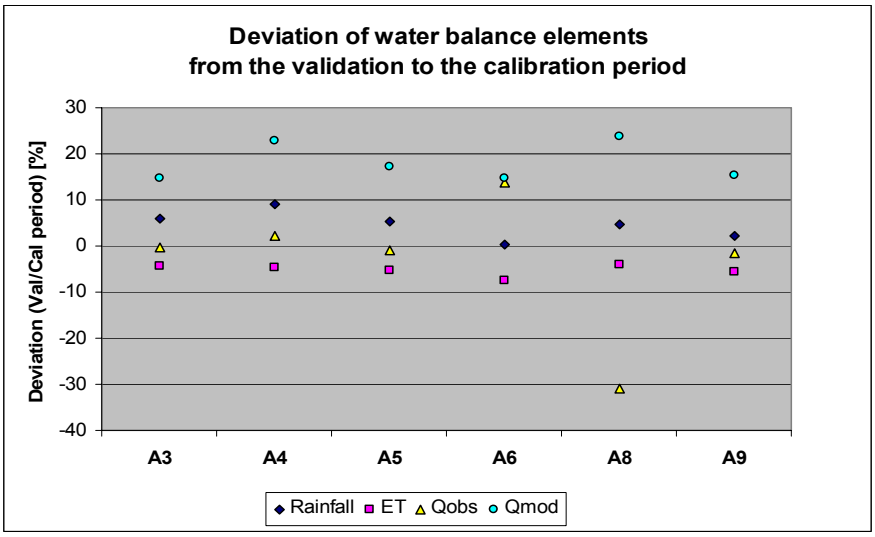

Fig. 6.32: Deviation of water balance elements from the validation to the calibration period in the study catchments in percent. The increase in rainfall and the decrease in evaporation cause an increase in simulated streamflow, which is not reflected in the observed discharge data.

Principally two reasons can be established to explain this effect:

a) Rainfall really was higher in the period 1992 – 96, but the catchments (maybe due to deep seepage into the fractured volcanic rocks) absorbed it so no increase in flow was noticed at the gauging stations.
b) Systematic measuring errors are involved – either the increase in rainfall could be a systematic error, or the discharge data would in reality show an increase which was missed because of underestimation of abstractions or the getting out-of-date of the rating equations. A reason that certainly explains a part of the deviations also is that discharge records are mainly missing in flood flow phases of the validation period.

Which explanation is right or if the reality is a combination of the two cannot be decided finally. If explanation a) were true, it would mean that the hydrology of the forest zone is not well understood yet concerning the absorption of water by deep seepage or the forest, and that more research has to be done to find out more about the processes.

Seasonal distribution of runoff: The plots of Pardé Coefficients and monthly deviations of simulated from naturalised observed runoff in the previous sections show that the model overestimates flood flows or wet season runoff and underestimates dry season runoff. Only at A6 the highest positive deviation occurs in the dry month of July. The deviations are considerable in some catchments and some months. The main reason is the lack of a possibility within the model to "save" water from the wet periods for the dry periods (a slower groundwater discharge cannot be reached with the current parameters – there is no possibility to let slow groundwater discharge start at a higher saturated zone moisture level). Other possible reasons include overestimation of evaporation in low flow periods (uneven distribution of evaporation pans in altitude), inaccurate rating equations for either low or high flows (or both), or larger-scale underground water movements that mitigate the differences between the seasonal flows in a way that is not yet understood.

Considering all factors, it can be said that modelling results are satisfactory in the catchments where the rain gauges are distributed evenly in altitude and exposition. The quality of the simulation decreases considerably where this is not the case, such as at A4 (altitudinal precipitation maximum missed) and at A8 and A9 (few rain gauges, interpolation of rainfall from gauges with different expositions).

6. 3. SENSITIVITY OF THE MODEL TO PARAMETER VALUES

6. 3. 1. Groundwater parameters

The groundwater parameters R1COEFF (long term groundwater discharge), R2COEFF (short term groundwater discharge), SSZTH (threshold of moisture in saturated zone separating the application of the long/short term coefficients) and SCOEFF (deep seepage coefficient) are the catchment-specific parameters that take the greatest influence on the shape of the modelled hydrograph. SCOEFF removes a part of the water from the water balance, assuming that this water is lost to deep aquifers and does not show up anymore within the considered area. R1COEFF, R2COEFF and SSZTH determine the shape of the recession curve or recession limb, the part of the hydrograph that reflects the depletion of groundwater/soil water into streamflow after rainfalls. The recession rate depends primarily on catchment geology (transmissivity, storativity of the aquifers) and the distance from stream channels to catchment boundaries, i.e. catchment size (Smakhtin 2001: 161).
All parameters are entered as constants into the control file of the model. This is a simplification that clearly represents a limitation of the model structure – there will never be

constant values that represent all of the mentioned processes optimally over the time period of several years with very different soil moisture conditions. So the parameters have to be optimised for a catchment and time period to represent a mean of the complex processes that they simulate. This can be done by trial and error, but there are also ways to determine estimates of the groundwater parameters that need only slight modification afterwards. One such method that was used in this study, is described in the Section 6.3.1.1.
Another simplification of the NRM^3 Streamflow Model structure is to assume a single groundwater reservoir. This way the water amounts for slow and fast groundwater discharge and deep seepage are all drawn from the shallow saturated zone. The shape of the observed hydrographs, however, rather suggests that different stores supply the water for the different processes, which fill up and drain on different time-scales.

6. 3. 1. 1. The recession parameters: R1COEFF, R2COEFF and SSZTH

Recession rates can be described mathematically by various recession equations, of which the exponential model is probably the most common and also the one used in the NRM^3 Streamflow Model. It takes the form:

$$R = (\ln Q_1 - \ln Q_2)/(t_1 - t_2) \qquad (\text{for } t_2 > t_1) \qquad (6.6)$$

with R = recession constant
Q_1 = discharge rate at time 1 (t_1) [m^3/s]
Q_2 = discharge rate at time 2

Various ways of deriving recession constants from the shape of the observed hydrograph are mentioned by Smakhtin (2001: 161) that range from plotting "today's flow" against "flow n days ago" (correlation method) to superimposing individual recession curves to construct a master recession curve (matching strip method). Most of these methods remain rather subjective.
For parameter estimation for the NRM^3 Streamflow Model, the additional difficulty is that two constants have to be estimated and a threshold established to separate the use of the two. A semi-quantitative way of providing estimates for the three values from the observed hydrograph and the results of a first model run was explored in the course of this study, which proved quite reliable and shall be described below:

- A first model run has to be done in order to have a series of soil moisture data from the saturated zone (SSZ) to accompany the observed streamflow record.
- From the observed hydrograph, periods of pure recession (no rainfall that produces new flow peaks) are sought out.
- By subjective estimation by eye, in these recession curves the "breaking points" from a steep to a flat curve are determined; the SSZ values on these days are averaged to form the estimate for SSZTH.
- The R values are determined using formula 6.6 for the part above and below the breaking points respectively for each selected curve and averaged. The average of all R's of the flat parts provides the estimate for R1COEFF, and the average of the R's of the steep parts will be the estimate for R2COEFF.

There are of course several steps in this method where subjectivity plays the major role, from the choice of the considered recession periods (they should be as long and as "characteristic" as possible) to the fixing of the threshold. In fact, the determination of the breaking point by eye depends very much on what scale is used in the x- and y-axis of the plot; on the other

hand, there is no right or wrong breaking point or SSZTH – it can be set at various values. Is it set higher, the values of R1COEFF and R2COEFF will just have to be higher as well (because both parts of the curve will have to be steeper) than if it is set at a low value.
For A5 with this method parameter values of 0.03 (R1COEFF), 0.27 (R2COEFF) and 19.98 (SSZTH) were calculated. The finally used set is (0.03, 0.3, 20).

Fig. 6.33 shows the effect of changing the recession parameter values on the modelled hydrograph and on measures of model performance. It can be seen that there is no clear "best set" of groundwater recession parameters. The visual inspection of the hydrographs shows that for example in the baseflow period at the end of May/beginning of June 1993, run a5500gw7 (the run with the highest recession parameter values) is in best accordance with the naturalised observed hydrograph, because with its parameter values, the SSZTH threshold (the "breaking point") is reached earliest and slow groundwater discharge is highest. After the next, less intense rainy period, however, run a5500gw3 is closer to the observed values: The transition to a slow groundwater discharge now happens at a lower discharge level, the observed "breaking point" is lower. Accordingly run a5500gw3 with the lower parameter values shows less deviations.
Towards the end of the shown period, after a long recession period (the small flow peaks in the recorded hydrograph are missed by the simulation because of lacking rainfall inputs), it can be seen that all runs produce a similarly low discharge, indicating that the groundwater store is nearly empty (SSZ values around 3 mm in run a5500gw7 and around 5 mm in run a5500gw4). This means that under the current model structure, there is no possibility to store groundwater over longer periods.
The performance measures show that a5500gw4 (the run with the lowest recession parameter values) shows the highest coefficients of determination because it follows the observed pattern best, but the lower E_2 indicates higher deviations in the absolute values. So the final overall best set will necessarily be a compromise. It is also shown, however, that all parameter values produce a similar simulation quality as the finally chosen "best set".

Here a main problem with the way the groundwater recession is simulated within the current structure of the NRM^3 Streamflow Model becomes obvious: The parameter values are constant and there is only a single groundwater reservoir (the shallow saturated zone). This is why the "breaking point" between the steep (short-term) recession and the flat (long-term) recession will always appear on a similar height in the modelled hydrograph. In the observed hydrographs this breaking point is usually significantly higher after a rainy season or period than after a dry one. Also, as shown in the graphs of the seasonal distribution of simulated and observed runoff (Section 6.2), the model is not able to "save" enough water over longer time periods. To be able to simulate a more realistic behaviour, the NRM^3 Streamflow Model structure would have to be altered

- either by introducing a variable SSZTH threshold value that depends on antecedent rainfall.
- or, more physically based, by introducing a second groundwater store. This way the lower (more long-term) store could be filled up by infiltration during wet periods, thereby reducing the flood flows. The breaking point in the modelled hydrograph, that would become visible as soon as the upper (short-term) groundwater store is depleted, would then not occur always at the same height, but the height the groundwater discharge from the lower store reaches at that particular time would be added. This way also the monthly deviations of the modelled from the naturalised observed discharge sums could be better minimised: Flood flows, that are often overestimated by the model, would be reduced by the filling-up of the lower long-term store during rainy periods, and low flows could be increased.

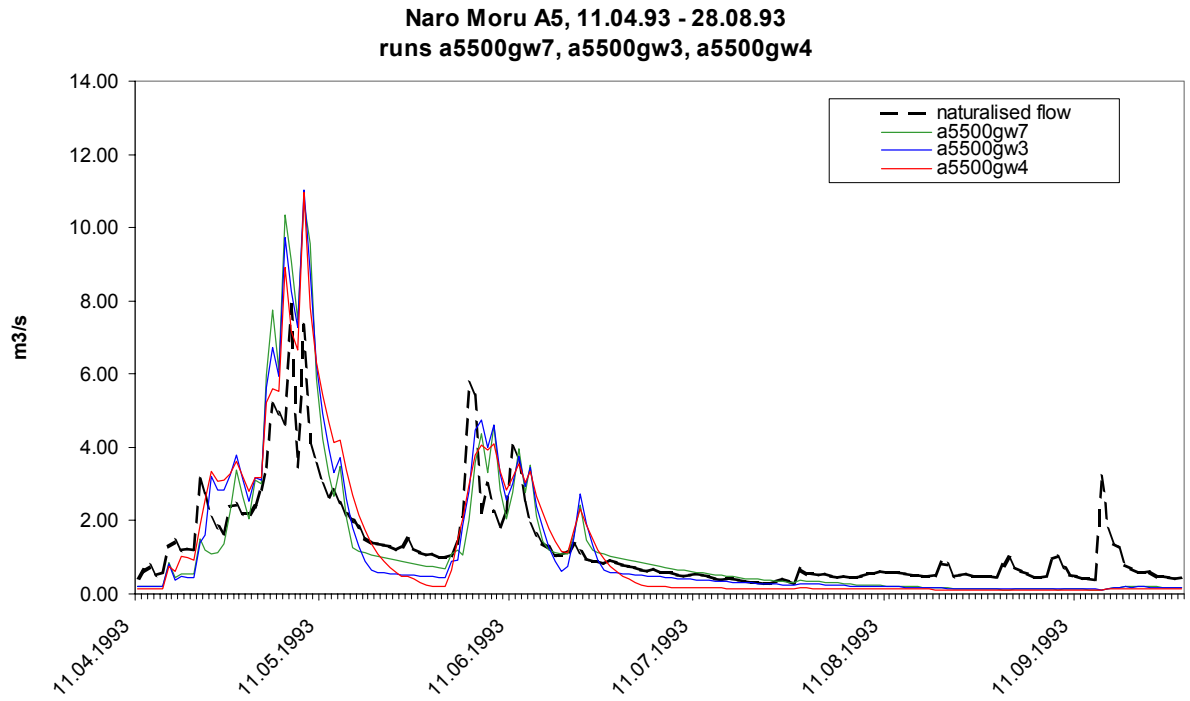

Run Name	Res.	R1 COEFF	R2 COEFF	SSZTH	S COEFF	RO COEFF	r^2 daily	E_2 daily	r^2 dec.	E_2 dec.	S – O /year [mm]	r^2 NMQ30
a5500gw3	500	**0.03**	**0.3**	**20**	0	0	0.655	0.693	0.820	0.760	-49.157	0.618
a5500gw4	500	**0.02**	**0.2**	**10**	0	0	0.664	0.649	0.824	0.707	-48.167	0.637
a5500gw7	500	**0.04**	**0.04**	**30**	0	0	0.622	0.703	0.803	0.774	-48.191	0.590

Fig. 6.33: The effect of changing the groundwater recession parameters. The parameter values and the respective measures of model performance for the calibration period show that there is no clear "best" set. Overall performance is similar in all runs. Under one parameter set, like in run a5500gw7, a high baseflow period (like the one in May/June in the given hydrograph) may be reproduced well, but a lower observed baseflow will be overestimated. Another parameter set, like in run a5500gw3, will reproduce low baseflows better but underestimate periods of high baseflows. A final set has to be chosen considering all performance measures and the visual impression of observed and modelled hydrographs.

6. 3. 1. 2. The deep seepage parameter: SCOEFF

The deep seepage parameter can be applied when modelled values are systematically higher than observed values. Since the parameter also is a constant and low flows are significantly reduced by its use as well, it was never chosen to be higher than zero for the final parameter sets in this study. Its effect is demonstrated by Fig. 6.34 for the A9 catchment: Although a reduction of the overestimation of annual runoff and a higher E_2 score could be reached by an increase of SCOEFF, for the final run it was decided to set its value to zero. The reason is that low flows are reduced too much and the overestimation of total runoff is rather caused by inappropriate or too high flow peaks in the simulation than by a systematic constant overestimation.

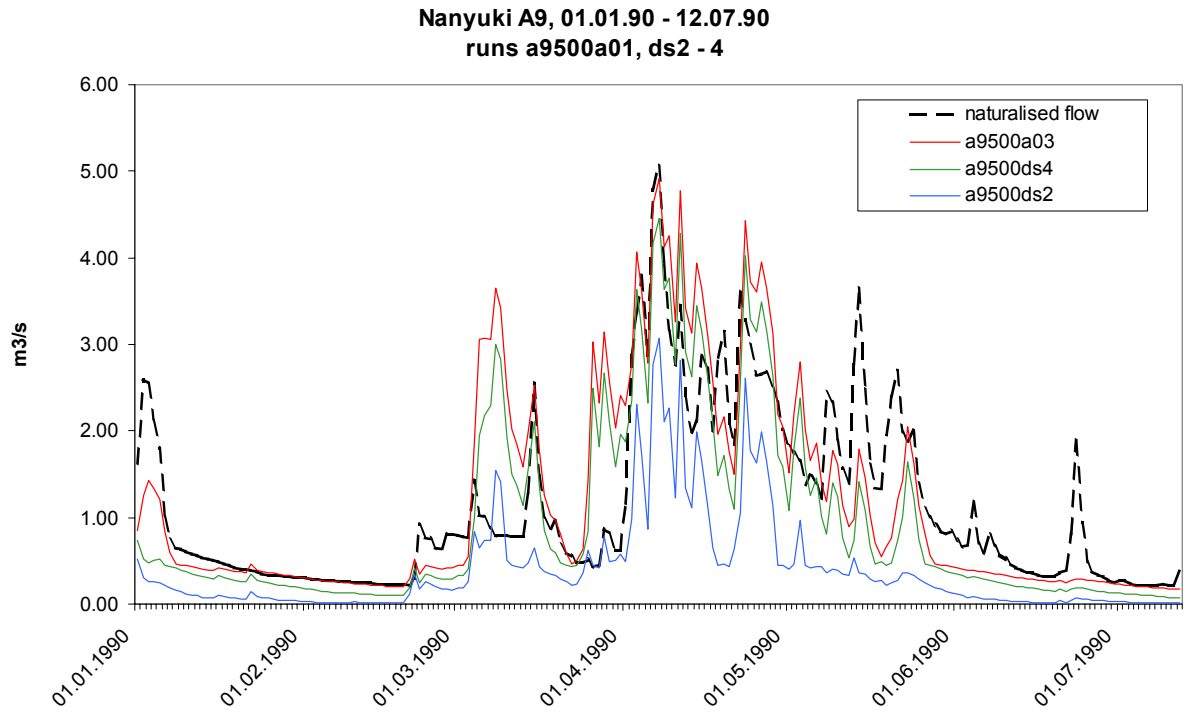

Run Name	Res.	R1 COEFF	R2 COEFF	SSZTH	S COEFF	RO COEFF	r^2 daily	E_2 daily	r^2 dec.	E_2 dec.	S – O /year [mm]	r^2 NMQ30
a9500a01	500	0.03	0.3	20	**0**	0	0.605	0.166	0.736	0.623	95.72	0.862
a9500ds4	500	0.03	0.3	20	**0.02**	0	0.601	0.454	0.738	0.528	11.22	0.853
a9500ds2	500	0.03	0.3	20	**0.1**	0	0.537	0.375	0.689	-0.153	-127.29	0.888

Fig. 6.34: The effect of changing the deep seepage parameter (SCOEFF) value at Nanyuki A9. Although the overestimation of annual runoff can be reduced, for the final run an SCOEFF value of zero was chosen, because low flows were too much reduced by SCOEFF and the overestimation of runoff is actually caused by inappropriate flow peaks. Abbreviations are listed on p. 12; run names are explained in Appendix D.1.1.

6. 3. 2. Runon

The runon coefficient ROCOEFF is intended to represent Hortonian Overland Flow which has been considered a dominant runoff generating mechanism in the study catchments (refer to Section 3.4.2). It makes a constant proportion of direct runoff from a cell flow on to downslope cells that still have infiltration capacity, where it is added to the incoming precipitation.

The net effect of the runon coefficient is to break flow peaks and provide more soil moisture for baseflow. It was found that in the study catchments its use only has a positive effect in the Naro Moru A6 catchment, the only catchment with a large area in the savannah zone. In the other catchments (A3 – A5, A8, A9) because of the shallower soils there are only few cells with infiltration capacity left after storms. Almost no effect is visible in the hydrograph even of a high ROCOEFF value in these catchments, and only a slight reduction in annual streamflow can be observed. At A6, in contrast, ROCOEFF was found to have a very positive effect and for the final run was set to 0.8.

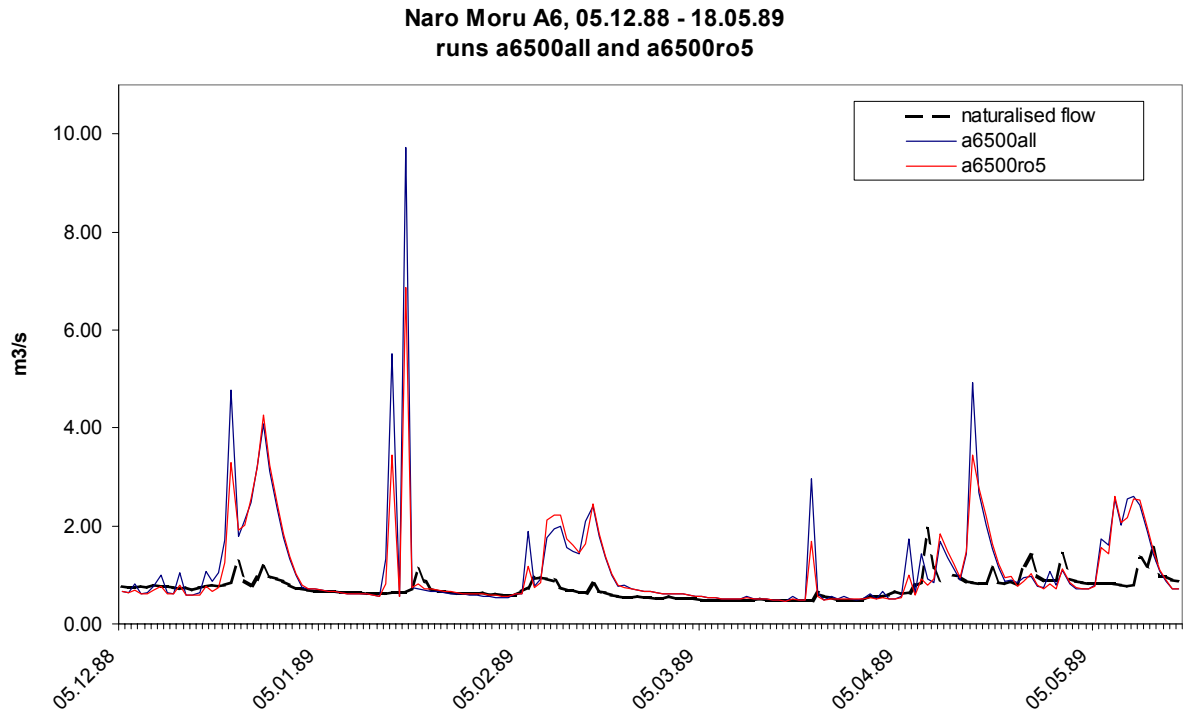

Run Name	Res.	R1 COEFF	R2 COEFF	SSZTH	S COEFF	RO COEFF	r^2 daily	E_2 daily	r^2 dec.	E_2 dec.	S – O /year [mm]	r^2 NMQ30
a6500all	500	0.02	0.25	18	0	**0**	0.443	0.416	0.649	0.450	26.192	0.792
a6500ro2	500	0.02	0.25	18	0	**0.2**	0.446	0.428	0.644	0.449	24.458	0.781
a6500ro3	500	0.02	0.25	18	0	**0.5**	0.457	0.450	0.645	0.463	21.690	0.792
a6500ro5	500	0.02	0.25	18	0	**0.8**	0.473	0.483	0.652	0.483	17.960	0.801

Fig. 6.35: Increasing the runon coefficient ROCOEFF at A6 clearly has the positive effect of reducing inappropriate flow peaks. In the other catchments, that only have very small savannah areas, ROCOEFF was found to have almost no effect. Abbreviations are listed on p. 12; run names are explained in Appendix D.1.1.

6. 3. 4. The dynamic curve number component (model version stm4d)

The seasonally dynamic curve numbers were introduced to account for the long-term moisture status of a catchment, especially the quality of the grass cover and its hydrological influence in savannah catchments (refer to Section 3.4.3). The seasonal deviations of catchment rainfall from the long-term annual mean are used to construct a series of average, dry or wet seasonal conditions. Base curve numbers are then reduced in wet seasons and increased in dry seasons (contrary to the final curve numbers which are increased by high antecedent rainfall and reduced by low antecedent rainfall – a "contradiction" that demonstrates that the curve numbers are a parameter used to account for two different effects; refer also to Section 3.4.1). The use of the dynamic curve number component was found to bring no improvement in the study catchments. There could be several reasons for this:

- The processes found to have a hydrological influence in the Mukogodo catchment, where the routine was first introduced, don't play a significant role in perennial meso-scale catchments on the Mt. Kenya slopes.
- Generally the curve numbers might have been chosen to low (see Section 6.3.5) and thus a dry season status will improve the simulation while a wet season status will reduce simulation quality. The net effect is neither negative nor positive.

- The principle is good but the method for the determination of average, wet or dry conditions has to be improved: seasons in this routine always include the same whole months, but the onset of wet or dry conditions varies considerably from year to year. So the positive effect of the dynamic curve numbers is lost to bad timing. For this theory speaks the fact that often the first flow peaks after a longer dry period are underestimated by the model because the soil has much infiltration capacity, while in reality the first rainfalls might produce a larger proportion of surface runoff due to the dried-out and crusted soil surface.

The effect of the dynamic curve numbers is demonstrated by Fig. 6.36 for the A6 catchment. The seasonal status is DRY until the end of September and WET from October to December of the illustrated period. It can be seen that the dry curve numbers cause significantly higher flow peaks at the beginning of the period, which are overestimated anyhow by the model. In the WET period, almost no difference between the two simulated hydrographs is visible.
The performance measures for the calibration period at A6 are lower for the run making use of the dynamic curve numbers than for the run without its use but otherwise the same settings.

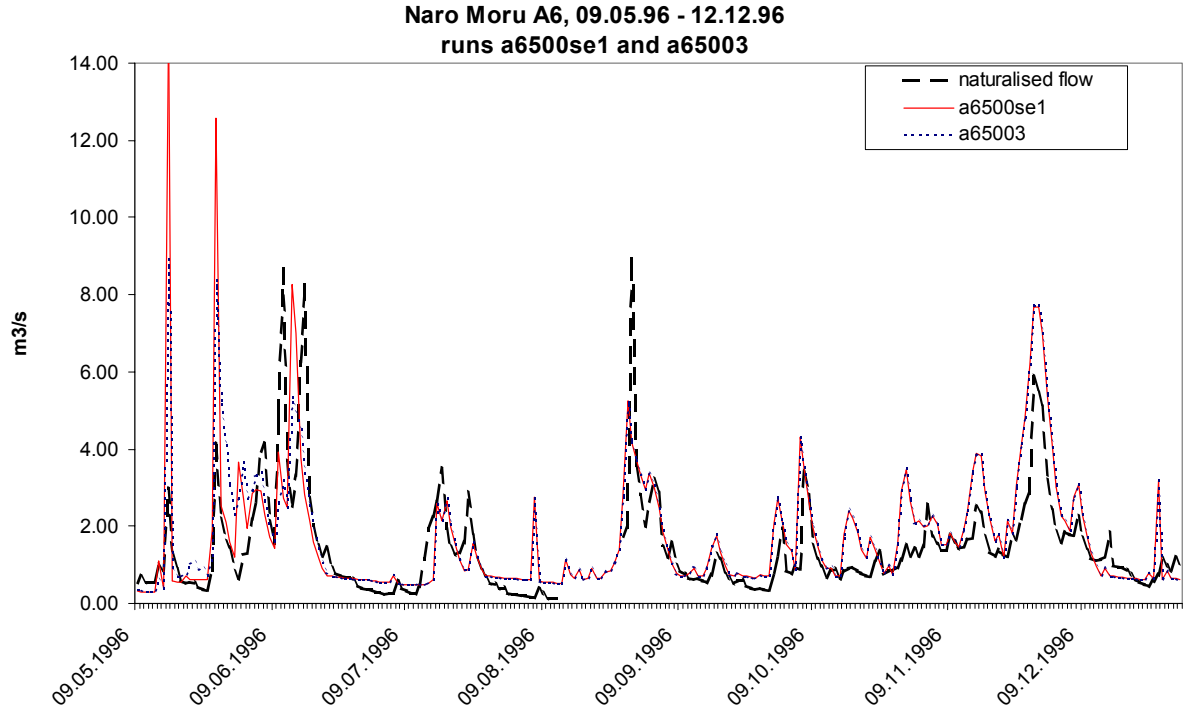

Run Name	Res.	R1 COEFF	R2 COEFF	SSZTH	S COEFF	RO COEFF	r^2 daily	E_2 daily	r^2 dec.	E_2 dec.	S – O /year [mm]	r^2 NMQ30
a65003	500	0.02	0.25	18	0	0	0.439	0.412	0.643	0.438	26.230	0.775
a6500se1	500	0.02	0.25	18	0	0	0.399	0.347	0.636	0.393	29.176	0.652

Fig. 6.36: The effect of the dynamic curve number component at A6. It can be seen that a DRY seasonal status (until 31.09.96) causes higher flow peaks while almost no difference between the two simulated hydrographs is visible when the seasonal status is WET (October to December 1996). The performance measures for the calibration period are inferior for the run using the routine (a6500se1). Abbreviations are listed on p. 12; run names are explained in Appendix D.1.1.

6. 3. 5. Curve numbers

Although the curve numbers are neither a catchment-specific parameter nor subject to calibration in this study, the effect of raising them by 10% was explored for the A5 catchment because of the underestimation of flow in the calibration period and the fact that some small flow peaks were missed by the simulation. Surprisingly it was found that the increased curve numbers resulted in a better overall simulation quality according to almost all considered performance measures except the NMQ30 in the validation period. A visual inspection of the simulated hydrographs (Fig. 6.37) reveals that especially small flow peaks in or after dry periods that are "swallowed up" by the original curve numbers, which makes the run with the increased curve numbers follow the observed pattern better. On the other hand, baseflow is slightly reduced, and total runoff in the validation period is more overestimated than in the run with the original curve numbers.

Two reasons could be responsible for the effect of better simulation quality with higher curve numbers:

a) the curve numbers of some or all of the land use classes in the study catchments are calibrated too low.

b) the curve numbers are OK but inaccurate rainfall inputs cause deviations that are partly made up for by the higher curve numbers.

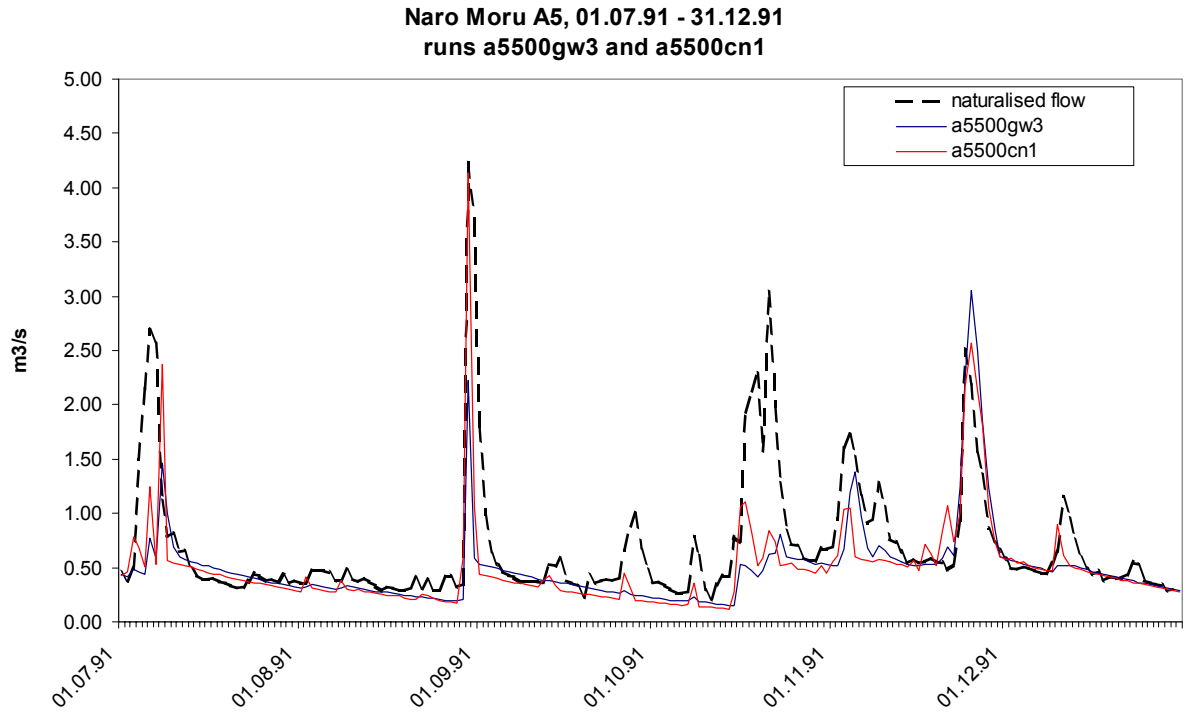

	Calibration period						Validation period					
Run Name	r^2 daily	E_2 daily	r^2 dec.	E_2 dec.	S – O /year [mm]	r^2 NMQ30	r^2 daily	E_2 daily	r^2 dec.	E_2 dec.	S – O /year [mm]	r^2 NMQ30
a5500gw3b	0.655	0.693	0.820	0.760	-49.157	0.618	0.564	0.513	0.721	0.659	13.044	0.906
a5500cn1	0.660	0.701	0.824	0.773	-45.865	0.651	0.586	0.540	0.732	0.689	16.386	0.892

Fig. 6.37: Sensitivity of the modelling results to changing curve numbers. The run with the increased curve numbers by 10% (a5500cn1) shows a better overall performance than the run with the original curve numbers.

6. 4. SENSITIVITY OF THE MODEL TO INPUT DATA

6. 4. 1. Sensitivity to meteorological input data

6. 4. 1. 1. Precipitation

Precipitation inputs are clearly the type of data that modelling results are most sensitive to and that represents the most limiting factor for hydrological modelling in the study area. There are several reasons for the difficulties in monitoring precipitation in the study area:

- The dominance of convective over advective rainfall generation causes many storms to have a very local extent. Storms that can cause many millimetres of rainfall in one place may not be felt just a few kilometres away.
- Orography additionally causes a vertical precipitation gradient, and it represents obstacles to the air movements that result in higher precipitation on the windward and lower precipitation on the leeward sides and turbulences in the air masses, resulting in a very complicated rainfall pattern.

The consequence for hydrological modelling is that observed flow peaks may not at all be simulated because rainfall inputs are lacking, or the reverse effect that peaks are modelled that were never recorded because storms that occurred in other catchments were interpolated to the catchment in question. A good example is the year 1987 in the Nanyuki catchment, shown in Fig. 6.38. In Nanyuki catchment a lot of the precipitation in the crucial runoff-generating areas of the upper forest and moorland zones is interpolated from the rain gauges along the Naro Moru Profile that are not so far away in kilometres but have a different exposition on the mountain.

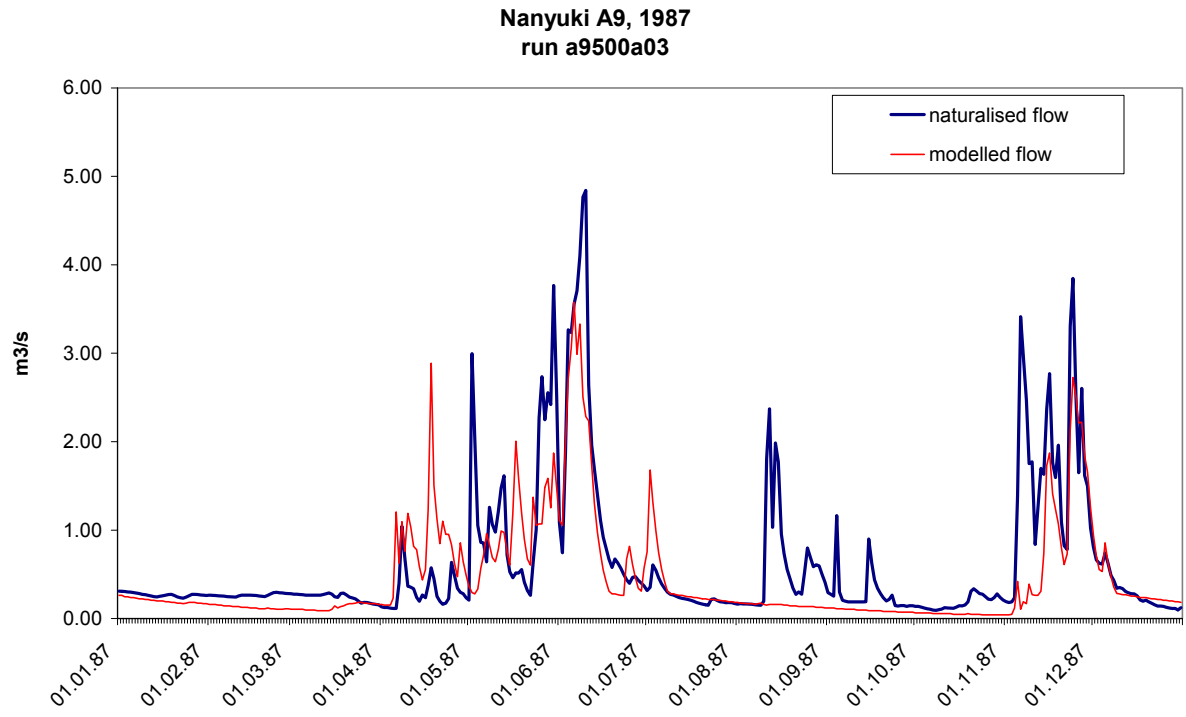

Fig. 6.38: The year 1987 at Nanyuki A9. It can be seen that some modelled flow peaks did not occur in reality while other observed flow peaks were completely missed by the model because of inaccurate catchment rain interpolation.

The introduction of an altitude-dependent interpolation of rainfall in combination with the currently used IDW would help to solve the altidude problem. But in order to capture all storms an extremely dense network of rain gauges would have to be maintained, which is not

realistic for financial reasons. New techniques, like remote sensing of cloud temperatures in order to monitor storms, are interesting options for the future.

Fig. 6.39 shows the effect of leaving away the data from all rain gauges installed by NRM^3 on a simulation run of the A5 catchment (using the data of only three gauges instead of six). The outcome is a clearly not acceptable simulation quality – the E_2 score for the calibration period sinks from 0.69 to 0.15. This illustrates the importance of the NRM^3 monitoring network – hydrological modelling as a method for predicting the state of water resources would not be an option for water management in the region if the monitoring network was discontinued.

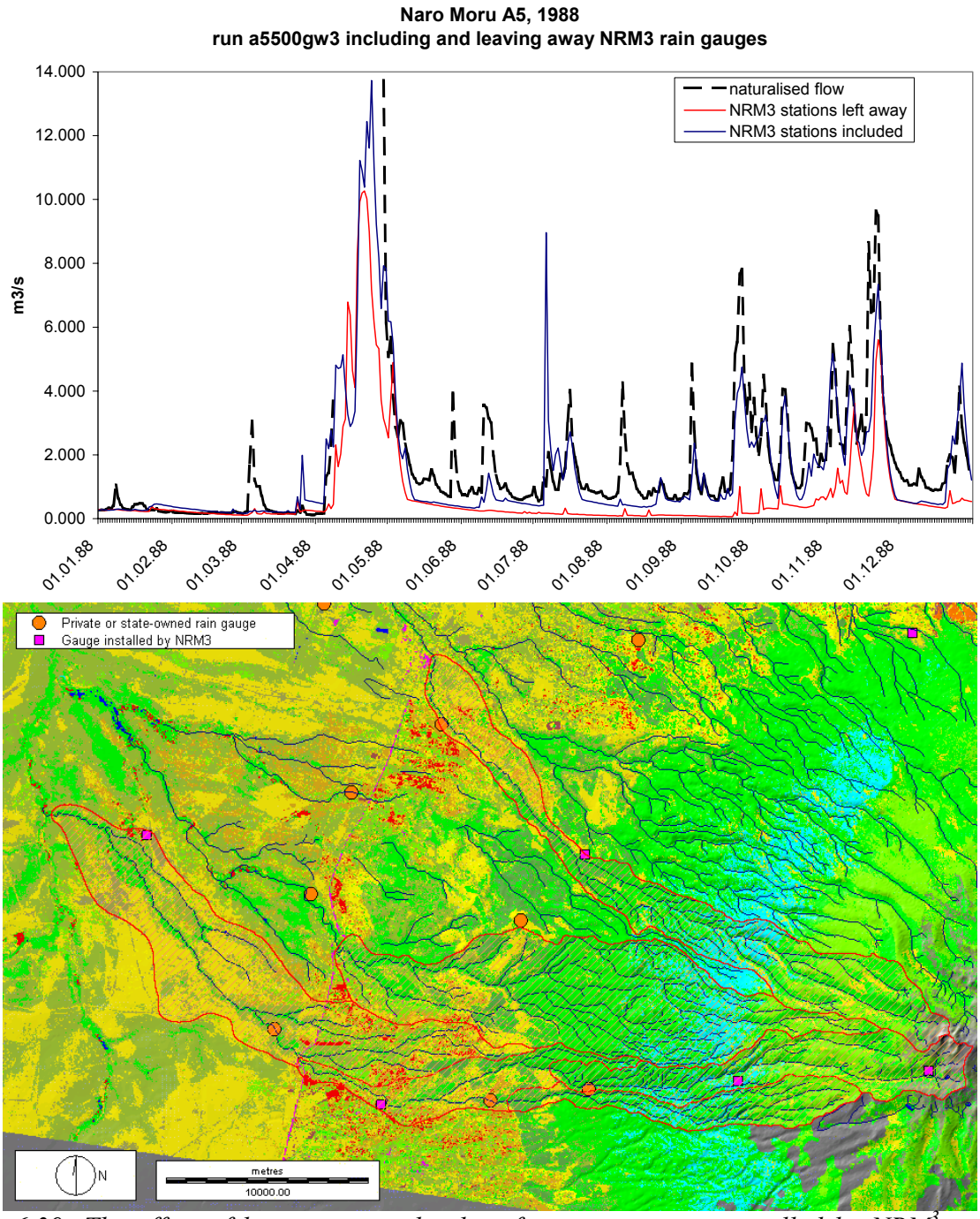

Fig. 6.39: The effect of leaving away the data from rain gauges installed by NRM^3 on the simulation quality (above: comparison of the hydrographs; below: map with the left-away gauges marked as squares). The result is a very low simulation quality – an E_2 score of 0.15 only is reached for the calibration period.

6. 4. 1. 2. Evaporation

Evaporation data plays a less important role than precipitation data. A model run using monthly averages over the whole calibration and validation period instead of daily measured data even reached better scores in some respects. Even the difference of total runoff deviations between calibration and validation period is reduced. The respective hydrographs are shown in Fig. 6.40 a) (runs a5500gw3 with daily measured evaporation data and run a5500eta with monthly averages).

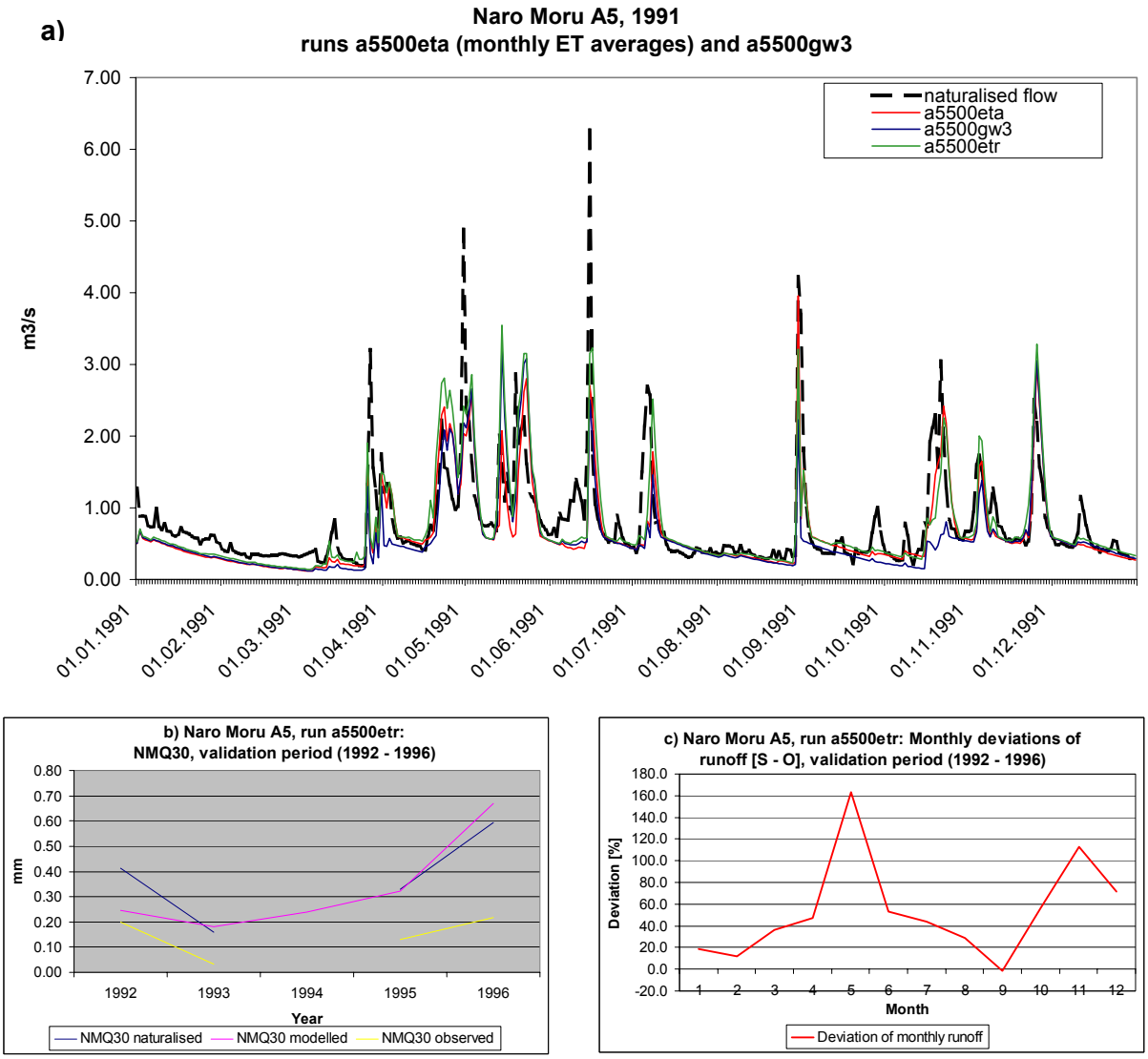

	Calibration period						Validation period					
Run Name	r^2 daily	E_2 daily	r^2 dec.	E_2 dec.	S – O /year [mm]	r^2 NMQ30	r^2 daily	E_2 daily	r^2 dec.	E_2 dec.	S – O /year [mm]	r^2 NMQ30
a5500gw3	0.655	0.693	0.820	0.760	-49.157	0.618	0.564	0.513	0.721	0.659	13.044	0.906
a5500eta	0.657	0.711	0.817	0.794	-44.755	0.617	0.549	0.516	0.702	0.653	0.482	0.856
a5500etr	0.670	0.700	0.823	0.780	2.517	0.586	0.569	0.476	0.723	0.638	50.790	0.773

Fig. 6.40: The effect of averaging and leaving away evaporation data at A5: the run a5500eta (red line in 6.40 a)) using monthly average ET values shows even some better scores than the final run a5500gw3 (blue line) and shows less under- and overestimation of total runoff in the calibration and validation period. Using average seasonal evaporation rates from 1983/84 for Teleki (4262 m a.s.l.) (run a5500etr, green line in 6.40 a)) resulted in less underestimation of low flows (Fig. 6.40 a), and NMQ30 in Fig. 6.40 b)), but significantly increased the monthly deviations and the overall overestimation in the validation period (Fig 6.40 c)).

It was also tried to improve the distribution of evaporation in altitude by using seasonal average evaporation rates measured by Decurtins (1992: 80) in the years 1983 and 1984 at the station Teleki (4262 m a.s.l.). This resulted in higher baseflows (Fig. 6.40 a) and b)), but raised the overestimation of flow in the validation period from 13 to 50 mm/year and significantly increased the overall monthly deviations of runoff (Fig. 6.40 c)). This means that in fact the lack of evaporation data at high altitudes is partly responsible for the underestimation of low flows (although they are still underestimated relative to the flood flows, and in the calibration period also in absolute terms, indicating that the main problem is inherent in the model structure), but also that an underestimation of average evaporation rates in wet season months in the upper catchment can cause significant additional deviations.

6. 4. 2. Sensitivity to GIS inputs

6. 4. 2. 1. Resolution

Simulation quality is expected to decrease with coarser resolution of GIS input data. A finer resolution, however, requires a higher monitoring effort to record the data, more disc storage space and more computation time for model runs. For example, a 10-year run in 500 m resolution on a PC using a Pentium(R) 4 1600 processor just takes 1 to 2 minutes, while the same run in 50 m resolution takes more than 24 hours. It was thus explored which is the critical resolution of GIS input data for a good simulation quality.

Fig. 6.41 shows the daily Efficiency Scores and the deviations of simulated from observed runoff for different resolutions in the validation period at A5. It can be seen that the efficiency as well as the runoff deviations remain stable up to a resolution of 500 m. The same can be said for the other catchments.

Zappa (2002: 49) established a function to calculate critical grid size from catchment area based on his findings and those of other authors:

$$\beta = 0.021 * \alpha^{0.61} \qquad (6.7)$$

where β is the critical grid size and α the catchment area. With this formula, the critical grid size for the study catchments would actually be lower (320 m for A5, 142 m for A4), but it has to be taken into consideration that a) this is a fitted function and the critical grid size of 500 m can be found for a catchment of 43.3 km^2 in the xy-plot for this function and b) that the NRM^3 Streamflow Model is not a distributed but a semi-distributed model: The resolution of GIS inputs influences modelling results mainly by way of the curve numbers; topography only plays a role in the determination of flowpaths for the runon routine (and not determination of cell rainfall, temperature for snowmelt, or exposition, or subsurface flowpaths like in more physically-based models).

Table 6.15 shows the average, maximum and minimum base curve numbers, the number of cells within the catchment and the actual catchment area for each resolution at the A5 catchment. The decreasing performance at resolutions of 1000 m and coarser coincides with increasing deviations of the average base curve number and low cell counts inside the catchment. This suggests that for running the model in other catchments, the criteria for a sufficient resolution could be formulated as:

- The average base curve number (or average land use and soils) should not deviate from the one in the highest resolution available by more than +/-1. This can be determined easily in Idrisi with the EXTRACT module.
- The number of cells within the catchment should be large enough – at least 50 to 100.

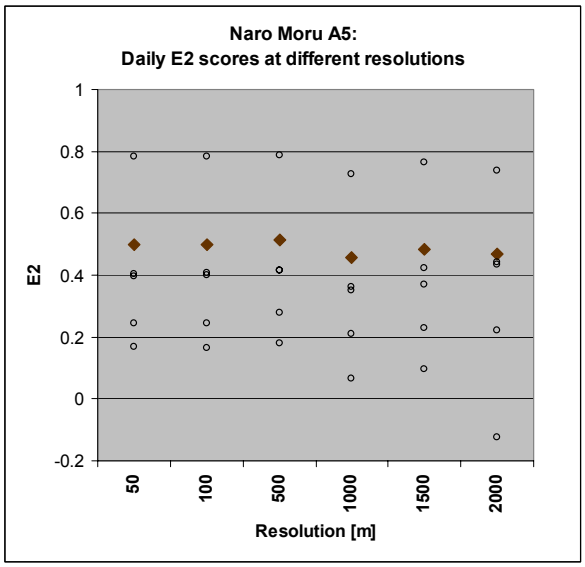

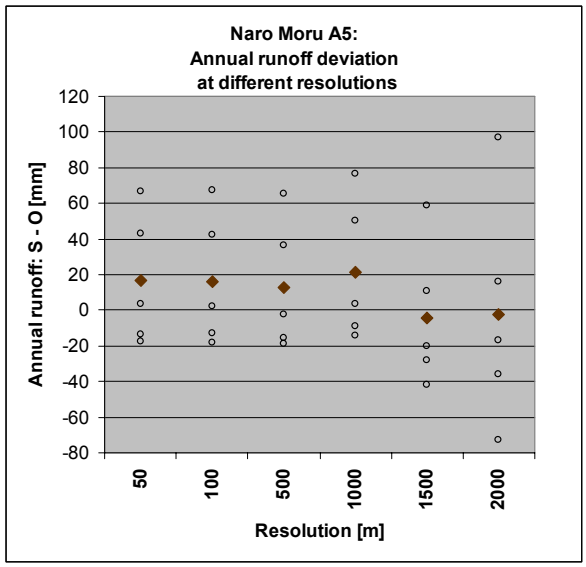

Fig. 6.41: Daily E_2 scores (left) and deviations of simulated from observed runoff (right) for different resolutions at Naro Moru A5. Circles indicate the performance in the single years, diamonds stand for the whole validation period.

The GIS catchment area is of minor importance since model outputs are given in millimetres and have to be converted into m^3/s outside the model (in this study done in the StreamflowAnalysisMacro, see Appendix C.7) where the real catchment area is used anyway.

Resolution [m]	50	100	500	1000	1500	2000
Average base CN	64.529	64.553	64.325	66.648	63.59	68.36
Min CN	47	47	47	47	47	47
Max CN	95	95	90	89	80	80
No. of cells in catchment	34800	8682	342	91	39	25
GIS catchment area [sqkm]	87	86.82	85.5	91	87.75	100

Table 6.15: Average, maximum and minumum base curve numbers, number of cells inside the catchment and actual GIS catchment area for A5 at different resolutions.

6. 4. 2. 2. Land use maps 1988 and 1995

The measures of model performance for the run a5100l95, using the 1995 land use map, compared to the performance of run a5100a01 (land use map 1988 used), are given in Table 6.16. The same parameters as for the final run a5500gw3 were used but GIS inputs were given in 100 m instead of 500 m resolution. The use of the land use map 1995 does not, as might be expected, result in better performance in the validation period – the simulation quality even decreases. Similar results were achieved in the other catchments.

	Calibration period (1987 – 1991)						Validation period (1992 – 1996)					
Run Name	r^2 daily	E_2 daily	r^2 dec.	E_2 dec.	S – O /year [mm]	r^2 NMQ30	r^2 daily	E_2 daily	r^2 dec.	E_2 dec.	S – O /year [mm]	r^2 NMQ30
a5100l95	0.660	0.675	0.824	0.741	-37.855	0.586	0.563	0.453	0.714	0.600	23.758	0.693
a5100a01	0.656	0.690	0.822	0.760	-45.779	0.622	0.563	0.499	0.722	0.646	16.132	0.903

Table 6.16: Runs at Naro Moru A5 in 100 m resolution, a5100l95 using the land use map 1995 and a5100a01 using the 1988 map. A5100l95 shows clearly inferior performance in the validation period, where is should be expected, to perform better.

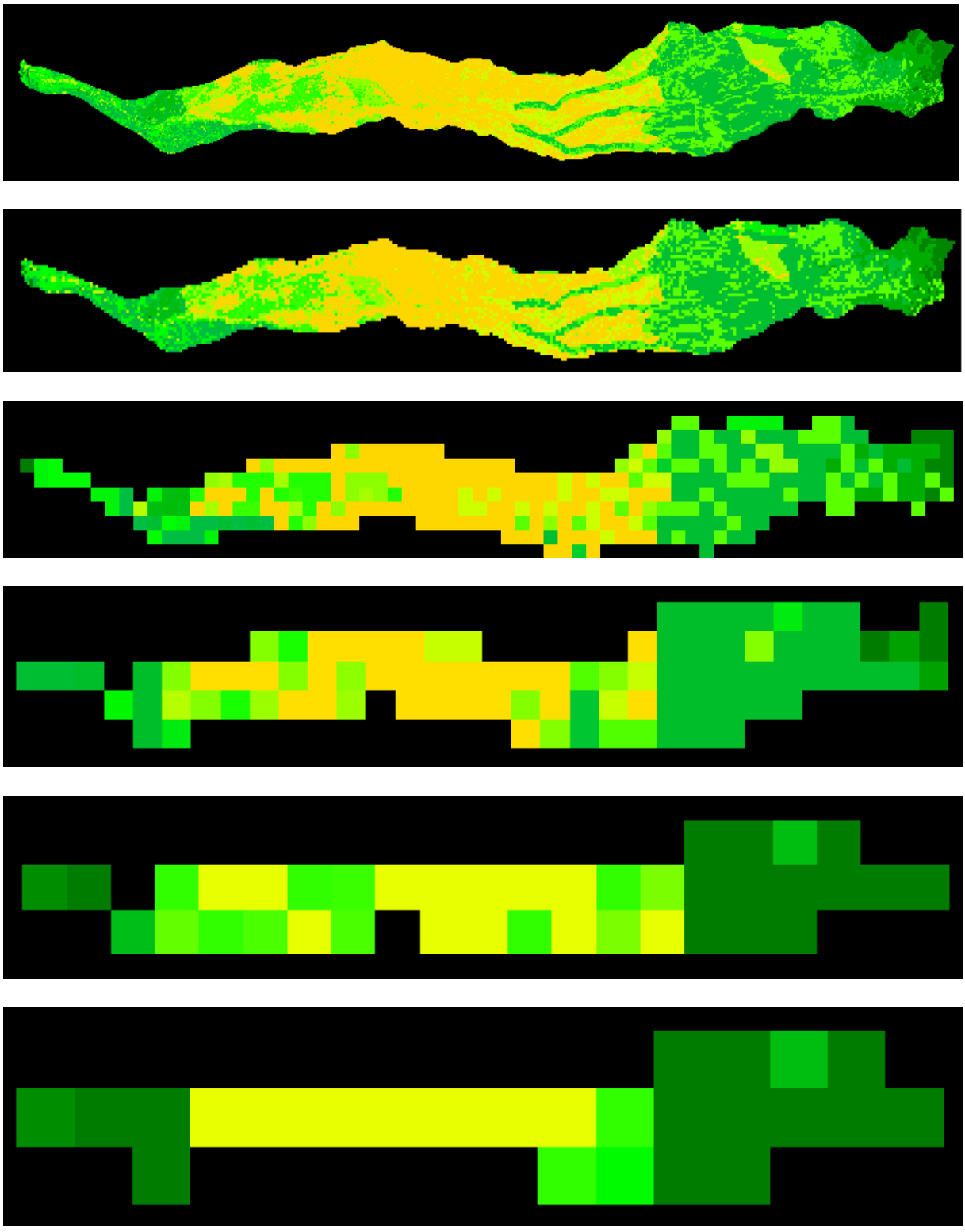

Fig. 6.42: Maps of the A5 base curve numbers at resolutions 50, 100, 500, 1000, 1500 and 2000 meters (from top to bottom; green = high curve numbers, yellow = low curve numbers).

The analysis of both land use maps (Fig. 6.43) reveals that on the 1995 map the proportion of forest (Td) is much lower than on the 1988 map, but grassland (G) has increased. The inspection of the maps shows that the changes do not so much affect the lower,

anthropogenically strongly influenced part of the catchment but mainly the moorland and alpine area. This is probably not so much due to real changes between 1988 and 1995 but to different ground conditions at the time when the satellite images were made or different classifying methods. The 1995 land use map results in a higher average base curve number (66.76 instead of 64.55 for A5), mainly effective in the upper parts of the catchment were most direct runoff is generated, raising the flow peaks in the period when they are overestimated by the model anyway.
For these reasons the 1988 land use map was used for all final runs.

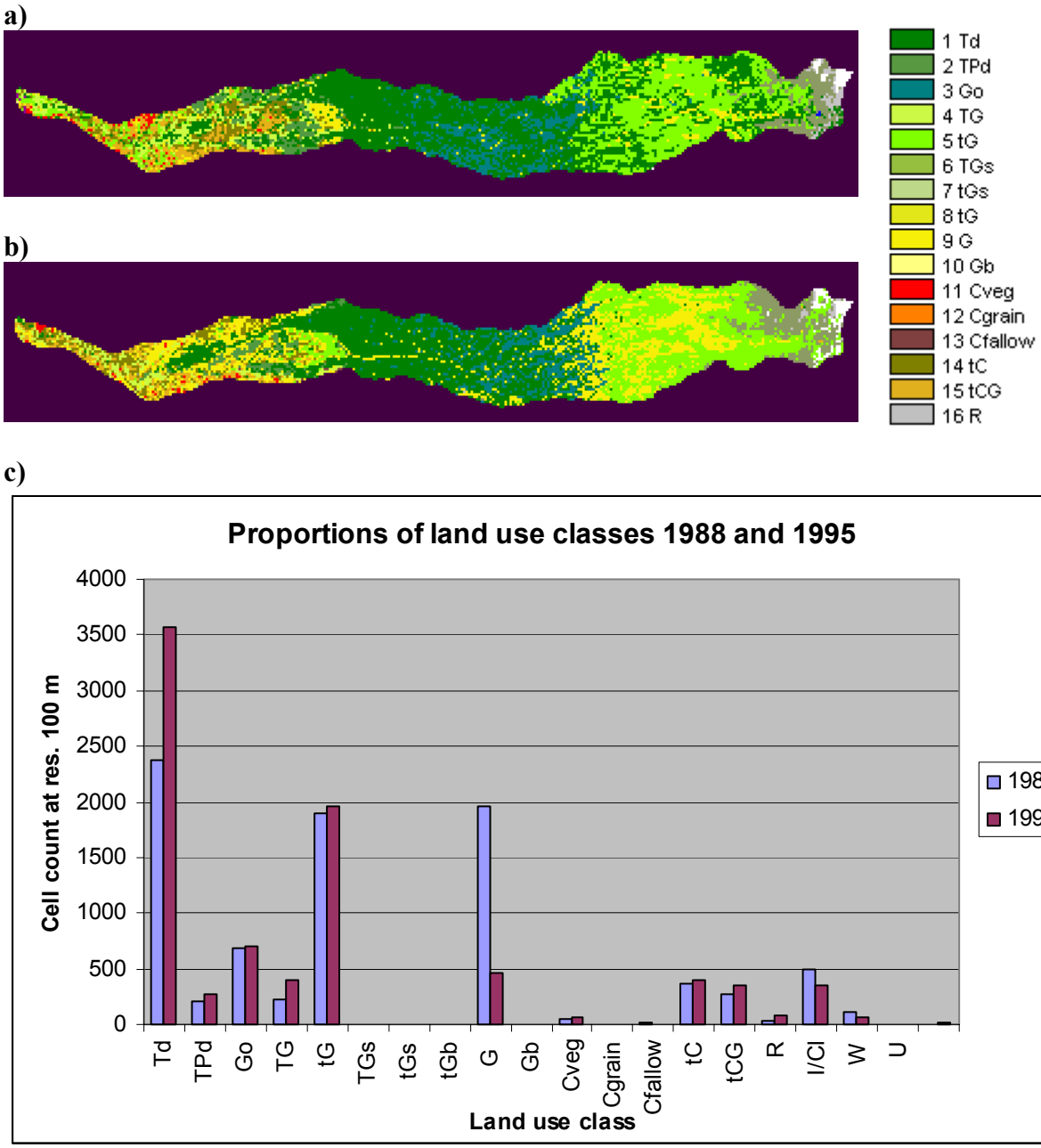

Fig. 6.43: a) land use map 1988 (Roth 1997); b) land use map 1995 (Niederer 2000), in 100 m resolution; c) histogram showing the differences in area proportions occupied by the land use classes. The land use categories and their associated parameter values can be viewed in Appendix A.5.

6. 5. FURTHER MODEL OUTPUTS

Besides daily discharge, there are other types of outputs from the NRM^3 Streamflow Model, that could not be used to evaluate the simulation quality in calibration and validation because there were no corresponding observed datasets available. Nevertheless these outputs can help in analysing the hydrological characteristics of catchments, even if their validity is not supported by measured data. The output maps of cell rain and runoff-generating areas and the soil moisture time series shall be presented as useful analysis tools in the following sections.

6. 5. 1. Runoff-generating areas

For days on which the rainfall threshold set in the control file is exceeded in the rainfall input data file, the model prints output maps in the Idrisi16 format of cell rain, final curve numbers, direct runoff generated on each cell, plant available water and soil moisture (see also Section 3.4.4). Examples of each map can be viewed in Appendix C.6.
Of great hydrological interest is the reaction of cells or hydrological response units to incoming rainfall. Fig. 6.44 shows cell rainfall and direct runoff generated in Naro Moru A5 catchment on a day in the dry season and on a day in the long rains season.
In the first example, on February 21, 1987 (Fig. 6.44 a), most rain is recorded at MetStation (29.7 mm). Accordingly the cells in this area generate most runoff, but there is a clear difference between forested cells, that even in close proximity to MetStation generate no direct runoff, while adjacent grassland cells with the same soils produce up to 3.35 mm runoff (all on humic andosols). The rock cells at the peak of Mt. Kenya also generate comparatively much runoff – 0.145 mm for 5.43 mm of precipitation. A little runoff (0.38 mm) is also generated by the "urban" (Naro Moru town) lowest cell of the catchment, that received 11.98 mm of rainfall on this day.
On April 6, 1987 (Fig. 6.44 b) rain increases with altitude, the maximum of 26.4 mm is recorded at Teleki. Accordingly the rocky areas around the peak generate most runoff, in the range of 11 mm. In the upper forest and moorland zone, rainfall is around 20 mm; grassland cells produce 4 – 6 mm of runoff, while forested cells generate some runoff (0.5 –1.5 mm) as long as they are located on shallow soils (dystric histosols or regosols). In the lower forest zone and footzone no direct runoff is generated, although rainfall is still in the range of 15 – 20 mm in the forest zone, 10 to 15 mm in the footzone and below 10 mm only in the lowest tip of the catchment.

6. 5. 2. Shallow saturated zone moisture

The water content of the shallow saturated zone, the groundwater reservoir of the NRM^3 Streamflow Model, is printed as daily output series in the outfile of every model run. Its analysis allows to assess the dynamics of baseflow contributions to streamflow.
Fig. 6.45 shows the average catchment saturated zone moisture for all Naro Moru catchments (A3 – A6) in the period 1990 and 1991, 1990 being a rather wet year (precipitation = 1223 mm) and 1991 being a dry year (precipitation = 809 mm). A4 catchment displays the highest variability (highest moisture peaks but also lowest values) and A6 the lowest variability. A3 catchment often shows the highest values in recession phases, indicating that this subcatchment sustains a substantial part of dry period flows. The graphs have to be looked at with care, however, since these values are pure simulation and not validated by any measurements. It would certainly be recommendable to evaluate modelled soil moisture and groundwater table time series with measured ones to find out more about the subsurface water

balance in the catchments, mainly at A4 (where total discharge is greatly underestimated by the model). Such measurements have in fact been carried out in the forest zone of Naro Moru catchment and will soon be analysed in a further MSc thesis within the framework of NRM[3].

a)

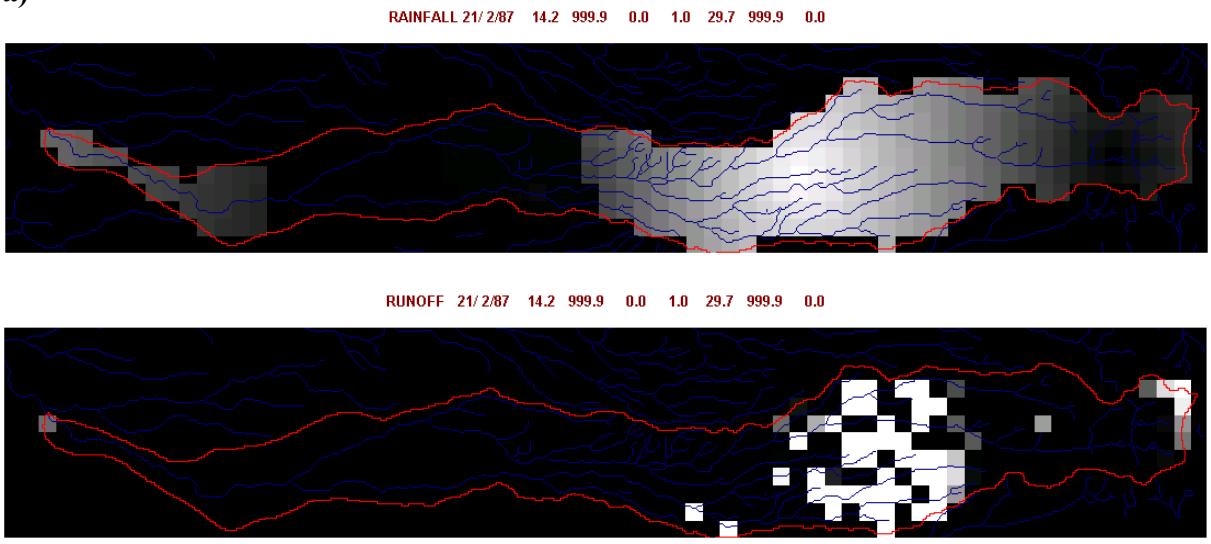

b)

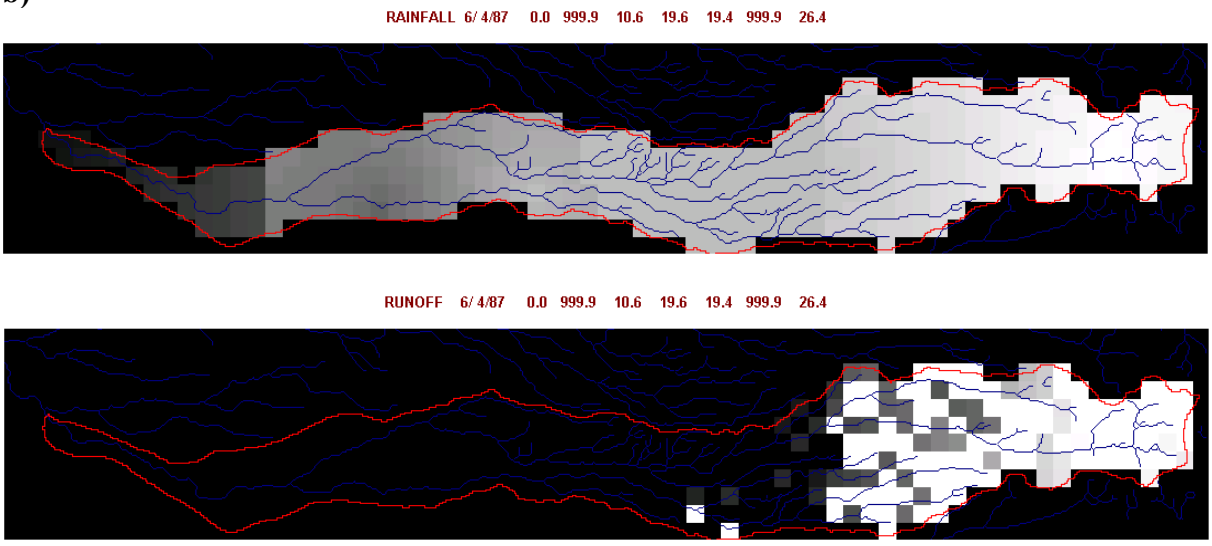

Fig. 6.44: Cell rainfall and direct runoff in Naro Moru catchment on 21/02/1987 (a) and 06/04/1987 (b) (white areas = high rain/runoff values). The figures indicate the rainfall amounts at measured at the gauges within the catchment (999.9 = missing value). Most direct runoff is generated from grassland and rock cells in the upper catchment. Forested cells only generate direct runoff as long as they are situated on shallow soils. The resolution of the grid layer is 500 m.

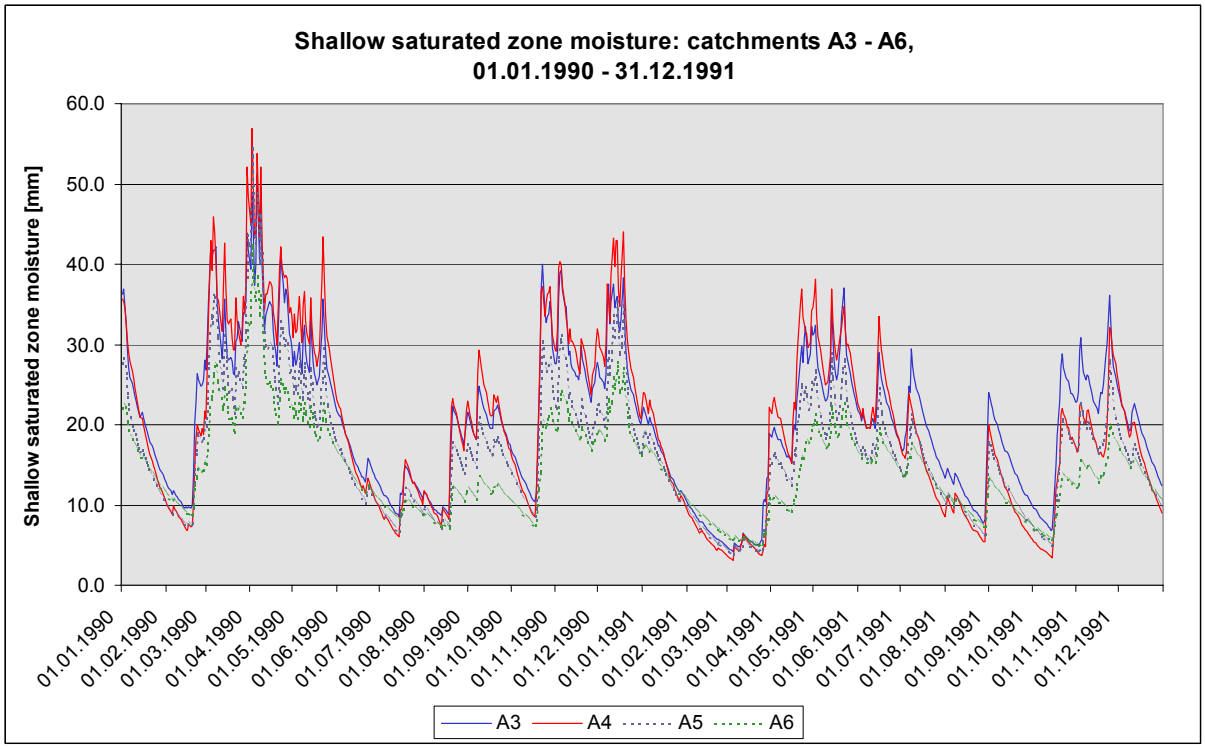

Fig. 6.45: Average catchment shallow saturated zone moisture for the Naro Moru A3 – A6 catchments.

6. 6. HANDLING AND USER-FRIENDLINESS

The successful use of the NRM^3 Streamflow Model as a tool for water management in the Upper Ewaso Ng'iro does not only depend on its ability to reliably simulate discharge from catchments, but also on its handling and user-friendliness. If a tool is too complicated or time-consuming or if the necessary skills to handle it are lacking in the context where it is to be applied, it will not be used, or mistakes are likely to occur. This is why this section is dedicated to the practical side of the NRM^3 Streamflow Model's applicability in the context of NRM^3 and the River Water Users Associations.

At present the NRM^3 Streamflow Model takes the form of an executable file, the actual programme, that is controlled by a control file, a simple text file. The input data files are text files as well; even the GIS files can be opened as text files and edited manually. Since some parameters are hardcoded in the executable file, for runs with certain features the source code has to be altered and recompiled. While this programme structure certainly gives the user a lot of control, it also makes the use of the model very time-consuming and is the source of many potential errors. The following elements should be introduced or changed to make the model more user-friendly:

- **Graphical user interface:** Most computer users today are accustomed to the windows-type graphical interface where buttons can be clicked on and information entered in dialog windows. When confronted with a command-line programme, many potential users might give up already. The introduction of such an interface would also help to eliminate error sources, since it would be possible to warn the user when invalid information is entered.

- **Outputs:** For the work on this study outputs were analysed with Excel macros which produced all summary statistics and graphs. The production of these macros is very time-consuming, and they can only be used as long as similar time periods are considered, since Excel stores dates as integer numbers and does recognize months or years – so when other time periods are considered, the whole macro has to be altered. In addition the Excel macros take up large amounts of disk space and have to be saved for every run if the data want to be kept available. The automatisation of analysis outputs would certainly be a very desirable feature.
- **Warnings and error messages:** under the current structure situations may occur where a simulation simply stops without any explanation. More often an error message is printed in the command prompt, but it is only understandable to someone with knowledge on Fortran77. Warning dialogues within the graphical users interface that would inform the user about invalid inputs and more understandable error messages for all possible errors would increase user-friendliness a lot. At present it can be very time-consuming to find errors – they might be very small things, such as a digit too much in a number or a start of a data series at the wrong line number.
- **Hardcoded parameters:** Certain parameters, such as the maximum number of cells that can be processed, the maximum number of rain gauges or the maximum number of soil types, soil layers or land cover types are at present hardcoded in the source code. Recompiling requires a compiling programme – which is free for Linux but has to be bought under Windows systems, causing additional costs. Additionally repeated recompiling results in a series of different versions of the same programme, which represents another source of error.
- **File conversions:** when running the model under Linux but analysing the outputs in Windows, in- and output files have to be converted from DOS to Unix format and back. The GIS files have to be converted between the older Idrisi16 format that the model uses and the newer Idrisi32 format that is more widespread today. These conversions are time-consuming and could be automated.
- **Handling of files:** currently all input files for a run have to be placed in the same folder for a model run. This results in many folders with many files of which many have the same names. This way disk space is unnecessarily occupied, and potential errors increase when files are copied back and forth.
- **Automatic re-running and parameter optimisation:** The fact that the control file name has to be entered manually every time a run is started at present even makes impossible to use scripts that would allow to automatically start several runs after each other. Almost luxurious would be an option to automatically look for optimised parameter sets – which certainly is one of the least urgent improvements, the number of catchment-specific parameters being so small.

All of these improvements would be very desirable. None of them is really necessary in order to run the model as long as a person with the necessary skills and lots of time available is using it. But realistically speaking the model would probably could be used much more easily if it was introduced into the context of NRM^3 and the RWUAs in an updated programme structure.

6. 7. CONCLUSIONS

The question whether the NRM^3 Streamflow Model can be applied as a potential tool for water management in the Upper Ewaso Ng'iro Basin – especially the demonstration of the effects of land use change and the prediction of low flows – has to be answered in three parts: the first one concerning the simulation quality, i. e. the actual ability of the model to predict streamflow, the second one concerning parameter calibration and data requirements, and the third one concerning its practical applicability in the context of NRM^3 and the River Water Users Associations.

6. 7. 1. Simulation quality

Considering the simple model structure and the basic data requirements, the simulation quality reached by the NRM^3 Streamflow Model is satisfactory in the catchments where good-quality rainfall data from a dense monitoring network are available. The performance measures in these catchments indicate a reasonably good simulation quality on the decadal time-step and an acceptable quality on the daily scale. Total runoff is underestimated in the calibration period and overestimated in the validation period. Overestimations of naturalised observed discharge occur at flow peaks and in wet months, while underestimation is common in low flow periods. Even if low flows are underestimated in absolute terms, the interannual pattern of the lowest monthly flows (NMQ30) is followed well. However, their systematic underestimation is a serious drawback in an area where the lowest flows are critical.
Two types of limitations to better simulation quality were identified:

- The quality and availability of input data: mainly the rainfall data represent a limitation to better simulation quality; model performance is good in the catchments that have a dense measuring network and decreases considerably where the distances to rain gauges increase and the distribution of rainfall in altitude is not represented well by the measuring network. Other datasets (mainly discharge and abstractions) would allow more valid conclusions if they were more reliable.
- Model structure: The very simple representation of groundwater discharge with a single reservoir and constant parameter values is one of the main limitations to better simulation quality. The model should be able to "save" water over longer time. This could be reached by the introduction of a second, deeper long-term groundwater store, or by making the groundwater discharge parameters adaptable to longer-term moisture conditions. The second great limitation is that the interpolation of rainfall and evaporation does not include the altitude of cells. The introduction of an altitude-dependent interpolation of the meteorological input variables would make the predictions more reliable in ungauged catchments and catchments with few rain gauges. The dynamic curve numbers, which try to incorporate long-term moisture, would probably lead to better result if the method of their determination were not dependent on months of the year but on a more flexible temporal season definition.

6. 7. 2. Data and parameter requirements

The sensitivity analyses to parameters and input data given in Sections 6.3 and 6.4 show that the NRM^3 Streamflow Model can be used without extensive calibration. The catchment-specific parameters (groundwater and runon parameters) can easily be estimated from observed hydrographs, if such are available, or from catchment characteristics and regionalisation techniques that could be explored in further studies.

The data requirements for evaporation and GIS inputs are easily met in the study area, as a coarse temporal (for evaporation) and spatial (for GIS data) resolution is sufficient for satisfactory simulation quality. The quality of the available rainfall data, however, represents a serious limitation that could be relieved by

- a denser rainfall monitoring network, or new monitoring techniques such as the estimation of rainfall from cloud temperatures in satellite pictures; and/or
- the introduction of altitude-dependent interpolation of rainfall in the model (as mentioned above).

6. 7. 3. Practical applicability in the context of NRM^3 and the RWUAs

The model in its present form is quite time-consuming to operate and requires understanding of the involved programmes and systems. With the command-line operation mode and the large number of conversion steps involved, there are many sources of potential errors. Graphic outputs and summary statistics for analysis have to be produced outside the model, which again increases time requirements. Some parameters are hardcoded, requiring recompiling when they need to be changed. Possibilities for automatisation or controlling simulations with scripts are lacking as well as adequate error warnings or messages.
For the practical application of the NRM^3 Streamflow Model in Kenya, a graphical user interface should be introduced to cut down on time requirements and potential error sources, and better guidelines should be given on how to operate the model (in the form of a manual and adequate error warnings within the programme). Without these improvements, the use of the NRM^3 Streamflow Model will require much outside support.

7. EXAMINATION OF ENVIRONMENTAL CHANGE SCENARIOS

In this part of the study, the NRM^3 Streamflow Model is applied to predict streamflow under scenarios of environmental change. Socio-economic developments on the regional as well as the global scale are expected to influence the physical basis of streamflow generation in the study region in the future:

- Population growth, immigration and the intensification of agriculture on the regional scale result in pressure on land and vegetation. Forests and savannah areas are converted to cropland or grazing land to satisfy food, income and energy (fuelwood) requirements.
- The anthropogenic emissions of greenhouse gases and aerosols on the global scale are expected to induce changes in global climate – in general a global warming of 1.4 to 5.8°C until 2100 and a general intensification of the water cycle is predicted by the IPCC (Intergovernmental Panel on Climate Change), but local climates may change much more dramatically.

Significant impacts of these developments on the water availability may be felt in the study region in the near future already, probably by the next generation. Thus it is important to incorporate predictions on water availability into long-term water management. In the Upper Ewaso Ng'iro Basin, where water is scarce today already, agreements on the distribution of water resources have to be reached considering not only the current state of the resource but also the possible changes in the near future.

Two kinds of scenarios are examined in this chapter:

- Five land use change scenarios were produced putting the forest, footzone and savannah zone under land use classes that might become dominant in the future. GIS land cover inputs for the NRM3 Streamflow Model were modified accordingly. It is not likely that any of these extreme scenarios will actually occur, but like this, conclusions can be drawn on which land use changes should be promoted or prevented in order to keep streamflow reliable.
- Two climate change scenarios, the IPCC Special Report on Emissions Scenarios (IPCC 2000) A2 and B2 illustrative marker scenarios, were used to produce meteorological input data series with the characteristics of the predicted climate of the years 2040 – 2069 according to the methodology proposed by the IPCC Task Group on on Scenarios for Climate Impact Assessment (IPCC-TCGIA 1999).

The scenarios are compared to a so-called base case representing current conditions. For the study, measured rain and evaporation data of the 15-year period 1987 – 2001 and the land use map 1988 were used for the base case. For the land use change scenarios, the GIS land cover map was modified and the meteorological records kept; for the climate change scenarios, the meteorological data modified according to the GCM predictions for each scenario replaced the measured records, and the land use map 1988 was kept. The impacts of the scenarios were analysed for the four nested Naro Moru catchments A3 – A6, with a focus on A5 because overall streamflow predictions have been shown to be most reliable for this catchment in calibration and validation.

7. 1. BASE CASE

The base case that the scenarios are compared to is intended to represent current conditions. It includes the 15-year period 1987 – 2001. The determination of the baseline period is mainly

based on the criteria given by IPCC-TGCIA (1999) concerning the available meteorological records:

- Data should be representative of present-day climate in study region
- The data series should be sufficient in duration to capture variability (including anomalies – droughts etc.)
- data should be available and distributed over space for all major climatic variables
- data quality should be sufficiently high
- data series is consistent or readily comparable with other baseline climatologies

Ideally a 30-year period should be chosen, at best the period 1961 – 1990 as it is the current international standard averaging period, in order to capture interdecadal variability and to be able to compare the results to most other impacts assessments. This is prevented by the availability of data, however – evaporation records start in March 1986, and it has been shown in Section 6.4 that the rainfall data of the Non-NRM^3 stations that already recorded before the 1980s alone are not sufficient as inputs for the NRM^3 Streamflow Model to make streamflow predictions.

The use of measured datasets from the baseline period was preferred to using data generated by a weather generator. Weather generators have the advantage that they can produce data series of any desired length that have the statistical characteristics of a recorded (mostly shorter) dataset used as input. Weather generators, like LARS-WG or ClimGen, are available from the internet. The newer "serial" type weather generators, like LARS-WG, model first the series of dry and wet periods based on the input datasets and then model other variables (temperature, precipitation, etc.) based on these – an improvement with respect to older weather generators that often failed to describe adequately the length of dry and wet periods.
The drawback with weather generators, however, is that datasets for each station are generated independently from each other, ignoring correlations in space. A weather generator might produce a long dry period in one year at one station, but another station would by chance experience a wet year at the same time. Mixing these datasets within the hydrological model to interpolate the catchment climate would result in an equalization and removal of weather extremes.
This problem does not exist when using measured data. Also applying monthly change fields to this data in climate impacts assessment is not an inferior method to what a weather generator would do – it would produce datasets with the same statistical characteristics.

The meteorological data 1987 – 2001 of the stations described in Table 7.1 make up the baseline climatology. Please refer to Appendix A for missing data. As base case land use map the 1988 map (Roth 1997) was chosen.

Station	UTM long	UTM lat	Altitude [m a.s.l.]	Variable (P = precipitation, ET = evaporation)	Record Start Date
Satima	278425	9983931	1950	P	01.01.1973
Munyaka	283658	9980282	2070	P + ET	27.11.1991
Naro Moru Forest Gate Post	289002	9980504	2195	P	01.01.1957
Naro Moru Gate	293829	9981024	2420	P + ET	01.01.1968
Naro Moru Met Station	301090	9981442	3050	P + ET	01.02.1978
Naro Moru Moorland	304420	9981854	3771	P	01.01.1990
Teleki	310446	9981925	4262	P	01.04.1978
Matanya	272189	9993443	1840	P + ET	01.03.1986

Table 7.1: Measuring stations of which 1987 – 2001 data were used as baseline meteorological data.

7. 1. 1. Weather in the baseline period

Fig. 7.1 shows monthly average rainfall and evapotranspiration for the A5 catchment in the baseline period. Monthly actual evapotranspiration rates are quite constant throughout the year in the range of 50 – 70 mm. Precipitation reaches peaks of 162.1 and 182.2 mm in the long rains and short rains seasons caused by the crossing of the equator of the ITCZ. The lowest value is reached in the dry season in February with 38.7; in the continental rains season (June to September) monthly precipitation lies around 60 mm.

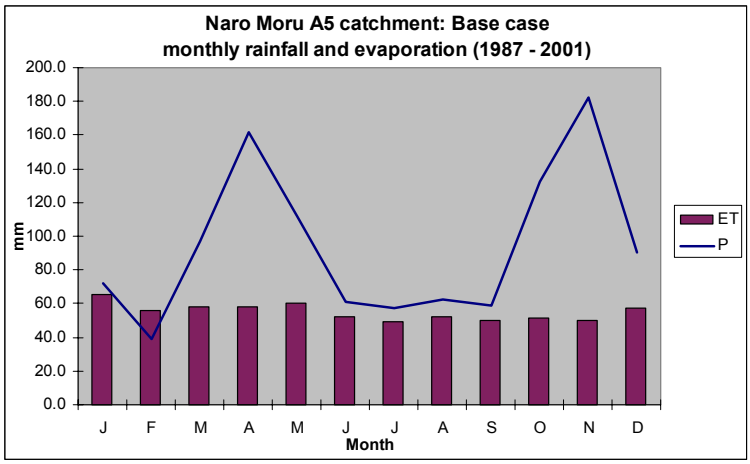

Fig. 7.1: Monthly average precipitation and evapotranspiration in the baseline period (1987 – 2001) in the Naro Moru A5 catchment.

The interannual variability of rainfall and evapotranspiration is illustrated in Fig. 7.2. For precipitation rates, the variability is considerable: In the wettest year, 1997, 121% of the average annual rainfall over the whole period were recorded; the driest year, 2000, saw only 59% of the annual mean precipitation. Evaporation is much less variable; it was also lowest in the driest year (when the least moisture was available) with 83% of the baseline period mean, and highest in the year 1995 (a wet year but not the wettest) with 110% of the average annual ET rate.
Among other factors, the high variability is caused by the ENSO (El Niño Southern Oscillation), that is responsible for the most extreme deviations from the annual means (such as the year 2000, for example).

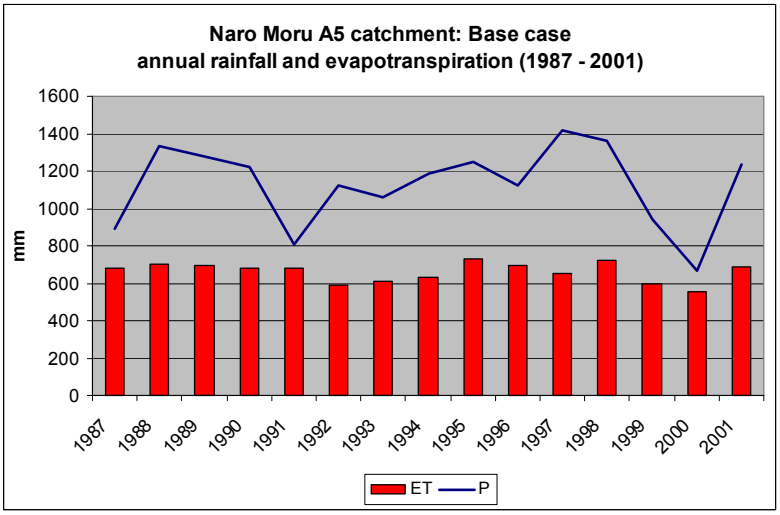

Fig. 7.2: Annual precipitation and evapotranspiration in the baseline period in the Naro Moru A5 catchment.

7. 1. 2. Base Case discharge

To avoid confusion between the changes caused by the deviations between simulated and modelled flow and the changes caused by the scenario conditions, the simulated scenario discharge data are not compared to the recorded flows of the baseline period but to simulated flows. The differences between simulated and observed discharge data are shown here as they also have to be considered when interpreting the scenario analysis results.

The monthly Pardé Coefficients for the baseline period are shown in Fig. 7.3 a). Logically the discharge regime follows the monthly precipitation pattern with peaks in the wet seasons. The simulated coefficients do not differ much from the observed.
The interannual variability (Fig. 7.3 b) of discharge is strongest in flood flows (upper quartile), but also mean discharge and low flows are affected. The modelled values of median and quartiles lie below the observed values and show less variability, but follow the pattern of the observed values well. This means that the absolute amounts of scenario streamflow and the variability of the scenario predictions will have to be corrected upwards when comparing them to real conditions today. The proportions of the changes should be quite reliable, however.

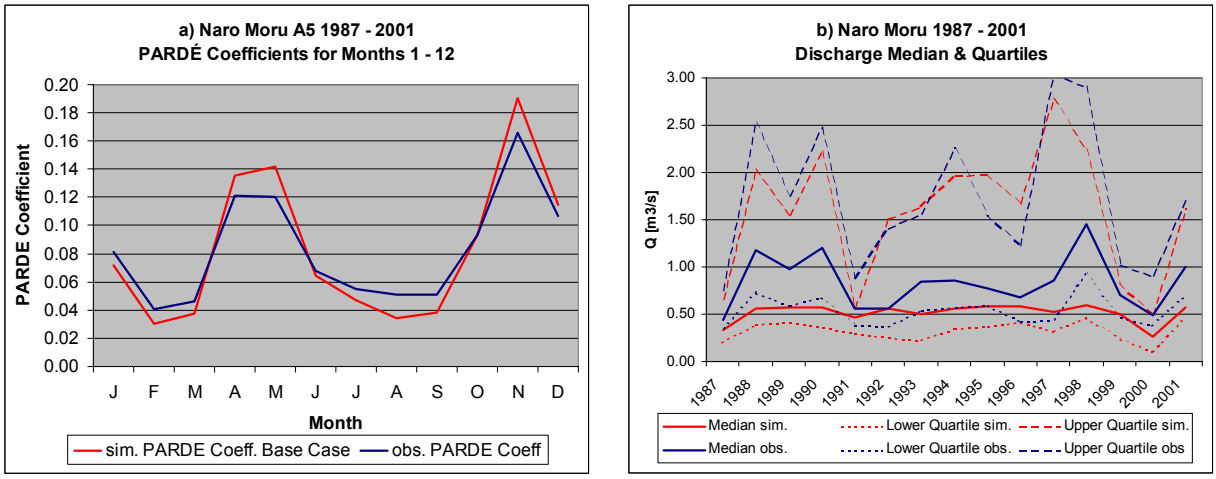

Fig. 7.3: a) Simulated and observed Pardé Coefficients in the baseline period; b) simulated and observed year-to-year median and quartiles of discharge.

7. 1. 3. Land use in the baseline period

The 1988 and 1995 land use maps have been presented and compared in Section 6.4.2.2 for the Naro Moru A5 catchment. The changes between 1988 and 1995 include an increase by almost 300% of bare grassland at the expense of the forest area; most of the increase can be observed in the upper catchment, however, indicating that not real changes but different atmospheric or vegetational conditions when the Satellite pictures were made or different classification methods cause a large part of the changes.
Some land use changes can also be observed in the lower catchment between 1988 and 1995: a slight reduction of the forest area and an increase in cropland and grassland. This shows that the trends based on which the land use scenarios were developed can be observed in the baseline period already. The shrinking of the forest area was almost stopped in 1998, however, when KWS (Kenya Wildlife Service) started driving illegal settlers, growers and trappers out of the Mt. Kenya National Park Area by force.

7. 2. LAND USE CHANGE SCENARIOS

Five land use change scenarios are examined, of which the fifth is repeated with modified soils. They include:

- **Scenario lcsc01:** Forest and Savannah zone converted to small-scale cropland (Cgrain)
- **Scenario lcsc02**: Forest and Savannah zone converted to small-scale cropland with trees (tC)
- **Scenario lcsc03:** Grassland with trees below 2000 m a.s.l., forest and bamboo between 2000 and 3200 m a.s.l.
- **Scenario lcsc04:** Catchment up to 2300 m a.s.l. converted to bare grassland
- **Scenario lcsc5a:** Catchment up to 3200 m a.s.l. converted to bare grassland, soils intact
- **Scenario lcsc5b:** Catchment up to 3200 m a.s.l. converted to bare grassland, humic acrisols and andosols on mountain slopes eroded by 50%

7. 2. 1. Method

For the land use scenarios examined in this study the savannah, footzone and forest zone are put under single land use categories that might become dominant or might be desirable to expand in the future. This way the impact of single land use classes can be distinguished.
Above 3200 m a.s.l. the land use is left in the state of 1988 in all scenarios. The transition of moderately well to well-drained humic Andosols characteristic for the forest zone to poorly drained moorland soils lies around this altitude (Decurtins 1992: 26), and it is assumed that the expansion of cultivated land would at the latest stop here - above crops would not grow anymore due to soils and climate.
In Scenario 1, 2, 4 and 5, the catchment is put under land use classes that are increasing under current trends: cropland and grassland. Scenario 2 tries to assess whether a positive hydrological impact (or less negative impacts) could be reached in comparison to Scenario 1 by promoting trees in and between the fields. Scenario 3 is represents the state of the catchment under “natural” conditions.

For the production of the input GIS maps, the 1988 land use map was modified in Idrisi32 with the help of the OVERLAY and the RECLASS module. To distinguish land use in the different altitude belts, the digital elevation model was first reclassed so that all cells had a value of 1, 100, or 10’000 assigned according to their location in one of the three altitude zones (below 2000 m, between 2000 and 3200 m, above). This reclassed raster layer was then overlain with the land use map in the multiplying mode, so that for example the land use class 12, if situated between 2000 and 3200 m a.s.l., got the new value 1200. In the last step, the land use categories in the three altitude zones could be replaced with the desired values.

7. 2. 2. Expected impacts of land use changes: past experiences

The impacts of land use changes on water availability in catchments have been evaluated in several past studies. Thomas (1993: 32) states, however, that no predictive power has been established from catchment studies so far, since response to treatment is highly variable. Plot experiments, on the other hand, give clearer results but they are difficult to extrapolate to the catchment scale. General past experiences and results shall be summarised in this section.

Deforestation generally causes higher total runoff and also higher low flow volumes, as demonstrated by several studies (Liniger & Weingartner 2000; see also Smakhtin 2001: 152 for an overview). In theory, both a reduction and an increase in low flows is possible: reduced evapotranspiration, interception and infiltration rates lead to higher soil moisture storage and increased surface runoff. This in turn leads to reduced groundwater recharge and increased gully erosion, which may result in lowering the groundwater table and reducing low flows originating from groundwater storage. No study describing these mechanisms has been published to date, however (Smakhtin 2001: 152). To model processes like this, a very complicated physically-based hydrological model would have to be used – the NRM[3] Streamflow Model cannot predict such feedbacks between different elements of catchment hydrology.
The effect of deforestation also depends on which land use forest is replaced with. A paired catchment study by EAAFRO (East Africa Agriculture and Forestry Research Organization) showed no long-term change in total streamflow when montane and bamboo forest on volcanic rocks were replaced by tea plantations, but the seasonal variations increased (Thomas 1993: 35). At Mbeya in Tanzania, the water yield was doubled after the replacement of the forest with smallholder cultivation on very steep slopes – the increase was mainly felt in the dry season baseflow due to very porous ash-derived soils (Liniger & Weingartner 2000: 353).

Afforestation has been shown to reduce streamflow due to increased interception losses, transpiration losses, infiltration and soil moisture holding capacity. Significant reductions in low flows may also be the case. A paired catchment approach in South Africa to assess the impact of eucalyptus and pine plantations showed that eucalypti reduce streamflow more than pines – low flows were reduced by up to 100% (Smakhtin 2001: 151). In an experiment pine plantations in East Africa initially caused a 19% reduction in total streamflow but no long-term effect (Thomas 1993: 35).

Conservation farming – aiming at maintaining good ground cover by contouring, terracing and mulching – is expected to reduce runoff volumes during both high- and low-flow periods. Plot-scale experiments demonstrate this effect (Liniger & Thomas 1998), but catchment case studies have not been identified (Smakhtin 2001: 152).

Other land use changes that might affect the study catchments in the future are the increase of urban areas (expected to reduce low flow runoff due to impervious surfaces) and the melting of the glaciers at the peak of Mt. Kenya. Their impacts are not explored in this study, however.

7. 2. 3. Impacts of land use changes: results of the scenario runs

The presentation of the results in the following sections focuses on the impacts of the land use changes on the A5 catchment. In some cases A6 shows a reverse response than the rest of the catchment, because more than half of its area is in the savannah zone, and conversion to a different land use class in some cases affects the average base curve number just the other way round. These cases are specially discussed.

7. 2. 3. 1. Scenario lcsc01: Forest and Savannah zone converted to small-scale cropland (Cgrain)

Fig 7.4: Land use under scenario lcsc01: the large area in orange is Cgrain (>50% cropland with grain). Boundaries of the Naro Moru A3 – A6 catchments are shown in red.

Catchment	Annual runoff [%]	Qmax [%]	Qmin [%]	Mean [%]	Median [%]	Lower Quartile [%]	Upper Quartile [%]	Mean NMQ30 [%]	Q/P ratio [+/- %]
A5	11.128	15.433	0.000	11.128	-3.846	0.000	0.699	-5.939	4.587
A3	6.937	19.438	-20.000	6.937	-3.030	0.000	4.489	-4.154	3.430
A4	10.587	22.668	-33.333	10.587	-8.046	-2.273	2.604	-10.375	5.072
A6	16.245	17.882	0.000	16.245	13.043	45.455	25.281	7.848	3.775

Table 7.2: Impacts of scenario lcsc01 on streamflow. The values shown are deviations to the base case values in percent.

Impacts: The main impact of the scenario lcsc01 (summarised in Table 7.2) is an increase of total streamflow by 6 – 16%, which is mainly caused by an increase in flood flows. The increase is most pronounced at A6 and is least felt at A3, which is explained by the different proportions of the changed area in the catchments. Low flows are slightly reduced in the A3 – A5 catchment, while at A6 an increase in the NMQ30 and the lower discharge quartile is predicted. The Q/P ratio (ratio of rainfall converted to runoff) is higher in the scenario than in the base case, due to a higher proportion of direct runoff. The discharge regime is not much affected: The Pardé Coefficients (Fig. 7.3 b) just increase slightly in wet months and are a little lower in the dry periods with respect to the base case.

Interpretation: For the subcatchments with a large forest area under base case conditions (A3 – A5) the overall curve numbers increase, producing more direct runoff. Root depth, kc factor (the factor determining actual from potential evaporation and land cover) and leaf interception are reduced, lowering the evapotranspiration rate. This results in higher discharges, except in dry periods: not so much water infiltrates when there is rain, and it is thus sooner gone afterwards. The decrease of the NMQ30 is less pronounced in the A3 and A5 catchments than in the A4 catchment, which indicates that the moorland and alpine zone contribute a major part to low flows.
At A6 a large proportion of the catchment area consists of savannah and other crop classes in the base case which are replaced by Cgrain under the scenario. The difference in the curve numbers is not as pronounced as in the other catchments. Thus not much less water infiltrates, which in combination with higher surface runoff also causes low flows to increase.

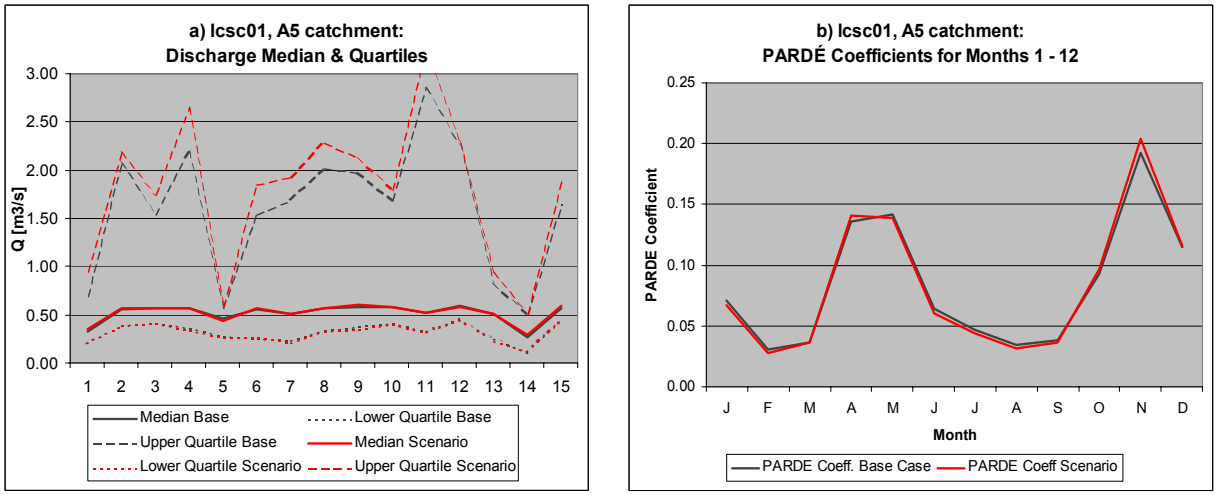

Fig. 7.3: Discharge median and quartiles for all simulation years under scenario lcsc01 at A5 (a) and average Pardé Coefficients (b).

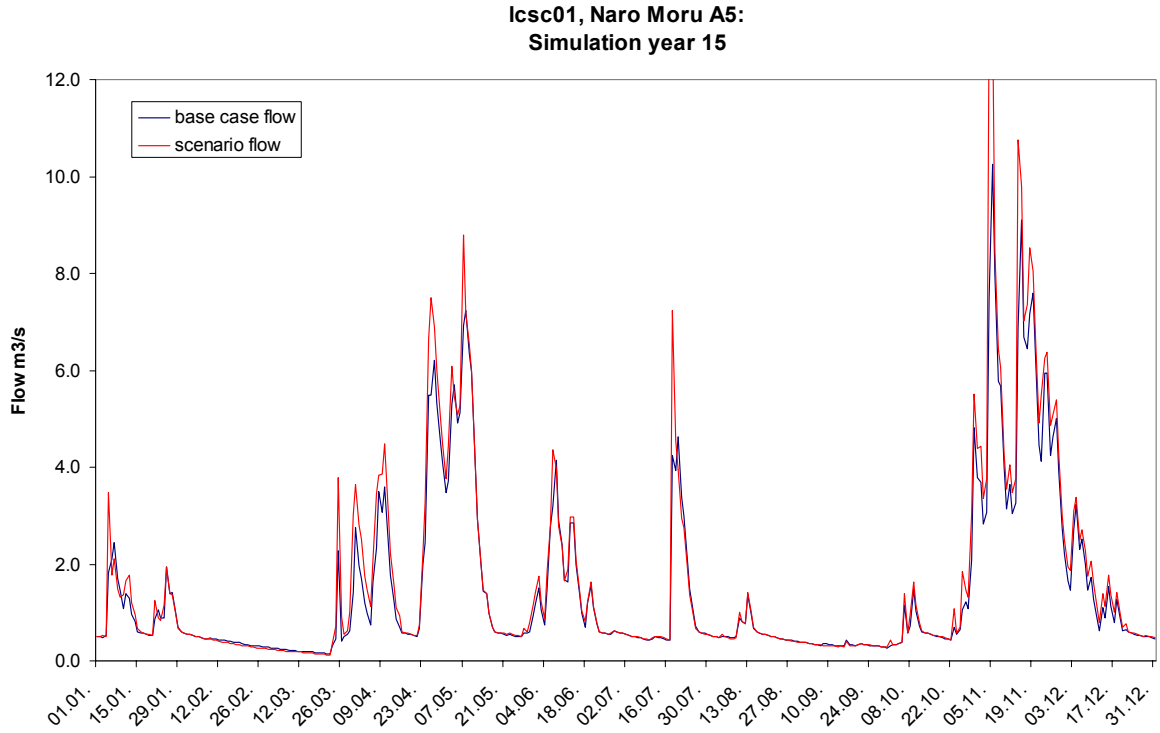

Fig. 7.4: Daily discharge under scenario lcsc01 in the simulation year 15 at A5. The differences are most visible at the flow peaks; baseflow is slightly reduced in the dry season (February and March).

7. 2. 3. 2. Scenario lcsc02: Forest and Savannah zone converted to small-scale cropland with trees (tC)

Fig. 7.5: Land use under the scenario lcsc02. The large area in brownish green is tC (cropland with 2 – 20% trees); catchment boundaries A3 – A6 are shown in red.

Catchment	Annual runoff [%]	Qmax [%]	Qmin [%]	Mean [%]	Median [%]	Lower Quartile [%]	Upper Quartile [%]	Mean NMQ30 [%]	Q/P ratio [+/- %]
A5	10.636	12.368	0.000	10.636	-3.846	0.000	1.224	-5.988	4.384
A3	6.921	16.976	-20.000	6.921	-3.788	0.000	4.334	-4.164	3.418
A4	10.512	20.425	-33.333	10.512	-6.897	0.000	2.778	-10.035	5.033
A6	15.133	15.568	0.000	15.133	13.043	45.455	28.090	8.590	3.518

Table 7.3: Impacts of scenario lcsc02 on streamflow. The values shown are deviations to the base case values in percent.

Impacts: With respect to the base case lcsc02 has very similar impacts as lcsc01, but they are less pronounced. The differences to lcsc01 are mainly visible at the flood flows (less increase in peak flows). For the low flows the impacts are almost identical as in the first scenario. This means that planting trees between fields does not help to mitigate the negative impact of a large cropland area on low flows, unless other cultivation practices, e. g. mulching or thin tillage are included.

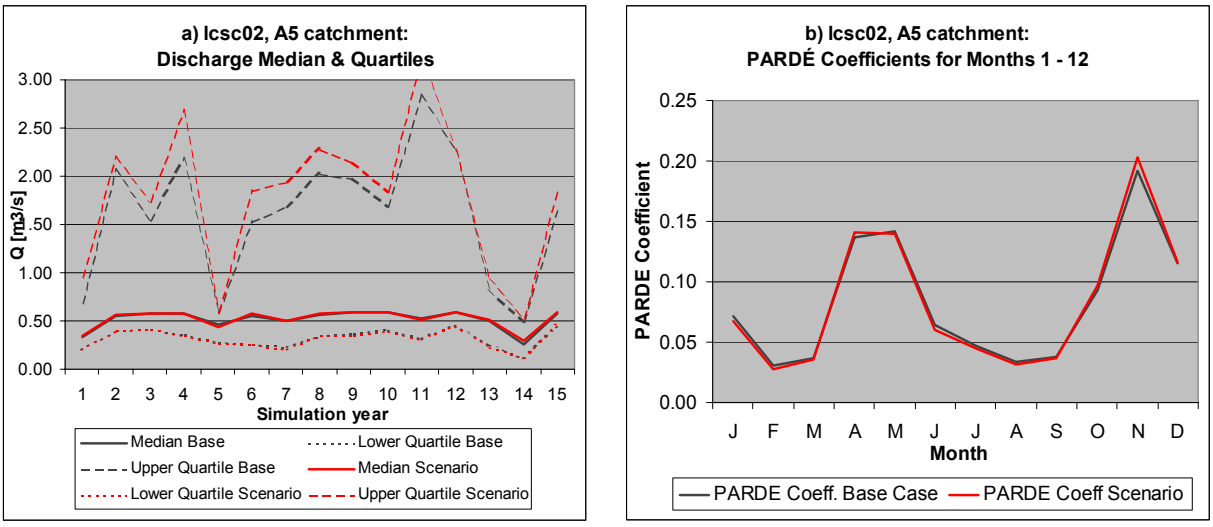

Fig. 7.5: Discharge median and quartiles for all simulation years under scenario lcsc02 at A5 (a) and average Pardé Coefficients (b).

Interpretation: The same changes are effective as under lcsc01, but in slightly smaller dimensions. The curve numbers of tC are a little lower than of Cgrain, causing less direct runoff, and root depth is increased, which raises evaporation.

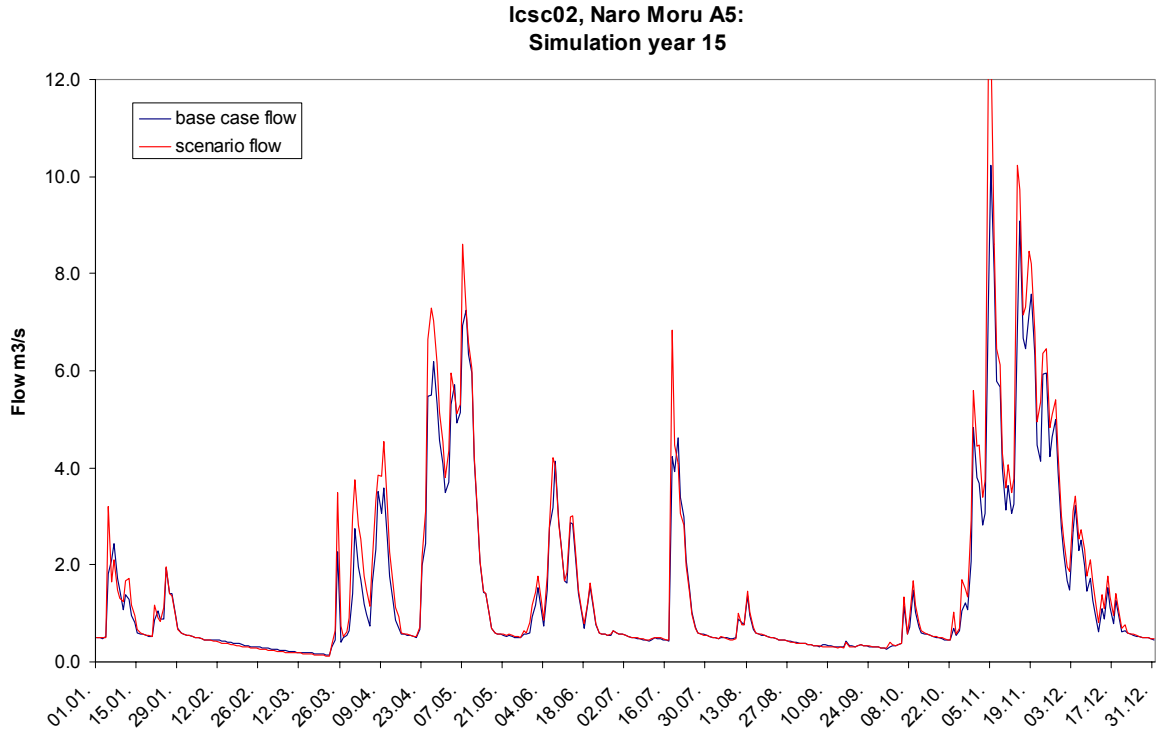

Fig. 7.6: Daily discharge under scenario lcsc02 in the simulation year 15 at A5. As under lcsc01, the greatest differences are found at the flow peaks, and baseflow is slightly reduced in the dry season (February and March).

7. 2. 3. 3. Scenario lcsc03: Grassland with trees below 2000 m a.s.l., forest and bamboo between 2000 and 3200 m a.s.l.

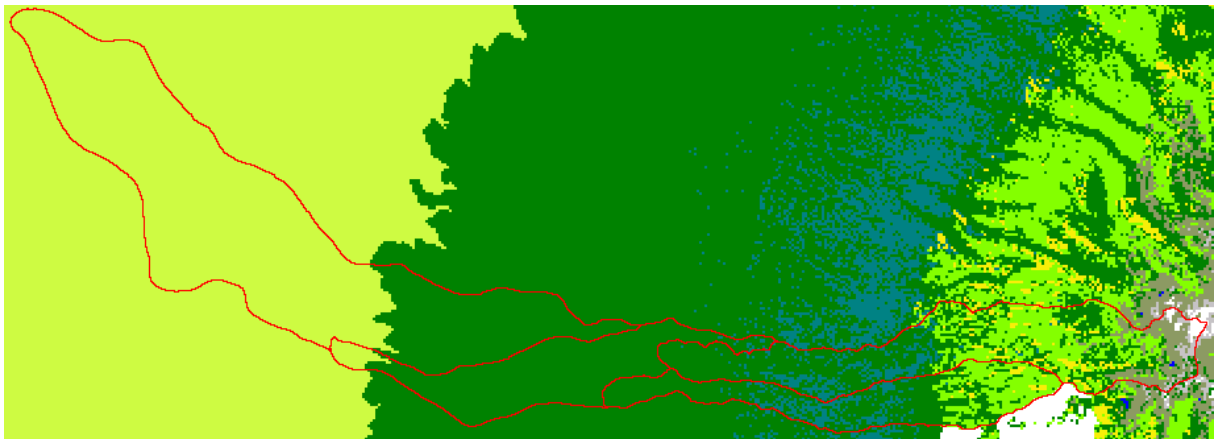

Fig. 7. 7: Land use under the scenario lcsc03. The light green areas to the left are tG (>50% grassland with 2 – 20% trees). The dark green areas in the middle are forest (Td – > 50% dense trees) interspersed with bamboo forest (Go - >50% bamboo) at higher altitudes. Catchment boundaries A3 – A6 are shown in red.

Catchment	Annual runoff [%]	Qmax [%]	Qmin [%]	Mean [%]	Median [%]	Lower Quartile [%]	Upper Quartile [%]	Mean NMQ30 [%]	Q/P ratio [+/- %]
A5	-1.592	-1.638	0.000	-1.592	-1.923	0.000	-14.685	0.980	-0.624
A3	-0.121	-1.598	0.000	-0.121	-3.030	0.000	-9.598	2.339	-0.058
A4	-0.462	-0.551	0.000	-0.462	-5.747	2.273	-15.972	3.831	-0.209
A6	-6.973	-18.093	0.000	-6.973	8.696	36.364	-12.360	-2.654	-1.612

Table 7.4: Impacts of scenario lcsc03 on streamflow. The values shown are deviations to the base case values in percent.

Impacts: Under this "natural" scenario, total streamflow is reduced by 0.12% (A3) up to 6.97% (A6 catchment). In the upper three subcatchments (A3 – A5) the reduction affects mainly the flood flows: peaks, upper quartile and median of discharge are lower than in the base case. Low flows increase a little – an increase of 0.1% at A5 up to 3.8% at A4 is predicted.
At the lower end of the savannah zone, at A6, conditions are different: the reduction in streamflow is effective at the peaks and in the lowest flows (NMQ30), but median and lower quartile are higher than in the base case.
In all catchments, a smaller proportion of rain is converted to runoff than in the base case. The discharge regime remains almost identical as shown by the Pardé Coefficients in Fig. 7.8 b) – only the short rains month of November suffers a relative decrease, and the dry season and continental rains month experience a small relative increase in streamflow.

Interpretation: Since the upper forest zone and the moorland zone generate most discharge, the two uppermost catchments A3 and A4 do not experience much change with respect to the base case conditions, neither in land use nor in streamflow. At A5 the reduction in streamflow is a little more effective: Since the interception rate, root depth and the kc factor of forest are high, evaporation is increased. The low curve numbers, however, let a large proportion of the rain infiltrate, thus raising baseflow.
At A6, the curve numbers are reduced on average as well, causing less direct runoff but creating more reserves for the recession phase after floods. Interception and kc factor are in some areas lowered and in some places raised, so their effects cancel each other out more or

less. The root depth of grassland with trees is about equal to other grassland categories but greater than on the cropland it replaces, which keeps up higher evaporation rates in longer drought period, thus causing the lowered NMQ30.

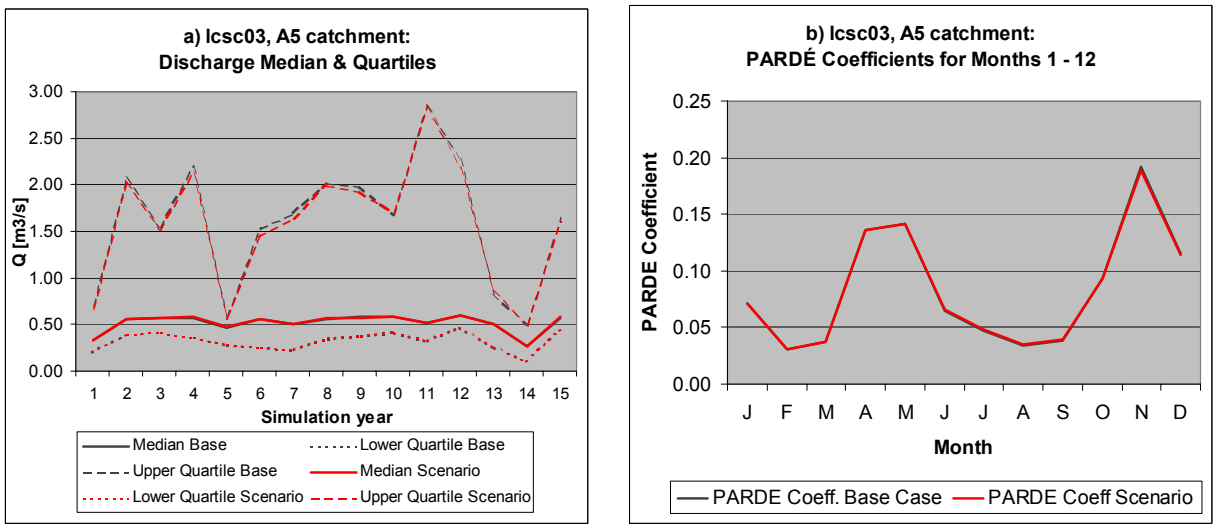

Fig. 7.8: Discharge median and quartiles for all simulation years under scenario lcsc03 at A5 (a) and average Pardé Coefficients (b).

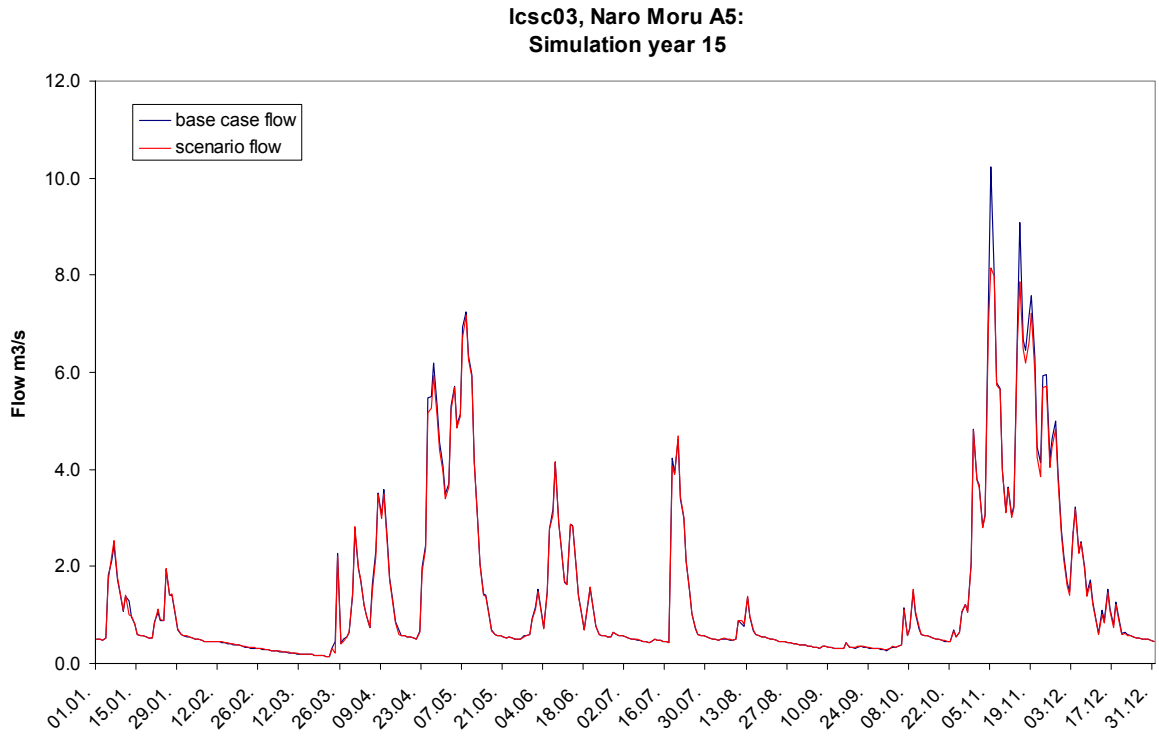

Fig. 7.9: Daily discharge in the simulation year 15 under lcsc03 at Naro Moru A5. The differences are most pronounced in the short rains season flow peaks. The baseflow increase in the dry season is hardly noticeable.

7. 2. 3. 4. Scenario lcsc04: Catchment up to 2300 m a.s.l. converted to bare grassland

Fig. 7.10: Land use under the scenario lcsc04. The ochre areas to the left Gb (>50% bare grassland). The areas above 2300 m a.s.l. remain unaffected. Catchment boundaries A3 – A6 are shown in red.

Catchment	Annual runoff [%]	Qmax [%]	Qmin [%]	Mean [%]	Median [%]	Lower Quartile [%]	Upper Quartile [%]	Mean NMQ30 [%]	Q/P ratio [+/- %]
A5	20.666	27.061	0.000	20.666	5.769	9.375	20.105	23.527	8.513
A3	0.041	0.000	0.000	0.041	-3.030	0.000	-10.526	0.116	0.021
A4	6.342	-1.338	0.000	6.342	-2.299	6.818	0.521	16.200	3.042
A6	80.982	90.252	0.000	80.982	39.130	72.727	169.101	55.594	19.186

Table 7.5: Impacts of scenario lcsc04 on streamflow. The values shown are deviations to the base case values in percent.

Impacts: Total streamflow is raised by 0 – 6% in the A3 and A4 catchments that are only affected at their lowest tips by the changes under this scenario. At A5 and A6 total runoff increases by 21% and 81% respectively.
At A5 and A6, the increase is most pronounced at the flow peaks, but the low flow measures are also raised. This is not caused by higher baseflow, as the inspection of the daily hydrograph reveals, but by small flow peaks after small storms.
At A3 and A4, the median and at A4 even the peaks are lowered but low flows are raised, which is caused by small flow peaks rather than higher baseflow, like in the lower catchments.
The discharge regime is not much affected. A relative decrease affects the months February to April, while the long rains and continental rains months experience a relative increase (see Fig. 7.11 b).

Interpretation: While the forest zone is largely undisturbed, the curve numbers in the footzone and savannah are higher than in the base case, converting the largest proportion of every rainfall into direct runoff, which is the cause for the numerous small flow peaks. Interception is down to zero, and the kc factor is reduced, resulting in a lowered actual evaporation rate. Baseflow remains thus stable despite lower infiltration rates.
At A3 and A4 the rather unexpected reduction in flow peaks and flood flows is due to some situations where the lower infiltration and the subsequently lowered soil moisture in the saturated zone result in lower baseflow contributions that cannot outweigh the higher direct runoff. The maximum flow peak over the whole simulation period at A4 (Table 7.5) is a good example. This peak occurs at November 8 in the 11th simulation year. In the base case, total streamflow is 25.41 mm, made up of 20.92 mm groundwater discharge and 4.49 mm direct

runoff. In the scenario, direct runoff is higher with 5.7 mm, but groundwater discharge amounts to only 19.37 mm, resulting in a total discharge of 25.07 mm. The higher groundwater discharge in the base case is due to higher water content in the shallow saturated zone– 82.22 mm under the base case, opposed to only 78.91 mm under the scenario.

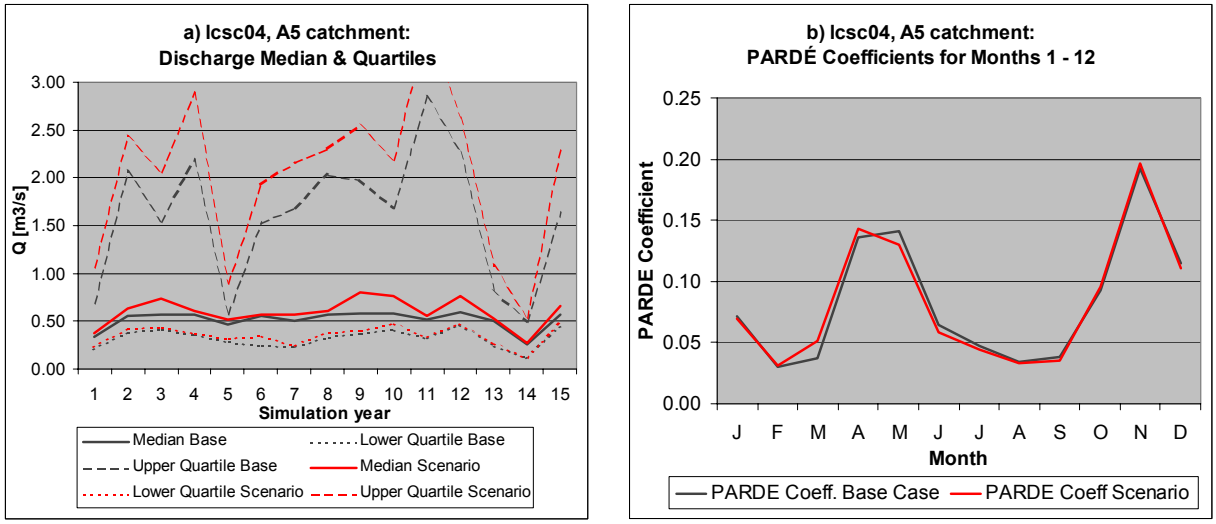

Fig. 7.11: Discharge median and quartiles for all simulation years under scenario lcsc04 at A5 (a) and average Pardé Coefficients (b).

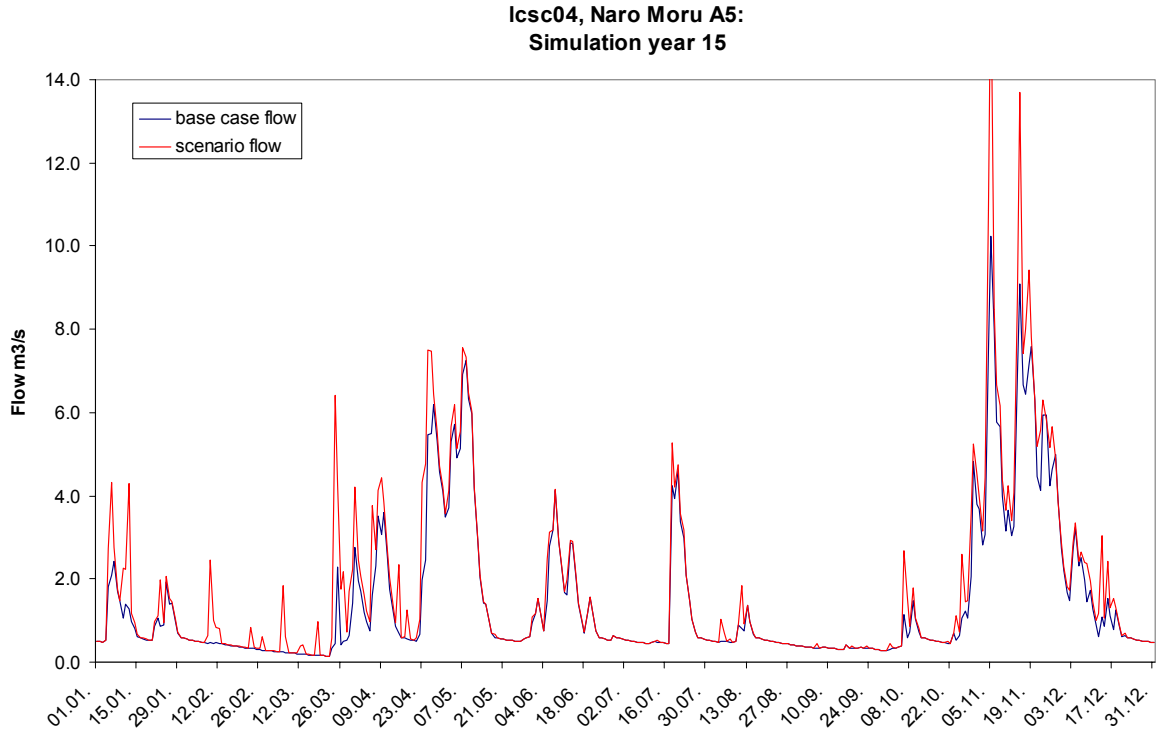

Fig. 7.12: Daily discharge in the simulation year 15 under lcsc04 at Naro Moru A5. The higher curve numbers cause much more direct runoff and additional flow peaks that under base case conditions are "swallowed up" by the vegetation.

7. 2. 3. 5. Scenario lcsc5a: Catchment up to 3200 m a.s.l. converted to bare grassland, intact soils

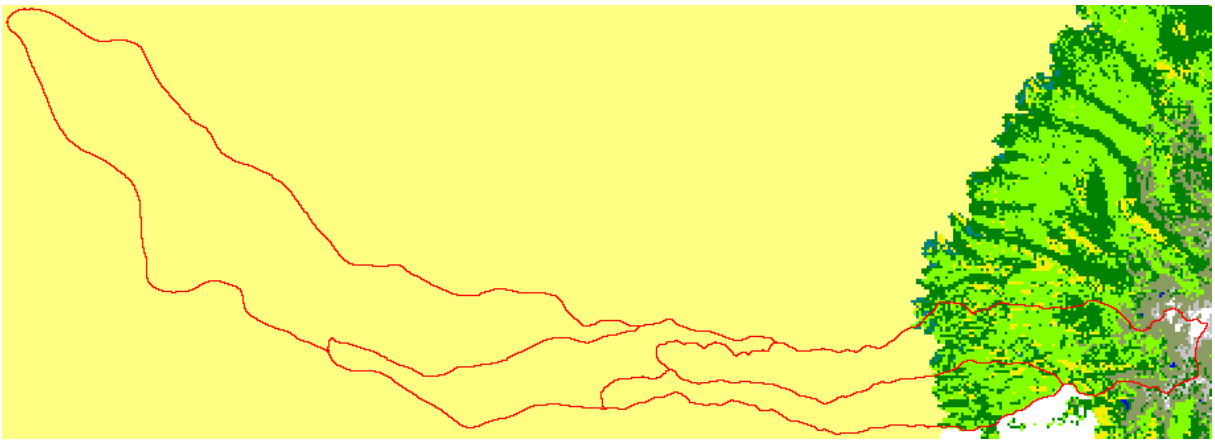

Fig. 7.13: Land use under the scenario lcsc05. The ochre areas to the left are Gb (>50% bare grassland). The areas above 3200 m a.s.l. remain unaffected. Catchment boundaries A3 – A6 are shown in red.

Catchment	Annual runoff [%]	Qmax [%]	Qmin [%]	Mean [%]	Median [%]	Lower Quartile [%]	Upper Quartile [%]	Mean NMQ30 [%]	Q/P ratio [+/- %]
A5	59.195	39.746	0.000	59.195	38.462	28.906	76.224	64.304	24.889
A3	31.861	45.832	-20.000	31.861	15.152	22.561	52.941	44.735	16.002
A4	49.184	57.261	-33.333	49.184	20.690	36.364	95.833	72.734	24.012
A6	127.243	114.376	0.000	127.243	78.261	118.182	263.483	138.784	30.541

Table 7.6: Impacts of scenario lcsc5a on streamflow. The values shown are deviations to the base case values in percent.

Impacts: The changes that affect the A5 and A6 catchment under scenario lcsc04 are stronger and affect the upper catchments A3 and A4 as well under this scenario, since bare grassland now reaches up to 3200 m a.s.l. and the forest zone has disappeared. Total streamflow is raised by 31.9% (A3) to 127% (A6 catchment). Again the changes are most pronounced at peaks and flood flows. But also median and low flows are raised. The minimum flows on the other hand remain equal (at A5 and A6) or are even reduced a little, showing that not baseflow increases but direct runoff: As under scenario lcsc04, every small rainfall is converted to runoff, little water infiltrates. This is also demonstrated by the increased Q/P ratio.
The months February to March, August and October suffer a relative streamflow reduction under this scenario, while May – June and December receive a greater proportion of flow, as shown by the Pardé Coefficients in Fig. 7.14 b).

Interpretation: As in scenario lcsc04, the changes are mainly caused by the high curve numbers of bare grassland that let only a small proportion of the rain infiltrate. No interception losses and low evaporation make up for a part of the lowered inputs to soil moisture so that the minimum flows can be sustained at A5 and A6, and are slightly reduced at A4 and A5 (the high percentages of –20% and –33% are due to the low absolute flow value).

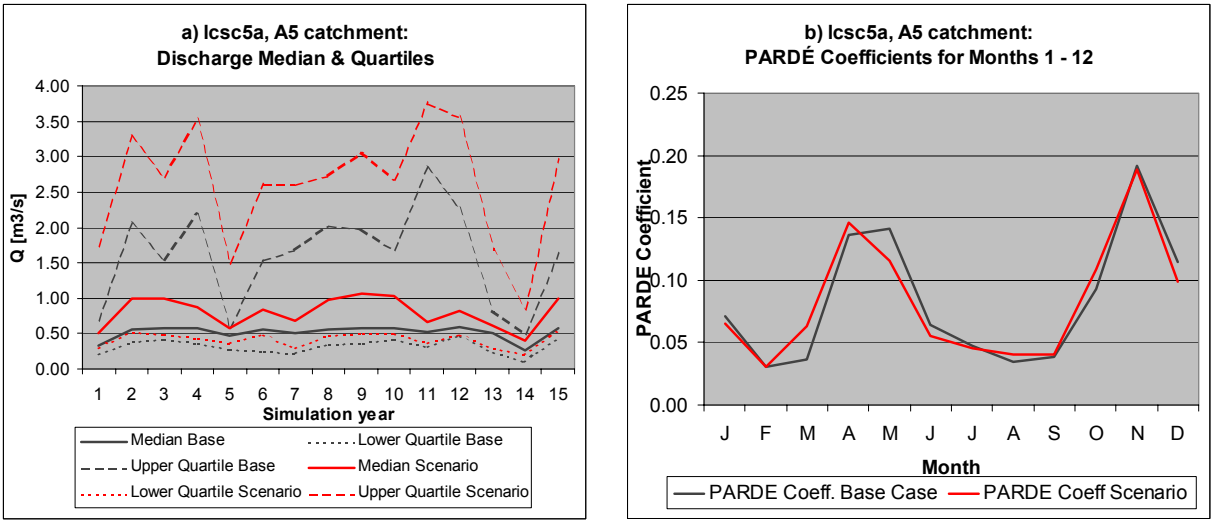

Fig. 7.14: Discharge median and quartiles for all simulation years under scenario lcsc5a at A5 (a) and average Pardé Coefficients (b).

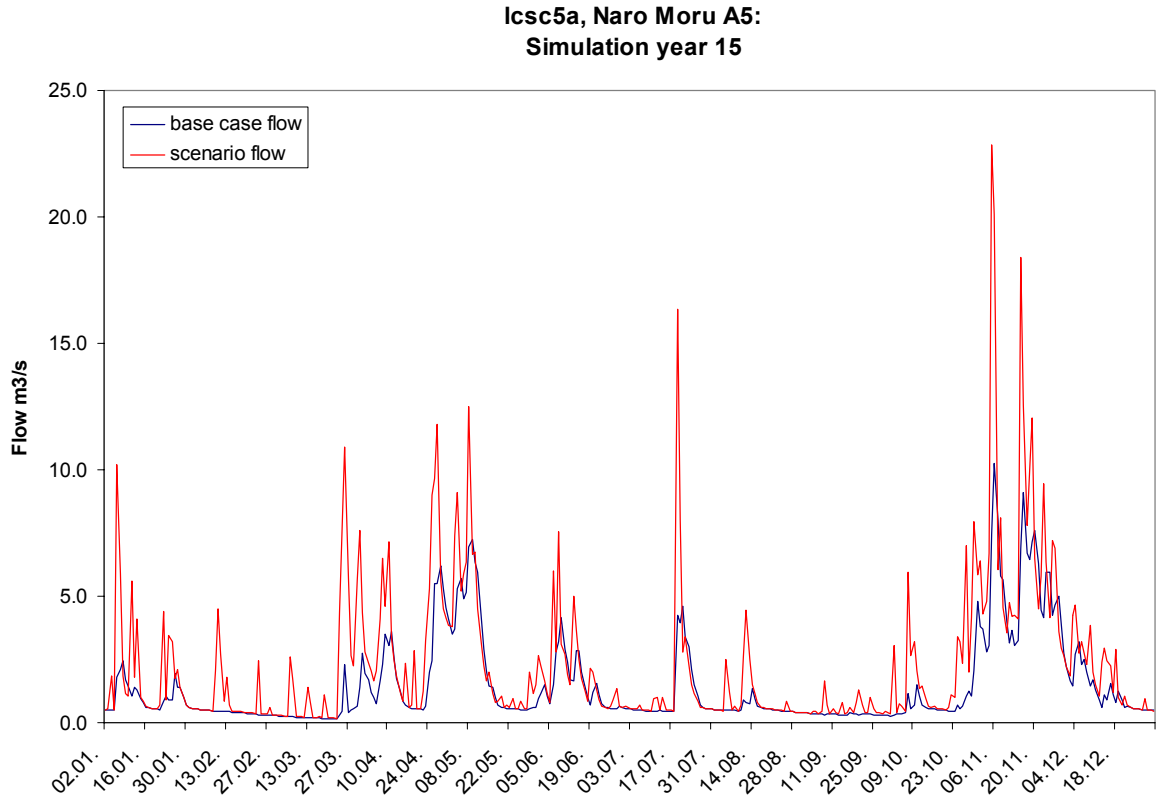

Fig. 7.15: Daily discharge at Naro Moru A5 under scenario lcsc5a: Many more small flow peaks appear in comparison with lcsc04, because the upper forest zone now also has low curve numbers and converts every rain to runoff.

7. 2. 3. 6. Scenario 5b: Catchment up to 3200 m a.s.l. converted to bare grassland, humic acrisols and andosols on mountain slopes eroded by 50%

Catchment	Annual runoff [%]	Qmax [%]	Qmin [%]	Mean [%]	Median [%]	Lower Quartile [%]	Upper Quartile [%]	Mean NMQ30 [%]	Q/P ratio [+/- %]
A5	59.274	39.746	0.000	59.274	38.462	28.906	76.224	62.574	24.930
A3	31.948	45.832	-20.000	31.948	15.152	22.561	53.251	43.580	16.054
A4	49.246	57.458	-33.333	49.246	20.690	36.364	96.354	71.723	24.051
A6	127.492	114.446	0.000	127.492	78.261	118.182	263.483	137.614	30.608

Table 7.7: Impacts of scenario lcsc5b on streamflow. The values shown are deviations to the base case values in percent. The impacts are almost identical to those of scenario lcsc5a.

Impacts: The impact of the scenario "bare grassland with eroded soils" are almost identical to the impacts of the same scenario with intact soils. Total streamflow is only increased by fractions of percent, and also the other measures deviate very little from the lcsc5a values.

Interpretation: The reason for the small differences to lcsc5a is that on one hand the humic acrisols and andosols do not cover a large area of the catchments (slopes in the mid and upper forest zone, without valley bottoms), and they still have a quite large maximum water capacity when reduced by 50% (humic andosols: 83 mm; humic acrisols: 223 mm) that is rarely reached anyhow, especially since the high curve numbers cause only little water to infiltrate. Accordingly the minimum soil moisture reached in the saturated zone is in both scenarios the same, amounting to 1.18 mm.

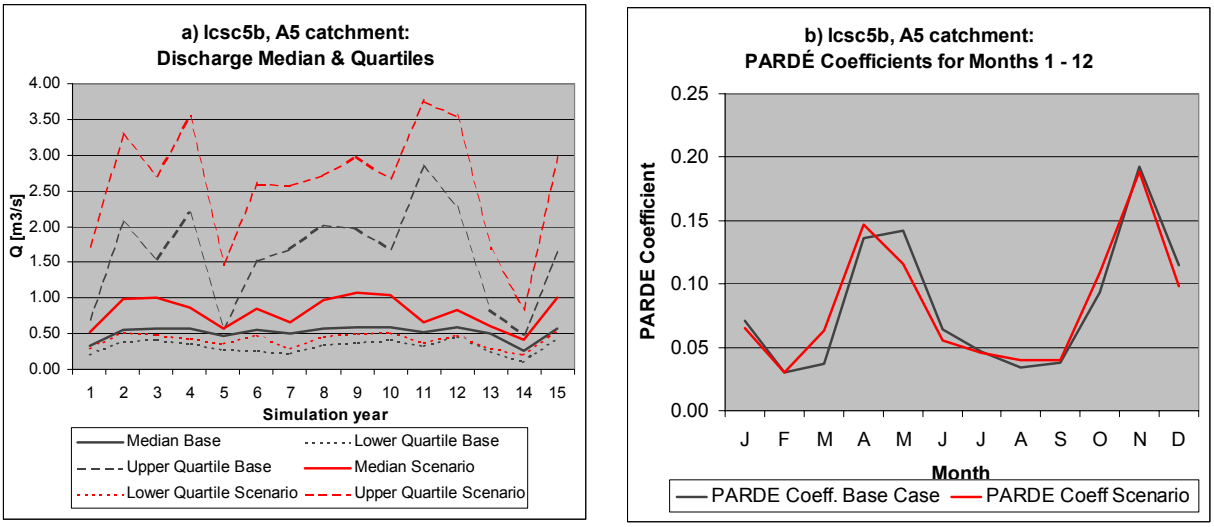

Fig. 7.16: Discharge median and quartiles for all simulation years under scenario lcsc5b at A5 (a) and average Pardé Coefficients (b). The graphs are almost identical to those of lcsc5a.

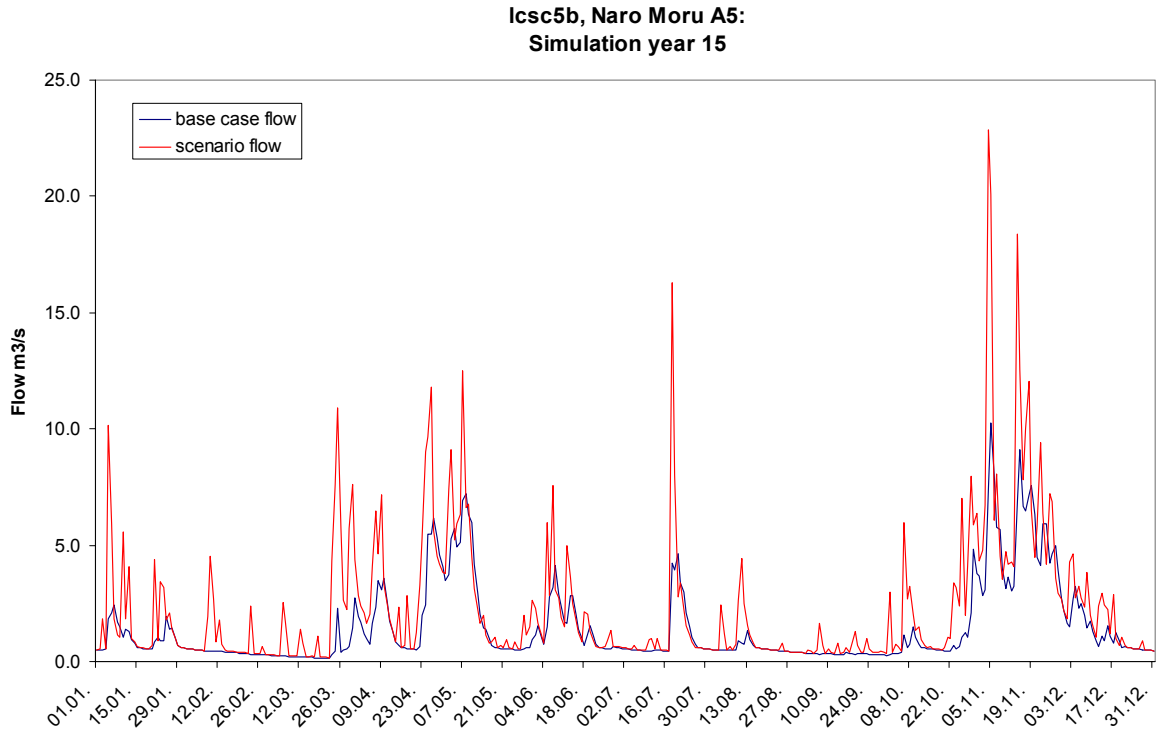

Fig. 7.17: Daily discharge at Naro Moru A5 under scenario lcsc5b: The eroded soils have almost no impact compared to lcsc5a, since their maximum water holding capacity is still rarely reached.

7. 3. CLIMATE CHANGE SCENARIOS

The impacts of two climate change scenarios on the Naro Moru subcatchments are examined in this section. The outputs of the GCM ECHAM4 were used of the following two scenarios from the IPCC Special Report on Emissions Scenarios (SRES) (IPCC 2000):

- **Scenario ccsc01:** IPCC SRES A2 illustrative marker scenario
- **Scenario ccsc02:** IPCC SRES B2 illustrative marker scenario

These are two out of forty scenarios that were developed for the Special Report and they were chosen because for GCM outputs from ECHAM4 (which was found to simulate the baseline climate best) are at present publicly available on the internet for these scenarios only. Characteristics and purpose of the IPCC SRES scenarios are described in the following section.

7. 3. 1. IPCC SRES scenarios

The IPCC already in 1990 and 1992 published long-term emissions scenarios that were widely used in the analysis of climate change and its impacts. The years after brought significant changes in the understanding of driving forces of emissions, like the carbon intensity of energy supply, sulfur emissions or the income gap between poorer and richer countries. This is why the IPCC plenary in 1996 decided to develop new emissions scenarios.

The scenarios from the 2000 Special Report are intended to represent the range of driving forces and emissions to reflect current understanding and underlying uncertainties. Only outlying “surprise” or “disaster” scenarios are excluded. No judgement is offered by IPCC as to the preference for any of the scenarios, and they are not assigned probabilities of occurrence.

As a framework for the scenarios, four so-called qualitative “storylines” (see Fig. 7.18) were developed: A1, A2, B1 and B2. Each storyline represents different demographic, social, economical, technological, and environmental developments. From these storylines the forty SRES scenarios were derived as quantitative interpretation of a qualitative storyline by six modelling teams. All scenarios based on the same storyline constitute a “scenario family”. The A1 family is subdivided into three scenario groups characterizing alternative developments in energy technologies: A1FI (fossil fuel intensive), A1T (predominantly non-fossil fuel) and A1B (balanced). The other families consist of just one group.
The scenarios can be further divided into those that share harmonized assumptions on global population, gross world product, and final energy use (denoted with HS in Fig. 7.18) and those that explore uncertainties beyond the harmonized scenarios (denoted with OS). Four illustrative marker scenarios (harmonized) were provided already in 1998 in draft form and included in revised form in the 2000 Special Report. It is these scenarios that the impact assessment in this study is based on.
The four storylines underlying the scenarios are shortly described in Box. 7.1.

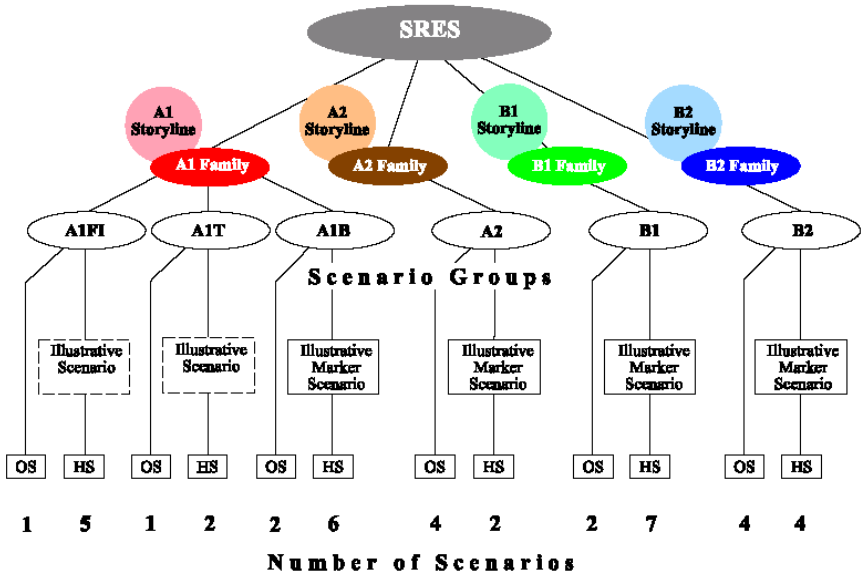

Fig. 7.18: Schematic illustration of the IPCC SRES scenarios. Abbreviations are explained in the text (Source: IPCC 2000).

THE FOUR SRES STORYLINES

- The A1 storyline and scenario family describes a future world of very rapid economic growth, global population that peaks in mid-century and declines thereafter, and the rapid introduction of new and more efficient technologies. Major underlying themes are convergence among regions, capacity building, and increased cultural and social interactions, with a substantial reduction in regional differences in per capita income. The A1 scenario family develops into three groups that describe alternative directions of technological change in the energy system. The three A1 groups are distinguished by their technological emphasis: fossil intensive (A1FI), non-fossil energy sources (A1T), or a balance across all sources (A1B).
- The A2 storyline and scenario family describes a very heterogeneous world. The underlying theme is self-reliance and preservation of local identities. Fertility patterns across regions converge very slowly, which results in continuously increasing global population. Economic development is primarily regionally oriented and per capita economic growth and technological change are more fragmented and slower than in other storylines.
- The B1 storyline and scenario family describes a convergent world with the same global population that peaks in mid-century and declines thereafter, as in the A1 storyline, but with rapid changes in economic structures toward a service and information economy, with reductions in material intensity, and the introduction of clean and resource-efficient technologies. The emphasis is on global solutions to economic, social, and environmental sustainability, including improved equity, but without additional climate initiatives.
- The B2 storyline and scenario family describes a world in which the emphasis is on local solutions to economic, social, and environmental sustainability. It is a world with continuously increasing global population at a rate lower than A2, intermediate levels of economic development, and less rapid and more diverse technological change than in the B1 and A1 storylines. While the scenario is also oriented toward environmental protection and social equity, it focuses on local and regional levels.

Fig. 7.19: Total global CO_2 emissions from all sources (energy, industry, and land use change) from 1990 to 2100 in gigatonnes of carbon per year. The 40 SRES scenarios are represented by the four storylines A1, A2, B1 and B2. The coloured bands show the range of harmonized and non-harmonized scenarios within each group. The illustrative marker scenarios for each scenario group are represented by the solid lines. (Source: IPCC 2000: 7¨)

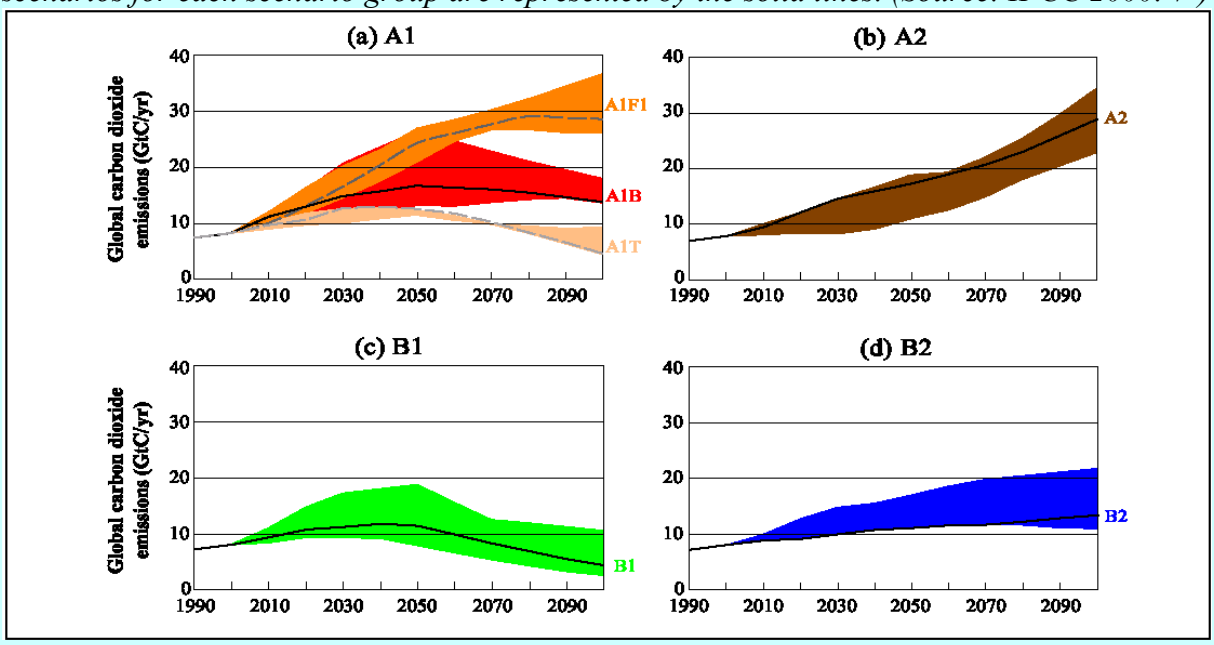

Box. 7.1: The four IPCC SRES storylines

7. 3. 2. Methods of climate impacts assessment

For the climate impacts assessment in this study the "Guidelines on the use of scenario data for climate impact and adaptation assessment" by the IPCC Task Group on Scenarios for Climate Impact Assessment (IPCC-TCGIA 1999) were followed.

The reasons for the selection of the baseline period and the datasets used have been described in Section 7.1. In order to construct daily rainfall and evaporation series that have the characteristics of changed climate as predicted by IPCC SRES scenarios, the following procedure was adopted:

1) Selecting appropriate GCM outputs
2) Extracting regional GCM outputs and downscaling of the data to the Naro Moru study catchments
3) Constructing change fields of temperature and evaporation by extracting GCM outputs for the baseline period 1987 – 2001, and comparing their monthly means to those of the scenario period 2049 – 2070
4) Applying the monthly change fields to the baseline measured data and running the NRM[3] Streamflow Model with the modified inputs

7. 3. 2. 1. Selection of GCM outputs

As mentioned in the previous section, six modelling teams have developed 40 SRES scenarios using different Global Circulation Models (GCMs). So it is not easy to select the most appropriate GCM predictions for an impacts assessment. However, there are some practical

limitations that narrow the breadth of choice, and some criteria given by IPCC-TGCIA which help to identify suitable outputs.
The practical limitations are that the IPCC data distribution centre (IPCC-DDC) has made available monthly prediction from the used GCMs on the internet, but only a small number of the 40 experiments is available by this way to date. They are shown in Table 7.8.
The criteria suggested for the selection of appropriate GCM outputs (IPCC-TGCIA 1999: 43) are:

- **Vintage:** in general, recent model simulations are likely (but not certain) to be more reliable than those of earlier vintage, because they are based on recent knowledge, incorporate more processes and feedbacks and are usually of higher spatial resolution than earlier models.
- **Resolution:** Some of the early GCMs operated on a horizontal resolution of some 1000 km with 2 – 10 levels in the vertical. More recent models are run at nearer 250 km resolution with around 20 vertical levels. This is likely to result in, but does not guarantee, a superior model performance.
- **Validity:** The models should be used that simulate present-day climate most faithfully. It should be noted that the relative performance of GCMs depends critically on the size of the region (small regions at sub-grid scale are less likely to be well-described than continent-scale areas) and its location (the level of agreement between GCM simulation and reality varies a lot from region to region). Furthermore it should be remembered that a high correlation of the simulation with today's climate does not necessarily mean more reliable predictions.
- **Representativeness of results:** If outputs of more than one GCM are used, it is recommended that models are chosen including a high range of predicted values for a variable. In addition, it is recommended that at least a 30-year period be used for averaging GCM output data in order to dampen the effects of inter-decadal variability.

Modelling centre	Model	Available SRES scenario runs	Resolution
Max Planck Institute for Meteorology	ECHAM4/ OPYC3	A2, B2	2.8° x 2.8°
Hadley Centre for Climate Prediction and Research	HadCM3	A2, B2	2.5° x 3.75°
Australia's Centre for Atmospheric Research	CSIRO-Mk2	A1, A2, B1, B2	3.2° x 5.6°
National Centre for Atmospheric Research	NCAR-CSM NCAR-PSM	A2 B2	3.7° x 3.7°
Geophysical Fluid Dynamics Laboratory	R30	A2, B2	4.5° x 7.5°
Canadian Center for Climate Modelling and Analysis	CGCM2	A2, B2	3.7° x 3.7°
Center for Climate Research Studies (CCSR) National Institute for Environmental Studies (NIES)	CCSR/NIES AGCM + CCSR OGCM	A1, A1FI, A1T, A2, B1, B2	5.6° x 5.6°

Table 7.8: GCM outputs available from the IPCC data distribution centre.

These criteria are followed in this study as far as possible given the availability of data and the time-frame. Concerning **vintage**, the most recent simulations available at the IPCC data distribution centre (IPCC-DDC) are used; the SRES scenarios are modelled with coupled atmosphere-ocean models (AOGCMs). They are able to simulate the time lags between a given change in atmospheric conditions and the response of climate and can more realistically simulate the transient-response of climate to a time-dependent change in greenhouse gas concentrations (in contrast, the earlier equilibrium models assumed a constant higher rate of greenhouse gases in the atmosphere with the climate equilibrium reached already). The recent AOGCMs are "warm-start" experiments, which means they begin by modelling historical forcing in the eighteenth or nineteenth century, on one hand enabling comparisons between today's climate and the outputs, and on the other hand avoiding the so-called "cold-start" problem that arises from assuming equilibrium conditions at present.

Concerning **resolution** and the distance of modelled grid points to the study catchments of Naro Moru, the ECHAM4 and HadCM3 GCMs are the models with the highest resolution and with grid points closest to Naro Moru.

Plotting the average monthly means over the baseline interpolated to the study area against the measured data allows to quantify the **validity** of the two GCM output datasets (Fig. 7.20; see next section for the employed method of downscaling GCM projections). It reveals that the ECHAM4 GCM represents present-day climate better than HadCM3. The crucial variable is precipitation, since temperature is not a direct input variable for the NRM[3] Streamflow Model, but is used indirectly to derive a change in evapotranspiration from a mean change. Both models underestimate rainfall and overestimate temperature, which is mainly the effect of altitude, but it can be seen that the ECHAM4 outputs follow the measured rainfall pattern better.

Concerning **representativeness**, it would have by far exceeded the time-frame given for this study to explore the whole range of predictions for rainfall and temperature. Using a thirty-year period to maximise the representativeness with respect to interdecadal variability is only possible for the scenario period, for which the years 2040 – 2069 (a standard period employed for climate change impacts assessment, IPCC-TGCIA 1999) are used. For the baseline the availability of measured data restricts the length of the period.
Based on the above findings, the projections of the model ECHAM4 were chosen to be used as basis for modifying the baseline meteorological data for the climate change scenarios in this study. A short description of the model can be found in Appendix C.10.

7. 3. 2. 2. Extracting GCM data and downscaling to the study area

The GCM data are provided by the IPCC Data Distribution Centre in the GRIB (GRIdded Binary) format, a data format that allows to pack information on a global grid with several layers into little storage space. FM 92 GRIB is widely used to represent forecast and analysis products in binary code. The GRIB specification is maintained and reviewed by the World Meteorological Organisation (WMO).

To graphically represent GRIB data, a programme called GRADS (Grid Analysis and Display System) can be downloaded from the IPCC data distribution centre (http://ipcc-ddc.cru.uea.ac.uk/dkrz/dkrz_index.html). In order to extract the values for the grid points around Naro Moru, the GRIB files first have to be converted to ascii format with a programme called grbconv.exe (available from the same site). This results in a text file in which the values for each grid point, each variable, each layer and each time step are simply

written one after another. To extract the values for every month for the desired gridpoints, a Fortran77 programme (climextract) was written and run under Linux. The source code can be viewed in Appendix. C.9.

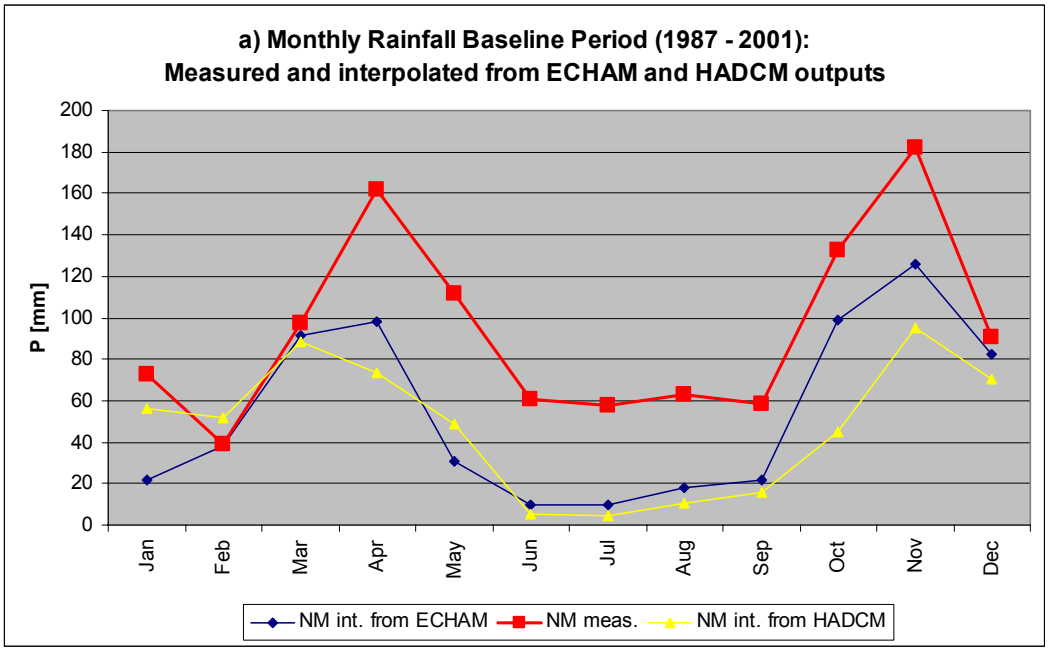

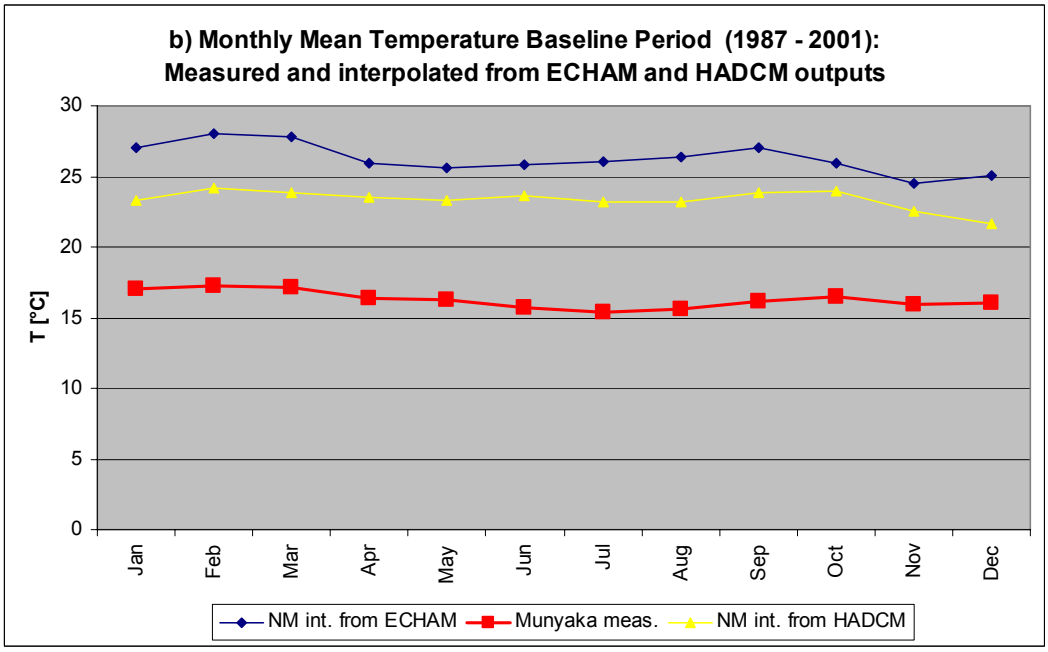

c) Correlation with measured data

	Precipitation	Temperature
r^2 HadCM3 - measured	0.976	0.210
r^2 ECHAM4 - measured	0.981	0.465

Fig. 7.20: Comparison of the monthly averaged outputs of the GCMs HADCM and ECHAM with the baseline period meteorological observations. ECHAM outputs show a higher level of agreement with the measured data in precipitation, the most crucial variable for the use of the NRM^3 Streamflow Model.

One of the major problems in applying GCM projections to regional impacts assessment is the coarse spatial resolution of the gridded estimates in relation to the exposure units studied. Several methods of this procedure known as "downscaling" or "regionalisation" are described by IPCC-TGCIA (1999: 48ff):

- The simplest method is to use the values of the nearest grid box. This is discouraged because of the lack of confidence in regional estimates of climate change.
- A little more sophisticated, but still simple is the method of interpolating the values from nearby grid boxes. The results are likely to be more reliable than those of the first method.
- Statistical downscaling techniques utilise statistical relationships between large-area and site-specific surface climates, or between atmospheric circulation types and local weather. This requires large amounts of observational data to establish the needed relations.
- High resolution experiments make use of numerical models over the area of interest. This can be done in various ways, from running a GCM at higher resolution in a limited number of years ("time slice" experiments) over running a GCM at various resolutions around the globe with the highest resolution over the area of interest ("stretched grid" experiments) up to using conventional GCM outputs to provide the boundary conditions for a high-resolution RCM (the "nesting" approach).

For this study the second method of interpolating the values from nearby grid boxes was adopted because of data availability and the given time-frame. The GCM output values from the four nearest grids were interpolated by Inverse Distance Weighting to the Naro Moru catchment.

7. 3. 2. 3. Constructing change fields

A scenario of future climate is obtained by adjusting the baseline observations by the difference or ratio between averaged results of the GCM experiment for the scenario period and the corresponding averages of the simulated baseline period (IPCC-TGCIA 1999: 47). Differences are usually applied for temperature changes ($Average_{ScenarioPeriod} - Average_{BaselinePeriod}$) and ratios are commonly used for precipitation changes ($Average_{ScenarioPeriod} / Average_{BaselinePeriod}$). The pattern of differences or ratios is known as "change field".

In this study, monthly change fields were constructed using differences for temperature and ratios for precipitation, using the formulae:

$$\Delta P_i = Psim_i[2040 - 2069] / Psim_i[1987 - 2001] \quad (7.1)$$

$$\Delta T_i = Tsim_i[2040 - 2069] - Tsim_i[1987 - 2001] \quad (7.2)$$

where ΔP_i = change field in precipitation for month i
ΔT_i = change field in temperature for month i
$Psim_i$ = simulated average precipitation over period […] for month i
$Tsim_i$ = simulated average temperature over period […] for month i

Since the NRM[3] Streamflow Model does not require temperature but evaporation as input variable, the temperature change fields have to be converted to evaporation change fields. This was done as in the work of Thomas (1993) applying a relationship that results in an increase of evaporation by 4% for an increase in temperature by 1°C (Budyko 1990 cited in Thomas 1993: 139).

The change fields for precipitation and evapotranspiration for the two examined scenarios are presented in Table 7.9.

Month	A2 scenario (ccsc01)		B2 scenario (ccsc02)	
	ΔP [%]	ΔET [%]	ΔP [%]	ΔET [%]
January	276.45	0.98	16.00	5.58
February	79.34	2.42	-9.97	6.82
March	-1.82	4.52	-4.05	7.50
April	0.59	7.20	40.47	3.83
May	19.68	5.95	4.67	5.40
June	-30.87	6.50	12.14	6.83
July	-39.59	7.40	68.33	6.99
August	-31.82	7.18	57.36	5.74
September	-6.51	6.32	-14.54	6.71
October	5.79	5.30	30.22	3.88
November	3.83	5.84	23.53	3.28
December	-5.62	6.35	3.91	3.57
YEAR	**22.45**	**5.50**	**19.00**	**5.51**

Table 7.9: Change fields for precipitation and evapotranspiration for the scenarios ccsc01 (IPCC SRES A2 scenario) and ccsc02 (IPCC SRES B2 scenario).

7. 3. 3. Projected climate changes for Africa

A characterization of regional climate change projections for the 21st century in Africa has been performed by Hulme et al. (2001). A range of atmospheric greenhouse gas loadings according to the four draft marker scenarios for the IPCC Special Report on Emissions Scenarios (IPCC 2000) was assumed.
Future warming across Africa ranges from 0.2°C per decade (B1 – low scenario) to 0.5°C per decade (A2 – high scenario). The warming is greatest over the semi-arid margins of the Sahara and central southern Africa. The range of the predictions is smallest over north Africa and the equator and greatest over the interior of Southern Africa.
For seasonal rainfall, the changes are less well defined. Under the lowest warming scenario, few areas only experience changes that exceed two standard deviations of natural variability by the middle of the 21st century. The exceptions are parts of East Africa where rainfall increases by 5 – 20% in December – February and decreases by 5 – 10% in June – August.
For annual rainfall, there is a general consensus for wetting in East Africa (IPCC 2001: 494).

Figures 7.21 and 7.22 show the median of the precipitation change projections of seven GCM experiments and the range of the projections for African Regions for the months December – February and June – August under the lowest (B1) and the highest scenario (A2) by the 2050's. It can be seen that the changes in East Africa are significant also under the low scenario, but the intermodel range with values between 48% up to almost 200% over the study area indicates how insecure the predictions are.

December - February

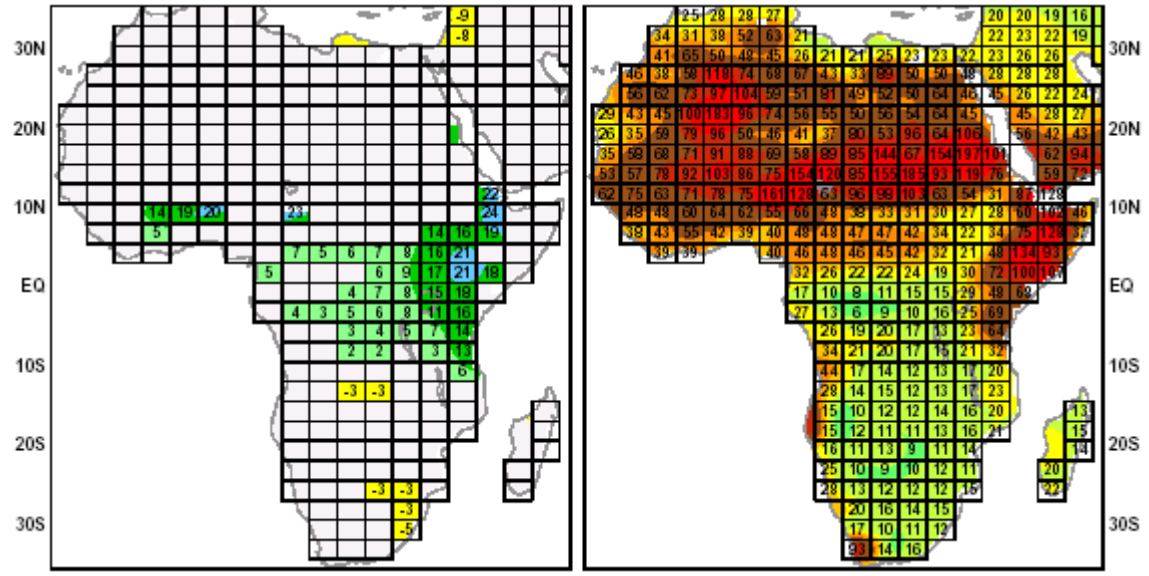

June – August

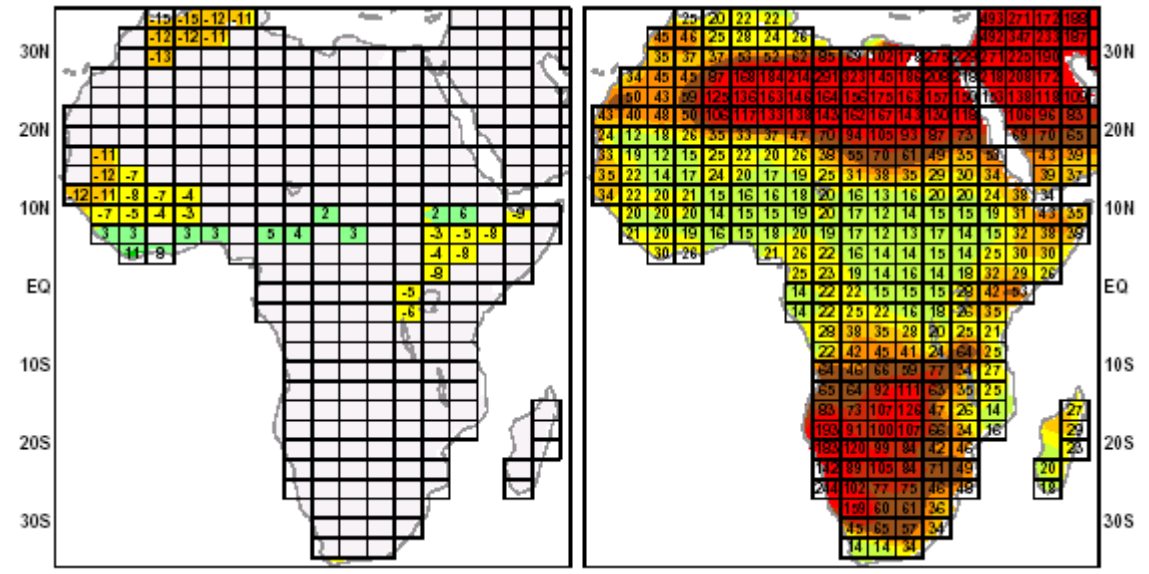

Fig. 7.21: Precipitation changes under the low B1 scenario in December – February (above) and in June – August (below). The maps on the left show the percentage of projected precipitation change (median of seven GCM experiments), the maps on the right the range of projected changes. For areas where the standard deviation of natural variability as defined by HadCM2 is not exceeded no change is shown in the left maps (Source: Hulme et al. 2001).

December – February

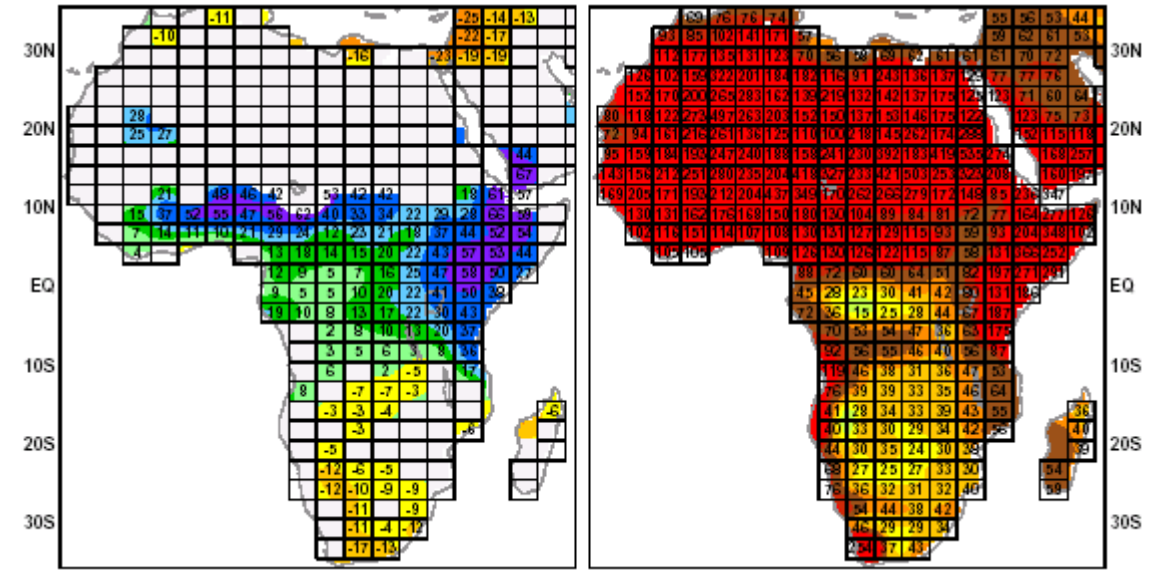

June – August

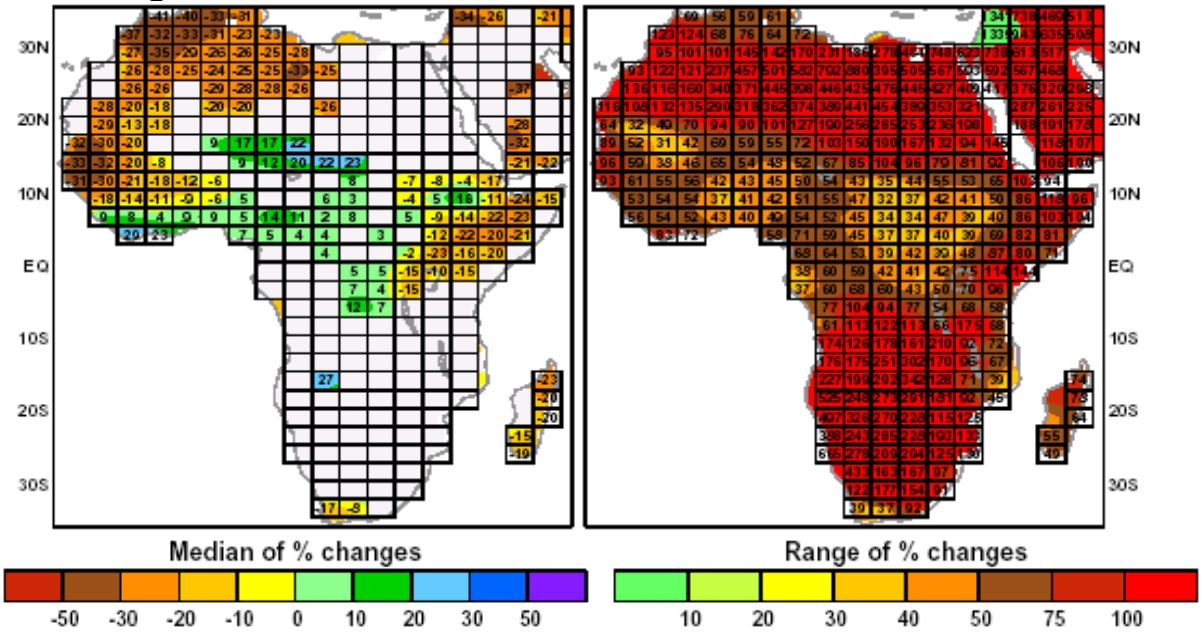

Fig. 7.22: Precipitation changes under the high A2 scenario in December – February (above) and in June – August (below). The maps on the left show the percentage of projected precipitation change (median of seven GCM experiments), the maps on the right the range of projected changes. For areas where the standard deviation of natural variability as defined by HadCM2 is not exceeded, no change is shown in the left maps (Source: Hulme et al. 2001).

Hulme et al. (2001) additionally identified some fundamental limitations to knowledge with regard to future African climate: Often the climate variability caused by the ENSO is poorly represented in the global climate models, and representation of regional changes in land cover and dust and biomass aerosol loadings is absent. These not well-understood processes may have significant impacts on future African climates.

7. 3. 4. Impacts of climate change: results of the scenario runs

7. 3. 4. 1. Scenario ccsc01: IPCC SRES A2 illustrative marker scenario

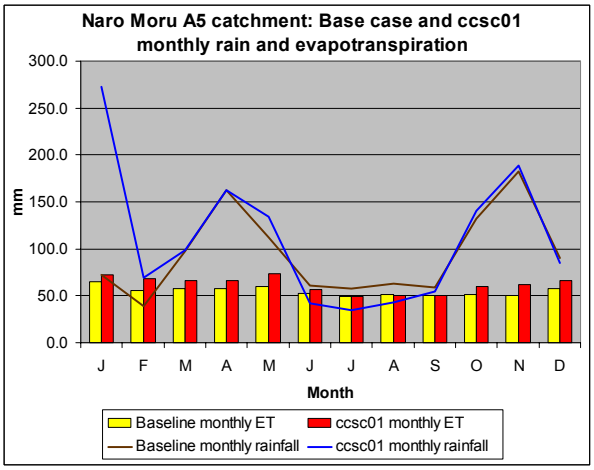

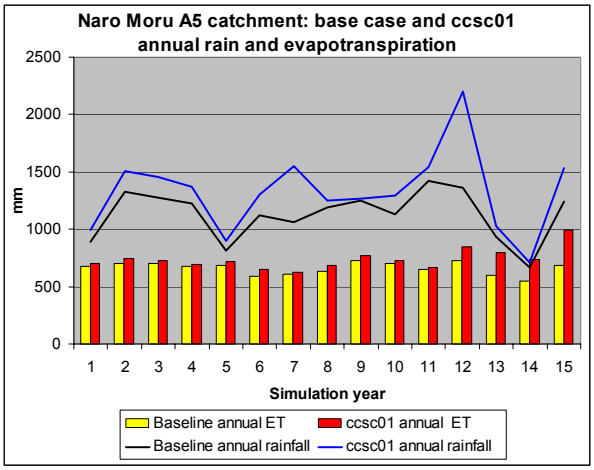

Fig. 7.23: Monthly (left) and annual (right) catchment precipitation and actual evapotranspiration for A5 under scenario ccsc01 compared to the base case.

Catchment	Annual runoff [%]	Qmax [%]	Qmin [%]	Mean [%]	Median [%]	Lower Quartile [%]	Upper Quartile [%]	Mean NMQ30 [%]	Rain [%]	Q/P ratio [+/- %]
A5	26.274	285.594	-75.000	26.274	-1.923	-12.500	23.404	-30.151	17.627	1.083
A3	19.990	189.960	-80.000	19.990	-3.030	-10.000	23.558	-28.846	16.188	-0.135
A4	20.096	247.658	-100.000	20.096	-6.897	-10.795	25.694	-30.513	16.587	-0.632
A6	59.008	546.108	0.000	59.008	14.286	18.750	49.580	-19.006	22.597	6.047

Table 7.10: Impacts of scenario ccsc01 on streamflow. The values shown are deviations to the base case values in percent.

Impacts: The impacts of this scenario on discharge are an increase in streamflow amounts as well as in streamflow variability. Total runoff is raised by 20% (A3) to 59% (A6 catchment). The increase is mainly felt in flood flows: The discharge peaks increase by 190 - 546% and the upper quartile by 23 – 50%.
At A3 – A5, median and low flow measures decrease. The NMQ30 is lowered by around 30%, the minimum discharges by 75% (A5) to 100% (A4), which would signify a drying.out of Naro Moru South.
At A6, the minimum flow stays the same as in the base case, the NMQ30 decreases by 19%, and all other measures show an increase under the scenario.
The discharge regime changes considerably: The months January to March experience a large relative increase in streamflow, as shown by the Pardé Coefficients in Fig. 7.25 b). In January the Pardé Coefficient is raised – from 7.18 to 30.89, which makes it the month with the most discharge. All other months suffer a relative decrease, which is felt strongest in the continental rains months.
Interannual variability increases, as indicated by Fig. 7.25 a). The high rainfall amounts in some months and the reduction in other months leads to extremely high or extremely low soil moisture, which results in more variable final curve numbers and infiltration capacity. In the dry 13th and 14th simulation year, actual evapotranspiration is relatively high, which is caused by the long droughts, subsequently reduced curve numbers and increased infiltration.

Interpretation: The increase in streamflow is logically due to an increase in annual rainfall, which is strongest in the dry season (January to March). The long rains and short rains months

also experience a moderate increase in rainfall. During the continental rains (June to August) rainfall decreases by around thirty percent, causing a very dry period during which streamflow is significantly reduced.
The effect that the discharge at A6 shows an increase of median and lower quartile, unlike in the other catchments, is partly due to the fact that the relative increase in rainfall is more pronounced in the lower catchment because under the base case meteorlogy it receives a higher proportion of rainfall in the months when the change field is most positive. The other reason is that in the upper catchments with the lower average curve numbers, more rain infiltrates into the soil. This way some flow peaks in the months when rainfall decreases are not even visible anymore in the scenario hydrographs of A3 – A5 (see June – August in Fig. 7.24, for example). In the A6 catchment the response to rainfall is more instantaneous. Baseflows also decrease in the continental rains months, but their decrease is hidden by the statistical measures that include the increase in the small flow peaks. Only the NMQ30 indicates the lowered baseflows.
The equal minimum discharge at A6 in the scenario as in the base case can be explained with a similar effect: In most years the annual minimum is lower in the scenario than in the base case. The absolute minimum over the whole period, however, is a case where also in the base case the soil water is down to a minimum due to lacking infiltration (0.4 mm in the saturated zone on October 17 of the 14th year), resulting in as little flow as in the scenario.

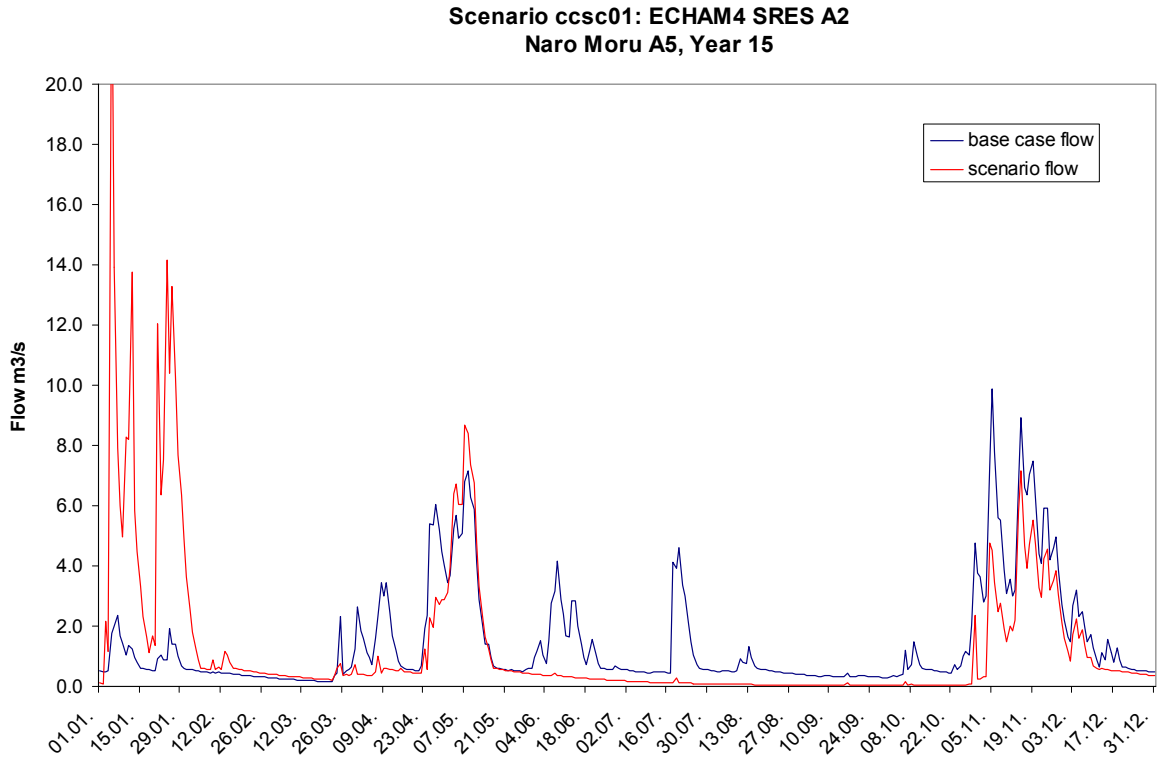

Fig. 7.24: Daily discharge at A5 under the scenario ccsc01 in the 15th simulation year. Note the increase in flow peaks in January and in the long rains season. In the continental rains season, flows are dramatically reduced.

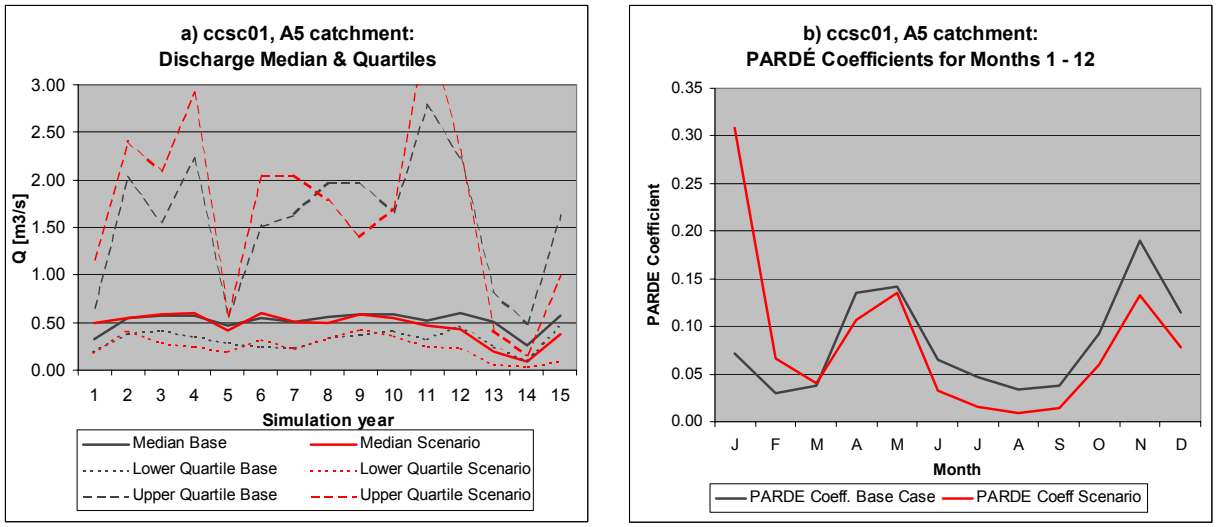

Fig. 7.25: Discharge median and quartiles for all simulation years under scenario ccsc01 at A5 (a) and average Pardé Coefficients (b).

7. 3. 4. 2. Scenario ccsc02: IPCC SRES B2 illustrative marker scenario

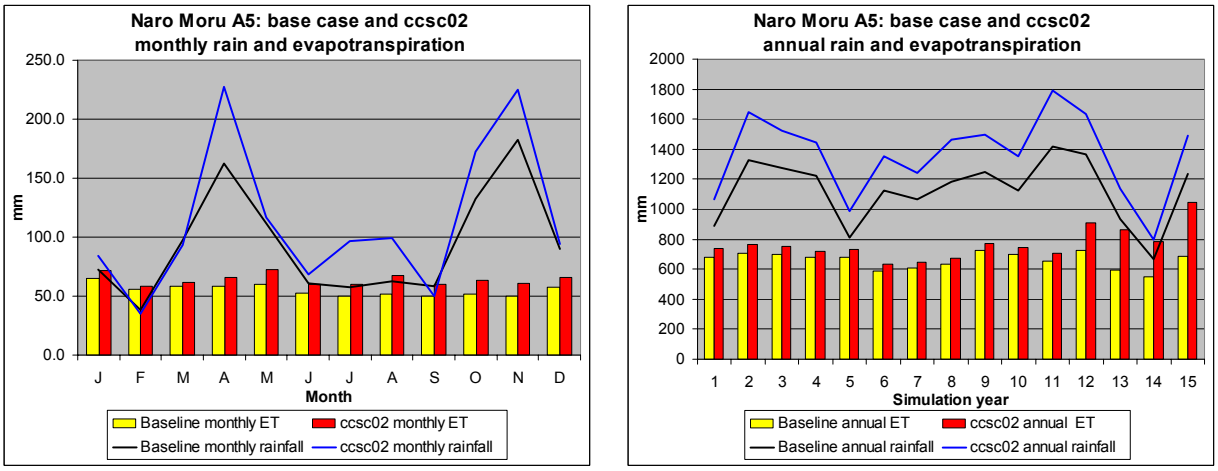

Fig. 7.26: Monthly (left) and annual (right) precipitation and actual evapotranspiration under scenario ccsc02 compared to the base case.

Catchment	Annual runoff [%]	Qmax [%]	Qmin [%]	Mean [%]	Median [%]	Lower Quartile [%]	Upper Quartile [%]	Mean NMQ30 [%]	Rain [%]	Q/P ratio [+/- %]
A5	28.458	34.776	-50.000	28.458	7.692	21.875	31.738	-7.042	20.853	1.936
A3	26.213	36.739	-20.000	26.213	7.576	22.500	40.705	-6.195	21.252	1.296
A4	25.514	58.756	-100.000	25.514	9.195	34.091	38.021	-9.695	21.127	1.057
A6	47.297	53.150	0.000	47.297	21.429	62.500	66.387	17.404	22.790	4.973

Table 7.11: Impacts of scenario ccsc02 on streamflow. The values shown are deviations to the base case values in percent.

Impacts: As in scenario ccsc01, under scenario ccsc02 the amount and the variability of streamflow is increased, as shown in Fig. 7.28 a). The changes are different in magnitude and distribution, however. The increase in total streamflow with 25.5 – 28.5% is greater than

under the first scenario in the upper three subcatchments A3 – A5. At A6, the increase amounts to 47%, which is less than under ccsc01.
Upper quartile, median and lower quartile of daily discharge are raised with respect to the base case. The increase is again most pronounced at the peaks and flood flows. The lowest monthly mean flows (NMQ30) are reduced at A3 – A5 by 7 – 10%; at A6, they increase by 17%. In general the range between low flows and peak flows is greater than under present conditions, but not as extreme as under the scenario ccsc01.
The discharge regime is not affected very much by this scenario, as shown in Fig. 7.28 b). Flows are relatively reduced in the dry season (February – March) and May, June and September. The other months experience a relative increase.
Interannual variability is increased for the same reasons as under scenario ccsc01. Especially towards the end of the simulation period, the baseline meteorology modified by the change fields results in long drought periods, increasing actual evaporation and reducing the Q/P ratio.

Interpretation: The increase in rainfall under this scenario affects mainly the rainy seasons and the months June to August. The dry season (January – March) experiences a slight reduction in rainfall (opposing the projections of the SRES A2 and B1 scenarios). This leads to a more constant increase in streamflow than under ccsc01 with less variability.

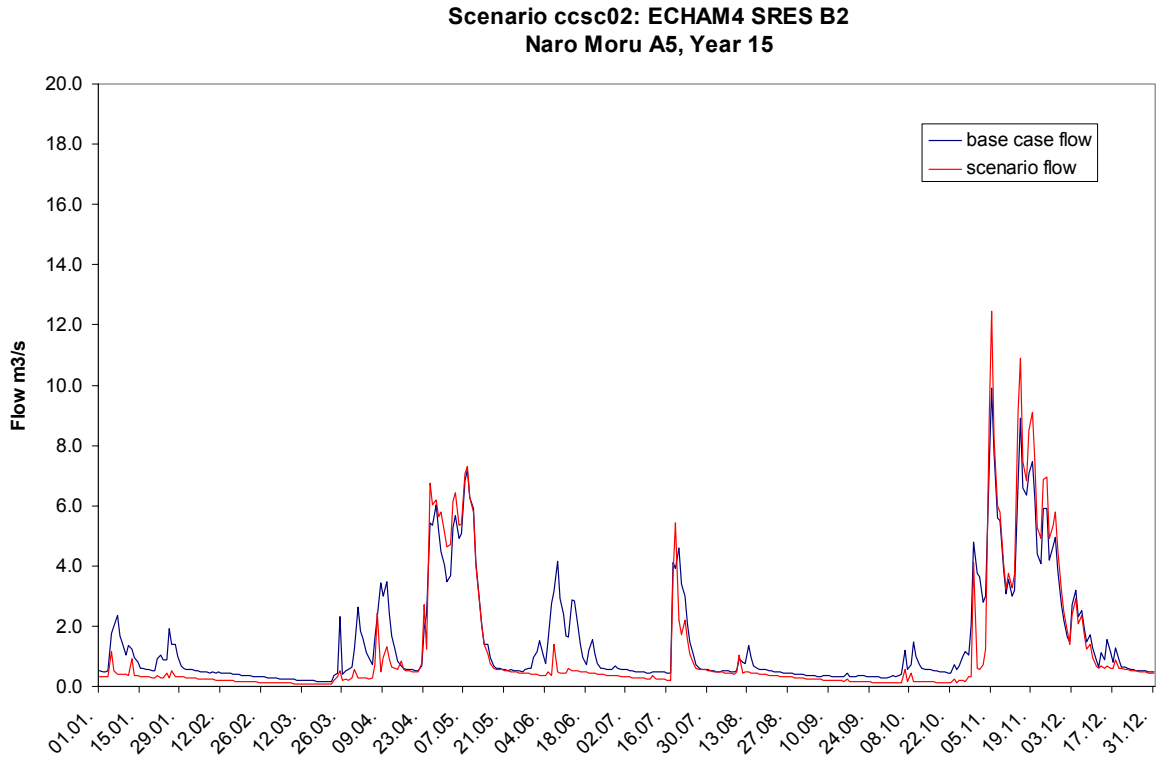

Fig. 7.27: Daily discharge at A5 under scenario ccsc02 in the 15th simulation year. The reduced low flows and raised peaks which are characteristic for this scenario can be seen. Not characteristic is total runoff – it is reduced by 19% compared to the base case in this year (over the whole simulation period it is raised by 28%). This is caused by long drought periods – the reduced soil moisture leads to low final curve numbers, which raises infiltration, and this in turn results in higher evaporation rates.

The contrasts between the upper and the lower subcatchments are less pronounced than under scenario ccsc01. This is explained by the fact that the increase in rainfall is almost equal in all subcatchments (under ccsc01 it is most pronounced in the A6 catchment), and by the final curve numbers raised by the more constantly higher soil moisture in the upper subcatchments, leading to more direct runoff. At A6 this effect is less pronounced than under ccsc01, as indicated by the lower Q/P ratio.

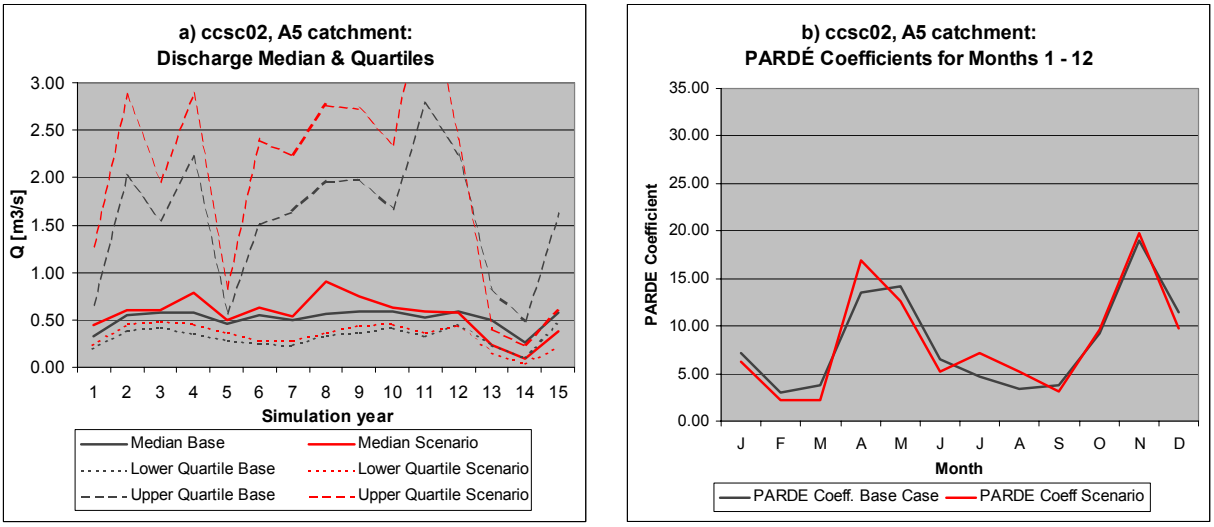

Fig. 7.28: Discharge median and quartiles for all simulation years under scenario ccsc01 at A5 (a) and average Pardé Coefficients (b).

8. DISCUSSION

8.1. ASSESSMENT OF GROUNDWATER AND ABSTRACTIONS INFLUENCES ON THE WATER BALANCES

8. 1. 1. Groundwater influences

The examination of the river profiles measurements of discharge, electric conductivity and temperature presented in Section 5.1 shows that in the Naro Moru and Burguret catchments, the footzone is characterized by groundwater contributions to baseflow and the savannah zone by transmission losses. This confirms findings from earlier studies on the water balance of Naro Moru River (Decurtins 1992, Gathenya 1992). In the Naro Moru catchment, it is shown that the modelled values at the outlets of the nested subcatchments lie within the range of the naturalised observed discharge for the days of the profile measurements. Influences of groundwater with long residence times are greatest in the Burguret catchment with the influence of spring-fed tributaries, but are found to contribute only a small proportion of dry season flow.
Based on these findings, hydrological modelling of the study catchments was considered possible without major changes in the model structure of the NRM^3 Streamflow Model. However, with the underestimation of total runoff in the calibration period and the overestimation in the validation period in almost all catchments, the modelling results indicate that longer-term underground movements of water in deep aquifers might in fact be effective - this can neither be confirmed or ruled out due to the lacking reliability of the input data.

The results are flawed by the very insecure estimates on anthropogenic influence (the unknown real amounts of abstracted water amounts at the time of the profile measurements that represent a great source of error concerning discharge, and pollution in the Nanyuki catchment affecting the electric conductivity measurements). In the Nanyuki catchment, these insecurities are so great that a safe statement on groundwater influences cannot be made. But also in the Naro Moru catchment, where abstractions estimates based on different assessment methods can be compared, the wide range between the lowest and the highest estimates indicates the insecurities. The drying out of Naro Moru river in the savannah zone due to the abstractions makes it impossible to know if any, and how much more water would be lost if there was any flow in the stretch that was dried out at the time of the profile measurements.
The way an assessment like this should be made is by officially agreeing with the water users on a schedule stating when they should not abstract water, so that undisturbed measurements could be made. In the current situation, where not even all water users are known, let alone would be reachable and convinceable that this action is necessary, it would be impossible to implement such a schedule, however.

It should also be remembered that the river profiles represent the situation on two days in a dry period. It is likely that groundwater influences are easiest to detect during a period when the discharge in a river is mainly made up of baseflow, but it just indicates and does not prove that the findings are generally valid.

8. 1. 2. Abstractions

Abstractions are quantified based on abstractions monitoring data in NRM^3 database (1987 – 1997 – different methods from daily over monthly monitoring to snapshot campaigns) and the 2001/02 snapshot abstractions campaigns, of which the one on Naro Moru was conducted during the field work period for this study (refer to Aeschbacher 2003). The daily sums of abstracted water in a catchment are added to the observed daily discharge, resulting in a naturalised flow series.

The problem with the abstracted water quantities is that they are highly variable in time and depend on various factors: the amount of water available in the river, the amount of rainfall and the necessity for irrigation, and the personal decisions and preferences of each water user. Especially the last factor is impossible to predict or extrapolate, thus necessarily leading to insecure estimates. The question is whether the estimates are in the range of the real amounts and which method of assessment is most efficient. The thesis of Jos Aeschbacher (2003) extensively deals with these subjects.
For the calibration and validation of the NRM^3 Streamflow Model, the measured datasets from the NRM^3 database (from earlier campaigns and monitoring) were used for flow naturalisation, because the naturalised flow series produced with the Abstractions Calculation Tool (Aeschbacher 2003) did not become available almost until the end of the work on this study. The use of the flow series naturalised with the data from the NRM^3 database also led to better performance measures. However, this does not necessarily mean that they are more accurate – it is more likely for the periods when extensive monitoring was done, like the daily monitoring on Naro Moru by Gathenya (1992), but questionable when only monthly measurements, and these with many gaps, are available.

The main message is that abstractions can be estimated in various ways requiring more or less financial and work effort, but the amounts remain insecure estimates, especially on the daily time-scale. It should be kept in mind that deviations from simulated to naturalised observed values in model calibration and validation may also in part be due to inaccurate abstraction estimates, since these can cause more than 100% deviation in low flow periods.

8. 2. EVALUATION OF THE NRM^3 STREAMFLOW MODEL

8. 2. 1. Simulation quality

Calibration and validation of the NRM^3 Streamflow Model has been carried out in the study catchments Naro Moru A3 – A6, Burguret A8 and Nanyuki A9. The simulation quality is found to be satisfactory in the catchments where good-quality rainfall input data from a dense-enough measuring network are available: the applied performance measures indicate a reasonably good simulation quality on the decadal time-step and an acceptable quality on the daily scale. Total runoff is overestimated in some periods and underestimated in others, which is mainly attributed to the difficulties in interpolating rainfall in mountainous areas with mainly convective local storms. Flood flows are generally overestimated and low flows underestimated. The interannual pattern of the lowest flows is followed well, but their general underestimation is a problem in an area where dry season flows are critical.

Limitations to better simulation quality are identified in the model structure as well as in the quality and reliability of the input and validation datasets.

The main limitation in the **model structure** is the representation of groundwater storage and discharge. Under the current model structure, just one reservoir represents the groundwater store, and the release of water from this store is steered by three constant parameters (two coefficients for slow and fast groundwater discharge and a threshold value of the water content to separate the use of the two). This does not allow to let slow groundwater discharge begin at different levels of total discharge, and water cannot be "saved" in the model over time periods longer than some months. The necessary modifications would either be the introduction of a second, lower groundwater store, or of a variable threshold parameter that depends on antecedent rainfall.
The second great limitation is the method of rainfall interpolation. Currently Inverse Distance Weighting is used. Topography is not considered. In the very mountainous terrain of Mt. Kenya with clearly orographic precipitation this leads to deviations from the interpolated to the probable real rainfall pattern where the measuring gauges are not well distributed in altitude with respect to the areas that rain is interpolated to. The introduction of altitude-dependent precipitation interpolation would increase the reliability of the simulation outputs.
A further, minor limitation in the model structure is the determination of beginning and end of seasons when using the dynamic curve number component: beginning and end dates should be flexible and not fixed to certain dates in the year, since dry or wet season onsets vary considerable over the years.
For the simulation of streamflow in larger catchments like A6 (170 km^2) the introduction of channel routing is necessary to avoid the time lag in flow peaks on the daily scale.

The variable **quality and reliability of the input and validation datasets** represents an even greater limitation. The biggest problem are the rainfall inputs: on one hand the monitoring network is too coarse to capture all tropical convective storms that may cause heavy rain in a very small area. On the other hand measuring stations at different altitudes that could capture the distribution of rainfall in altitude only exist along the Naro Moru profile. Correspondingly, the NRM^3 Streamflow Model performs best in this area. In the Burguret and Nanyuki catchments, where only two more rain gauges are situated in the lower forest zone, and in the small A4 catchment, where the probable altitudinal peak of rainfall is not represented by any rain gauge, the simulation quality is considerably lower, mainly with respect to total runoff. In addition, some rainfall data had to be excluded from the analysis because they were obviously erroneous.
The lacking reliability of the measured discharge data represents a limitation to evaluating the simulated model outputs. The rating equations used for the river gauging stations (with their natural cross-sections) have been the same for years and are based on relatively few gaugings, especially towards the upper and lower end of the flow range. The sometimes large gaps in the discharge data prevent the closer assessment of certain flow periods. Certain data periods also had to be removed because of strong suspicion that measurement errors were involved (weir leakage, stuck water recorder needle).

It should be noted that the quality of the NRM^3 Streamflow Model Simulations could only be evaluated based on the comparison to measured discharge. Several authors (Beven 2001, Zappa 2002) point out the importance of evaluating a hydrological model with as many observed variables as possible in order not to reach the best scores but to reach a model structure that reproduces the natural processes as closely and physically plausible as possible. Only this way a maximum reliability can be reached when using the model to predict streamflow in ungauged catchments or in the future. It is thus recommended that the NRM3 Streamflow Model be tested with respect to other output variables as well if datasets become available – of soil moisture, for example, or peak flows.

8. 2. 2. Sensitivity to parameters and input data

The experiences from calibration and validation and the sensitivity analyses to the catchment-specific **parameters** show that the NRM^3 Streamflow Model can be applied without extensive calibration. In fact, most catchment-specific parameters can be estimated from physical catchment characteristics and need only little modification in calibration.
The catchment-specific parameters that the model is most sensitive to are the groundwater discharge coefficients. If discharge measurements from a catchment are available, the groundwater coefficients can be estimated from these; if not, regionalization approaches can be tried – for example, in the study catchments with similar geology, soils and vegetation, the groundwater parameters seem to depend on catchment size to a certain extent.
The only further catchment-specific parameter is the runon coefficient, which has been found to improve simulation quality in the large half-savannah catchment A6 but affects the results only very marginally in the smaller, more mountainous and forested catchments.
The use of the dynamic curve number component has brought no improvement of the simulation in any of the catchments. This may in part be due to the fact that the beginning and end of the seasons are fixed to certain dates in the year, but is also attributed to the fact that the subroutine was mainly introduced to account for the effects the quality of the grass-cover in savannah catchments has on hydrology. On the other hand, increased base curve numbers after longer droughts could be an improvement – the first flow peaks after dry periods, that at present in many cases are underestimated (probably due to the fact that when soils are very dry, less water infiltrates), would be simulated higher.

Concerning the temporal and spatial resolution of the **input data**, the rainfall data again have to be mentioned as the most crucial inputs. Leaving away only some of the available stations results in a large decrease in simulation quality. This shows the necessity of the NRM^3 monitoring network – without it, rainfall-runoff modelling would not be possible in the area. Of course, such a network has to be paid for, and given the fact that with the station density available today still many storms are missed, for the future new methods like the estimation of rainfall from cloud temperatures monitored by satellites are an option to explore.
Evaporation inputs are less crucial: Running the model using monthly average evaporation rates instead of daily data does not have negative impacts on the results, if the averages have been calculated over several years. The main factor that needs consideration is the realistic representation of overall catchment evaporation – it should be watched that the evaporation gauges are well distributed in altitude. An under- or overestimation of evaporation mainly affects baseflow.
The resolution of the GIS input layers is shown not to affect simulation quality up to a resolution of 500 m. At coarser resolutions, the performance decreases. The NRM^3 Streamflow Model is thus generally less sensitive to the spatial resolution of GIS inputs than most distributed hydrological models, which is explained by the simpler model structure: The resolution affects simulated discharge mainly by way of the curve numbers. Topography, which in other models influences rain, evaporation, and subsurface flowpaths, plays a role in the NRM^3 Streamflow Model only for the computation of surface flowpaths for the runon routine.
The use of the land use maps 1988 (Roth 1997) or 1995 (Niederer 2000) only marginally affects simulation quality. Anyway, the majority of the differences in land use between the two maps (the increase in grassland in the moorland zone at the expense of dense trees) is more likely to be due to different vegetational or atmospheric conditions at the time the satellite pictures were taken or different classification methodologies than to real land use changes.

8. 2. 3. Practical applicability and user-friendliness

Considering the simulation quality reached in the catchments with good rainfall data, given the simple model structure and the available input data, the NRM^3 Streamflow Model could be a useful tool for future water management in meso-scale catchments in the Upper Ewaso Ng'iro Basin. Possible applications include:

- Exploring the effects of land-use on hydrology
- Estimating discharge in ungauged catchments (given good-quality rainfall data)
- Generating simulated discharge series to determine requirements to water supply works and other engineered installations
- Assessing the impacts of scenarios of climate change

Besides the recommended modifications to the model structure, a need for improvements is also identified in the user-friendliness of the programme. At present, running the NRM^3 Streamflow Model is very time-consuming and requires above-average computer knowledge to deal with eventual problems. There are many potential sources of error since many procedures have to be completed manually. The introduction of a graphical user interface and the automatisation of procedures (mainly the production of output graphs and summary statistics) would be very desirable if the model is to be used in the context of NRM^3 and the River Water Users Associations.

8. 3. EXAMINATION OF ENVIRONMENTAL CHANGE SCENARIOS

The modelled outputs of the scenario runs in the four nested Naro Moru subcatchments show that the current trends in land use and climate change will, if continued, result in more total streamflow in most cases, but also increased variability, causing the crucial dry season flows to decrease. The impacts of climate change are much more dramatic than the impacts of land use change – at least the way the NRM^3 Streamflow Model predicts them.

There are no surprises in the results of the **land use change scenarios**: It is shown that conversion of the land use to crops results in raised overall water yield but a slight reduction in low flows. Conversion to grassland has more dramatic impacts – the ability of the catchments to absorb rainfall is significantly reduced, and every small rain results in an instant flow peak in the river; rains in the upper catchment areas this way also increase dry season flows on average, but water storage and baseflows are low. The erosion of half the soil depth of the humic andosols and acrisols on the upper mountain slopes affects streamflow only slightly – the infiltration capacity of the remaining soils still exceed actual infiltration in most cases, given the high curve numbers and low infiltration rates of bare grassland.
Conversion to a natural land use only results in very small differences to current conditions, indicating that land use changes up to the present are only responsible for a small part of changes in streamflow regime up to today.

The examined **climate change scenarios** result in quite dramatic changes in the discharge regime. Total discharge is increased as well as discharge variability.
Under the high IPCC SRES A2 scenario, rainfall in the dry season (especially January and February) is increased by a multiple. The continental rains season, by contrast, experiences a significant decrease in rainfall. The increase in streamflow is most pronounced at the flood flows. Low flows are reduced. Interannual variability in streamflow increases as well: The

longer droughts and heavier rainy seasons cause a higher range of the final curve numbers, so that the ratio of discharge to precipitation varies considerably over the years.
The lower SRES B2 scenario has similar but less dramatic impacts. The main difference to the A2 scenario is that the dry season does not become wetter, but the two rainy seasons do. The result is also an increase in overall streamflow but with less extremes – peaks are not raised as much and low flows not reduced as much as under the A2 scenario. Still the impacts of the scenario on the low flows are considerable in the dry years and would require drastic water-saving measures if the projections were to come true.

The **validity** of this impact assessment can of course be questioned for various reasons. First there are the deviations from simulated to real discharge, that are in some cases considerable, as shown in the calibration and validation of the NRM^3 Streamflow Model. The part of the deviations that is not caused by the model structure but by erroneous input data (what part this is, we cannot know) of course does not have to be taken into consideration in the scenarios.

The most important factor concerning the validity of the projections is that the NRM^3 Streamflow Model is a simple model that cannot reproduce all possible feedbacks between the elements of the hydrological system. The feedbacks that cannot be simulated include:

- the impact of land use change on erosion and subsequently the groundwater table
- the impact of land use changes on the internal soil structure (gradual development of other soil types due to different vegetation)
- the impact of climate change on land use and vegetation
- the higher evaporation rates under a high CO_2 environment due to increased transpiration by plants

A further source of errors are the GCM predictions that the climate change scenarios are based on – Hulme (2001) identifies shortcomings mainly in the representation of the current ENSO variability, and the lack of representation of dust and biomass aerosol loadings and regional land use changes – and the way the GCM predictions are downscaled to the study area: a statistical approach or the use of a regional circulation model would certainly be better than simple interpolation, but besides the given short time-frame for this study the necessary data and models are not available.

If the impacts of climate change are predicted to be more dramatic by the modelling experiments than the impacts of land use change, it has to be considered that apart from directly influencing the runoff-generating processes in a catchment and thus the water yield, land use changes may also lead to changes in water quality and sediment transport, and, most important, in the case of conversion to more intensive agriculture, to an increase in river water abstractions (since the new crops also have to be irrigated). This way land use changes may cause significant additional reductions in streamflow that have not yet been included in the predictions made in this study.

Last but not least it can be questioned how probable it is that the examined scenarios will occur – here the scope for speculations is wide, predictions in the classic sense are impossible. The land use change scenarios are not intended to be realistic – extreme situations were used to be able to be able to distinguish the impact of single land use classes. The IPCC SRES scenarios are intended to be realistic alternatives for the future development of global climate – but also there, no probability of occurrence is assigned to any of the scenarios.

8. 4. RECOMMENDATIONS AND OUTLOOK

A hydrological model has been tested as a potential tool for water management. The experiences from its evaluation show that rainfall-runoff modelling is a feasible method of assessing and managing water resources in the study area. The findings and results could be made more valid, however, if the NRM^3 Streamflow Model structure could be adapted according to the findings presented in this study, if the quality and reliability of the data in the NRM^3 database was higher, and if some still existing knowledge gaps on the hydrology of the study catchments could be closed.

It is important, for example, that more discharge gaugings be made to establish the rating equations for the river gauging stations. The effort this would take is not great compared to the overall effort that the monitoring of gauge heights requires, and the reliability of the data could be increased greatly.
The meteorological network should be kept up and no more rainfall or evaporation gauges closed down. The modelling results show that reliable rainfall data from an as dense as possible monitoring network are crucial inputs. Of course this is also very much a matter of money. The reliability of the datasets could already be increased if the quality-control procedures were applied more strictly and if sufficient financial resources were available to do so. Recent financial constraints have had a negative impact on data quality.

Some hydrological processes in the study catchments are still not understood well enough. The question of groundwater re- and discharge by deep aquifers has not been clarified completely. Although the results of the river profile measurements generally confirm earlier findings and do not indicate great influences of deep seepage, the modelling results lead to question this because of the deviations of simulated and observed water yield in some catchments and time periods (especially the underestimation of total runoff in the calibration period opposed to the overestimation in the validation period). But again, these deviations could as well be due to measurement errors. Further research and more reliable data are required to bring clarification.

Besides the above-mentioned improvements on model structure and user-friendliness (with the modification of the simulation of groundwater discharge, altitude-dependent interpolation of rainfall and a graphical user interface as the most urgent needs) an evaluation of the modelling results with respect to other output variables than daily discharge would be desirable in order to increase the reliability of the model predictions. A comparison of modelled to observed soil moisture or peak flows, for example, would be possible if observed datasets become available.

Concerning the predictions that are made for the future, should the examined scenarios come (partly) true, the expected decrease of the water resources in the dry seasons means that the present problems of water scarcity will be aggravated. To mitigate impacts, it is extremely important that the River Water Users Associations be strengthened and that basin-wide agreements can be reached on the allocation of the scarce resource. The promotion of water-saving technologies and land uses must be part of the strategy as well as the installation of water supply works and water storage facilities. The failure to implement such water management activities would most probably result in heavy conflicts between upstream and downstream water users. An increase of economic activity in the region would help to solve the problems, but even more important is the strengthening of the attitude of the farmers towards cooperation with one another and towards taking responsibility for the natural resource water. Miracles cannot be counted on…


MAXIMUM
MIRACLE
CENTRE

REFERENCES

- Aeschbacher, J. (2003): Development of Water Use and Water-Shortage in the Naro Moru Catchment (Upper Ewaso Ng'iro Basin, Kenya). MSc thesis, Institute of Geography, University of Berne
- Barben, M. and Weingartner, R. (1998): Klimaänderung und Wasserhaushalts-simulation – Murg und Ergolz. Publikation Gewässerkunde Nr. 210. Gruppe für Hydrologie, Geographisches Institut der Universität Bern
- Berger, P. (1989): Rainfall and Agroclimatology of the Laikipia Plateau, Kenya. Geographica Bernensia. Institute of Geography, University of Berne
- Beven, K. (2001): Rainfall-Runoff Modelling. John Wiley & Sons. Chichester
- Decurtins, S. (1992): Hydrogeographical Investigations in the Mt. Kenya Subcatchment of the Ewaso Ng'iro River. Group for Development and Environment, Institute of Geography, University of Berne
- Flury, M. (1987): Rain-fed Agriculture in the Central Division (Laikipia District, Kenya). Geographica Bernensia. Institute of Geography, University of Berne
- Gathenya, J. M: (1992): Water Balance for Sections of Naro Moru River. MSc thesis. University of Nairobi
- Gichuki F. N., Liniger H.P., Schwilch G. (1998a): Knowledge about Highland-Lowland Interactions: The Role of a Natural Resource Information System. In: Eastern and Southern Africa Geographical Journal, Vol. 8, p. 5 – 14. Department of Geography, University of Nairobi
- Gichuki F. N., Liniger H.P., McMillan L., Schwilch G., Gikonyo J. K. (1998b): Scarce Water: Exploring Source Availability, Use and Improved Management. In: Eastern and Southern Africa Geographical Journal, Vol. 8, p. 15 – 28. Department of Geography, University of Nairobi
- Gichuki, F. N., Ngigi, S. (2001): Community Management of Matanya Irrigation Project. Water Users Associations Support Initiative Report No. 5. NRM^3, Nanyuki, Kenya
- Gichuki, F. N. (2001): Water Scarcity and Associated Conflicts – Experiences from the Upper Ewaso Ng'iro North Basin. Water Users Associations Support Initiative Report No. 8. NRM^3, Nanyuki, Kenya
- Gichuki F. N., Njeru J. L., Liniger H. P. (2001): Rivers of Ewaso Ngiro North Basin – Constraints and Opportunities. Draft Working Paper for the Water Users Association Support Initiative Report No. 8. NRM^3, Nanyuki, Kenya
- Gichuki, F. N., Njeru, L., Kihara, J., Gikonyo, J., Liniger, H. P. (2002a): Developing a water information system. Water Information System Series Report No. 4. NRM^3, Nanyuki, Kenya
- Gichuki, F. N., Gichuki, Ph. G., Muni, R. K. (2002b): Characterisation of the Flow Regime of Ewaso Ng'iro River. Water Information System Series Report No. 6. NRM^3, Nanyuki, Kenya
- Gichuki, F. N., Gikonyo, J., Liniger, H. P. (2002c): Water Allocation – Guidelines, Procedures and Impacts. Water Users Associations Support Initiative Report No. 18. NRM^3, Nanyuki, Kenya

- Gikonyo, J. K. (2003): River Water Accounting and Water Allocation Modelling: A Case Study of the Upper Ewaso Ng'iro Basin. Unpublished, draft of PhD thesis. Institute of Geography, University of Berne
- Giorgetta, M. (2002): ECHAM4 short description. Max Planck Institute for Meteorology http://www.mpimet.mpg.de/en/extra/models/echam/echam4_description.php
- Hulme, M., Doherty, R., Ngara, T., New, M., Lister, D. (2001): African Climate Change: 1900 – 2100. In: Climate Research 17, p. 145 – 168. Inter-Research
- IPCC (Intergovernmental Panel on Climate Change): Data Distribution Centre. http://ipcc-ddc.cru.uea.ac.uk
- IPCC (Intergovernmental Panel on Climate Change) (2000): Special Report on Emissions Scenarios. Nakicenovic, N. and Swart, R. (eds.). Cambridge University Press, Cambridge, United Kingdom. http://sres.ciesin.org
- IPCC (Intergovernmental Panel on Climate Change) (2001): Climate Change 2001: Impacts, Adaptation and Vulnerability. Vol. II.
- IPCC-TCGIA (1999): Guidelines in the Use of Data for Climate Impact and Adaptation Assessment. Version 1. Prepared by Carter, T. R., M. Hulme, and M. Lal, Intergovernmental Panel on Climate Change, Task Group on Scenarios for Climate Impact Assessment
- Kenyatta, J. (1965): Facing Mount Kenya. Vintage Books. New York
- Kihara, J., Gichuki, F. N., Njeru, L., Gikonyo, J., Liniger, H. P., Schwilch, G. (2002): Data Access and Utilization. Water Information System Series Report No. 3. NRM^3, Nanyuki, Kenya
- Klingl, T. (1996): GIS-gestützte Generierung synthetischer Bodenkarten und landschaftsökologische Bewertung der Risiken von Bodenwasser- und Bodenverlusten. Die Fallstudie Laikipia East, Kenya. Geographica Bernensia. Institute of Geography, University of Berne
- Leibundgut C., Berger P., Brodbeck A., Brunner R., Decurtins S., Kohler T., Moeri T., Müller I., Schotterer U., Winiger M. (1986): Hydrogeographical Map of Mount Kenya. Geographica Bernensia, African Studies Series Vol. A3. Institute of Geography, University of Berne
- Liniger, H.P. (1992): Water and Soil Resource Conservation and Utilization on the Northwest Side of Mt. Kenya. In: Mountain Research and Development, Vol. 12, No 4, pp. 363 – 373. Centre for Development and Environment, Institute of Geography, University of Berne
- Liniger, H.P., Thomas D. B. (1998): GRASS – Ground Cover for Restoration of Arid and Semi-Arid Soils. In: Advances in GeoEcology 31, pp. 1167 – 1178. Catena, Reiskirchen
- Liniger, H.P., Gichuki, F. N., Kironchi G., Njeru L. (1998a): Pressure on the Land: The Search for Sustainable Use in a Highly Diverse Environment. In: Eastern and Southern Africa Geographical Journal, Vol. 8, pp. 29 - 44. Department of Geography, University of Nairobi
- Liniger, H.P., Weingartner R., Grosjean M., et al. (1998b): Mountains of the World, Water Towers for the 21st century – A Contribution to Global Freshwater Management. Mountain Agenda, Paul Haupt, Bern

- Liniger, H.P., Weingartner, R. (2000): Mountain forests and their role in providing freshwater resources. In: Price, M. F. and Butt, N (eds.): Forest in sustainable mountain development: a state of knowledge report for 2000. IUFRO research series, No. 5, pp. 370 – 380. Oxon and New York
- McMillan, L. (1996): User's Notes for NRM^3 /LRP Rating Equations: Version I. Not published. Filename: 1usents.doc
- McMillan, L. (1997): NRM^3 /LRP Rating Equations. Version 2a. Not published. Filename: RatingCurves.doc
- McMillan, L. (2003): Establishment of a Rainfall-Runoff Model for Exploration of Land-Use Change Impacts on the Water Balance of Small Catchments in Tropical Africa. PhD thesis, Institute of Geography, University of Berne
- Niederer P. (2000): Classification and Multitemporal Analysis of Land Use and Land Cover in the Upper Ewaso Ng'iro Basin (Kenya) using Satellite Data and GIS. MSc thesis. Centre for Development and Environment, Institute of Geography, University of Berne
- Notter, Benedikt (2002): Water Balances in the Upper Ewaso Ng'iro Basin. Research Practice Paper. Centre for Development and Environment, Institute of Geography, University of Berne
- NRM^3 (2002): NRM^3 database. NRM^3 (Natural Resource Monitoring, Modelling and Management), Nanyuki, Kenya.
- NRM^3 (Natural Ressource Monitoring, Modelling and Management) (2001): Water Abstractions Monitoring Campaign for the Nanyuki River, Upper Ewaso Ng'iro Basin. NRM3, Nanyuki, Kenya
- NRM^3 (Natural Ressource Monitoring, Modelling and Management) (2002a): Water Abstractions Monitoring Campaign for the Burguret River, Upper Ewaso Ng'iro Basin. NRM^3, Nanyuki, Kenya
- NRM^3 (Natural Ressource Monitoring, Modelling and Management) (2002b): Water Abstractions Monitoring Campaign for the Nghushishi River, Upper Ewaso Ng'iro Basin. NRM^3, Nanyuki, Kenya
- Roth, S (1997): Land Use Classification of the Upper Ewaso Ng'iro Basin in Kenya by means of Landsat TM Satellite Data. MSc thesis. Centre for Development and Environment, Institute of Geography, University of Berne
- Schotterer, U. and Mueller, I. (1985): The Use of Isotopes, Hydrochemistry, and Geophysics in Groundwater Research in Laikipia District, Kenya. Laikipia Reports Nr. 4. Institute of Geography, University of Berne
- Semenov, M. A. and Barrow, E. M. (2002): LARS-WG: A Stochastic Weather Generator for Use in Climate Impact Studies. Users Manual, Version 3.0. Rothamsted Research, Harpenden, Hertfordshire, U.K. / Canadian Climate Impacts Scenarios Project, Regina, Canada
- Smakhtin, V. U. (2001): Low flow hydrology: A review. In: Journal of Hydrology Nr. 240, p. 147 – 186. Elsevier.
- Speck, H. (1983): Mt. Kenya Area: Ecological and Agricultural Significance of the Soils – with 2 Soil Maps. Geographica Bernensia. Institute of Geography, University of Berne

- Spreafico, M. (2000): Modellierung hydrologischer Systeme und Prozesse. Lecture script. Institute of Geography, University of Berne
- Sturm, B. (2002): Development and Use of Long- and Short-Term Precipitation Interpolation Models in the Ewaso Ng'iro Basin. MSc thesis, Institute of Geography, University of Berne
- Thenya, Th., Gichuki, F. N., Liniger, H. P. (2001): Managing Wetland Ecosystems. WUA Support Initiative Report No 9. NRM3, Nanyuki, Kenya
- Thomas, M. K. (1993): Development of a Streamflow Model for a Rural Catchment in Kenya. MSc thesis. Cornell University, USA
- USDA SCS (1985): National Engineering Handbook, Section 4 - Hydrology. Washington, D.C.
- Weingartner, R. and Aschwanden, H. (1989): Discharge regimes. Plate 5.2 of the Hydrological Atlas of Switzerland (HADES)
- Wiesmann, U. (1998): Sustainable Regional Development in Rural Africa: Conceptual Framework and Case Studies from Kenya. Institute of Geography, University of Berne
- Zappa, M. (2002): Multiple-response verification of a distributed hydrological model at different spatial scales. PhD thesis. ETH Zürich.

APPENDIX

APPENDIX A: DATA

A. 1. Overview of rainfall data used in the study

A. 1. 1. Gauges

Station	Station ID	GIS code	UTM long	UTM lat	Altitude	reliable yes/no	StartDate
Satima	82	56	278425	9983931	1950	(yes)	01.01.1973
Munyaka	53	31	283658	9980282	2070	(yes)	27.11.1991
NMFGP	59	36	289002	9980504	2195	?	01.01.1957
NMGate	61	38	293829	9981024	2420	yes	01.01.1968
NMMet	62	39	301090	9981442	3050	yes	01.02.1978
NMMoor	58	40	304420	998154	3771	yes	
Teleki	90	63	310446	9981925	4262	yes	01.04.1978
Matanya	44	43	272189	9993443	1840	(yes)	01.03.1986
Nanyuki FS	40	49	293597	9992492	2337	yes	01.01.1989
Nanyuki KAF	57	25	280874	10004724	1860	?	01.01.1971
Ontulili FS	75	48	296238	10002954	2130	?	01.01.1957
Gathiuru FS	17	44	290497	9989256	2330	yes	01.01.1959
Loruku	38	45	286629	9998807	2040	no	01.01.1963
Jacobson	23	46	282215	9995527	1905	no	01.01.1934
Nicolson	66	47	280194	9990523	1950	yes	01.01.1970
Teleswani (NRM)	91	50	309631	10003267	2724	yes	20.03.1992

A. 1. 2. Data periods

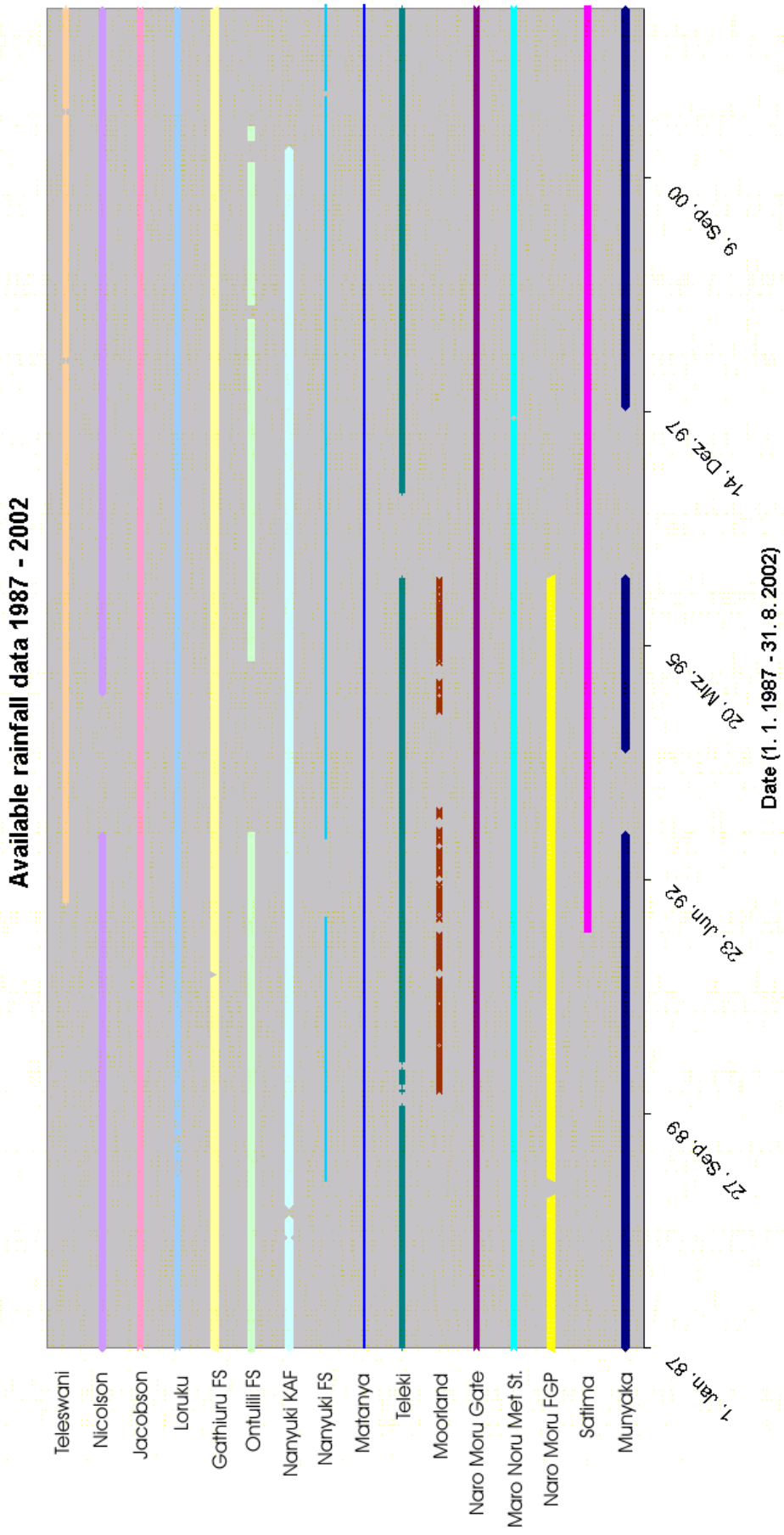

A. 2. Overview of evaporation data used in the study

A. 2. 1. Evaporation pans

Station	Station ID	GIS code	UTM long	UTM lat	Altitude	reliable yes/no	StartDate
Munyaka	53	31	283658	9980282	2070	(yes)	27.11.1991
NMGate	61	38	293829	9981024	2420	yes	12.03.1986
NMMet	62	39	301090	9981442	3050	yes	12.03.1986
Matanya	44	43	272189	9993443	1840	(yes)	12.03.1986
Teleswani (NRM)	91	50	309631	10003267	2724	yes	20.03.1992

A. 2. 2. Available data

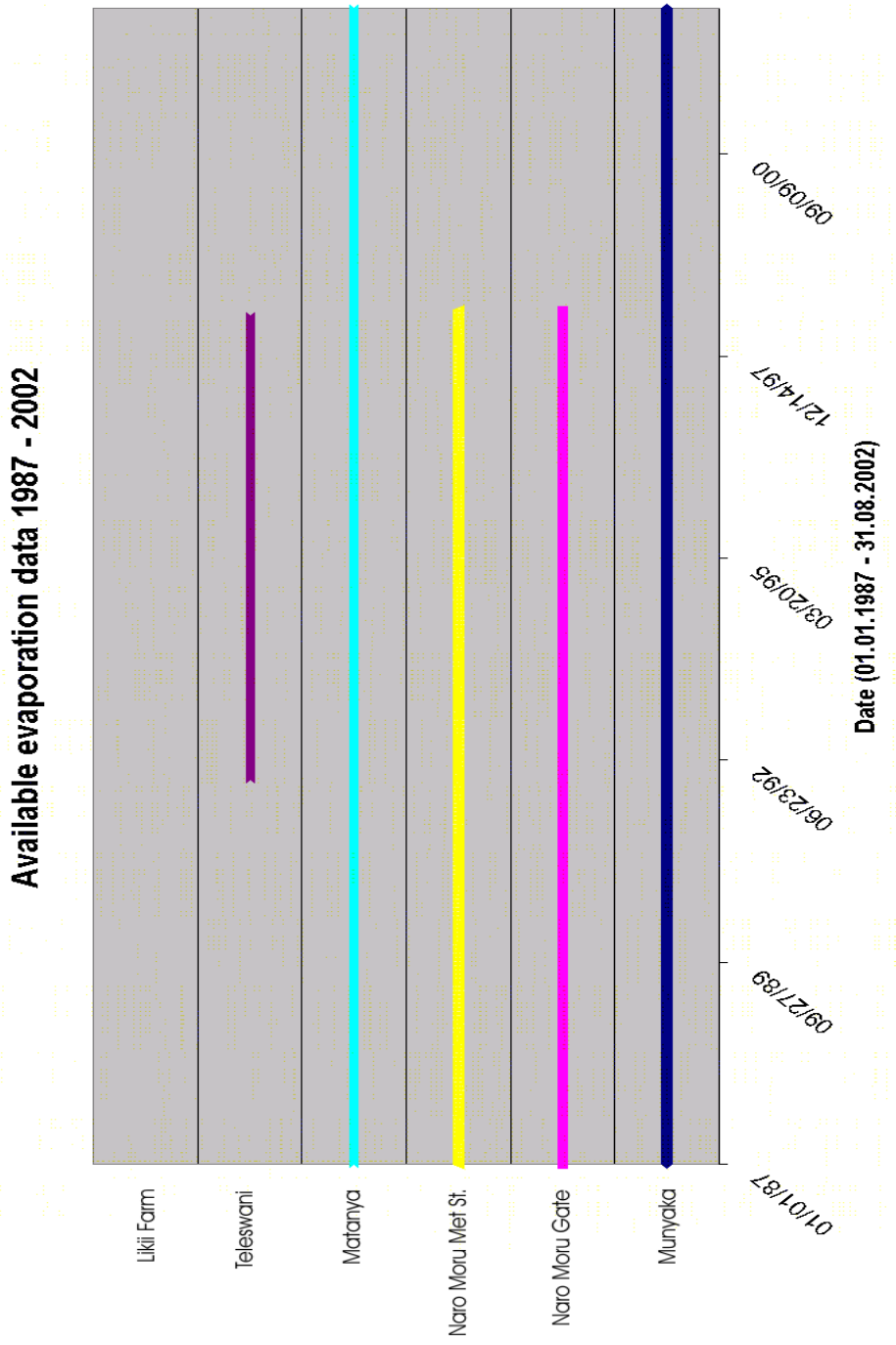

A. 3. Overview of discharge data used in the study

A. 3. 1. River gauging stations

Station ID	Name	MoWD-No.	Area	UTM long.	UTM lat.	Altitude	Operational at present
A1	N.M. ALPINE		5.14	310129	9981754	N. A.	No
A2	N.M. MOORLAND		14.08	304128	9982405	N. A.	No
A3	N.M. FOREST (N)		40.21	291885	9982075	2329	Yes
A4	N.M. FOREST (S)		23.12	289775	9980427	2235	Yes
A5	N.M. FOOTZONE	5BC2	63.34	279555	9982618	1990	Yes
A6	N.M. SAVANNAH		17.22	367553	9994237	1818	Yes
A7	N.M. MWICHUIRI		173.59	279769	9982652	N. A.	No
A8	BURGURET	5BC6	98.87	281477	9987966	1936	Yes
A9	NANYUKI	5BE1	68.37	286208	10002270	1968	Yes

A. 3. 2. Available data

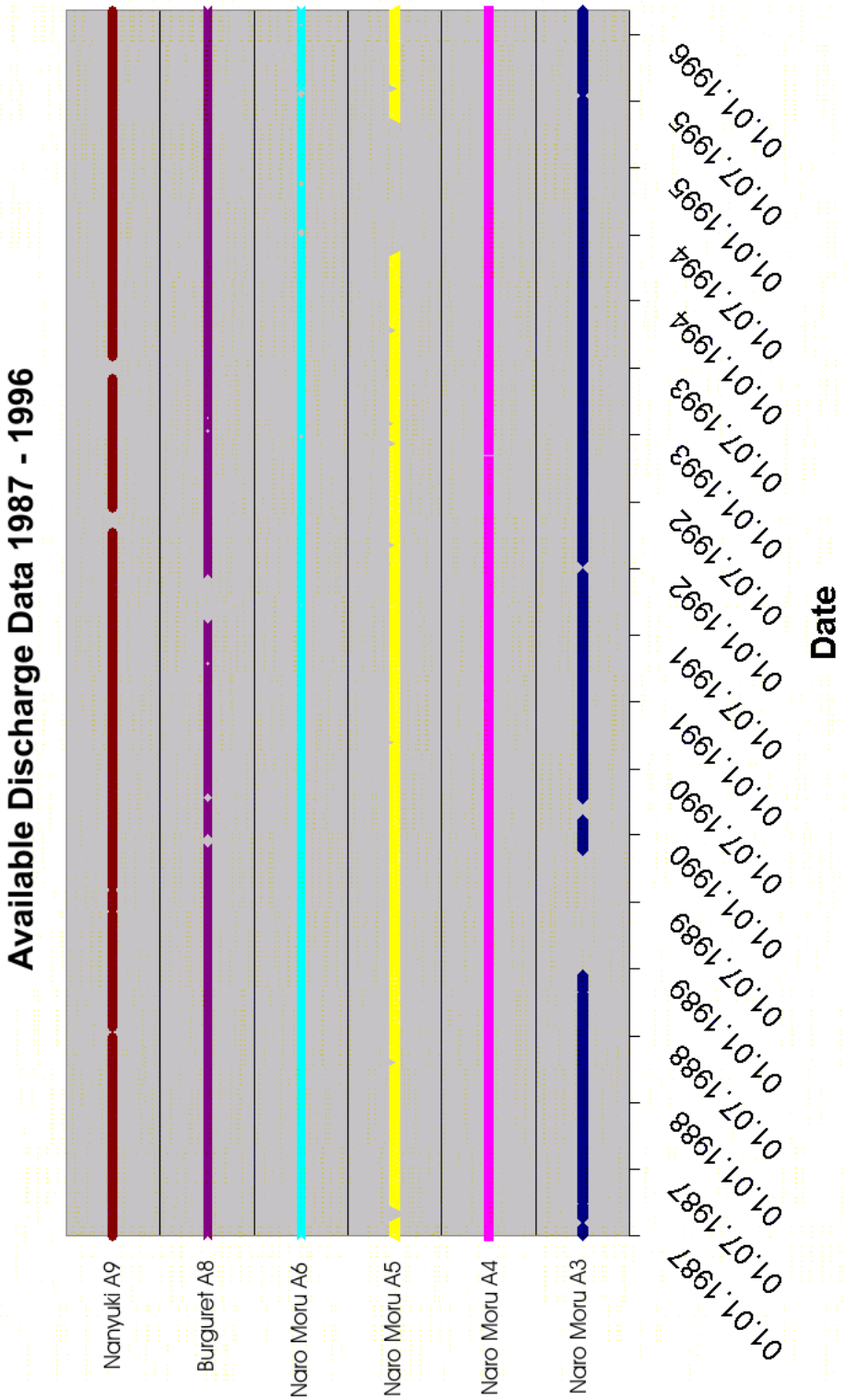

A. 3. 3. Rating equations

Compiled by L MacMillan, NRM[3], September 1997. Version 2a.

LRP	MWLRRD	NAME	Rating	Stage m	Equation	Error	Gaugings Used	Application
A0	5E3	Archers Post	A	≥ 0.0	$Q = 66.5426(H+0.021)^{1.8735}$	0.06748	7/3/58-1/10/92	7/3/58 - date
A1	n/a	Naro Moru	A	≥ 0.0	$Q = 0.8239(H-0.058)^{1.0181}$ *logged 'ghts' pre-2/10/95 must be inverted	0.04698	27/7/82-11/1/91	1981- date*
A2	n/a	Naro Moru	A	≥ 0.0	$Q = 1.6304(H+0.078)^{4.863}$ *logged 'ghts' pre-2/10/95 must be inverted	0.03965	23/11/81-24/11/94	1981-date*
A3	n/a	Naro Moru	A	≥ 0.0	$Q = 18.1176(H+0.079)^{3.6485}$ *logged 'ghts' pre-29/8/95 must be inverted	0.07838	25/5/81-18/10/95	1981-date*
A4	n/a	Naro Moru	A	≥ 0.0	$Q = 6.1291(H-0.05)^{2.6446}$ *logged 'ghts' pre-29/8/95 must be inverted	0.05105	8/11/84-18/10/95	1981-date*
A5	5BC2	Naro Moru	A	≥ 0.00	$Q = 15.973(H+0.012)^{1.762}$	0.06869	30/4/48-12/11/82	30/4/48-25/4/83
			B	≤ 0.10	$Q = 36.4200(H-0.0)^{2.374}$	n/a	18/5/83-8/4/94	26/4/83-17/5/95
			B	0.10<H≤0.30	$Q = 19.8976(H-0.033)^{1.8001}$			
				> 0.30	$Q = 14.3615(H-0.07))^{1.4035}$			
			C	≥ 0.00	$Q = 8.1040(H-0.039)^{2.5616}$	0.03125	5/10/95-28/10/95	18/5/95 - date
A6	n/a	Naro Moru	A	≥ 0.0	$Q = 2.3292(H+0.076)^{1.6767}$	0.15707	3/3/82-3/11/95	3/3/82 - date
A8	5BC6	Burguret	A	≤ 0.3	$Q = 5.3567(H-0.031)^{1.2959}$	0.07362	30/4/48-26/10/95	30/4/48-date
				> 0.3	$Q = 11.929(H-0.056)^{1.7692}$			
A9	5BE1	Nanyuki	A	≤ 0.56	$Q = 2.4322(H-0.003)^{1.4923}$	0.05332	14/4/50-10/6/92	14/4/50-5/6/93
				0.56<H≤1.30	$Q = 6.8644(H-0.06)^{2.7791}$			
				≥ 1.30	$Q = 7.5500(H-0.06)^{2.325}$			
			B	≤ 0.21	$Q = 15.30(H-0.0)^{2.325}$	n/a	8/4/94-29/11/95	6/6/93 - date
				> 0.21	$Q = 13.42(H-0.102)^{1.573}$			

A. 3. 4. Monthly average query

This Microsoft Access Query was used for the determination of average monthly abstracted river water amounts.

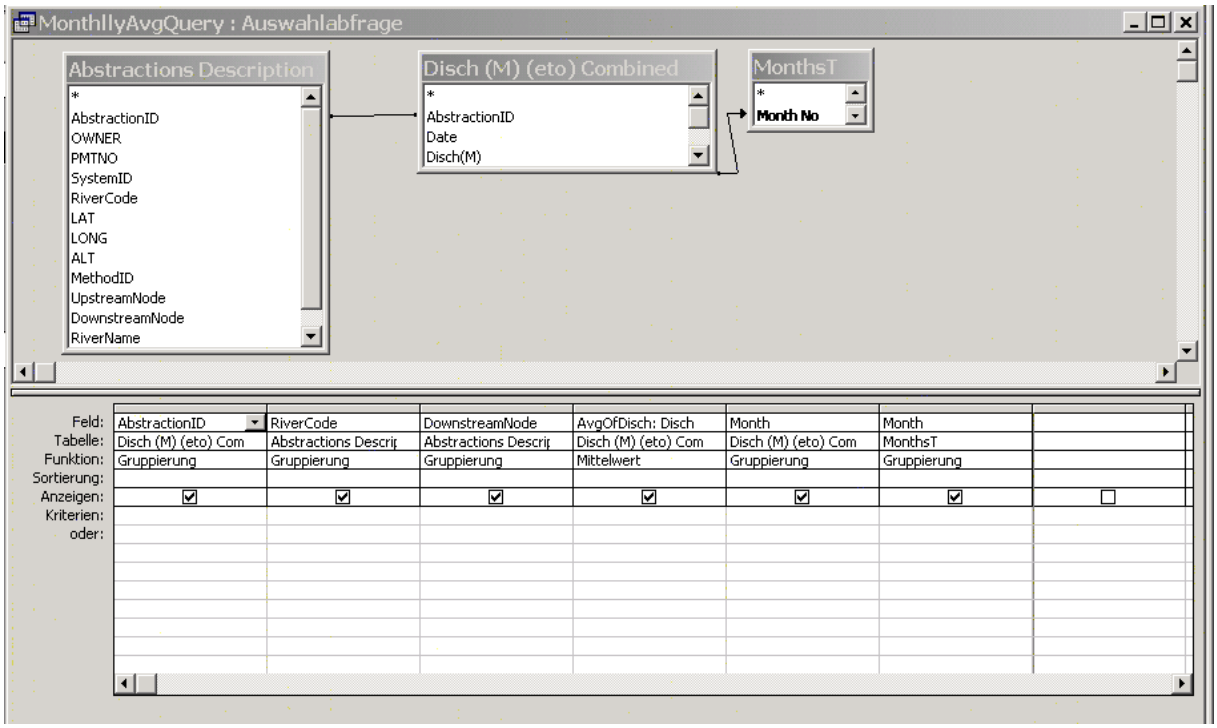

A. 4. Soil categories and associated parameters

Soil category	Depth [mm]	Max. plant avail.water [mm]	cracking soil	GIS ID
eut.Leptosol, lithic, rudic phase	150	9	n	1
eut.Leptosol, lithic, rudic phase	400	36	n	2
chr.,ferr. Lixisol, eut.,chrom.Cambisol	700	70	n	3
chr.,ferr. Lixisol, eut.,chrom.Cambisol	1800	227	n	4
chr.,ferr. Lixisol, eut.,chrom.Cambisol	500	62	n	5
chr.,ferr. Lixisol, eut.,chrom.Cambisol	800	107	n	6
chr. Lixisol, vert. Luvisol	1500	213	n	7
eut. Fluvisol	1800	227	n	8
hap., ando.,luv. Phaeozems	1800	277	n	9
luv. Phaeozems	500	69	n	10
verto.-luv. Phaeozems, eut. Vertisol	1500	221	y	11
gleyic soils, Fluvisols	800	86	n	12
ferr.Luvisol, badly eroded	500	69	n	13
ferr.Luvisol	1500	235	n	14
Gleysols, Histosols	1800	264	n	15
chr.Cambisols, chr. Luvisols, Regosols	600	79	n	16
vertic Luvisols	1200	185	y	17
calc. Cambisols, calc, Luvisols	800	105	n	18
Calcisols, Cambisols	1200	145	n	19
eut., vert. Cambisols	1500	221	n	20
eutric Planosols	1500	221	n	21
luvic Phaoezems/Humic Alisol/Acrisol	1200	187	n	22
humic Acrisols, dystric Regosols, dystric Gleysols	800	118	n	23
dystric Nitosols, humic Nitosols	1800	274	n	24
humic Acrisols	1500	223	n	25
complex mixtures of 22 and 24	1000	170	n	26
humic Andosols	800	132	n	27
dystric Histosols, partly humic Andosols	700	70	n	28
Rankers, dys Regosols, hum Andosols, hum Gleysols	400	38	n	29
humic Andosols, partly distric Histosols	750	107	n	30
hum Andosols, dys Regosols, partly dist Histosols	400	40	n	31
dystric Histosols, humic Andosols	800	78	n	32
Rankers, dystric Regosols, humic Andosols	800	78	n	33
Rankers, dystric fluvisols, dystric and humic Gleysols	700	74	n	34
dystric Regosols, Lithosols, Rankers	250	29	n	35
Lithosols, dystric Regosols	100	10	n	36

(Source: McMillan 2003)

A. 5. Land cover categories and associated parameters

ID	Class	Curve numbers for median conditions on SCS soil groups A - D				depth [mm]	root depth [mm]	Interception [mm]	kc	Prone to crusting (Yes/No)
		A	B	C	D					
1	Td	18	47	57	65	400	3000	3.6	1.1	N
2	TPd	18	47	57	65	400	3000	3.6	1.1	N
3	Go	25	55	70	77	300	3000	1.6	1.1	N
4	TG	35	59	73	79	230	2300	1.5	1.1	N
5	tG	38	60	74	80	210	2100	1.2	1.1	N
6	TGs	46	69	81	87	195	2300	0.8	0.7	Y
7	tGs	52	73	84	90	165	2100	0.6	0.6	Y
8	tGb	69	82	90	93	120	2100	0.2	0.4	Y
9	G	39	61	74	80	200	2000	1.1	1	N
10	Gb	74	85	92	95	100	2000	0	0.3	Y
11	C	58	72	81	85	250	1200	1.2	0.8	N
12	Cg	61	73	81	84	200	1200	1.4	0.8	N
13	Cf	74	83	87	90	200	1200	0	1	N
14	tC	55	70	80	84	255	1400	1.3	0.8	N
15	tCG	51	68	79	83	245	1500	1.2	0.9	N
16	R	72	82	87	89	100	100	0	0.7	N
17	tRG	61	75	83	86	140	800	0.4	0.8	N
18	I	72	82	87	89	100	100	0	0.7	N
19	W	95	95	95	95	3000	3000	0	1	N
20	U	74	84	90	92	100	500	0	0.7	N

(Source: McMillan 2003)

APPENDIX B: FIELD WORK

B. 1. River Profiles Checklist

Checklist used for the recording of information at the river profile points.

River Profiles Checklist

Date		
Team		
River		
No. of measuring point (uppermost on river = 1)		
GPS Reading 1	Lat	Long
GPS Reading 2	Lat	Long
Altitude		
Photo Film No.		
Photograph No.		
Electroconductivity		
Temperature		
Sample No.		
Current Meter Reading		
Discharge		

Draft of river cross-section:

B. 2. Current meter gauging sheet

Sheet used for the infilling of information during the current meter gaugings.

REPUBLIC OF KENYA — W.D. 480A

HYDROLOGY SECTION

CURRENT METER GAUGING (MID-SECTION METHOD)

NAME OF OBSERVER .... Date .... 19 ....

RIVER .... DRAINAGE AREA .... STATION (*See* Notes) ....

METHOD (Strike out where not applicable): Wading, boat, cableway, bridge (down or up-stream face) ....

METER: Make .... W.D.D. No. .... Prop. No. .... Weight .... kg.

TIME OF STARTING .... Time of Finishing .... Initial Point ....

GAUGE HEIGHT: at Start .... at Finish .... MEAN ....

NOTES.—(1) If discharge is not taken on line of standard section, state actual site below.

(2) If discharge taken at a site other than a regular gauging station, describe position of discharge site, give Lat. and Long. and number of cadastral sheet or other full description.

....

....

MEANS AND TOTALS

AREA .... sq. m. MEAN VEL. .... m./sec. G.Ht .... DISCHARGE .... cumecs.

Dist. from Initial point	Depth	Width	Area	Discharge	Velocity		Time Secs.	Revs.	Depth of Observation from Surface	Remarks
					Mean in vertical	At point				
	TOTAL ..									

Sheet No. .... *of* .... *Sheet Comp. by* .... *Check by* ....

B. 3. Rainfall data record sheet

Sheet used for the infilling of the rainfall data at the respective gauges.

LAIKIPIA RESEARCH PROGRAMME
P. O. BOX 141 NANYUKI Tel (0176)-22574

RAINFALL OBSERVATIONS AT Marula (Ol Jogi Farm) ..... FOR THE YEAR ~~19~~ 2000
METEOROLOGICAL No. .....
RECORDED BY .....

Day	Jan	Feb	Mar	Apr	May	Jun	Jul	Aug	Sep	Oct	Nov	Dec	Day
1													1
2													2
3													3
4					14,5		7,5						4
5					5,5								5
6					5								6
7											7,5		7
8								20		9			8
9								13		2,5			9
10					9								10
11						8,5						2	11
12								76					12
13								1,5					13
14													14
15									3				15
16					2			6				5	16
17												8,5	17
18								11					18
19								5			4		19
20								14,5	2,5				20
21													21
22							22						22
23											20		23
24								9,5			2		24
25								2,5					25
26						8,5		2,5			2		26
27				2									27
28													28
29													29
30							1						30
31							1						31
1 st of	Feb	Mar	Apr	May	Jun	Jul	Aug	Sep	Oct	Nov	Dec	Jan	
Total	0	0	0	2	36	17	31,5	161,5	5,5	11,5	28		
#Days													
Avg													

NOTE: 1. Rainfall amounts should be entered on the day of ~~measurement~~ rainfall

Comments: _____

B. 4. River profiles data

Data gathered during the profile measurements on Naro Moru, Burguret and Nanyuki, and the springs measured for comparison.

River/Water Body	Date	Time	Description	Discharge [l/s]	Electric Conductivity	Temperature	Turbidity	Altitude	UTM Lat.	UTM Long.
Naro Moru North	26.07.02	08.30	60m upstream A3	85.1	40.9	8.8	2.36	2329	9982047	292056
Naro Moru South	26.07.02	09.45	40m downstream A4	62.1	34.3	10.4	2.205	2235	9980482	289755
Naro Moru North	26.07.02	11.40	above confluence with NM South	14.8	46.8	16.3	67.5	2137	9980671	286430
Naro Moru South	26.07.02	12.20	above confluence with NM North	39.2	37.3	15.8	3.68	2116	9980598	286464
Naro Moru	26.07.02	13.00	70m downstream confluence NM North/South	*54*	39.3	17.1	1.8	2134	9980529	286232
Naro Moru	26.07.02	14.00		29.3	60.4	20.7	21.39	2082	9980129	284402
Naro Moru	26.07.02	15.15		34.8	72.0	20.6	10.1	2066	9980644	283457
Naro Moru	26.07.02	16.05		28.1	85.6	17.4	22.01	2045	9981405	282088
Naro Moru	26.07.02	16.45	A5 (below small bridge)	38.4	91.9	19.3	71.5	1990	9982498	279601
Naro Moru	27.07.02	08.55	A5 (below small bridge)	(gauge height 17cm)	93.6	13.5	N. A.	1990	9982498	279601
Naro Moru	27.07.02	09.30	Satima Farm	23.9	97.4	14.2	8.275	1945	9984094	278465
Naro Moru	27.07.02	11.05	railway bridge	21.3	105	16.3	6.08	1911	9985548	275801
Naro Moru	27.07.02	11.55		0	*128*	*15*	12.22	1890	9987418	274603
Naro Moru	27.07.02	12.30		0	*185*	*14.5*	85.5	1878	9989341	272844
Naro Moru	27.07.02	13.45	upstream Matanya Bridge	*1*	236	19.0	5.7	1841	9992820	270420
Naro Moru	27.07.02	14.55	Matanya Bridge	*1*	245	23.6		1834	9993219	270298
Naro Moru	27.07.02	14.15	A6	0	275	17.8	27.9	1818	9994330	267804
Waguziru	20.08.02	9.30	Tributary to Burguret	*max. 0.5*	*225-230*	14.5	N. A.	2296	9984871	290605
Burguret North	20.08.02	9.55	upstream from Bridge	159.2	30	11.4	7.835	2243	9986677	291315
Burguret South	20.08.02	10.55	underneath bridge	51.2	31.2	12	14.85	2265	9985430	290418
Burguret			addition of 1A and 1B	*210.4*						
Burguret	20.08.02	12.00		244.1	33.8	12.9	3.505	2112	9986890	287696
Waguziru	20.08.02	14.10	before confluence w/ Burguret	3.8	366	19.1	N. A.	1980	9987378	282253

Burguret	20.08.02	16.15	upstream of confluence w/ dry tributary	195.2	35.0	15.5	2.85	*2065*	9986998	285218
Burguret	20.08.02	17.45	upstream of Tarmac	171.2	64.7	17.1	4.425	1936	9988195	281468
Burguret	21.08.02	8.15	A8		63.9	15.1				
Burguret	21.08.02	8.40		160	70.7	15.9	8.67	1881	9991038	278957
Burguret	21.08.02	9.20		143.8	72.4	16.4	11.09	1872	9991711	276348
Burguret	21.08.02	10.15	underneath railway bridge	152	74.1	17.1	12.82	1856	9992468	274989
Burguret	21.08.02	12.30		134.1	77.7	19.4	20.94	1840	9994530	273471
Burguret	21.08.02	13.45		113.5	84.5	19.7	34.81	1832	9997518	271992
Rongai	21.08.02	16.00	before swamp	9.8	99.3	21.5	187	1829	9999409	271540
Burguret	21.08.02	14.45	before confluence w/ Ewaso Ng'iro	67.7	79.5	22.0	125.0	1803	647	268068

Nanyuki	22.08.02	8.20	upstream of confluence w/ tributary		35.5	10.6	N. A.	2327	9991742	294583
Nanyuki	22.08.02	8.50	downstream of confl. w/ tributary	204.4	37.5	11.9	0.61	2254	9992966	292663
Nanyuki	22.08.02	10.25	downsteam of intake gravity pipe	138.8	37.5	13	0.83	*2237*	9993706	291741
Nanyuki	22.08.02	11.15	upstream of bridge	88.4	37.7	14.6	2.74	2135	9995918	290136
Nanyuki	22.08.02	12.30		139	41.1	18.6	2.855	2051	9998311	287780
Nanyuki	22.08.02	13.35	upstream of bridge	95.7	44.4	18.6	2.28	1994	9999932	286107
Nanyuki	22.08.02	14.35	between tarmac and A9	60.4	47.4	19.8	3.91	1968	2126.5	286168
Nanyuki	23.09.02	9.00	20m above "No. 6"	23.7	69	14	27.26	1949	2088	286174
Nanyuki	23.09.02	9.45	near "Hilde's Place"	17.9	86.5	14.4	17.98	1916	4347	284470
Nanyuki	23.09.02	10.30	Above confluence w/ Likii River	21	211	14.5	25.7	1869	7348	283188
Likii	23.09.02	11.05	Above confluence w/ Nanyuki River	200.8	75.6	16.3	5.45	1885	7340	283501
Nanyuki				221.8						
Nanyuki	23.09.02		~200m below confluence w/ Likii River		90.5	16.1				
Nanyuki	23.09.02	12.45		211.6	73.6	17.1	7.83	1818	12656	281148

Nanyuki	23.09.02	14.50		253.5	81.2	17.3	3.96	1815	14787	280736
Nanyuki	23.09.02	15.40	Above confluence w/Timau River	156.1	78.7	17.5	10.7	1782	16330	280665
Timau	23.09.02	16.10	Above confluence w/ Nanyuki River	167.4	157	16.8	252.5	1787	N. A.	280771
Nanyuki	23.09.02		Station 5BE20	347 l/s (Gauge height = 101cm); Addition 13A+13B=323.5	116	17.1				

Borehole Satima Farm	27.07.02	10.30	Satima Farm		301	25.5		1957	9983896	298383
Mureru Springs	30.07.02	09.15	Burguret Catchment	*8.5*	400	20.6		1986	9986342	280938
Karichota Spring	30.07.02	09.40	Burguret Catchment	*2.5*	303	21.1		2014	9985996	283864
Burguret Springs	30.07.02		Burguret Catchment	*very little*	*562*	22		1948	9990218	282571
Ragati Spring	30.07.02		Burguret Catchment	*0.5*	760	20.5		1959	9992204	283723

APPENDIX C: NRM^3 STREAMFLOW MODEL DESCRIPTION AND TOOLS

C. 1. Model subroutines

(Source: McMillan 2003)

PROGRAM STREAM1

STREAM1 Main calling program for model

- **CONTROL** Reads in control file information; files and run parameters
- **CATCH** Derives a single array within the entire space denoting cells within the catchment
- **ELEVS** Reads in elevations from coverage file
- **RAININST** Reads in rain gauge information from coverage file
- **RAINWGHT** For each cell calculates the nearest two rain gauges and their weights
- **EVAPINST** Reads in pan evaporation gauge information from coverage file
- **EVAPWGHT** For each cell calculates the nearest three evaporation pans
- **COORD** Returns (row,col) IDRISI coordinates from single array position
- **DRNET** Reads in drainage network from coverage file
- **ELEVCHK** Checks elevation array to ensure all catchment cells have an elevation, if not, assigned
- **FLOWPATH** For each cell returns the position of a neighbouring cell to which flow will go
  - **REFER** Returns the single array position in entire space from IDRISI coordinates
  - **DIRECT** For each cell returns the direction of slope
  - **SLFACTOR** Computes SL factor for use in USLE soil erosion model
  - **PTFLCELL** Prints flowcell coverage in GIS format
    PTDOCFL Prints out document file for flowcell GIS coverage
  - **ELEVUP** Updates elevation coverage if changes have been made via screen
- **ORDER** Ranks the cells in order: edge of catchment (flow out only), cells which receive flow, drainage network cells
- **READLCOV** Reads land cover information datafile
- **READSOL** Reads soil information datafile
- **LCOVGIS** Reads land cover type from coverage file
- **SOLGIS** Read soil type from coverage file
- **MAXPAW1** Calculates the maximum plant available water
- **SOILEROD** Computes the soil erodibility factor for the soils of each cell
- **OPENDATA** Opens the rainfall and evaporation datafile and moves to run start date
- **SIMUL** Main routine for simulation of water balance

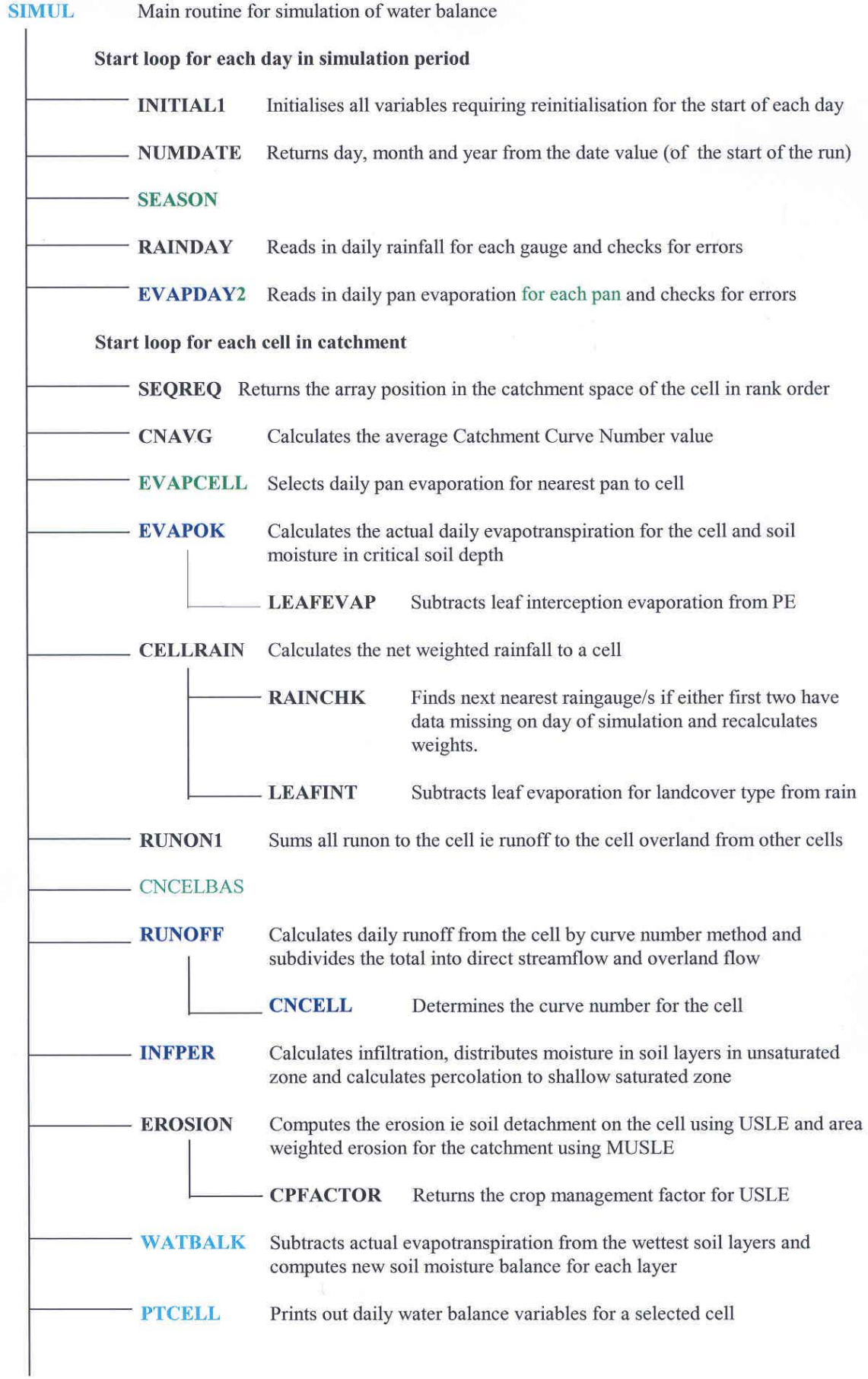
SIMUL
Main routine for simulation of water balance
Start loop for each day in simulation period
INITIAL1
Initialises all variables requiring reinitialisation for the start of each day
NUMDATE
Returns day, month and year from the date value (of the start of the run)
SEASON
RAINDAY
Reads in daily rainfall for each gauge and checks for errors
EVAPDAY2
Reads in daily pan evaporation for each pan and checks for errors
Start loop for each cell in catchment
SEQREQ
Returns the array position in the catchment space of the cell in rank order
CNAVG
Calculates the average Catchment Curve Number value
EVAPCELL
Selects daily pan evaporation for nearest pan to cell
EVAPOK
Calculates the actual daily evapotranspiration for the cell and soil moisture in critical soil depth
LEAFEVAP
Subtracts leaf interception evaporation from PE
CELLRAIN
Calculates the net weighted rainfall to a cell
RAINCHK
Finds next nearest raingauge/s if either first two have data missing on day of simulation and recalculates weights.
LEAFINT
Subtracts leaf evaporation for landcover type from rain
RUNON1
Sums all runon to the cell ie runoff to the cell overland from other cells
CNCELBAS
RUNOFF
Calculates daily runoff from the cell by curve number method and subdivides the total into direct streamflow and overland flow
CNCELL
Determines the curve number for the cell
INFPER
Calculates infiltration, distributes moisture in soil layers in unsaturated zone and calculates percolation to shallow saturated zone
EROSION
Computes the erosion ie soil detachment on the cell using USLE and area weighted erosion for the catchment using MUSLE
CPFACTOR
Returns the crop management factor for USLE
WATBALK
Subtracts actual evapotranspiration from the wettest soil layers and computes new soil moisture balance for each layer
PTCELL
Prints out daily water balance variables for a selected cell

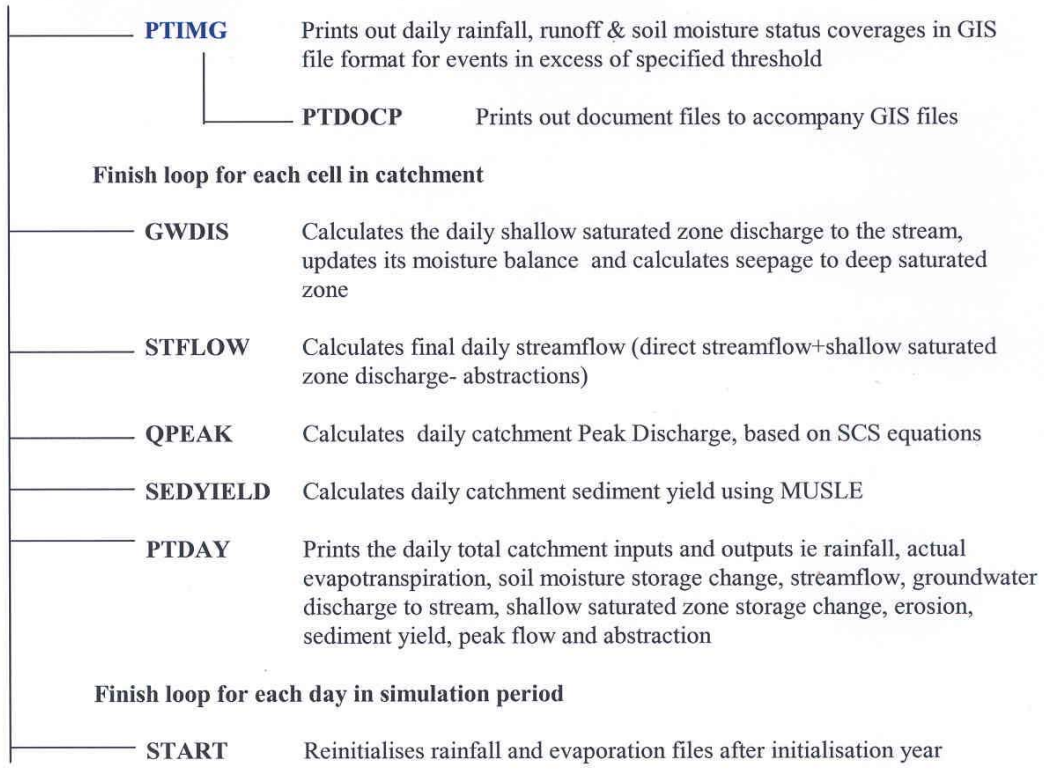

Note: Dark blue routines have major changes from original model version provided by Thomas
Pale blue routines have minor changes from original model version provided by Thomas
Black routines may have very minor changes from original model version provided by Thomas

Lcm/modseqlcmfinvers.doc/7/7/01

C. 2. Running the NRM^3 Streamflow Model: A manual

Software requirements:

Windows/Linux systems
Idrisi16 or Idrisi32
Arc/Info and ArcView, if the GIS database format is Arc/Info
Fortran compiler (Linux: f77)
Dos2Unix text converter (can also be done in UltraEdit)
Microsoft Excel

Brief:

The input files have to be placed together in one folder with the executable file streamlm.exe. Most relevant information has to be entered in the control file (extension .con). Important are mainly the names of the input files; of the parameters the groundwater discharge coefficients are most important to be optimised for a specific catchment, all other parameters can be left the same for the start.
A run is started by double-clicking on the icon of this file or by entering streamlm.exe (in Windows) or streamlm (in Linux) in the command prompt. The program will first ask to enter the name of the control file. Then it checks the input files before starting the actual simulation. If sink cells are identified press "Enter" (in Windows) or type go (in Linux) to continue.

Required files:

The NRM^3 Streamflow Model needs the following input files in order to be run:
(Note: There are two model versions – stm2ci and stm4d, the latter incorporating dynamic curve numbers accounting for long-term moisture status of the seasons. The difference in simulation is minimal).

a) The control file

This file has the extension .con; its name can be set by the user (8 characters). It contains all information associated with a specific run, ie the parameters and the names of the input files.
Note: The control file is a little different in the two model versions. In the version stm4d a part is added at the bottom which refers to the season .prn file and the curve numbers that have to be altered.

b) Meteorological time series input files:

- Daily rainfall
- Daily pan evaporation
- Model version stm4d: season status file (how to produce it is described in chapter 4 of Lindsay McMillans thesis)

The files have to be in the .prn format and are produced the easiest in Excel and then saved as .prn files.

Note:

- ➔ The Date column has to be formatted as MM/DD/YY
- ➔ The model does not recognize the millennium change; the years after 2000 will be recognized as 1901, 1902, etc. It is not possible to model periods that contain the millennium change, but one can alter the year values of the dates (take care with the leap years!)

➔ The rain and evaporation data have to be formatted in Excel as numbers with (at least) one digit after the point.
➔ If a meteorological time series input file contains a row of data from a station that is not included in the GIS station file, errors will result
➔ For runs on Linux, the data have to start on the sixth row (error warning when not)

b) Soil and Land Use input files
- soil input file
- land use input file

These files have the extension .gen and contain information associated with each soil and land use type (Curve Number, soil depth, etc).

c) GIS input files (refer to GISSteps.doc):
- catchment area
- elevation
- drainage
- land cover
- soils
- rain gauges
- evaporation pans

These files are required to be in the Idrisi16 raster format, so there is a .doc and an img. File for each coverage. The extents and the resolution have to be the same in all files. Filenames have to be 8 characters long.

d) The executable file streamlm.exe (or streamlm in Linux)

e) The empty but essential file temp.req

Output files

A model run will produce the following output files:

a) Text files
- Runname1.out (name can be specified in the control file)
- Cellxxxx.out (name can be specified in the control file)

These files contain columns of values of the daily water balance, the first one for the whole catchment, the second one for a single cell whose location is also specified in the control file. The column containing the simulated discharge values is the one called STORMFLOW in the catchment file.

➔ It is recommended to analyse outputs in Excel spreadsheets. An analysis spreadsheet called StreamflowAnalysis.xls for the calibration and verification in the Ewaso Ng'iro Basin has been prepared and can be used for other applications as well. For its usage refer to its first table (Contents) (just take care of the Feb 29th's when going to other time periods).

b) GIS output files:
- 1cnkbase: base curve number from soil and veg overlay
- 1cnkf001: final curve number on a given day
- 1flow001: runoff on a given day
- 1pawe001: plant available water in the critical soil depth on a given day (at the start of the day)

- 1paws001 – soil moisture status on a given day
- 1rain001: rainfall on a given day
- 1flowcell: flow directions for runoff

1cnkbase and 1flowcell are produced in every model run. The rest of the output files is produced for every day that the rainfall at one station exceed PTRESH (can be set in the control file, line 53).

NOTE FURTHER:

- The maximum number of GIS coverage cells, rain and evaporation gauges used, soil and land use types etc. is specified in parms.for (model code file). If the model does not work it may be that one of these numbers is exceeded. In this case alter the number in parms.for and recompile the program (refer to RunLinux.doc). The maximum number of rain gauges also occurs in the file rainday.for on line 21 (comment) and 24.
- Never open and save an Idrisi .doc file in Word; it is actually a text file and Word will add some formats to it that make it unreadable for Idrisi.

C. 3. Running the NRM^3 Streamflow Model under the LINUX system

When running the NRM^3 model with large arrays of cell sizes (for example Naro Moru catchment in a resolution of 100 or 50 m) the compiling capacity of standard Windows Fortran Compilers is exceeded. So the model needs to be run in the LINUX operating system. The following steps have to be carried out in order to do so.

Required software:	KDE/LINUX
	Gcc (Linux fortran compiler)
	Dos2Unix/Unix2Dos (text file converter)
Optional:	Emacs (LINUX text editor)

1. Before compiling the model codes in LINUX, all input files have to be run through the Dos2Unix program in Windows with the command

    Dos2unix <file-name>

This converts the CR/LF line ending in DOS files into the LF only which is used in UNIX.
Alternative way: In case a file is not converted and one is already in LINUX, it can also be done in the editor XEmacs.
To open a file in XEmacs, type the following command in the command line

    xemacs <file-name>

Then in XEmacs, type

    Ctrl + x, enter, f

"File coding system" will be displayed. Choose "undecided Linux" by clicking on it with the middle mouse button.

2. The file parms.for has to be modified when one moves to larger cell arrays so that the
    Number of cells in space
    Number of cells inside catchment
    Number of rain gauges
    Etc.
indicated in this file are equal or greater than the real number of these parameters used in the simulation. (If this is not the case, the program will return the dialog "segmentation problem" when opening the first GIS input file.)
An easy way to count the cells is for example the command

    wc –l <file-name> (means "word count, lines") or
    grep 5 <file-name> ¦ wc –l

3. The maximum number of rain gauges that can be included is also hardcoded in the routine rainday.for. The number in line 24, cols 29/30 (set to 14 in the version received by LCM) has

to be changed to be equal or greater than the number of rain gauges used. Also the comment in line 21 should be changed.

4. Now the source codes can be compiled using the command

```
f77 -o streamlm streamlm.for –lm
```

of which action the executable file streamlm will result.

5. After this, the model can be run by typing the command

```
streamlm
```

Alternative: If a model run has to be repeated because of problems, all outfiles that have already been written have to be removed again from the folder that the model is being run in. The linux shell run.sh (currently in: /home/notter/run/a65001) automatically removes all outfiles and initialises a new model run. It is called by typing

```
run.sh
```

Observe the following details:

- In LINUX it does matter whether a command or a filename is written in capital letters or not. Thus the filenames indicated in the control file and the real filenames have to correspond in this way also
- A model run can be interrupted typing Ctrl + c
- When starting a new run in the same directory that was used before, all output files have to be removed, otherwise the program will ask you to specify a new name for the run (which is not fatal but may not be your wish). This can easily be done using the command

  ```
  rm –f *.out flowcell.* 1cnkbase.*
  ```

  (which means all files with the ending .out and all files of all types called flowcell will be removed). This step is included in run.sh.

C. 4. Preparing the GIS input layers for the NRM^3 Streamflow Model

Required GIS software: Arc/Info
ArcView
Idrisi32

1. Base layers are stored in the **Arc/Info** format in the CDE database in:

P:\Kenya\laikewas\GIS\	hydro:	ewaswsh0 – catchment boundaries
		laikriv050 – drainage network
	climate:	ewasrnf1 – rainfall and ET stations
	topo:	ewasdtm050 – terrain model
	soil:	ewassot1 – soil types
	land:	ewaslco95

2. The vector layers have to be converted to grids using the command

```
Arc: Polygrid <in-cover> <out-grid> {value-item}          or
Arc: Linegrid <in-cover> <out-grid> {value-item}          or
Arc: Pointgrid <in-cover> <out-grid> {value-item}
```

The value item assigned to the grid cells has to be specified especially for the soil map: there it has to be "lcmped". For the other coverages it is not necessary.

A dialog will ask for the resolution of the resulting grid (here in meters). The grids, if they are not in the resolution wanted, have to be resampled. This can be done in the GRID module of Arc/Info with the command:

```
Grid: <out-grid> = resample (<in-grid>, <cell-size>)
```

3. The extent actually needed (has to be the same for all layers) has to be cut out with the command

```
Arc: gridclip <in-grid> <out-grid> <x1> <y1> <x2> <y2>
```

4. In **ArcView** (set the spatial analyst as extension) the grids have to be converted to the .flt interchange format using File -> Export Data Source -> Binary Raster. For each layer there should be now at least an .flt and a .hdr file (for some there is also a .prj file)

5. Now all the .hdr files have to be opened with an editor and the x/y corners corrected, because they may be a little offset after the above conversions (but have to match exactly in order to run the model).

6. In **Idrisi32** the files have to be imported with File -> Import -> Software-specific formats -> ESRI -> ArcRaster. They will be saved as .rst files (+ one .rdc for each)

7. If categories have to be reclassified, it can be easily done with the button "reclass" in Idrisi32. This has to be done for the catchment boundary layers and maybe the land cover & soil layers. In- or excluding rainfall/evaporation stations can also be done this way, or later by manually adding or removing the station ID's in the .img files.

a) This has to be done for the **catchment boundary** layers. For example, for the catchment boundary layer of A5, the areas belonging to A1 – A5 (which have the values 17 – 22 in the original layer) have to be classed together with the value 5, and the rest of the map has to be zero (value inside catchment has to be identical with "catchment ID" in the control file!).
b) The **Land Cover type** values have to correspond to the ones in satveg.gen. They can either be reclassed in Idrisi32 or the satveg.gen file can be altered.
   Note: The 1988 and the 1995 land use map do not use the same categories! The following list contains the values associated with each category in both maps. The 1988 categories are the ones also currently used in the model. See Appendix A for a listing of these categories ("Land Use classes and associated parameters" → ID) Similarly, the **soil cover type** values have to correspond to allsol.gen. Here nothing has to be changed, though, since there is only one land use map in the database that was also used as basis for allsol.gen.

   For convenience, the reclassification scheme can also be saved as an .rcl file in Idrisi32, so if more than one layers have to be treated the same way, it has to be written only once, then saved and used again. The proceeding in Idrisi is self-explanatory.

8. With Reformat -> CONVERT the files have to be converted from binary file type to ASCII file type

9. With File -> Idrisi File Conversion 16/32 the ASCII files have to be converted to the (older) Idrisi for Windows (16bit) format. The result should be a .doc and an .img file for each layer. Note: to run the model, the names of the GIS input files need to be exactly 8 characters long.

10. The rain and evaporation layers have to be modified further so that the gauges with their ID correspond in the rainfall input file and the GIS files. Note that the ID's of the NRM3 Access database and not the ones in the CDE GIS-database are used!
If rainfall/evaporation stations have to be edited or added, it can be done directly by opening the .img-file with an editor that shows the line numbers. This (ASCII) file contains a single column of numbers, most of which are zero, and the rest are the rain/ET gauge ID's. To add a rain gauge, it's position in this array (the line number) has to be determined. It is calculated the following way:

$$Icol = (Xrg - X1)/R$$
$$Irow = tROW - [(Yrg - Y1)/R]$$
$$AP = (Irow - 1)*tCOL + (Icol - 1)$$

with Coordinates of rain gauge: Xrg, Yrg
Lower left corner of map: X1, Y1
Resolution of grid: R
Total Rows in map: tROW

Total Columns in map: tCOL
Row/Column no. of rain gauge in map: Irow, Icol
Final Array Position/Line number in .img file: AP

Then simply the ID of the station has to be placed in the correct AP/line number; if a new ID exceeds the max. value indicated in the .doc file, then it has to be adapted too.

C. 5. GIS input layers (example: Naro Moru A5 catchment in 500m resolution)

Catchment boundaries

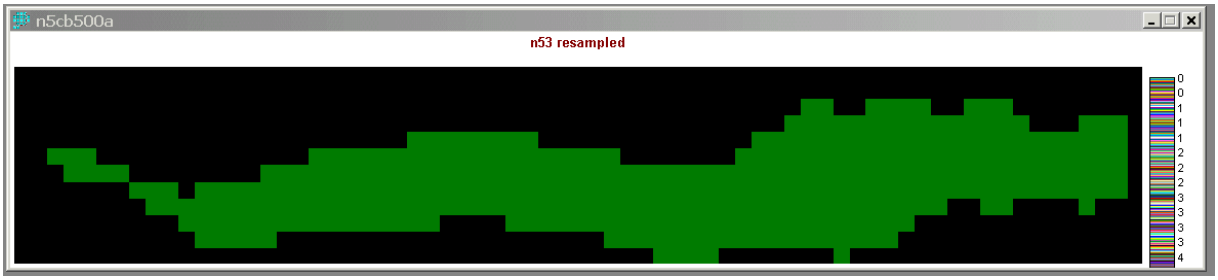

Elevation/Topography

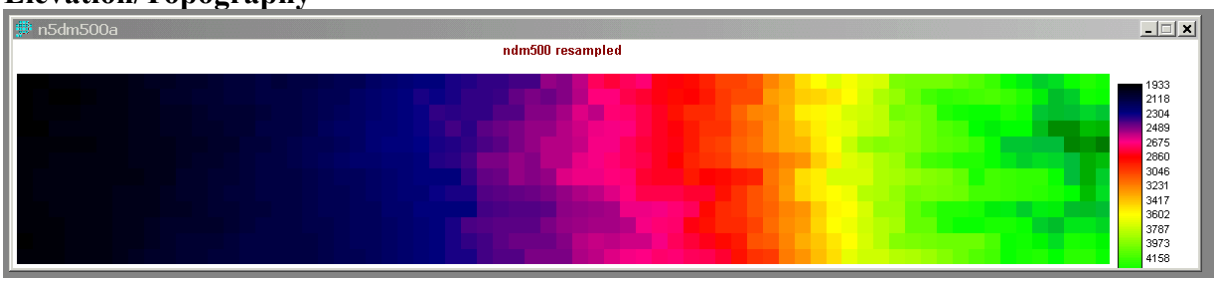

Drainage network

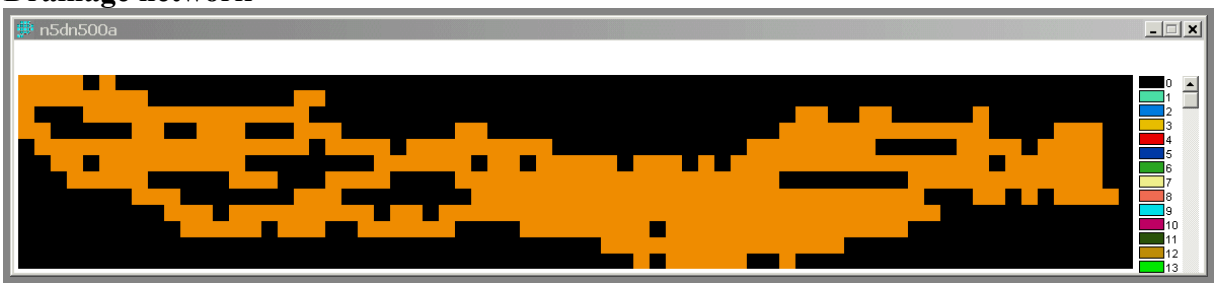

Evaporation pans

Rain gauges

Soil types

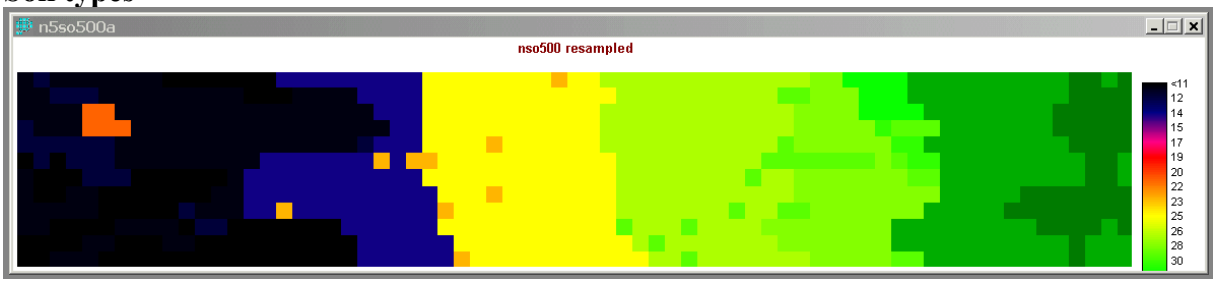

Land Use/Vegetation cover

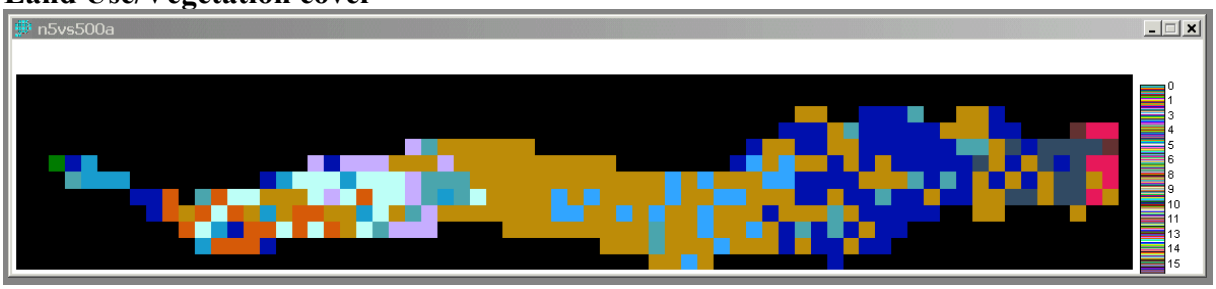

C. 6. GIS output files (example: Naro Moru A5 in 500m resolution)

Base Curve Numbers

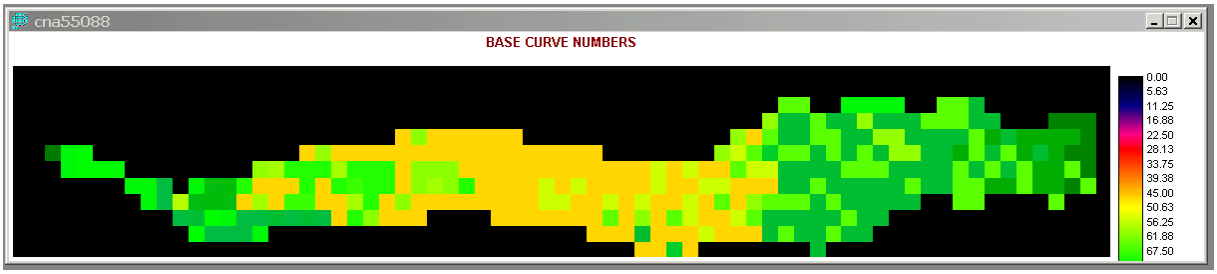

Flow Directions

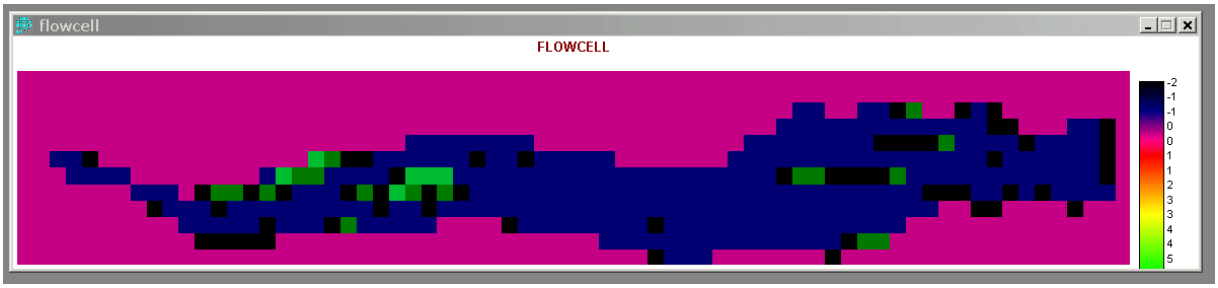

Final curve number on a given day (when rain of 1 station exceeds PTRESH)

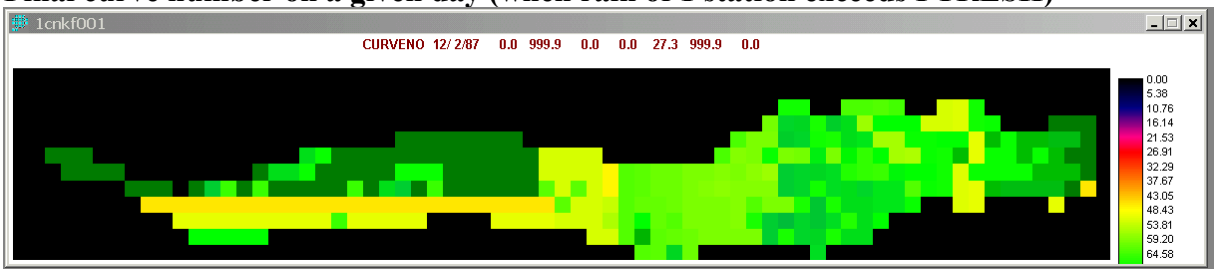

Runoff on a given day (when rain of 1 station exceeds PTRESH)

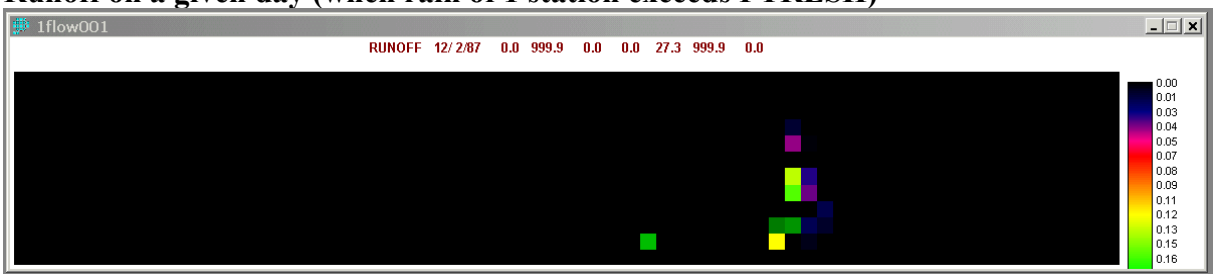

Plant available water at the start of a given day (when rain of 1 station exceeds PTRESH)

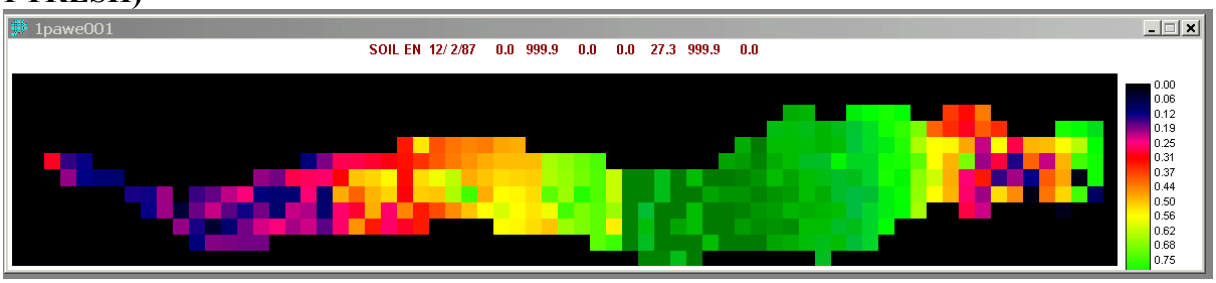

Soil status on a given day (when rain of 1 station exceeds PTRESH)

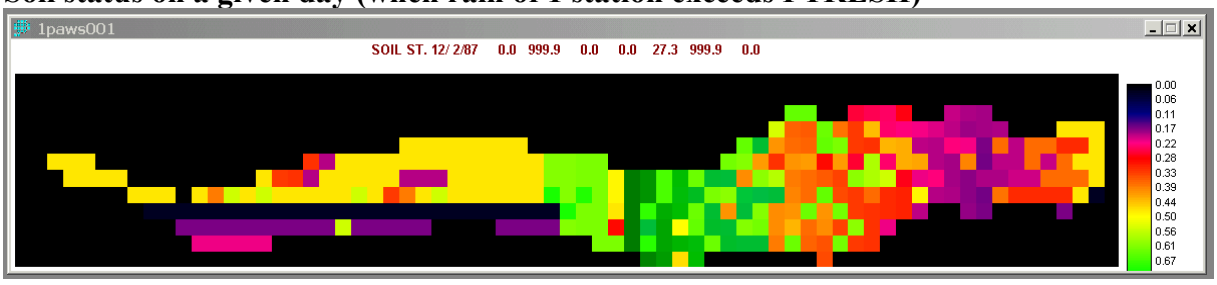

Interpolated rainfall on a given day (when rain of 1 station exceeds PTRESH)

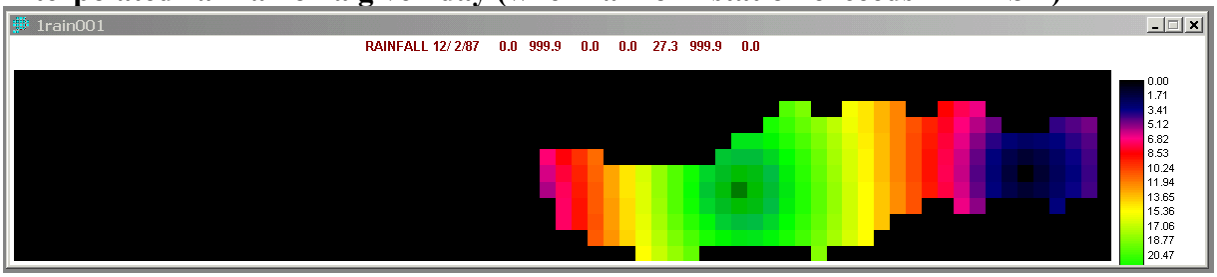

C. 7. Streamflow Analysis Excel Spreadsheet/Makro

Excel Spreadsheet used for the analysis of the calibration and validation runs – sample tables. (Fields marked in yellow have to be filled in with the valid information for each run.)

	A	B	C	D	E	F	G	H	I	J	K	L	M	N	O	P	Q	R	S
1	Naro Moru A5					Model Run:	a5500gw3			model versio	stm2ci								
2	500.0	m grid				runon coeff:	0.0			comp system	windows								
3	coverage cells					land cover class	satveg1.gen			rcoeff1	0.03	mm		0.03					
4	catchment cells					soil class file	allsol1.gen			rcoeff2	0.3	mm		0.200					
5	area	87.0	km2			initpawf	0.5			sszth	20	mm		50.00					
6		87000000.0	m2			initial ssz	0.0	threshold for low flow analysis			0.730	m/3							
7																			
8		modelled	modelled	modelled	modelled	modelled		observed	naturalised	observed	naturalised						residual	square	positi
9	DATE	RAIN	ETP	streamflow	gwdis	streamflow		flow	flow	flow	flow	SWDIFF	SSZDIFF	SSZ	SUMPCK	gwq	nat-mod	residuals	residu
10		mm	mm	mm/day	mm/day	m3/s		m3/s	m3/s	mm	mm	mm	mm	mm	mm				
11	01.01.1987	0	2.02	0.49	0.49	0.493	13.725	0.242	0.367	0.24	0.36	-2.02	-0.49	15.89	0	#BEZUG!	-0.126	0.016	0.12
12	02.01.1987	0.96	1.53	0.48	0.48	0.483	0.050	0.217	0.341	0.22	0.34	-0.57	-0.48	15.41	0	0.4767	-0.141	0.020	0.14
13	03.01.1987	0.3	1.77	0.46	0.46	0.463		0.198	0.322	0.20	0.32	-1.47	-0.46	14.95	0	0.4623	-0.140	0.020	0.14
14	04.01.1987	1.46	1.69	0.45	0.45	0.453		0.208	0.332	0.21	0.33	-0.23	-0.45	14.5	0	0.4485	-0.120	0.014	0.12
15	05.01.1987	0	2.19	0.44	0.44	0.443		0.196	0.320	0.19	0.32	-2.19	-0.44	14.07	0	0.435	-0.122	0.015	0.12
16	06.01.1987	0	1.91	0.42	0.42	0.423		0.149	0.273	0.15	0.27	-1.91	-0.42	13.64	0	0.4221	-0.149	0.022	0.14
17	07.01.1987	0.45	1.79	0.41	0.41	0.413		0.132	0.256	0.13	0.25	-1.35	-0.41	13.23	0	0.4092	-0.156	0.024	0.15
18	08.01.1987	0.33	1.84	0.4	0.4	0.403		0.139	0.263	0.14	0.26	-1.52	-0.4	12.84	0	0.3969	-0.139	0.019	0.13
19	09.01.1987	0.82	1.82	0.39	0.39	0.393		0.154	0.278	0.15	0.28	-1	-0.39	12.45	0	0.3852	-0.114	0.013	0.11
20	10.01.1987	1.11	2.02	0.37	0.37	0.373		0.131	0.256	0.13	0.25	-0.91	-0.37	12.08	0	0.3735	-0.116	0.013	0.11
21	11.01.1987	0	1.76	0.36	0.36	0.363		0.120	0.244	0.12	0.24	-1.76	-0.36	11.72	0	0.3624	-0.117	0.014	0.11
22	12.01.1987	0	1.88	0.35	0.35	0.352		0.120	0.244	0.12	0.24	-1.88	-0.35	11.36	0	0.3516	-0.107	0.012	0.10
23	13.01.1987	0	1.79	0.34	0.34	0.342		0.120	0.244	0.12	0.24	-1.79	-0.34	11.02	0	0.3408	-0.097	0.009	0.09
24	14.01.1987	3.25	1.79	0.33	0.33	0.332		0.123	0.247	0.12	0.25	1.04	0.08	11.11	0.41	0.3306	-0.085	0.007	0.08
25	15.01.1987	2.81	1.54	0.35	0.33	0.352		0.182	0.307	0.18	0.30	1.25	-0.33	10.78	0.01	0.3333	-0.045	0.002	0.04
26	16.01.1987	6.61	1.31	0.44	0.32	0.443		0.233	0.357	0.23	0.35	5.04	-0.18	10.6	0.15	0.3234	-0.085	0.007	0.08
27	17.01.1987	1.72	2.24	0.32	0.32	0.322		0.145	0.270	0.14	0.27	-0.52	-0.32	10.28	0	0.318	-0.052	0.003	0.05
28	18.01.1987	0	2.21	0.31	0.31	0.312		0.161	0.285	0.16	0.28	-2.21	-0.31	9.97	0	0.3084	-0.027	0.001	0.02
29	19.01.1987	0	2.46	0.3	0.3	0.302		0.126	0.250	0.13	0.25	-2.46	-0.3	9.67	0	0.2991	-0.051	0.003	0.05
30	20.01.1987	0	2.26	0.29	0.29	0.292		0.104	0.228	0.10	0.23	-2.26	-0.29	9.38	0	0.2901	-0.063	0.004	0.06
31	21.01.1987	0	1.69	0.28	0.28	0.282		0.091	0.215	0.09	0.21	-1.69	-0.28	9.1	0	0.2814	-0.066	0.004	0.06
32	22.01.1987	0	1.79	0.27	0.27	0.272		0.085	0.209	0.08	0.21	-1.79	-0.27	8.83	0	0.273	-0.062	0.004	0.06
33	23.01.1987	1.41	1.74	0.26	0.26	0.262		0.078	0.202	0.08	0.20	-0.33	-0.26	8.57	0	0.2649	-0.059	0.004	0.05
34	24.01.1987	8.48	1.87	0.29	0.26	0.292		0.093	0.218	0.09	0.22	4.41	1.91	10.47	2.16	0.2571	-0.074	0.005	0.07
35	25.01.1987	4.17	1.96	0.31	0.31	0.312		0.126	0.250	0.12	0.25	2.12	-0.22	10.25	0.09	0.3141	-0.062	0.004	0.06
36	26.01.1987	0	2.15	0.31	0.31	0.312		0.105	0.230	0.10	0.23	-2.15	-0.31	9.94	0	0.3075	-0.082	0.007	0.08
37	27.01.1987	0	2.18	0.3	0.3	0.302		0.093	0.217	0.09	0.22	-2.18	-0.3	9.64	0	0.2982	-0.084	0.007	0.08
38	28.01.1987	0	1.68	0.29	0.29	0.292		0.090	0.214	0.09	0.21	-1.68	-0.29	9.35	0	0.2892	-0.078	0.006	0.07
39	29.01.1987	1.59	1.9	0.28	0.28	0.282		0.068	0.192	0.07	0.19	-0.32	-0.27	9.09	0.01	0.2805	-0.089	0.008	0.08
40	30.01.1987	0	1.8	0.27	0.27	0.272		0.066	0.190	0.07	0.19	-1.8	-0.27	8.82	0	0.2727	-0.081	0.007	0.08
41	31.01.1987	0	1.9	0.26	0.26	0.262		0.061	0.185	0.06	0.18	-1.9	-0.26	8.55	0	0.2646	-0.076	0.006	0.07
42	01.02.1987	0	2.09	0.26	0.26	0.262		0.055	0.163	0.05	0.16	-2.09	-0.26	8.29	0	0.2565	-0.098	0.010	0.09
43	02.02.1987	0	1.97	0.25	0.25	0.252		0.049	0.157	0.05	0.16	-1.97	-0.25	8.05	0	0.2487	-0.094	0.009	0.09
44	03.02.1987	0	1.89	0.24	0.24	0.242		0.056	0.165	0.06	0.16	-1.89	-0.24	7.8	0	0.2415	-0.076	0.006	0.07
45	04.02.1987	0	1.85	0.23	0.23	0.232		0.053	0.161	0.05	0.16	-1.85	-0.23	7.57	0	0.234	-0.070	0.005	0.07
46	05.02.1987	0.3	1.75	0.23	0.23	0.232		0.046	0.154	0.05	0.15	-1.45	-0.23	7.34	0	0.2271	-0.077	0.006	0.07
47	06.02.1987	0	1.58	0.22	0.22	0.222						-1.58	-0.22	7.12	0	0.2202			
48	07.02.1987	0	1.66	0.21	0.21	0.211						-1.66	-0.21	6.91	0	0.2136			
49	08.02.1987	0	1.63	0.21	0.21	0.211						-1.63	-0.21	6.7	0	0.2073			
50	09.02.1987	1.63	1.55	0.2	0.2	0.201						0.08	-0.2	6.5	0	0.201			

alldata | day2dec | DecData | ModelPerf | qqplots | monthsum | annwb | lowflowdata | lowflowanalysis | allflows8696 | 1987 | 1988 | 1989 | 1990 | 1991 | 1992 | 1993 | 1994 | 1995 | 19

	A	B	C	D	E	F	G	H	I	J	K	L	M	N	O	P	Q
1	**Model Performance**																
2																	
3																	
4	**Calibration Period**																
5																	
6																	
7		**Mean obs Q**	**Mean sim Q**	**Median**	**Median**	**Lower Quart**	**Lower Quart**	**Upper Quart**	**Upper Quart**	**simulated**	**simulated**	**sim tot Q**	**nat. obs.**	**Sim - Obs**			No. Of nat. o
8				**nat. obs.**	**simulated**	**nat. obs.**	**simulated**	**nat. obs.**	**simulated**	**rainfall**	**total Q**	**if obs Q av.**	**total Q**	**Q [mm/y]**			
9	**1986 - 1991**	1.23	1.12588171	0.73	0.50	0.39	0.30	1.53	1.18	5005	2057.06	1887.18	2132.9653	-49.1570595			1986 - 91
10	**1987**	0.72	0.68043836	0.36	0.33	0.26	0.20	0.74	0.65	890	248.36	238.66	228.465568	10.194432			1987
11	**1988**	1.52	1.52699454	0.95	0.55	0.48	0.39	1.95	2.01	890	558.88	410.85	524.958961	-114.108961			1988
12	**1989**	1.41	1.32608219	0.86	0.55	0.49	0.37	1.63	1.33	1193	485.22	482.86	514.365975	-31.5059748			1989
13	**1990**	1.69	1.51909589	1.19	0.57	0.58	0.35	2.35	2.20	1223	554.47	544.97	587.592961	-42.6229609			1990
14	**1991**	0.76	0.57569863	0.54	0.46	0.38	0.29	0.84	0.56	809	210.13	209.84	277.581832	-67.7418324			1991
15																	
16																	
17	**Daily values:**																
18			**Root Mean**	**Mean**	**Efficiency**				**Maximum discharge 1987 - 1991**								
19		**R2**	**Square Error**	**Abs. Dev**	**score**				**Simulated**	**observed**	**nat. obs.**						
20			**(RMSE)**	**(MAD)**	**(E2)**				13.7246528	13.5731481	13.7345296						
21	**1986 - 1991**	0.6553238	0.91718372	0.48597292	0.69252182												alldata:
22	**1987**	0.57849965	0.63989388	0.30375127	0.61377501												
23	**1988**	0.66085148	1.03716938	0.5472017	0.70084273												
24	**1989**	0.64674812	1.24374857	0.68159104	0.4325176				**Minimum discharge 1987 - 1991**								
25	**1990**	0.76532098	0.96094244	0.60275399	0.67567955				**Simulated**	**observed**	**nat. obs.**						
26	**1991**	0.42549914	0.55359505	0.29439882	0.48293326				0.05034722	0.00370833	0.11541						
27																	
28																	
29	**Decadal values:**																
30			**Root Mean**	**Mean**	**Efficiency**												
31		**R2**	**Square Error**	**Abs. Dev**	**score**												
32			**(RMSE)**	**(MAD)**	**(E2)**												
33	**1986 - 1991**	0.82023897	0.63750211	0.40643196	0.75994935												DecData
34	**1987**	0.75972927	0.38056546	0.2405064	0.71816692												
35	**1988**	0.91440083	0.6068105	0.45836945	0.85194994												
36	**1989**	0.7417936	0.92970001	0.58640146	0.52352399												
37	**1990**	0.87488316	0.74866546	0.50802682	0.76800101												
38	**1991**	0.68089164	0.30684451	0.24359801	0.49289088												
39	Thomasperio	0.84523675															
40	(Sep 89 - Aug 91)																
41																	
42																	
43																	
44	**Verification Period**																
45																	
46																	
47		**Mean obs Q**	**Mean sim Q**	**Median**	**Median**	**Lower Quart**	**Lower Quart**	**Upper Quart**	**Upper Quart**	**simulated**	**simulated**	**sim tot Q**	**nat. obs.**	**Sim - Obs**			No. Of nat. o
48				**nat. obs.**	**simulated**	**nat. obs.**	**simulated**	**nat. obs.**	**simulated**	**rainfall**	**total Q**	**if obs Q av.**	**total Q**	**Q [mm/y]**			

alldata / day2dec / DecData / ModelPerf / qqplots / monthsum / annwb / lowflowdata / lowflowanalysis / allflows8696 / 1987 / 1988 / 1989 / 1990 / 1991 / 1992 / 1993 / 1994 / 1995 / 19

	A	B	C	D	E	F	G	H	I	J	K	L	M	N	O	P	Q	R
1	**Low Flow Analysis**																	
2																		
3	**Calibration period**																	
4																		
5			**naturalized**	**modelled**	**naturalized**	**modelled**	**NMQ30**	**NMQ30**	**NMQ30**									
6		**R2 below thre**	**days below**	**days below**	**olume belo**	**volume belo**	**naturalized**	**simulated**	**observed**									
7							**(May - April)**	**(May - April)**	**(May - April)**									
8	**1987 - 91**	0.20451936	939	1250	348.232619	473.27												
9	**1987**	0.45811617	283	279	80.1680552	82.12	0.18	0.06	0.06						RowNo			
10	**1988**	0.18800511	142	222	42.2826802	91.54	0.47	0.43	0.34					alldata:	11 - 1836			
11	**1989**	0.08823229	146	229	65.3925284	94.68	0.37	0.23	0.22						11			
12	**1990**	3.6146E-07	122	208	50.9082015	84.22	0.33	0.15	0.16						376			
13	**1991**	0.46633309	246	312	109.481154	120.71	0.37	0.08	0.17						742			
14			**r2(duration)**	0.80576262	**r2(volume)=**	0.52395139	**r2(NMQ30)=**	0.61763332							1107			
15															1472			
16														DecData	11 - 190			
17															11			
18															47			
19															83			
20															119			
21	**Verification Period**														155			
22																		
23			**naturalized**	**modelled**	**naturalized**	**modelled**	**NMQ30**	**NMQ30**	**NMQ30**									
24		**R2 below thre**	**days below**	**days below**	**olume belo**	**volume belo**	**naturalized**	**simulated**	**observed**						RowNo:			
25							**(May - April)**	**(May - April)**	**(May - April)**					alldata:	1837 - 3663			
26	**1992 - 96**	0.38923773	1142	1105	298.439594	418.274653									1837			
27	**1992**	0.51760181	230	236	76.2843091	86.8892361	0.41	0.23	0.20						2203			
28	**1993**	0.16490203	185	232	78.8900972	75.1180556	0.16	0.09	0.03						2568			
29	**1994**	0.9363075	343	211	36.4416056	77.39375		0.18							2933			
30	**1995**	0.01527673	205	218	23.1746612	87.6142361	0.33	0.26	0.13						3298			
31	**1996**	#NV	179	208	83.6489204	91.259375	0.59	0.52	0.22					DecData	191 - 370			
32			**r2(duration)**	0.07001909	**r2(volume)=**	0.00877793	**r2(NMQ30)=**	0.90623891							191			
33															227			
34															263			
35															299			

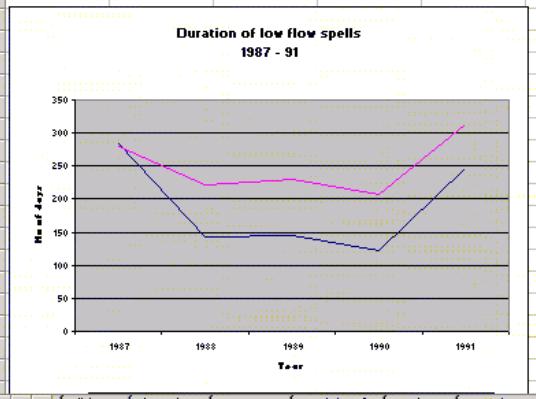

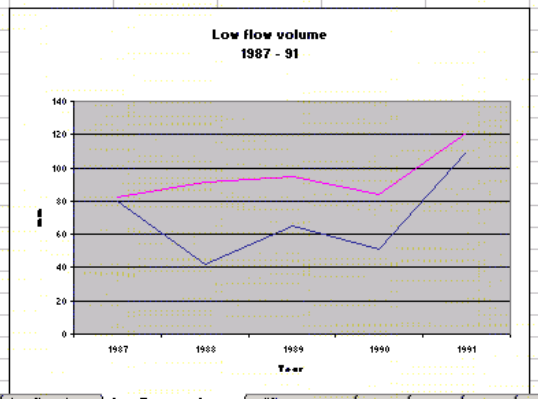

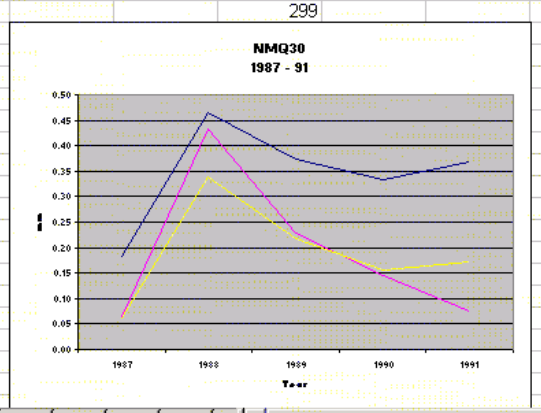

alldata | day2dec | DecData | ModelPerf | qqplots | monthsum | annwb | lowflowdata | **lowflowanalysis** | allflows8696 | 1987 | 1988 | 1989 | 1990 | 1991 | 1992 | 1993 | 1994 | 1995 | 19

C. 8. Scenario Analysis Excel Spreadsheet/Makro

Excel Spreadsheet used for the analysis of the scenario runs – sample tables. (Fields marked in yellow have to be filled in with the valid information for each run.)

	A	B	C	D	E	F	G	H	I	J	K	L	M	N	O	P	Q	R
1	Naro Moru A5					Model Run:	echama2s			model versio	stm2ci		*ECHAM SRES A2 Scenario predictions for 2040 - 2069*					
2	500.0	m grid				runon coeff:	0.0			comp system	windows							
3	coverage cells					land cover class	satveg1.gen			rcoeff1	0.03	mm		0.03				
4	catchment cells					soil class file	allsol1.gen			rcoeff2	0.3	mm		0.200				
5	area	87.0	km2			initpawf	0.5			sszth	20	mm		50.00				
6		87000000.0	m2			initial ssz	0.0	threshold for low flow analysis			1.000	m/3						
7																		
8	SIMULATION	scenario	scenario	scenario	scenario	scenario	scenario	scenario	scenario	scenario	scenario		BaseCase	BaseCase	BaseCase	BaseCase	BaseCase	BaseC
9	DAY	RAIN	ETP	streamflow	gwdis	streamflow	SWDIFF	SSZDIFF	SSZ	SUMPCK	gwq		streamflow	streamflow	rain	ET	SWDIFF	SSZDI
10		mm	mm	mm/day	mm/day	m3/s	mm	mm	mm	mm			m3/s	mm/day	mm	mm	mm	mm
11	01.01.01	0	1.96	0.48	0.48	0.483	-1.96	-0.48	15.63	0	#BEZUG!		0.493	0.49	0	2.02	-2.02	
12	02.01.01	3.61	1.48	0.47	0.47	0.473	1.99	-0.32	15.3	0.14	0.4689		0.483	0.48	0.96	1.53	-0.57	
13	03.01.01	1.11	1.76	0.46	0.46	0.463	-0.66	-0.44	14.86	0.01	0.459		0.463	0.46	0.3	1.77	-1.47	
14	04.01.01	5.5	1.7	0.45	0.45	0.453	2.71	0.63	15.48	1.07	0.4458		0.453	0.45	1.46	1.69	-0.23	
15	05.01.01	0	2.26	0.46	0.46	0.463	-2.26	-0.46	15.02	0	0.4644		0.443	0.44	0	2.19	-2.19	
16	06.01.01	0	2.06	0.45	0.45	0.453	-2.06	-0.45	14.57	0	0.4506		0.423	0.42	0	1.91	-1.91	
17	07.01.01	1.69	1.93	0.44	0.44	0.443	-0.24	-0.44	14.13	0	0.4371		0.413	0.41	0.45	1.79	-1.35	
18	08.01.01	1.24	1.99	0.42	0.42	0.423	-0.75	-0.42	13.71	0	0.4239		0.403	0.4	0.33	1.84	-1.52	
19	09.01.01	3.09	1.91	0.44	0.41	0.443	0.37	0.38	14.09	0.79	0.4113		0.393	0.39	0.82	1.82	-1	
20	10.01.01	4.18	2.12	0.42	0.42	0.423	1.04	0.6	14.69	1.02	0.4227		0.373	0.37	1.11	2.02	-0.91	
21	11.01.01	0	1.84	0.44	0.44	0.443	-1.84	-0.44	14.25	0	0.4407		0.363	0.36	0	1.76	-1.76	
22	12.01.01	0	2.08	0.43	0.43	0.433	-2.08	-0.43	13.82	0	0.4275		0.352	0.35	0	1.88	-1.88	
23	13.01.01	0	2.01	0.41	0.41	0.413	-2.01	-0.41	13.4	0	0.4146		0.342	0.34	0	1.79	-1.79	
24	14.01.01	12.24	2	0.87	0.4	0.876	4.98	4.39	17.79	4.79	0.402		0.332	0.33	3.25	1.79	1.04	
25	15.01.01	10.57	1.62	1.89	0.53	1.903	3.29	3.76	21.55	4.3	0.5337		0.352	0.35	2.81	1.54	1.25	
26	16.01.01	24.89	1.33	5.45	1.07	5.488	13.4	4.72	26.27	5.78	0.6465		0.443	0.44	6.61	1.31	5.04	
27	17.01.01	6.47	2.32	2.64	2.48	2.658	0.32	1.19	27.46	3.67	0.7881		0.322	0.32	1.72	2.24	-0.52	
28	18.01.01	0	2.33	2.84	2.84	2.860	-2.33	-2.84	24.63	0	0.8238		0.312	0.31	0	2.21	-2.21	
29	19.01.01	0	2.78	1.99	1.99	2.004	-2.78	-1.99	22.64	0	0.7389		0.302	0.3	0	2.46	-2.46	
30	20.01.01	0	2.73	1.39	1.39	1.400	-2.73	-1.39	21.25	0	0.6792		0.292	0.29	0	2.26	-2.26	
31	21.01.01	0	2.15	0.97	0.97	0.977	-2.15	-0.97	20.27	0	0.6375		0.282	0.28	0	1.69	-1.69	
32	22.01.01	0	2.33	0.68	0.68	0.685	-2.33	-0.68	19.59	0	0.6081		0.272	0.27	0	1.79	-1.79	
33	23.01.01	5.3	2.27	0.78	0.59	0.785	0.63	1.62	21.21	2.21	0.5877		0.262	0.26	1.41	1.74	-0.33	
34	24.01.01	31.94	2.26	11.14	0.96	11.217	2.19	16.35	37.56	17.32	0.6363		0.292	0.29	8.48	1.87	4.41	
35	25.01.01	15.69	2.24	6.33	5.87	6.374	9.92	-2.8	34.76	3.06	1.1268		0.312	0.31	4.17	1.96	2.12	
36	26.01.01	0	2.3	5.03	5.03	5.065	-2.3	-5.03	29.73	0	1.0428		0.312	0.31	0	2.15	-2.15	
37	27.01.01	0	2.49	3.52	3.52	3.544	-2.49	-3.52	26.21	0	0.8919		0.302	0.3	0	2.18	-2.18	
38	28.01.01	0	1.96	2.46	2.46	2.477	-1.96	-2.46	23.75	0	0.7863		0.292	0.29	0	1.68	-1.68	
39	29.01.01	6	2.26	2.11	1.72	2.125	0.36	1.28	25.03	3	0.7125		0.282	0.28	1.59	1.9	-0.32	
40	30.01.01	0	2.1	2.11	2.11	2.125	-2.1	-2.11	22.92	0	0.7509		0.272	0.27	0	1.8	-1.8	
41	31.01.01	0	2.29	1.48	1.48	1.490	-2.29	-1.48	21.44	0	0.6876		0.262	0.26	0	1.9	-1.9	
42	01.02.01	0	2.63	1.03	1.03	1.037	-2.63	-1.03	20.41	0	0.6432		0.262	0.26	0	2.09	-2.09	
43	02.02.01	0	2.54	0.72	0.72	0.725	-2.54	-0.72	19.69	0	0.6123		0.252	0.25	0	1.97	-1.97	
44	03.02.01	0	2.46	0.59	0.59	0.594	-2.46	-0.59	19.1	0	0.5907		0.242	0.24	0	1.89	-1.89	
45	04.02.01	0	2.42	0.57	0.57	0.574	-2.42	-0.57	18.52	0	0.573		0.232	0.23	0	1.85	-1.85	
46	05.02.01	0.52	2.3	0.56	0.56	0.564	-1.78	-0.56	17.97	0	0.5556		0.232	0.23	0.3	1.75	-1.45	
47	06.02.01	0	2.02	0.54	0.54	0.544	-2.02	-0.54	17.43	0	0.5391		0.222	0.22	0	1.58	-1.58	
48	07.02.01	0	2.21	0.52	0.52	0.524	-2.21	-0.52	16.91	0	0.5229		0.211	0.21	0	1.66	-1.66	
49	08.02.01	0	2.17	0.51	0.51	0.514	-2.17	-0.51	16.4	0	0.5073		0.211	0.21	0	1.63	-1.63	
50	09.02.01	2.94	2.07	0.49	0.49	0.493	0.87	-0.49	15.91	0	0.492		0.201	0.2	1.63	1.55	0.08	

Contents | alldata | day2dec | DecData | monthlydata | lowflowdata | FlowComp | LowflowComp | WBComp | Tabelle1 | DailyChart | DecFlowChart

Flow Comparison: BaseCase run vs Scenario run

SIMULATION YEAR	BaseCase Mean Q	Scenario Mean Q	BaseCase Median	Scenario Median	BaseCase Lower Quart	Scenario Lower Quart	BaseCase Upper Quart	Scenario Upper Quart	BaseCase Qmin	Scenario Qmin	BaseCase Qmax	Scenario Qmax	Scenario total Q [mm]	BaseCase total Q [mm]	Scen - Base Q [mm/y]	BaseCase rainfall
1 to 15	1.28	1.62	0.52	0.51	0.32	0.28	1.42	1.75	0.04	0.01	19.08	73.58	8810.55	6977.33	122.214667	16902.43
1	0.69	0.88	0.33	0.49	0.20	0.18	0.65	1.16	0.05	0.02	5.29	11.22	320.23	248.36	71.87	889.79
2	1.54	1.92	0.55	0.55	0.39	0.41	2.02	2.40	0.17	0.17	13.72	15.34	697.75	558.88	138.87	1330.01
3	1.56	1.96	0.57	0.58	0.41	0.29	1.55	2.08	0.24	0.06	16.62	32.28	711.93	565.80	146.13	1275.33
4	1.53	1.89	0.57	0.59	0.35	0.24	2.22	2.91	0.20	0.10	12.10	14.23	684.45	554.62	129.83	1223.39
5	0.58	0.71	0.46	0.42	0.29	0.20	0.56	0.57	0.12	0.03	3.26	9.31	258.34	210.32	48.02	809.18
6	1.21	1.53	0.55	0.59	0.25	0.32	1.51	2.05	0.06	0.15	8.58	11.74	557.39	438.57	118.82	1123.37
7	1.32	2.63	0.50	0.50	0.23	0.22	1.63	2.05	0.11	0.08	11.03	41.90	951.93	477.54	474.39	1062.52
8	1.48	1.52	0.56	0.49	0.34	0.34	1.96	1.79	0.07	0.13	13.29	13.42	549.48	536.64	12.84	1186.14
9	1.43	1.38	0.58	0.58	0.37	0.43	1.97	1.40	0.14	0.18	11.21	12.40	499.19	520.03	-20.84	1248.75
10	1.25	1.63	0.58	0.55	0.41	0.36	1.66	1.70	0.20	0.21	8.94	28.06	593.83	455.35	138.48	1126.15
11	1.94	2.19	0.52	0.46	0.32	0.25	2.78	3.55	0.08	0.09	19.08	19.88	792.33	704.44	87.89	1420.18
12	2.01	4.14	0.59	0.43	0.46	0.23	2.24	2.31	0.27	0.11	11.97	73.58	1499.05	728.57	770.48	1364.49
13	0.83	0.43	0.50	0.20	0.24	0.07	0.83	0.42	0.10	0.01	7.22	23.76	154.59	302.09	-147.50	937.37
14	0.43	0.13	0.26	0.09	0.11	0.04	0.48	0.16	0.04	0.01	3.96	2.15	48.88	155.02	-106.14	667.68
15	1.44	1.36	0.57	0.38	0.45	0.09	1.61	0.98	0.15	0.02	9.89	24.89	491.18	521.10	-29.92	1238.08

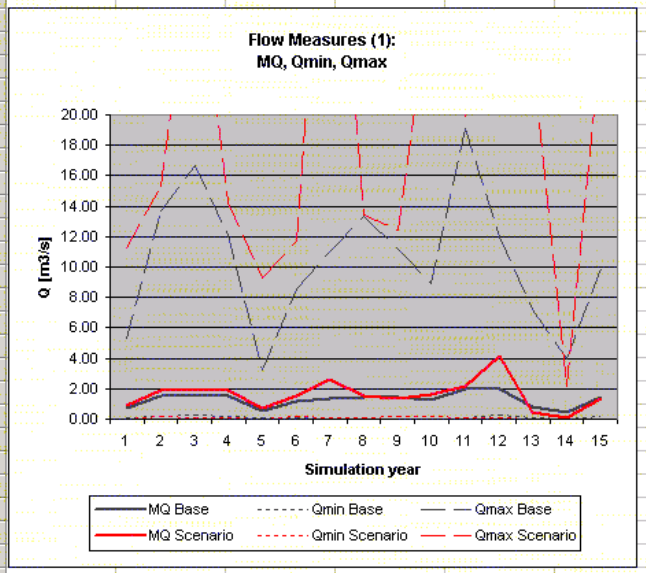

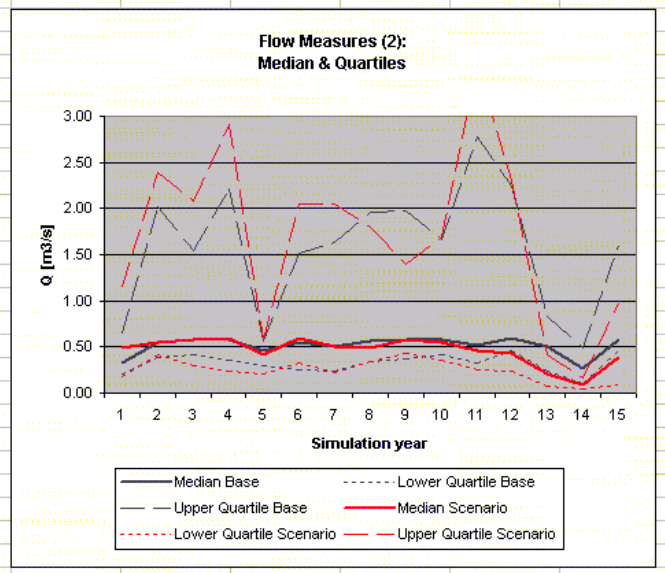

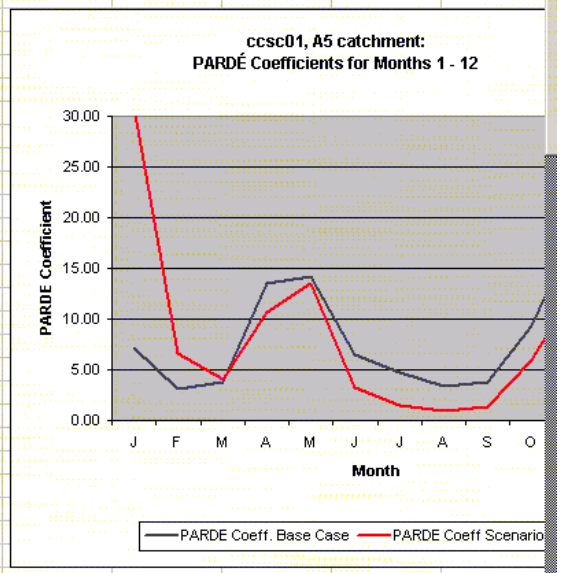

Contents | alldata | day2dec | DecData | monthlydata | lowflowdata | FlowComp | LowflowComp | WBComp | Tabelle1 | DailyChart | DecFlowChart

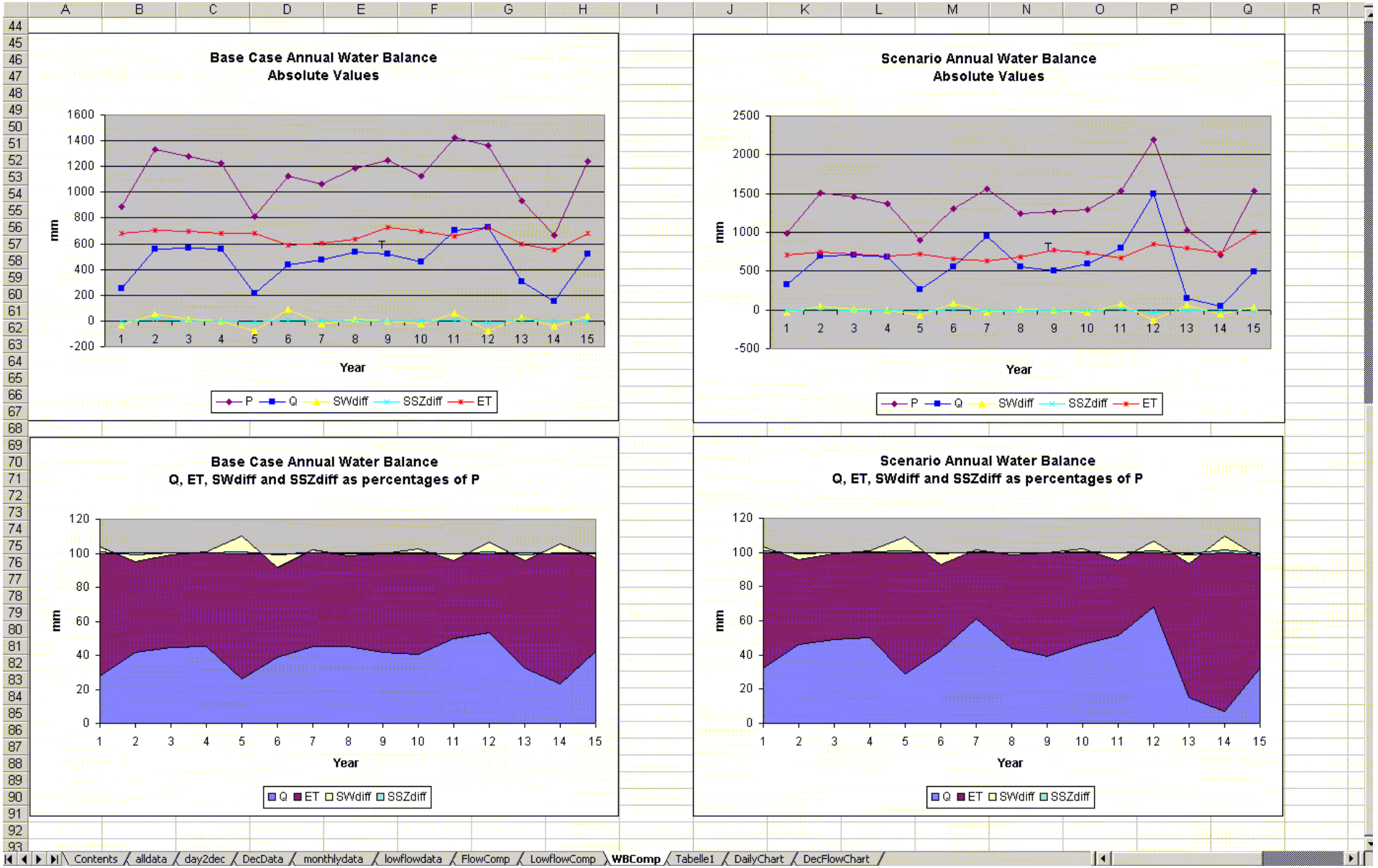
Base Case Annual Water Balance
Absolute Values
mm
Year
P
Q
SWdiff
SSZdiff
ET
Scenario Annual Water Balance
Absolute Values
mm
Year
P
Q
SWdiff
SSZdiff
ET
Base Case Annual Water Balance
Q, ET, SWdiff and SSZdiff as percentages of P
mm
Year
Q
ET
SWdiff
SSZdiff
Scenario Annual Water Balance
Q, ET, SWdiff and SSZdiff as percentages of P
mm
Year
Q
ET
SWdiff
SSZdiff
Contents
alldata
day2dec
DecData
monthlydata
lowflowdata
FlowComp
LowflowComp
WBComp
Tabelle1
DailyChart
DecFlowChart

C. 9. Climextract source code

Climextract is a fortran77 programme used for the extraction of temperature and precipitation values for the 4 grid points around Naro Moru from a global climate file in the GRIB format. The line increments for different GCM outputs have to be set in the control file.

```
      PROGRAM CLIMEXTRACT

C     WRITTEN BY BENEDIKT NOTTER
C     22/04/2003
C     modified 19/05/2003
C     READS GCM OUTPUT GRIB FILES IN ASCII FORMAT
C     AND WRITES TIME-SERIES OF OUTPUT PARAMETER OF 4 GRID POINTS AROUND
C     NARO MORU CATCHMENT
C     NOTE: SET NAMES OF IN- AND OUTFILE AND LINE INCREMENTS FOR USED GCM
C     IN CONTROL FILE

C*********************************************************************

      REAL A, B, C, D
      REAL K, L, M

      CHARACTER*12 CONTROLFILE
      CHARACTER*12 INFILE
      CHARACTER*12 OUTFILE

C*********************************************************************

      WRITE(*,50)
60    FORMAT(/10X, 'ENTER NAME OF CONTROLFILE:')
      READ(*,51) CONTROLFILE
61    FORMAT(A8)

      OPEN(UNIT=3,FILE=CONTROLFILE,STATUS='OLD')
      READ(3,*)
      READ(3,*)
      READ(3,62) INFILE
62    FORMAT(37X,A8)
      READ(3,63) OUTFILE
63    FORMAT(37X,A8)
      READ(3,64) K
64    FORMAT(13X,I3)
      READ(3,65) L
65    FORMAT(13X,I2)
      READ(3,66) M
66    FORMAT(13X,I3)

      OPEN(UNIT=1,FILE=INFILE,STATUS='OLD')
      OPEN(UNIT=2,FILE=OUTFILE,STATUS='NEW')

      DO 30 i = 1, K
         READ(1,*)
30    CONTINUE

110   READ(1,20) A, B
20    FORMAT(13X,E13.6,E13.6)

      DO 40 i = 1, L
         READ(1,*)
40    CONTINUE
```

```
      READ(1,20) C, D
      WRITE(2,21) A, B, C, D
21    FORMAT(E13.6,1X,E13.6,1X,E13.6,1X,E13.6)

      DO 50 i = 1, M
         READ(1,*)
50    CONTINUE

      GOTO 110

      STOP
      END
```

```
CLIMEXTRACT CONTROL FILE

INFILE  (NAME MUST BE 8 CHARACTERS):
OUTFILE (NAME MUST BE 8 CHARACTERS):
INCREMENT 1: 499
INCREMENT 2: 15
INCREMENT 3: 1009


Note:
- For ECHAM outputs: Increment 1 = 499
                     Increment 2 = 15
                     Increment 3 = 1009
- For HADCM outputs: Increment 1 = 434
                     Increment 2 = 11
                     Increment 3 = 864
```

C. 10. ECHAM4 short description

(Source: Giorgetta 2002)

This is a short overview of the atmospheric general circulation model ECHAM. The model is based on the weather forecast model of the European Centre for Medium Range Weather Forecasts (ECMWF). Numerous modifications have been applied to this model at the Max Planck Institute for Meteorology and the German Climate Computing Centre (DKRZ) to make it suitable for climate forecasts, and it is now a model of the fourth generation. A detailed description of the ECHAM4 model can be found in Roeckner et al. (1996).

- In the standard model version a 19-level hybrid sigma-pressure coordinate system is used. The vertical domain extends up to the pressure level of 10 hPa. Prognostic variables are vorticity, divergence, logarithm of surface pressure, temperature, specific humidity and mixing ratio of total cloud water. Except for the water components the prognostic variables are represented by spherical harmonics with triangular truncation at wavenumber 42 (T42) in its standard version. A semi-implicit time stepping scheme is used together with a weak time filter. The time step for dynamics and physics is 24 min (for T42 horizontal resolution). The radiation time step is 2 hours. Both seasonal and diurnal cycles in solar forcing are simulated. For the transport of water vapour and cloud water a semi-Lagrangian scheme is used (Williamson and Rasch, 1994).
- **Horizontal diffusion** is expressed in the form of a hyper-Laplacian which essentially confines the damping to the high-wavenumber end of the spectrum. To avoid fictituous reflection at the upper boundary, a high-diffusion sponge zone is realized through a gradual decrease of the order of the scheme in the lower stratosphere. The diffusion operator is applied to vorticity, divergence and temperature but not to the water components which are advected by the semi-Lagrangian scheme.
- The **turbulent surface fluxes** are calculated from Monin-Obukhov similarity theory (Louis, 1979). Within and above the atmospheric boundary layer, a higher-order closure scheme is used to compute the turbulent transfer of momentum, heat, moisture, and cloud water. The eddy diffusion coefficients are calculated as functions of turbulent kinetic energy E which is obtained from the respective rate equation (Brinkop and Roeckner, 1995), including turbulent transport of E, generation or destruction by wind shear and buoyancy flux, and dissipation. The interaction between cloud and turbulence is represented by processes such as the vertical exchange of turbulent kinetic energy generated through radiative cooling at cloud top, the impact of cloud water on the buoyancy flux, and cloud top entrainment through the turbulent flux of cloud water.
- **Gravity wave drag** associated with **orographic** gravity waves is simulated after Miller et al. (1989), using directionally dependent subgrid-scale orographic variances obtained from a high-resolution U.S. Navy dataset. Surface stress due to gravity waves excited by stably stratified flow over irregular terrain is calculated from linear theory and dimensional considerations. The surface wave stress is a function of low-level wind, orographic variance and buoyancy frequency. In addition, high-drag states are considerd when the flow becomes hydraulic at low levels due to the breaking of lee waves. The vertical profile is calculated from a local wave Richardson which describes the onset of turbulence due to convective instability and the turbulent breakdown approaching a critical level.
- The **soil model** comprises the budgets of heat and water in the soil, the snow pack over land and the heat budget of land ice. Vegetation effects such as the interception of rain and snow in the canopy and the stomatal control of evapotranspiration are parameterized in a highly idealized way. The local runoff scheme is based on catchment considerations and takes into account subgrid-scale variations of field capacity over inhomogeneous terrain. Land surface parameters such as background albedo, roughness length, vegetation type, leaf area index and soil parameters like water holding capacity, heat capacity and thermal conductivity have been compiled for ECHAM 4 (Claussen et al., 1994), consistent with the Olson et al. (1983) definition of ecosystem complexes.
- The parameterization of **cumulus convection** (shallow, mid-level, and deep), is based on the bulk mass flux concept of Tiedtke (1989). However, according to the suggestions of Nordeng (1994), organized entrainment is related to buoyancy instead of moisture convergence, organized detrainment is computed for a spectrum of clouds detraining at

different heights, and an adjustment-type closure is used for deep cumulus convection instead of the moisture convergence closure applied in the Tiedtke scheme. Moreover, the water loading is considered in the buoyancy calculation, the cloud water detrained at the top of cumulus clouds is entering as a source term in the stratiform cloud water equation.

- The **stratiform cloud** water content is calculated from the respective budget equation including sources and sinks due to phase changes and precipitation formation by coalescence of cloud droplets and gravitational settling of ice crystals (Roeckner, 1995). The convective cloud water detrained at the top of cumulus clouds is used as a source term in the stratiform cloud water equation. Fractional cloud cover is parameterized in terms of relative humidity.
- The **radiation** code has been adopted from the ECMWF model (Fouquart and Bonnel, 1980; Morcrette et al., 1986) with a few modifications like the consideration of additional greenhouse gases (methane, nitrous oxide and 16 CFCs), the 14.6 μm band of ozone and various types of aerosols (optionally). Moreover, the water vapour continuum has been revised to include temperature weighted band averages of e-type absorption and also a band dependent ratio of (p-e)-type to e-type continuum absorption (Giorgetta and Wild, 1995). The single scattering properties of cloud droplets and ice crystals are derived from Mie theory with suitable adaptation to the broad-band model (Rockel et al., 1991), and the effective radius of droplets and ice crystals is parameterized in terms of the liquid and ice water content, respectively (Roeckner, 1995).

APPENDIX D: RESULTS

D. 1. Calibration and validation runs with the NRM^3 Streamflow Model in the study catchments

Note: Runs in blue are the ones with the highest overall performance (can be several per catchment)
Runs in bold blue are the final runs for each catchment

D. 1. 1. Run description

Run Name	Catch-ment	comp system	model version	description	Resolu-tion	R1COEFF	R2COEFF	SSZTH	SCOEFF	ROCOEFF
a5500gw3b	**A5**	**windows**	**stm2ci**	**gw run 3**	**500**	**0.03**	**0.3**	**20**	**0**	**0**
a5500gw2b	A5	windows	stm2ci	gw run 2	500	0.02	0.2	20	0	0
a5500gw4b	A5	windows	stm2ci	gw run 4	500	0.02	0.2	10	0	0
a5500gw5b	A5	windows	stm2ci	gw run 5	500	0.01	0.2	15	0	0
a5500gw1b	A5	windows	stm2ci	gw run 1	500	0.04	0.4	20	0	0
a5500gw6b	A5	windows	stm2ci	gw run 7	500	0.02	0.04	25	0	0
a5500gw7	A5	windows	stm2ci	gw run 8	500	0.04	0.04	30	0	0
a5500ro1	A5	windows	stm2ci	runon = 0.1	500	0.03	0.3	20	0	0.1
a5500ro2	A5	windows	stm2ci	runon = 0.5	500	0.03	0.3	20	0	0.2
a5500ro3	A5	windows	stm2ci	runon = 0.2	500	0.03	0.3	20	0	0.5
a5500ro4	A5	windows	stm2ci	runon = 0.8	500	0.03	0.3	20	0	0.8
a5500cn1	A5	windows	stm2ci	curve numbers increased by 10%	500	0.03	0.3	20	0	0
a5500se1	A5	windows	stm4d	dynamic CN's	500	0.03	0.3	20	0	0
a5100l95	A5	linux	stm4d	lc1995	100	0.03	0.3	20	0	0
a5100a01	A5	linux	stm4d	lc 1988	100	0.03	0.3	20	0	0
a5100ro1	A5	linux	stm4d	runon = 0.1	100	0.03	0.3	20	0	0.1
a5500eta	A5	windows	stm2ci	monthly average ET values	500	0.03	0.3	20	0	0
a5500et2	A5	windows	stm2ci	Munyaka data left away	500	0.03	0.3	20	0	0
a5050a01	A5	linux	stm4d	resolution	50	0.03	0.3	20	0	0
a5500act	A5	windows	stm2ci	abstraction calculation tool values	500	0.03	0.3	20	0	0
a3500a01	A3	windows	stm2ci	lc map 1988	500	0.02	0.4	25	0	0
a3500a02	A3	windows	stm2ci	lc map 1988	500	0.03	0.5	30	0	0
a3500a03	**A3**	**windows**	**stm2ci**	**lc map 1988**	**500**	**0.03**	**0.4**	**26**	**0**	**0**
a3500a04	A3	windows	stm2ci	lc map 1988	500	0.04	0.4	34	0	0
a3500ds1	A3	windows	stm2ci	deep seepage = 0.2	500	0.03	0.4	26	0.2	0
a3500ds2	A3	windows	stm2ci	deep seepage = 0.05	500	0.03	0.4	26	0.05	0
a3500ds3	A3	windows	stm2ci	deep seepage = 0.02	500	0.03	0.4	26	0.02	0
a3500ro1	A3	windows	stm2ci	runon = 0.1	500	0.03	0.4	26	0	0.1
a3500ro2	A3	windows	stm2ci	runon = 0.2	500	0.03	0.4	26	0	0.2
a3500ro3	A3	windows	stm2ci	runon = 0.5	500	0.03	0.4	26	0	0.5
a350095a	A3	windows	stm2ci	lc map 1995	500	0.03	0.4	26	0	0
a3500se1	A3	windows	stm4d	seasons	500	0.03	0.4	26	0	0

a3100a01	A3	linux	stm4d	lc map 1988	100	0.03	0.4	26	0	0
a31kma01	A3	windows	stm2ci	lc map 1988	1000	0.03	0.4	26	0	0

a45001	A4	windows	stm2ci	lc map 1988	500	0.02	0.4	25	0	0
a45002	A4	windows	stm2ci	lc map 1988	500	0.03	0.36	25	0	0
a45003	A4	windows	stm2ci	lc map 1988	500	0.05	0.5	35	0	0
a45004	**A4**	**windows**	**stm2ci**	**lc map 1988**	**500**	**0.04**	**0.4**	**30**	**0**	**0**
a4500ro1	A4	windows	stm2ci	runon = 0.1	500	0.04	0.4	30	0	0.1
a4500ro2	A4	windows	stm2ci	runon = 0.2	500	0.04	0.4	30	0	0.2
a4500ro3	A4	windows	stm2ci	runon = 0.5	500	0.04	0.4	30	0	0.5
a450095a	A4	windows	stm2ci	lc map 1995	500	0.04	0.4	30	0	0
a4500se1	A4	windows	stm2ci	seasons	500	0.04	0.4	30	0	0
a41001	A4	linux	stm4d	lc map 1988	100	0.04	0.4	30	0	0

a65001	A6	linux	stm4d	calc gw parms 1	500	0.02	0.3	16	0	0
a65002	A6	linux	stm4d	calc gw parms 2	500	0.02	0.25	14	0	0
a65003	A6	linux	stm4d	gw run	500	0.02	0.25	18	0	0
a650095a	A6	linux	stm4d	lc map 1995	500	0.02	0.25	18	0	0
a6500se1	A6	linux	stm4d	seasons	500	0.02	0.25	18	0	0
a6500all	A6	linux	stm4d	all rain gauges used	500	0.02	0.25	18	0	0
a6500ro1	A6	linux	stm4d	runon = 0.1	500	0.02	0.25	18	0	0.1
a6500ro2	A6	linux	stm4d	runon = 0.2	500	0.02	0.25	18	0	0.2
a6500ro3	A6	linux	stm4d	runon = 0.5	500	0.02	0.25	18	0	0.5
a6500ro4	A6	linux	stm4d	runon = 0.8	500	0.02	0.25	18	0	0.8
a6500ro5	**A6**	**linux**	**stm4d**	**runon = 0.8, all rain gauges**	**500**	**0.02**	**0.25**	**18**	**0**	**0.8**
a6100a01	A6	linux	stm4d	runon = 0.8, all rain gauges	100	0.02	0.25	18	0	0.8

a8500a01	A8	linux	stm4d	all rain gauges used	500	0.03	0.25	18	0	0
a8500a02	A8	linux	stm4d	calculated gw parms	500	0.04	0.4	25	0	0
a8500a03	A8	linux	stm4d	gw run	500	0.02	0.2	16	0	0
a8500ro1	A8	linux	stm4d	runon = 0.1	500	0.03	0.25	18	0	0.1
a8500ro2	A8	linux	stm4d	runon = 0.2	500	0.03	0.25	18	0	0.2
a8500ro3	A8	linux	stm4d	runon = 0.5	500	0.03	0.25	18	0	0.5
a8500se1	A8	linux	stm4d	seasons	500	0.03	0.25	18	0	0
a8500nmr	A8	linux	stm4d	only NM rain gauges used	500	0.03	0.25	18	0	0
a85001st	A8	linux	stm4d	only GathiuruFS	500	0.03	0.25	18	0	0
a8500a8r	A8	linux	stm4d	only A8 gauges	500	0.03	0.25	18	0	0
a850095a	A8	linux	stm4d	lc 1995	500	0.03	0.25	18	0	0
a8100a01	A8	linux	stm4d	prm like a8500a01	100	0.03	0.25	18	0	0

a9500a01	A9	linux	stm4d	all rain gauges; estimated gw parameters	500	0.03	0.3	20	0	0
a9500a02	A9	linux	stm4d	gw comparison run	500	0.04	0.4	25	0	0
a9500a03	A9	linux	stm4d	gw comparison run	500	0.02	0.25	18	0	0

a9500nmr	A9	linux	stm4d	only NM rain stations	500	0.03	0.3	20	0	0
a95001st	A9	linux	stm4d	only Nanyuki Forest	500	0.03	0.3	20	0	0
A9500a9r	A9	linux	stm4d	only A9 stations	500	0.03	0.3	20	0	0
a9500ds1	A9	linux	stm4d	ds = 0.28	500	0.03	0.3	20	0.28	0
a9500ds2	A9	linux	stm4d	ds = 0.1	500	0.03	0.3	20	0.1	0
a9500ds3	A9	linux	stm4d	ds = 0.05	500	0.03	0.3	20	0.05	0
a9500ds4	A9	linux	stm4d	ds = 0.02	500	0.03	0.3	20	0.02	0
a9500ro1	A9	linux	stm4d	runon = 0.1	500	0.03	0.3	20	0	0.1
a9500ro2	A9	linux	stm4d	runon = 0.2	500	0.03	0.3	20	0	0.2
a9500ro3	A9	linux	stm4d	runon = 0.5	500	0.03	0.3	20	0	0.5
a950095a	A9	linux	stm4d	land use 1995	500	0.03	0.3	20	0	0
a9500se1	A9	linux	stm4d	seasons	500	0.03	0.3	20	0	0

D. 1. 2. Calibration period (1987 – 1991)

Run Name	Daily		Decadal		Sim - Obs [mm/y]	*Low flow analysis*			
	r2	E2	r2	E2		threshold [m3/s]	duration sim - obs [days]	vol/day sim - obs [m3/s]	r2 (NMQ30)
a5500gw3b	**0.655**	**0.693**	**0.820**	**0.760**	**-49.157**	**0.730**	**62.200**	**0.018**	**0.618**
a5500gw2b	0.654	0.698	0.823	0.752	-47.921	0.730	40.600	-0.043	0.634
a5500gw4b	0.664	0.649	0.824	0.707	-48.167	0.730	28.000	-0.126	0.637
a5500gw5b	0.664	0.641	0.824	0.700	-48.343	0.730	26.800	-0.135	0.570
a5500gw1b	0.647	0.680	0.814	0.758	-49.717	0.730	50.200	0.016	0.609
a5500gw6b	0.647	0.655	0.810	0.748	-50.291	0.730	70.400	-0.003	0.629
a5500gw7	0.622	0.703	0.803	0.774	-48.191	0.730	9.200	0.016	0.590
a5500ro1	0.655	0.692	0.820	0.760	-49.167	0.730	62.200	0.008	0.618
a5500ro2	0.655	0.692	0.820	0.760	-49.217	0.730	62.200	0.008	0.618
a5500ro3	0.655	0.692	0.820	0.760	-49.183	0.730	62.200	0.008	0.618
a5500ro4	0.655	0.692	0.820	0.760	-49.297	0.730	62.200	0.008	0.618
a5500cn1	0.660	0.701	0.824	0.773	-45.865	0.730	58.000	0.004	0.651
a5500se1	0.655	0.692	0.820	0.760	-49.003	0.730	61.800	0.008	0.618
a5100l95	0.660	0.675	0.824	0.741	-37.855	0.730	59.200	-0.009	0.586
a5100a01	0.656	0.690	0.822	0.760	-45.779	0.730	61.400	0.008	0.622
a5100ro1	0.655	0.689	0.822	0.760	-45.851	0.730	61.600	0.008	0.623
a5500eta	0.657	0.711	0.817	0.794	-44.755	0.730	58.800	0.022	0.617
a5500et2	0.649	0.673	0.816	0.738	-37.477	0.730	60.400	0.009	0.620
a5050a01	0.656	0.690	0.822	0.760	-45.629	0.730	61.400	0.008	0.621
a5500act	0.672	0.674	0.748	0.674	-78.119	0.730	94.600	-0.087	0.846
a3500a01	0.308	0.466	0.531	0.905	5.880	0.320	9.400	0.115	0.958
a3500a02	0.304	0.506	0.525	0.920	8.160	0.320	-41.000	0.160	0.952
a3500a03	**0.306**	**0.514**	**0.533**	**0.917**	**8.062**	**0.320**	**-22.000**	**0.158**	**0.960**
a3500a04	0.298	0.554	0.520	0.926	11.488	0.320	-73.000	0.047	0.930
a3500ds1	0.194	-0.187	0.391	0.719	-283.096	0.320	108.200	-0.115	0.838
a3500ds2	0.273	0.322	0.475	0.861	-157.884	0.320	57.200	0.000	0.957
a3500ds3	0.295	0.487	0.517	0.909	-78.350	0.320	21.600	0.069	0.960
a3500ro1	0.306	0.514	0.533	0.917	8.064	0.320	-22.000	0.158	0.960
a3500ro2	0.306	0.514	0.533	0.917	8.046	0.320	-22.000	0.158	0.960

a3500ro3	0.306	0.513	0.533	0.917	8.070	0.320	-21.600	0.159	0.960
a350095a	0.308	0.473	0.535	0.908	20.544	0.320	-18.600	0.140	0.954
a3500se1	0.306	0.514	0.533	0.917	8.118	0.320	-22.000	0.158	0.960
a3100a01	0.282	0.456	0.509	0.904	25.956	0.320	-25.600	0.170	0.963
a31kma01	0.312	0.450	0.542	0.901	32.976	0.320	-22.000	0.152	0.972

a45001	0.593	0.535	0.715	0.978	-181.125	0.320	70.800	-0.206	0.679
a45002	0.595	0.587	0.728	0.980	-180.125	0.320	74.800	-0.129	0.604
a45003	0.583	0.628	0.744	0.982	-178.115	0.320	42.800	-0.064	0.468
a45004	**0.595**	**0.625**	**0.741**	**0.982**	**-178.943**	**0.320**	**83.600**	**-0.015**	**0.514**
a4500ro1	0.595	0.625	0.741	0.982	-178.987	0.320	83.600	-0.015	0.514
a4500ro2	0.595	0.625	0.741	0.982	-178.955	0.320	83.600	-0.015	0.514
a4500ro3	0.595	0.625	0.741	0.982	-178.937	0.320	84.000	-0.014	0.514
a450095a	0.592	0.615	0.741	0.982	-170.463	0.320	82.400	-0.032	0.428
a4500se1	0.595	0.625	0.741	0.982	-178.927	0.320	83.600	-0.015	0.514
a41001	0.533	0.598	0.699	0.981	-147.807	0.320	79.000	-0.010	0.638

a65001	0.440	0.377	0.632	0.402	25.986	0.610	32.000	0.027	0.771
a65002	0.450	0.377	0.648	0.403	25.842	0.610	40.400	0.017	0.751
a65003	0.439	0.412	0.643	0.438	26.230	0.610	1.800	0.028	0.775
a650095a	0.434	0.398	0.641	0.414	25.486	0.610	8.600	0.022	0.800
a6500se1	0.399	0.347	0.636	0.393	29.176	0.610	5.600	0.028	0.652
a6500all	0.443	0.416	0.649	0.450	26.192	0.610	1.200	0.028	0.792
a6500ro1	0.443	0.420	0.643	0.443	25.364	0.610	3.000	0.029	0.776
a6500ro2	0.446	0.428	0.644	0.449	24.458	0.610	3.400	0.029	0.781
a6500ro3	0.457	0.450	0.645	0.463	21.690	0.610	5.000	0.029	0.792
a6500ro4	0.468	0.474	0.646	0.476	18.446	0.610	7.000	0.030	0.802
a6500ro5	**0.473**	**0.483**	**0.652**	**0.483**	**17.960**	**0.610**	**6.800**	**0.030**	**0.801**
a6100a01	0.415	0.358	0.578	0.300	-1.906	0.610	36.000	-0.008	0.850

a8500a01	0.650	0.569	0.729	0.414	-148.615	0.770	76.200	-0.005	0.610
a8500a02	0.605	0.577	0.720	0.424	-146.915	0.770	61.000	-0.085	0.603
a8500a03	0.664	0.545	0.737	0.395	-150.059	0.770	61.400	-0.131	0.655
a8500ro1	0.651	0.569	0.729	0.413	-148.739	0.770	76.400	-0.075	0.610
a8500ro2	0.651	0.570	0.729	0.413	-148.829	0.770	76.800	-0.075	0.609
a8500ro3	0.652	0.570	0.729	0.411	-149.129	0.770	76.800	-0.076	0.614
a8500se1	0.650	0.569	0.730	0.414	-148.573	0.770	76.200	-0.075	0.610
a8500nmr	0.618	0.549	0.692	0.420	-133.435	0.770	72.600	-0.080	0.592
a85001st	0.352	0.040	0.531	-0.195	-229.939	0.770	115.200	-0.179	0.410
a8500a8r	0.646	0.559	0.740	0.447	-137.065	0.770	73.000	-0.082	0.652
a850095a	0.650	0.563	0.731	0.411	-148.101	0.770	76.200	-0.082	0.563
a8100a01	0.604	0.443	0.682	0.289	-154.415	0.770	82.000	-0.138	0.441

a9500a01	0.605	0.166	0.736	0.623	95.719	0.450	47.000	0.011	0.862
a9500a02	0.596	0.155	0.733	0.621	96.677	0.450	-4.800	-0.025	0.821
a9500a03	0.613	0.175	0.740	0.620	95.285	0.450	46.200	-0.045	0.905
a9500nmr	0.571	-0.336	0.694	0.494	150.091	0.450	39.600	0.021	0.664
a95001st	0.271	0.007	0.383	0.078	5.789	0.450	95.600	-0.069	0.611
A9500a9r	0.602	-0.165	0.739	0.550	128.825	0.450	42.800	0.005	0.915
a9500ds1	0.428	-0.014	0.632	-0.751	-191.125	0.450	160.000	-0.226	0.860
a9500ds2	0.537	0.375	0.689	-0.153	-127.289	0.450	137.400	-0.164	0.888
a9500ds3	0.579	0.499	0.721	0.256	-63.585	0.450	112.200	-0.119	0.913
a9500ds4	0.601	0.454	0.738	0.528	11.221	0.450	84.800	-0.061	0.853

a9500ro1	0.606	0.166	0.736	0.623	95.541	0.450	46.800	0.010	0.862
a9500ro2	0.606	0.167	0.736	0.623	95.345	0.450	46.800	0.010	0.862
a9500ro3	0.606	0.166	0.736	0.622	94.677	0.450	47.600	0.011	0.859
a950095a	0.607	0.077	0.740	0.606	106.123	0.450	46.400	0.001	0.812
a9500se1	0.605	0.166	0.740	0.606	95.747	0.450	46.400	0.001	0.812

D. 1. 3. Validation period (1992 – 1996)

Run Name	Daily		Decadal		Sim - Obs [mm/y]	*Low flow analysis*			
	r2	E2	r2	E2		thre-shold [m3/s]	duration sim - obs [days]	volume sim - obs [m3/s]	r2 (NMQ30)
a5500gw3b	**0.564**	**0.513**	**0.721**	**0.659**	**13.044**	**0.730**	**h**	**0.013**	**0.906**
a5500gw2b	0.559	0.525	0.714	0.647	13.896	0.730	-28.800	0.065	0.646
a5500gw4b	0.562	0.461	0.716	0.593	15.118	0.730	-39.000	-0.005	0.569
a5500gw5b	0.562	0.456	0.716	0.588	15.216	0.730	-41.400	-0.016	0.541
a5500gw1b	0.560	0.498	0.722	0.667	12.602	0.730	-20.200	0.126	0.652
a5500gw6b	0.557	0.445	0.721	0.648	12.728	0.730	4.200	0.108	0.656
a5500gw7	0.551	0.582	0.716	0.718	11.350	0.730	-66.200	0.105	0.671
a5500ro1	0.564	0.513	0.721	0.659	13.044	0.730	-7.400	0.013	0.906
a5500ro2	0.563	0.512	0.721	0.658	12.990	0.730	-7.400	0.117	0.666
a5500ro3	0.564	0.512	0.721	0.659	13.018	0.730	-7.400	0.117	0.666
a5500ro4	0.562	0.511	0.721	0.658	12.934	0.730	-7.400	0.117	0.666
a5500cn1	0.586	0.540	0.732	0.689	16.386	0.730	-13.800	0.115	0.662
a5500se1	0.556	0.516	0.721	0.659	13.432	0.730	-8.000	0.117	0.665
a5100l95	0.563	0.453	0.714	0.600	23.758	0.730	-9.400	0.102	0.693
a5100a01	0.563	0.499	0.722	0.646	16.132	0.730	-6.800	0.012	0.903
a5100ro1	0.561	0.497	0.721	0.645	16.042	0.730	-7.000	0.118	0.668
a5500eta	0.549	0.516	0.702	0.653	0.482	0.730	-2.000	0.108	0.856
a5500et2	0.571	0.498	0.729	0.653	19.544	0.730	-8.400	0.118	0.675
a5050a01	0.563	0.499	0.722	0.645	16.470	0.730	-7.400	0.013	0.904
a5500act	0.636	0.599	0.744	0.677	22.825	0.730	84.800	-0.190	0.734
a3500a01	0.582	0.177	0.837	0.875	82.499	0.320	65.600	-0.012	0.904
a3500a02	0.566	0.270	0.839	0.897	81.365	0.320	7.400	-0.001	0.914
a3500a03	**0.578**	**0.280**	**0.841**	**0.892**	**81.867**	**0.320**	**29.800**	**0.004**	**0.914**
a3500a04	0.559	0.391	0.845	0.909	81.211	0.320	-18.000	-0.016	0.940
a3500ds1	0.317	-0.430	0.672	0.716	-367.485	0.320	181.000	-0.107	0.965
a3500ds2	0.515	0.233	0.805	0.902	-170.805	0.320	110.400	-0.059	0.980
a3500ds3	0.554	0.335	0.833	0.921	-46.371	0.320	74.400	-0.029	0.955
a3500ro1	0.578	0.280	0.841	0.892	81.839	0.320	29.800	0.004	0.914
a3500ro2	0.578	0.280	0.841	0.891	81.853	0.320	29.800	0.004	0.914
a3500ro3	0.577	0.279	0.841	0.891	81.805	0.320	29.800	0.004	0.914
a350095a	0.576	0.200	0.843	0.868	100.409	0.320	33.000	-0.003	0.890
a3500se1	0.578	0.280	0.841	0.891	81.921	0.320	29.800	0.004	0.914
a3100a01	0.579	0.252	0.852	0.885	96.635	0.320	27.000	0.006	0.919
a31kma01	0.564	0.170	0.831	0.860	110.867	0.320	28.000	0.000	0.895
a45001	0.513	0.198	0.625	0.974	-87.569	0.320	64.600	-0.067	0.042
a45002	0.519	0.290	0.632	0.976	-89.525	0.320	65.400	-0.047	0.037
a45003	0.517	0.405	0.635	0.978	-92.807	0.320	20.200	-0.036	0.047
a45004	**0.520**	**0.362**	**0.635**	**0.977**	**-91.337**	**0.320**	**75.800**	**-0.011**	**0.037**

a4500ro1	0.520	0.362	0.635	0.977	-91.327	0.320	75.800	-0.011	0.037
a4500ro2	0.520	0.362	0.635	0.977	-91.333	0.320	76.000	-0.011	0.037
a4500ro3	0.519	0.361	0.635	0.977	-91.295	0.320	76.200	-0.011	0.037
a450095a	0.521	0.343	0.639	0.976	-81.531	0.320	73.200	-0.017	0.056
a4500se1	0.520	0.362	0.635	0.977	-91.365	0.320	75.800	-0.011	0.037
a41001	0.509	0.338	0.629	0.977	-76.911	0.320	74.000	-0.010	0.028

a65001	0.529	0.459	0.838	0.772	11.543	0.610	-1.000	0.124	0.762
a65002	0.524	0.456	0.845	0.773	11.173	0.610	12.200	0.109	0.769
a65003	0.516	0.478	0.843	0.785	10.713	0.610	-32.000	0.117	0.754
a650095a	0.508	0.460	0.837	0.767	11.181	0.610	-26.800	0.104	0.774
a6500se1	0.482	0.441	0.846	0.788	12.375	0.610	-31.600	0.117	0.764
a6500all	0.533	0.499	0.842	0.791	9.325	0.610	-32.000	0.117	0.756
a6500ro1	0.522	0.485	0.843	0.787	9.885	0.610	-31.600	0.117	0.757
a6500ro2	0.527	0.492	0.842	0.789	9.031	0.610	-31.400	0.116	0.765
a6500ro3	0.545	0.513	0.840	0.795	6.403	0.610	-29.000	0.117	0.774
a6500ro4	0.562	0.534	0.836	0.797	3.457	0.610	-26.800	0.117	0.791
a6500ro5	**0.570**	**0.542**	**0.835**	**0.797**	**2.633**	**0.610**	**-26.200**	**0.118**	**0.792**
a6100a01	0.537	0.461	0.794	0.732	-19.655	0.610	4.400	0.047	0.835

a8500a01	0.558	0.631	0.649	0.611	37.359	0.770	20.200	-0.110	0.040
a8500a02	0.525	0.624	0.642	0.638	36.819	0.770	2.800	-0.075	0.057
a8500a03	0.561	0.608	0.650	0.595	38.379	0.770	6.200	-0.158	0.022
a8500ro1	0.558	0.631	0.648	0.611	37.313	0.770	19.800	-0.111	0.040
a8500ro2	0.557	0.630	0.648	0.610	37.243	0.770	19.600	-0.111	0.040
a8500ro3	0.555	0.628	0.646	0.608	37.093	0.770	20.000	-0.111	0.040
a8500se1	0.558	0.631	0.649	0.612	37.391	0.770	20.200	-0.110	0.040
a8500nmr	0.533	0.510	0.632	0.473	65.225	0.770	14.200	-0.111	0.058
a85001st	0.286	0.415	0.386	0.216	-90.023	0.770	74.800	-0.249	0.643
a8500a8r	0.567	0.588	0.655	0.555	46.409	0.770	22.400	-0.112	0.052
a850095a	0.565	0.621	0.655	0.597	39.579	0.770	18.000	-0.116	0.060
a8100a01	0.538	0.475	0.629	0.390	25.593	0.770	33.400	-0.177	0.003

a9500a01	0.554	-0.350	0.712	0.597	139.145	0.450	41.400	-0.001	0.377
a9500a02	0.553	-0.308	0.713	0.618	138.737	0.450	-7.600	-0.033	0.344
a9500a03	0.558	-0.364	0.711	0.569	138.805	0.450	44.800	-0.041	0.417
a9500nmr	0.546	-1.398	0.703	0.306	214.097	0.450	28.000	0.006	0.331
a95001st	0.331	-0.635	0.445	0.119	95.771	0.450	82.600	-0.042	0.063
A9500a9r	0.516	-0.496	0.685	0.532	144.427	0.450	45.800	0.000	0.474
a9500ds1	0.382	-0.113	0.543	-0.814	-172.919	0.450	180.200	-0.170	0.122
a9500ds2	0.496	0.341	0.669	-0.120	-104.355	0.450	151.200	-0.113	0.180
a9500ds3	0.539	0.403	0.694	0.295	-33.683	0.450	116.600	-0.080	0.246
a9500ds4	0.548	0.208	0.706	0.546	49.889	0.450	77.800	-0.049	0.304
a9500ro1	0.553	-0.351	0.712	0.597	138.995	0.450	41.600	-0.001	0.379
a9500ro2	0.552	-0.352	0.711	0.597	138.873	0.450	41.800	-0.001	0.377
a9500ro3	0.547	-0.356	0.708	0.596	138.447	0.450	42.200	-0.001	0.375
a950095a	0.557	-0.469	0.719	0.566	149.921	0.450	36.800	-0.011	0.489
a9500se1	0.554	-0.350	0.719	0.566	139.139	0.450	36.800	-0.011	0.489

D. 2. Scenario Runs with the NRM^3 Streamflow Model

Land Use Change Scenarios

lcsc01 Cgrain (>50% cropland with grain) below 3200 m a.s.l.

lcsc02 tC (>50% cropland with 2 - 20% trees) below 3200 m a.s.l.

lcsc03 tG (>50% grassland with 2 - 20% trees) below 2000 m a.s.l., td (>50% dense trees) and Go (>50% bamboo) between 2000 and 3200 m a.s.l.

lcsc04 Gb (>50 bare grassland) up to 2300 m a.s.l.

lcsc05a Gb (>50 bare grassland) up to 3200 m a.s.l., soils unchanged

lcsc05b Gb (>50 bare grassland) up to 3200 m a.s.l., humic acrisols and andosols on mountain slopes eroded by 50%

Climate Change Scenarios

ECHAMA2 IPCC SRES A2 emissions scenario, modelled with the GCM ECHAM; baseline climate modified by monthly average change fields for the years 2040 - 69

ECHAMB2 IPCC SRES B2 emissions scenario, modelled with the GCM ECHAM; baseline climate modified by monthly average change fields for the years 2040 - 69

Baseline Period: 1987 - 2001

Values given are the differences of measures Scenario - Base Case

A5 Catchment

Scenario	Annual runoff [mm]	Annual runoff [%]	Qmax [m3/s]	Qmax [%]	Qmin [m3/s]	Qmin [%]	Mean [m3/s]	Mean [%]	Median [m3/s]	Median [%]	Lower Quartile [m3/s]	Lower Quartile [%]	Upper Quartile [m3/s]	Upper Quartile [%]	Mean NMQ30 [m3/s]	Mean NMQ30 [%]	Low flow duration [days /year]	Rain [mm /year]	Rain [%]	Q/P ratio [+/- %]
lcsc01	52.26	11.13	2.94	15.43	0.00	0.00	0.14	11.13	-0.02	-3.85	0.00	0.00	0.01	0.70	-0.01	-5.94	-8.60	0.00	0.00	4.59
lcsc02	49.95	10.64	2.36	12.37	0.00	0.00	0.14	10.64	-0.02	-3.85	0.00	0.00	0.02	1.22	-0.01	-5.99	-7.67	0.00	0.00	4.38
lcsc03	-7.47	-1.59	-0.31	-1.64	0.00	0.00	-0.02	-1.59	-0.01	-1.92	0.00	0.00	-0.21	-14.69	0.00	0.98	0.73	0.00	0.00	-0.62
lcsc04	97.04	20.67	5.16	27.06	0.00	0.00	0.27	20.67	0.03	5.77	0.03	9.38	0.29	20.10	0.04	23.53	-21.27	0.00	0.00	8.51
lcsc05a	277.96	59.19	7.57	39.75	0.00	0.00	0.77	59.19	0.20	38.46	0.09	28.91	1.10	76.22	0.12	64.30	-51.33	0.00	0.00	24.89
lcsc05b	278.33	59.27	7.57	39.75	0.00	0.00	0.77	59.27	0.20	38.46	0.09	28.91	1.10	76.22	0.12	62.57	-51.13	0.00	0.00	24.93
ECHAMA2	122.21	26.27	54.50	285.59	-0.03	-75.00	0.34	26.27	-0.01	-1.92	-0.04	-12.50	0.33	23.40	-0.06	-30.15	1.27	198.63	17.63	1.08
ECHAMB2	132.38	28.46	6.64	34.78	-0.02	-50.00	0.36	28.46	0.04	7.69	0.07	21.88	0.45	31.74	-0.01	-7.04	-14.00	234.98	20.85	1.94

A3 Catchment

Scenario	Annual runoff [mm]	Annual runoff [%]	Qmax [m3/s]	Qmax [%]	Qmin [m3/s]	Qmin [%]	Mean [m3/s]	Mean [%]	Median [m3/s]	Median [%]	Lower Quartile [m3/s]	Lower Quartile [%]	Upper Quartile [m3/s]	Upper Quartile [%]	Mean NMQ30 [m3/s]	Mean NMQ30 [%]	Low flow duration [days /year]	Rain [mm /year]	Rain [%]	Q/P ratio [+/- %]
lcsc01	40.19	6.94	2.09	19.44	0.00	-20.00	0.05	6.94	-0.01	-3.03	0.00	0.00	0.03	4.49	0.00	-4.15	-5.33	0.00	0.00	3.43
lcsc02	40.09	6.92	1.83	16.98	0.00	-20.00	0.05	6.92	-0.01	-3.79	0.00	0.00	0.03	4.33	0.00	-4.16	-5.53	0.00	0.00	3.42
lcsc03	-0.70	-0.12	-0.17	-1.60	0.00	0.00	0.00	-0.12	-0.01	-3.03	0.00	0.00	-0.07	-9.60	0.00	2.34	0.07	0.00	0.00	-0.06
lcsc04	0.24	0.04	0.00	0.00	0.00	0.00	0.00	0.04	-0.01	-3.03	0.00	0.00	-0.08	-10.53	0.00	0.12	-0.13	0.00	0.00	0.02
lcsc05a	184.56	31.86	4.93	45.83	0.00	-20.00	0.23	31.86	0.05	15.15	0.04	22.56	0.40	52.94	0.05	44.73	-27.87	0.00	0.00	16.00
lcsc05b	185.06	31.95	4.93	45.83	0.00	-20.00	0.24	31.95	0.05	15.15	0.04	22.56	0.40	53.25	0.05	43.58	-27.80	0.00	0.00	16.05
ECHAMA2	113.69	19.99	19.86	189.96	-0.02	-80.00	0.14	19.99	-0.01	-3.03	-0.02	-10.00	0.17	23.56	-0.03	-28.85	-1.67	190.31	16.19	-0.14
ECHAMB2	149.09	26.21	3.84	36.74	0.00	-20.00	0.19	26.21	0.02	7.58	0.04	22.50	0.29	40.71	-0.01	-6.19	-14.20	249.84	21.25	1.30

A4 Catchment

Scenario	Annual runoff [mm]	Annual runoff [%]	Qmax [m3/s]	Qmax [%]	Qmin [m3/s]	Qmin [%]	Mean [m3/s]	Mean [%]	Median [m3/s]	Median [%]	Lower Quartile [m3/s]	Lower Quartile [%]	Upper Quartile [m3/s]	Upper Quartile [%]	Mean NMQ30 [m3/s]	Mean NMQ30 [%]	Low flow duration [days /year]	Rain [mm /year]	Rain [%]	Q/P ratio [+/- %]
lcsc01	65.26	10.59	1.54	22.67	0.00	-33.33	0.05	10.59	-0.02	-8.05	0.00	-2.27	0.01	2.60	-0.01	-10.38	-9.33	0.00	0.00	5.07
lcsc02	64.79	10.51	1.39	20.43	0.00	-33.33	0.05	10.51	-0.02	-6.90	0.00	0.00	0.01	2.78	-0.01	-10.04	-9.13	0.00	0.00	5.03
lcsc03	-2.85	-0.46	-0.04	-0.55	0.00	0.00	0.00	-0.46	-0.01	-5.75	0.00	2.27	-0.06	-15.97	0.00	3.83	0.53	0.00	0.00	-0.21
lcsc04	39.09	6.34	-0.09	-1.34	0.00	0.00	0.03	6.34	-0.01	-2.30	0.01	6.82	0.00	0.52	0.01	16.20	-3.80	0.00	0.00	3.04
lcsc05a	303.17	49.18	3.88	57.26	0.00	-33.33	0.22	49.18	0.05	20.69	0.04	36.36	0.37	95.83	0.04	72.73	-29.20	0.00	0.00	24.01
lcsc05b	303.55	49.25	3.90	57.46	0.00	-33.33	0.22	49.25	0.05	20.69	0.04	36.36	0.37	96.35	0.04	71.72	-29.47	0.00	0.00	24.05
ECHAMA2	123.87	20.10	16.80	247.66	-0.01	-100.00	0.09	20.10	-0.02	-6.90	-0.01	-10.80	0.10	25.69	-0.02	-30.51	-6.20	213.51	16.59	-0.63
ECHAMB2	157.27	25.51	3.98	58.76	-0.01	-100.00	0.11	25.51	0.02	9.20	0.04	34.09	0.15	38.02	-0.01	-9.69	-15.53	271.94	21.13	1.06

A6 Catchment

Scenario	Annual runoff [mm]	Annual runoff [%]	Qmax [m3/s]	Qmax [%]	Qmin [m3/s]	Qmin [%]	Mean [m3/s]	Mean [%]	Median [m3/s]	Median [%]	Lower Quartile [m3/s]	Lower Quartile [%]	Upper Quartile [m3/s]	Upper Quartile [%]	Mean NMQ30 [m3/s]	Mean NMQ30 [%]	Low flow duration [days /year]	Rain [mm /year]	Rain [%]	Q/P ratio [+/- %]
lcsc01	36.30	16.25	5.12	17.88	0.00	0.00	0.20	16.25	0.06	13.04	0.10	45.45	0.23	25.28	0.01	7.85	-9.13	0.00	0.00	3.78
lcsc02	33.81	15.13	4.46	15.57	0.00	0.00	0.19	15.13	0.06	13.04	0.10	45.45	0.25	28.09	0.01	8.59	-8.47	0.00	0.00	3.52
lcsc03	-15.58	-6.97	-5.18	-18.09	0.00	0.00	-0.09	-6.97	0.04	8.70	0.08	36.36	-0.11	-12.36	0.00	-2.65	3.93	0.00	0.00	-1.61
lcsc04	180.94	80.98	25.84	90.25	0.00	0.00	0.99	80.98	0.18	39.13	0.16	72.73	1.51	169.10	0.09	55.59	-44.20	0.00	0.00	19.19
lcsc05a	284.30	127.24	32.74	114.38	0.00	0.00	1.56	127.24	0.36	78.26	0.26	118.18	2.35	263.48	0.22	138.78	-73.93	0.00	0.00	30.54
lcsc05b	284.86	127.49	32.76	114.45	0.00	0.00	1.57	127.49	0.36	78.26	0.26	118.18	2.35	263.48	0.22	137.61	-73.93	0.00	0.00	30.61
ECHAMA2	141.54	59.01	147.89	546.11	0.00	0.00	0.78	59.01	0.08	14.29	0.06	18.75	0.59	49.58	-0.05	-19.01	-14.60	208.17	22.60	6.05
ECHAMB2	113.45	47.30	14.39	53.15	0.00	0.00	0.62	47.30	0.12	21.43	0.20	62.50	0.79	66.39	0.04	17.40	-30.13	209.96	22.79	4.97